

Shimane University
Interdisciplinary Graduate School of Science and Engineering
Department of Geoscience



Doctoral Thesis

**Geological and geochemical studies
of the Neogene Siwalik Group, Khutia Khola section,
Nepal Himalaya and comparison with the Middle Bengal
Fan sediments: implications for provenance, paleoclimate
and Himalayan tectonics**

by
Swostik Kumar Adhikari
(S149845)

28th July 2017

**Geological and geochemical studies
of the Neogene Siwalik Group, Khutia Khola section,
Nepal Himalaya and comparison with the Middle Bengal Fan
sediments: implications for provenance, paleoclimate and
Himalayan tectonics**

A dissertation submitted to the Department of Geoscience
in partial fulfillment of the requirements for the Degree of
DOCTOR OF SCIENCE
at the interdisciplinary Graduate School of Science and Engineering
Shimane University, Japan

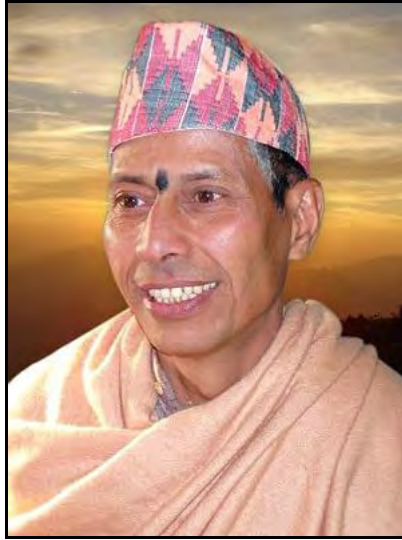
by
Swostik Kumar Adhikari
(S149845)

Supervisor
Prof. Tetsuya Sakai

Examination Committee
Prof. Hiroaki Ishiga
Prof. Hiroshi Usuki
Prof. Toshiaki Irizuki
Prof. Hiroki Hayashi

28th July 2017

DEDICATION



This thesis is dedicated to my beloved father late Mr. Sanad Kumar Adhikari, who would have been really proud of me for my achievements in this foreign land, and as my sincere respect to him I am committed to follow the path he has shown, the principle "live every moment, not survive".

CONTENTS

ABSTRACT	I-IV
LIST OF FIGURES	V-XII
LIST OF TABLES	XIII-XIV

CHAPTER ONE

INTRODUCTION	1-7
1.1 Introduction.....	1
1.2 Objectives.....	5

CHAPTER TWO

METHODOLOGY	8-10
2.1 Field study.....	8
2.2 Laboratory method.....	9

CHAPTER THREE

GEOLOGY OF NEPAL HIMALAYA	11-26
3.1 Introduction.....	11
3.2 Tectonic divisions of Nepal Himalaya.....	12
3.2.1 Tibetan-Tethys zone.....	13
3.2.2 Higher Himalayan zone.....	14
3.2.3 Lesser Himalayan zone.....	15
3.2.4 Sub-Himalayan zone (Siwalik or Churia Group).....	16
3.2.5 Terai zone.....	16
3.3 Stratigraphy of the Siwalik Group, Nepal Himalaya.....	18
3.4 Regional geology of the far western Nepal Himalaya.....	24

CHAPTER FOUR

LITHOSTRATIGRAPHY **27-47**

4.1 Introduction.....	26
4.2 Method.....	29
4.3 Lithostratigraphy.....	30
4.3.1 Jagati Formation.....	30
4.3.1.1 Type locality.....	30
4.3.1.2 Lithology.....	30
4.3.1.2.1 Lower member.....	33
4.3.1.2.2 Middle member.....	36
4.3.1.2.3 Upper member.....	37
4.3.2 Kala Formation.....	38
4.3.2.1 Type locality.....	38
4.3.2.2 Lithology.....	38
4.3.2.2.1 Lower member.....	39
4.3.2.2.2 Middle member.....	41
4.3.2.2.3 Upper member.....	42
4.4 Correlation with magnetostratigraphic data.....	43
4.5 Lithostratigraphy and comparison.....	46

CHAPTER FIVE

DEPOSITIONAL FACIES ANALYSIS **48-70**

5.1 Introduction.....	48
5.2 Methodology.....	50
5.3 Depositional facies.....	52
5.4 Architectural elements.....	56
5.5 Facies association.....	61
5.5.1 Facies association 1 (FA1).....	62
5.5.2 Facies association 2 (FA2).....	63
5.5.3 Facies association 3 (FA3).....	65
5.5.4 Facies association 4 (FA4).....	68

5.6 Correlation with magnetostratigraphic data.....	69
---	----

CHAPTER SIX

GEOCHEMICAL ANALYSIS **71-124**

6.1 Introduction.....	71
6.2 Sample preparation.....	72
6.3 XRF analysis.....	73
6.4 Results.....	74
6.4.1 Major elements.....	75
6.4.2 Trace elements.....	76
6.5 Element-Al ₂ O ₃ covariations.....	77
6.5.1 Major elements.....	78
6.5.2 Trace elements.....	83
6.6 Geochemical classification.....	91
6.7 Comparison with UCC by lithotypes.....	91
6.8 Provenance signatures by lithotypes.....	94
6.9 Weathering indices.....	96
6.10 Stratigraphic variation by lithotypes.....	105

CHAPTER SEVEN

PETROGRAPHICAL ANALYSIS **125-149**

7.1 Introduction.....	125
7.2 Methodology.....	126
7.3 Results.....	128
7.3.1 Jagati Formation (Meandering river system- FA1-FA2).....	128
7.3.2 Kala Formation (Braided river system- FA3-FA4).....	129
7.4 Sandstone classification.....	132
7.5 Provenance and tectonic setting.....	134
7.6 Climatic indexes.....	139
7.7 Stratigraphic variations in petrographic modes.....	142

CHAPTER EIGHT

The Middle Bengal Fan turbidites	150-175
8.1 Introduction.....	150
8.2 Samples.....	152
8.2.1 Sample preparation and analysis.....	152
8.2.2 Data processing.....	154
8.3 Result.....	155
8.3.1 Site U1450 (A & B).....	155
8.3.2 Site U1451 (A & B).....	156
8.4 Textural classification of sediments.....	157
8.5 Frequency curve.....	161
8.6 Comparison of the Siwalik Group sediments and the Bengal Fan turbidites.....	162

CHAPTER NINE

DISCUSSION	176-194
9.1 Fluvial setting.....	176
9.1.1 Significance in change from FA1 to FA2.....	177
9.1.2 Significance in change from meandering to braided river system.....	179
9.2 Geochemical variation.....	181
9.2.1 Source lithology.....	181
9.2.2 Change in fluvial style and weathering intensity.....	185
9.3 Climate change.....	187
9.3.1 Siwalik sedimentation and correlation with other studies along the Khutia Khola section.....	187
9.3.2 Comparative studies on paleoclimate and Himalayan tectonics.....	190

CHAPTER TEN

CONCLUSIONS	195-201
ACKNOWLEDGEMENTS	202-203
REFERENCES	204-233

ABSTRACT

The Neogene fluvial sediments (Siwalik Group) forming the southernmost hills in the Himalaya are one of the best archives of the climatic history and uplift of the Himalayas. This study focuses on geological and geochemical studies of a small river system at the time of Siwalik Group deposition, and compares the results with those from a large river system, to decipher the differences between the fluvial systems, as well as the provenance, tectonic setting and weathering regime of the sediments. The Siwalik Group in the Khutia Khola section is the target of this study. The Khutia Khola section contains finer sediments and thinner sandstone units than that of the neighboring Siwalik successions. These features indicate the deposition from a small river system. . Results are compared with equivalent sediments in the adjacent Karnali River section, which are known to have been deposited by the large palco-Karnali River system. The river deposits in these two sections are important records of tectonism and climatic change in the western part of the Nepal Himalaya, and the local variation of these key processes during middle to late Miocene times. Furthermore, the grain sizes of coeval turbidite beds from the Middle Bengal Fan were also analyzed. These sediments were originally eroded from the Himalaya and deposited in the Bengal Fan. The results from

both studies are compared to decipher the effect on sedimentation and climatic changes interlinked with Himalayan tectonics.

The newly established stratigraphy of the Khutia Khola area comprises the Jagati Formation (2110 m, equivalent to the Lower Siwalik) and the Kala Formation (2050 m, equivalent to the Middle Siwalik) in ascending order. The Jagati Formation consists of bioturbated, reddish-brown, brown to variegated mudstones, interbedded with very fine- to medium-grained, grey, reddish-grey to brown sandstones. The Kala Formation comprises thinly- to thickly-bedded, medium- to very coarse-grained, light-grey and grey to greenish-grey 'salt and pepper' sandstones and pebbly sandstones, interbedded with greenish-grey and brown to reddish-brown mudstones.

Depositional facies description from the Khutia Khola section shows the same sequences of facies associations that are recognized in other Siwalik sections in Nepal Himalaya. These comprise a fine-grained meandering river system (FA1), a flood-flow dominated meandering river system (FA2), and deep (FA3) and shallow (FA4) sandy braided river systems. FA1-FA2 corresponds to the Lower Siwalik, and FA3-FA4 to the Middle Siwalik. The timing of the appearance of FA2 is crucial for determining the timing of increased precipitation due to monsoon intensification, and accelerated sediment supply associated with tectonic uplift. FA2 appears at around 13.5 Ma in the

Khutia Khola section, which corresponds with timing in the adjacent Karnali River section.

Changes in geochemical indices including provenance, sorting effects, and intensity of weathering are well synchronized with the changes in depositional facies. Petrographic study shows that the compositions of the Khutia Khola sandstones are similar to other Siwalik sandstones in the Nepal Himalaya. Comparable petrographic and geochemical provenance indices suggest a common source for the Khutia Khola and Karnali River sediments. Stratigraphic elemental ratio plots (e.g. Ga/Rb, K_2O/Al_2O_3 , Na_2O/Al_2O_3 , SiO_2/Al_2O_3) identify more intense weathering, uniform source, and greater sorting fractionation in the meandering river systems. Systematic upward changes in such elemental ratios reflect change in fluvial style in the Lower to Middle Siwaliks, with shift from meandering to braided river systems.

Collectively, the dominance of the finer sediments and thinner sandstone units compared to neighboring Siwalik successions indicate that the Khutia Khola section was deposited by a small river system. This system was located at the western margin of the paleo-Karnali River system, or may represent the interfluvial setting of major river systems. FA2 appears in the Khutia Khola and the Karnali River sections the same time, as noted above. This implies increased discharge and accelerated erosion from the frontal

part of the Himalaya at around 13.5 Ma in the far-western Nepal Himalaya, earlier than in the central and eastern Nepal Himalaya (9.5 to 10.5 Ma). There is no significant variation in the record of monsoon intensification between the small and large river systems in the Siwalik Group in this area.

Grain size analyses of the turbidite beds from the Middle Bengal Fan, IODP Expedition 354 show that inversely graded beds are dominant in site U1450, and thicker massive beds dominantes in site U1451. Vertical variations in mean grain size show slight coarsening upward, and this may be associated with shifting of levees. In this instance, the variation in the grain size in the Middle Bengal Fan turbidites cannot be correlated with lithological changes in the Khutia Khola section of the Siwalik Group, probably because the change around 13.5 Ma was not strong enough to cause the sediment characteristics from the far western Himalaya to be transmitted to the Ganges River mouth.

List of Figures

Chapter One

Page no.

Fig. 1.1: Location map of the study area (after Upreti and Le Fort, 1999)6

Chapter Three

Fig. 3.1. Physiographic subdivisions of the Himalayan arc (after Gansser, 1964).....13

Fig. 3.2: Generalized geological map of the Nepal Himalaya (after Upreti and Le Fort, 1994).....17

Fig. 3.3. Regional geological map of Far Western Nepal (Sharma et al., 2007).....22

Chapter Four

Fig. 4.1. (A) Geological map of the Siwalik Group along the Khutia Khola section.

(B) Cross-section along X-Y (Adhikari and Sakai, 2015).....31

Fig. 4.2. Outcrop photographs of the Jagati Formation. A) Variegated mudstone alternating with fine-grained sandstone. B) Alternating sandstone and mudstone beds. C) Brown mudstone with bioturbation, rootlets and nodules. D) A vertebrate fossil found in mudstone. E) Very thick bedded sandstone near the boundary of the Jagati and Kala Formations. F) Cross-lamination in sandstone bed.....32

Fig. 4.3. Typical columnar sections. Jagati Formation (A and B, lower member; C, middle member; and, D upper member). Kala Formation (E, lower member; F,

middle member; and, G, upper member).....	34
Fig. 4.4. The distribution of various rocks in the Khutia Khola area. A) Distribution of sandstones, mudstones and pebbly sandstones. B) Distribution of various sandstones.....	35
Fig. 4.5. Outcrop photographs of the Kala Formation. A) Ripple lamination in sandstone. B) Coal lens. C) Thick sandstone beds. D) Finely laminated greenish-grey mudstone. E) Quartzite pebble-cobble in sandstone. F) Fractured zone around the MDT (between the southern and central belt of the Siwalik Group).....	40
Fig. 4.6. Magnetostratigraphy and lithostratigraphy divisions of the Siwalik Group along the Khutia Khola section (modified from Ojha et al., 2000).....	45

Chapter Five

Fig. 5.1. A) Geological map of the Siwalik Group along the Khutia Khola section. Red stars with alphabet along the Khutia Khola section indicate the location of columnar sections.....	51
Fig. 5.2. Outcrop photographs of the lithofacies. A) Laminated mudstone (Fl). B) Massive mudstone (Fm). C and D) Paleosols with burrow and rhizoliths (P). E) Planar-cross-bedded sandstone (Sp). F) Trough-cross-bedded sandstone (St). G) Ripple cross-laminated sandstone (Sr). H) Horizontally laminated sandstone (Sh).....	54
Fig. 5.2. cont. Outcrop photographs of the lithofacies. I) Convolute laminated sandstone (Sc). J) Massive sandstone (Sm). K) Horizontally stratified gravel (Gh). L)	

Trough-cross-bedded gravel (Gt).....55

Fig. 5.3. Examples of channel deposit element, CH, (outcrops and sketches). A) Thin- to medium-bedded, fine- to medium-grained sandstone succession deposited as seasonal (minor) channel deposit in middle member of the Jagati Formation. B) Medium- to very thick-bedded, medium- to very coarse-grained sandstones and gravely sandstones deposited as perennial (major) channel deposit in upper member of the Kala Formation.....59

Fig. 5.4. Examples of different types of architectural elements. A) Lateral-accretion (LA) patterns in upper member of the Jagati Formation. B) Downstream-accretion (DA) pattern in lower member of the Kala Formation. C and D) Sandy bedform (SB) deposits in lower and middle members of the Kala Formation, respectively. E) Floodplain (FF) deposits and Crevasse splay (CS) deposits in middle member of the Jagati Formation. F and G) Shallow lake (SL) deposits in middle and upper members of the Jagati Formation.....60

Fig. 5.4. cont. Examples of different types of architectural elements. E) Floodplain (FF) deposits and Crevasse splay (CS) deposits in middle member of the Jagati Formation. F and G) Shallow lake (SL) deposits in middle and upper members of the Jagati Formation.....61

Fig. 5.5. Detail representative columnar sections of facies associations FA1, FA2, FA3 and FA4.....67

Chapter Six

- Fig. 6.1. Major element (Si, Na, Ca) – Al₂O₃ variation diagrams (anhydrous normalized basis) for the Siwalik Group sandstones (sst) and mudstones (mst) from the Khutia Khola section.....79
- Fig. 6.2. Major element (Ti, Fe, Mg) – Al₂O₃ variation diagrams (anhydrous normalized basis) for the Siwalik Group sandstones (sst) and mudstones (mst) from the Khutia Khola section.....81
- Fig. 6.3. Major element (K, Mn, P) – Al₂O₃ variation diagrams (anhydrous normalized basis) for the Siwalik Group sandstones (sst) and mudstones (mst) from the Khutia Khola section.....82
- Fig. 6.4. Trace element (Ba, Pb, Sr) – Al₂O₃ variation diagrams (anhydrous normalized basis) for the Siwalik Group sandstones (sst) and mudstones (mst) from the Khutia Khola section.....85
- Fig. 6.5. Trace element (Cr, Ni, V) – Al₂O₃ variation diagrams (anhydrous normalized basis) for the Siwalik Group sandstones (sst) and mudstones (mst) from the Khutia Khola section.....86
- Fig. 6.6. Trace element (Sc, Rb, Ga) – Al₂O₃ variation diagrams (anhydrous normalized basis) for the Siwalik Group sandstones (sst) and mudstones (mst) from the Khutia Khola section.....87
- Fig. 6.7. Trace element (Nb, Ce, Y) – Al₂O₃ variation diagrams (anhydrous normalized basis) for the Siwalik Group sandstones (sst) and mudstones (mst) from the Khutia Khola section.....88

Fig. 6.8. Trace element (Th, Zr) – Al ₂ O ₃ variation diagrams (anhydrous normalized basis) for the Neogene Siwalik Group sandstones (sst) and mudstones (mst) from the Khutia Khola section.....	89
Fig. 6.9. Log (SiO ₂ /Al ₂ O ₃) – log (Fe ₂ O ₃ /K ₂ O) geochemical classification diagram for the Khutia Khola Siwalik Group sandstones and mudstones.....	92
Fig. 6.10. UCC-normalized spidergrams of average sandstones and mudstones from the Siwalik Group, Khutia Khola section.....	93
Fig. 6.11. Oxide/Al ₂ O ₃ ratio provenance discriminant for the Siwalik Group sandstones (sst) and mudstones (mst), Khutia Khola section.....	95
Fig. 6.12. A-CN-K plot (Nesbitt and Young, 1984) for the Siwalik Group sandstones (sst) and mudstones (mst), Khutia Khola section.....	98
Fig. 6.13. A–CNK–FM plot (Nesbitt and Young, 1989) for the Siwalik Group sandstones (sst) and mudstones (mst), Khutia Khola section.....	99
Fig. 6.14. MFW plot (Ohta and Arai, 2007) for the Siwalik Group sandstones (sst) and mudstones (mst), Khutia Khola section.....	101
Fig. 6.15. S-A-M plot (Krooncnburg, 1994) for the Siwalik Group sandstones (sst) and mudstones (mst), Khutia Khola section.....	104
Fig. 6.16. Ga/Rb–K ₂ O/Al ₂ O ₃ plot (Roy and Roser, 2013) for the Siwalik Group sandstones (sst) and mudstones (mst), Khutia Khola section.....	105
Fig. 6.17. Stratigraphic variation (<i>raw data</i>) in SiO ₂ /Al ₂ O ₃ ratios and Basicity Index in the Khutia Khola Siwalik sandstones and mudstones.....	108
Fig. 6.18. Stratigraphic variation (<i>raw data</i>) in Th/Sc and Na ₂ O/Al ₂ O ₃ ratios in the Khutia Khola Siwalik sandstones and mudstones.....	109

Fig. 6.17. Stratigraphic variation (*five-point moving averages*) in $\text{SiO}_2/\text{Al}_2\text{O}_3$ ratios and Basicity Index in the Khutia Khola Siwalik sandstones and mudstones.....114

Fig. 6.18. Stratigraphic variation (*five-point moving averages*) in Th/Sc and $\text{Na}_2\text{O}/\text{Al}_2\text{O}_3$ ratios in the Khutia Khola Siwalik sandstones and mudstones....115

Fig. 6.19. Stratigraphic variation (*five-point moving averages*) in $\text{K}_2\text{O}/\text{Al}_2\text{O}_3$ and Ga/Rb ratios in the Khutia Khola Siwalik sandstones and mudstones.....116

Chapter Seven

Fig. 7.1. Photomicrographs of sandstones from the Jagati and Kala Formations.....131

Fig. 7.2: Ternary diagram for sandstone composition based on schemes proposed by A) Pettijohn (1975); Q-F-L (quartz, feldspar, lithic fragments), and B) Folk (1980); Q-F-R (quartz, feldspar, rock fragments).....133

Fig. 7.3. Comparison of sandstones classification from different sections of the Siwalik Group, Nepal (after Folk 1980).....134

Fig. 7.4. Ternary diagram for provenance discrimination (after Dickinson et al. 1983). A) Qt-F-L (Quartz, feldspar, lithic fragments). B) Qm-F-Lt (Monocrystalline quartz, feldspar, total lithic grains).....137

Fig. 7.5. Ternary diagram for provenance discrimination. (A) Qp-Lv-Ls (Polycrystalline quartz, volcanic lithic fragment, sedimentary lithic fragment) and (B) Qm-P-K (Monocrystalline quartz, plagioclase, K-feldspar) (after Dickinson 1985). (C) Lv-Ls-Lm (Volcanic lithic fragment, sedimentary lithic fragment, metamorphic lithic fragment) (after Ingersoll and Suczek 1979).....138

Fig. 7.6. (A) Bivariant log/log plot of $Q_p/(F+R)$ (polycrystalline quartz to feldspar plus rock fragments) against $Q_t/(F+R)$ (total quartz to feldspar plus rock fragments) (after Suttner and Dutta, 1986). (B) Ternary Q-F-R (quartz, feldspar, rock fragments) diagram for the effect of source rock on the composition as a function of climate (after Suttner et al., 1981).....140

Fig. 7.7. Bivariant log-ratio plot of Q/F (quartz to feldspar) against Q/R (quartz to rock fragments) (after Weltje et al., 1998).....141

Fig. 7.8. Plots showing the stratigraphic variations. (A) Carbonate. (B) Feldspar. (C) Mica. (D) $Q_p/(F+R)$ (Polycrystalline quartz to feldspar plus rock fragments). (E) $Q_t/(F+R)$ (Total quartz to feldspar plus rock fragments).....144

Chapter Eight

Fig. 8.1. Location of Expedition 354 drill sites (France-Lanord et al., 2016).....152

Fig. 8.2. Representative examples of turbidites.....153

Fig. 8.3. Depth variation of textural components of site U1450 sediments. A) Mean grain size, B) Standard deviation (sorting), C) Skewness, and D) Kurtosis.....158

Fig. 8.4. Depth variation of textural components of site U1451 sediments. A) Mean grain size, B) Standard deviation (sorting), C) Skewness, and D) Kurtosis.....159

Fig. 8.5. Ternary plots of sand-silt-clay of site U1450 (after Shepard, 1954).....160

Fig. 8.6. Ternary plots of sand-silt-clay of site U1451 (after Shepard, 1954).....	160
Fig. 8.7. Frequency curve plots against grain size (phi) showing different bed types. A) Normally graded bed (Hole U1450A). (B) Inversely graded bed (Hole U1450A). (C) Massive (homogeneous) bed (Hole U1451A).....	161

Chapter Nine

Fig. 9.1. Oxide/ Al_2O_3 ratio provenance discriminant (Roser and Korsch, 1988) for the Siwalik Group sandstones (sst) and mudstones (mst), Khutia Khola section and comparison with the Karnali River and Bakiya Khola sections.....	183
Fig. 9.2. Qt-F-L (Quartz, feldspar, lithic fragments) Ternary diagram for provenance discrimination (after Dickinson et al., 1983). Field 1 = Karnali River section, far western Nepal (modified from Sigdel and Sakai, 2013), Field 2 = Surai Khola section, western Nepal and Bakiya Khola section, central Nepal, and Field 3 = Potwar Plateau, Pakistan (modified from Critelli and Intersoll 1994).....	184
Fig. 9.3. Comparison of the stratigraphic variation in SiO_2/Al_2O_3 of different Siwalik sections.....	186
Fig. 9.4. Correlation of present study with Ojha et al. (2000) study along the Khutia Khola section.....	189
Fig. 9.5 Correlation of climatic indices in the Bengal Fan sediments and the Siwalik Group sediments.....	193

List of Tables

Chapter Three

Page no.

Table 3.1: Classification of the Siwalik Groups of the Nepal Himalaya.....	23
--	----

Chapter Four

Table 4.1. Classification of the Siwalik Group of the Nepal Himalaya and its correlation.....	47
---	----

Chapter Five

Table 5.1. Description and interpretation of the depositional facies types found in the Khutia Khola section.....	53
Table 5.2. Description and interpretation of the architectural elements found in the Khutia Khola section.	57
Table 5.3. Facies associations recognized in the Siwalik Group, Khutia Khola section.....	69

Chapter Six

Table 6.1: XRF analyses of Siwalik sandstones and mudstones from the Jagati and Kala Formations, Khutia Khola section, Nepal.....	117
Table 6.2: Average compositions of the Siwalik sandstones and mudstones from the Khutia Khola area, by facies associations.....	124

Chapter Seven

Table 7.1. Framework parameters used in this study.....127

Table 7.2. Recalculated framework (%) and other parameters for the Jagati and Kala Formations, Khutia Khola section.....147

Chapter Eight

Table 8.1. Grain size analysis data of sites U1450 and U1451 (IODP Bengal Fan Expedition 354).....163

Chapter Nine

Table 9.2. Comparison of the fluvial systems180

CHAPTER ONE

INTRODUCTION

1.1 Introduction

The Himalayan orogeny started about 60 million years before by the collision of Indian plate with Eurasian plate. This tectonic activity formed the largest foreland basin in the south of the Himalaya (Burbank et al., 1996). The sediments yielded in association with Himalayan uplift were transported by rivers and were accumulated in foreland basin, which is collectively known as the Siwalik Group. A thick pile of fluvial sediments in the Siwalik Group was deposited during the middle Miocene to early Pleistocene (Gansser, 1964; Prakash et al., 1980; Tokuoka et al., 1986). The Siwalik Group is tectonically separated from the Indo-Gangatic Plain by the Main Frontal Thrust (MFT) in the south and from the Lesser Himalaya by the Main Boundary Thrust (MBT). The age of the Siwalik Group in the Nepal Himalaya ranges from 15.8 to 1 Ma based on the paleomagnetic studies (Tokuoka et al., 1986; Appel et al., 1991; Harrison et al., 1993; Appel and Rosler, 1994; Gautam and Appel, 1994; Gautam and Fujiwara, 2000; Ojha et al., 2000). The Siwalik Group is expected to be one of the best archives of climate history and uplift of the Himalayas.

The uplift of the Himalaya affected the monsoon precipitation, in particular, Indian Summer Monsoon (ISM) and resulted in changes in fluvial system (cf. Nakayama and Ulak, 1999). Several approaches have been made to reveal the linkage between uplift of Himalayas and evolution of ISM from the Siwalik Group. Carbon isotope analysis shows shift from a wetter to drier climate (a timing of monsoon intensification) at 7-8 million years ago (Quade et al., 1995) and 10 million years ago (Tanaka, 1997). Similarly, oxygen isotope studies suggest the onset of monsoon prior to 10.7 million years ago (Dettman et al., 2001).

Fluvial facies studies of the Siwalik Group detected the change in fluvial facies from meandering to braided river systems. In meandering river system, the facies change from meandering river system (FGM) to flood-flow dominated meandering river system (FFDM) indicates the increase in discharge (i.e. increase in precipitation due to ISM intensification). The timing of this change is, however, different among locations: at about 10.5 million years ago in the Bakiya Khola, central Nepal; 10 and 9.5 million years ago in the Tinau Khola and Surai Khola, west-central Nepal (Nakayama and Ulak, 1999; Ulak and Nakayama, 2001). This reveals disynchronous precipitation increase throughout Nepal Himalaya. Possibly, the catchment size of the rivers is the reason for these diachronous changes. Rivers with large catchment basins

can suppress local fluctuation of water supply to river, and respond only to regional climate change. In contrast, rivers with small catchment basins are expected to be sensitive to changes in precipitation induced by local uplift and minimal climatic change. Detail studies considering catchment size are important to reveal the precise climatic history in the Himalayas.

Sigdel and Sakai (2016) studied detailed river facies to reveal the regional climatic change in a large catchment basin along the Karnali River section, far western Nepal. The presence of much thicker river channel deposits and lesser proportion of mudstone beds show that the sediments were supplied from a large catchment area. The detailed fluvial facies study showed the appearance of FFMD around 13.5 million years ago. This age is much earlier than the eastern part of the Nepal Himalayas. This can be explained by the earlier uplift of the western part of Nepal Himalayas (Sigdel and Sakai, 2016).

The present study aims to reconstruct the depositional facies and geochemical analysis from the Siwalik Group sediments which were supplied from a small catchment area, and compare this system with that from a river with a large catchment basin, to decipher the differences between climatic changes due to local as well as regional precipitation on different catchment basin size and its relation with the

Himalayan tectonics. With this prospective, the location of small rivers near the Karnali River section was firstly estimated, as it has been most recently studied. The Khutia Khola lies about 50 km west from the Karnali River (Fig. 1.1). Previous studies on this area indicate the muddier sediment succession in the Khutia Khola section than in other Siwalik successions (cf. Tokuoka et al., 1986, 1988; Sah et al., 1994; Corvinus and Nanda, 1994; Dhital et al., 1995; Ulak and Nakayama, 1998; Sigdel et al., 2011), so that the Siwalik Group sediments along the Khutia Khola section are expected to have been small at the time of deposition. This succession is important for understanding of the Himalayan Uplift and climatic changes as well as environmental changes in the following points: (1) The muddy Siwalik succession could be a better archive than the sand-dominated Siwalik succession because the loss of sediment succession by stream erosion could be smaller than the sand-dominated cases, and (2) the sediments may provide a good example of interfluvial environments of the Siwalik phase. Magnetostratigraphic study is essential to determine the time frame. This area has been dated from 13.30 to 7.65 million years (Ojha et al., 2000), which allows comparison of fluvial facies with the Karnali River section.

This study also focuses on the grain size analysis of the turbidite beds of the Middle Bengal Fan sediments obtained from International Ocean Discovery Program,

Bengal Fan Expedition 354. The Bengal Fan is the world's largest submarine fan and the Himalaya is the main source of sediment in the basin (Curry and Moore, 1971; Emmel and Curry, 1984; Cochran, 1990). These sediments contain a record of the erosion and the uplift of the Himalayas (Curry and Moore, 1971). Spatial and temporal variation in grain size distribution of the turbidites in holes U1450 and U1451 (France-Lanord et al., 2016) may be helpful for understanding the impact of climate change and tectonics. Thus, this study focuses on the fluvial facies and geochemical studies of the Neogene Siwalik sediments as well as the grain size study of the Middle Bengal Fan turbidite sediments on the implications for provenance, palaeoclimate and Himalayan tectonics.

1.2. Objectives

- To establish a detailed lithostratigraphy of the Khutia Khola area, which permit comparison and correlation among different sections of the Siwalik Group in the Nepal Himalaya.
- To study and reconstruct the depositional environment of the Siwalik river systems based on fluvial facies analysis.
- To determine the changes in sediment provenance, sorting effects and weathering regime, based on whole-rock geochemical analysis by X-ray Fluorescence (XRF)

method.

- To analyze the sandstone petrography for understanding the provenance, tectonic setting and climate.
- To compare the detail study with the nearby Karnali River section and the other Siwalik Group in the Nepal Himalaya to decipher the differences between the climatic changes due to the local as well as regional precipitation on different catchment basin size and its relation with the Himalayan tectonics.
- To analyze the grain size of turbidite beds of the Middle Bengal Fan and to understand the variations in sediment distribution in the Bengal Basin, and compare the results with the Siwalik Group.

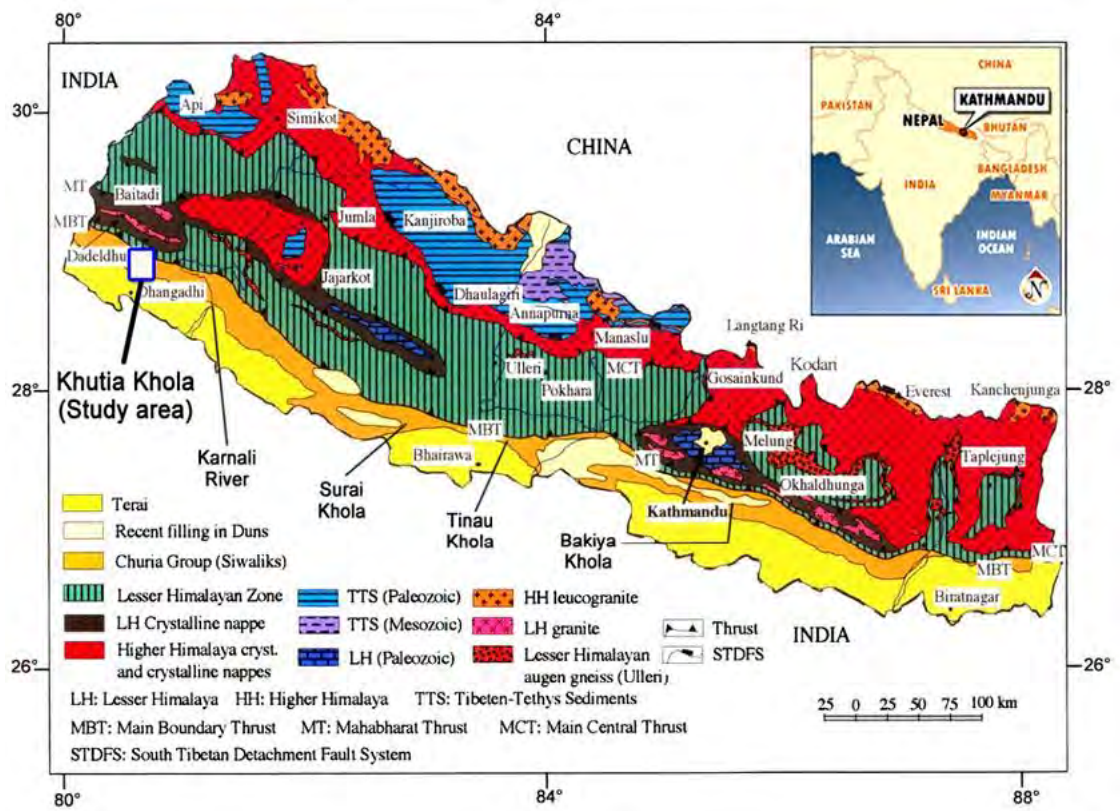


Fig. 1.1. Location map of the study area. The Khutia Khola area is indicated in box. (after Upreti and Le Fort, 1999)

CHAPTER TWO

METHODOLOGY

The present study was carried out for the establishment of lithostratigraphy, depositional facies analysis, whole rock geochemical analysis and petrographical analysis for the reconstruction of fluvial system, depositional environment, provenance and tectonic setting as well as sorting and weathering regime of the sediments. The grain size analysis of the turbidite beds of the Middle Bengal Fan sediments (IODP Bengal Fan Expedition 354) from two sites (U1450 and U1451) were also carried out to understand variations in grain size distribution in the turbidite beds.

2.1 Field study

Detailed description of lithology was carried out during the field study. At first, detailed stratigraphic work was carried out by measuring thickness of the individual beds and their characteristics. A geological map was prepared by using 1:25,000 scales topographical map. Detailed description of outcrop features such as bed geometry, texture, sedimentary structures, erosional surfaces, and color of the sandstone and mudstone were carefully observed to interpret the depositional environments.

Representative columnar sections of the individual facies were measured at good exposures. Topographical maps of the Chaumala (Sheet no. 288003D) and Sayal (Sheet No. 288003B) areas at 1:25,000 scale published by the Survey Department, Government of Nepal were used for this study. Field descriptions were aided with the use of grain size chart to standardize grain size descriptions, and Munsell soil color charts (2000) to standardize color description. Samples from measured sections were collected for whole rock geochemical analysis and petrographical analysis.

Similarly, sand and mud samples of selective turbidite beds were collected onboard from sites U1450 and U1451 for the pilot grain size analysis during IODP Bengal Fan Expedition 354 (France-Lanord et al., 2016). Later, more samples from different horizons of well-preserved turbidite beds were taken during post-cruise sampling party in Kochi Core Centre, Kochi, Japan. The samples were mainly taken from base, middle and top (sandy part) and upper muddy part of thicker and coarser turbidite beds.

2.2 Laboratory method

Whole rock geochemical analysis by X-ray Florescence (XRF) method was performed in laboratory to examine the influence of provenance, sorting and weathering

regime on the basis of major elements and 14 trace elements compositions. For this study, total 122 samples were collected from the Jagati and Kala Formations (formations, mentioned in chapter 4).

Petrography of 67 Siwalik Group sandstone samples from the Khutia Khola section were studied using standard thin-section petrographic analysis and framework modal analysis was quantified using the Gazzi-Dickinson method (Dickinson 1970; Ingersoll et al. 1984; Dickinson 1985). A total of 500 grains were counted per thin section by using a Swift point counter with horizontal grid spacing 0.3 mm to avoid individual grains being counted more than once.

Grain size analyses of 311 samples were performed from different horizons of 66 thicker and coarser turbidite beds from two sites (U1450 and U1451) (IODP Bengal Fan Expedition 354).

All samples were prepared for analysis using the standard methods applied in the Department of Geoscience, Shimane University, Japan.

CHAPTER THREE

GEOLOGY OF NEPAL HIMALAYA

3.1. Introduction

Nepal occupies the north-central position in south Asia, and is geographically sandwiched between Tibet (China) in the north and India in the south. The Nepal Himalaya is located in the central part of about 2400 km long Himalayan arc and covers about one-third of its length (Fig. 3.1). The Mechi and Mahakali rivers mark the eastern and western political boundaries of the country.

The Himalaya is the youngest and the highest mountain range which was formed by collision of the northward moving Indian continent with Asian landmass, started at about 60 Ma (Patriat and Achache, 1984; Jackson and Bilham, 1994; Rowley, 1996) and continue at present day at the rate of 5 cm per year (Seeber and Armbruster, 1981; DeMets et al., 1990; Pandey et al., 1995). This northward movement is accommodated within the Himalayas by the movement of various thrusts and folds, regional metamorphism and generation of leucogranite plutons (Le Fort, 1975, 1996; Yeats et al., 1992; Harrison et al., 1998; Powers et al., 1998). The entire Himalayan range is longitudinally controlled by three major thrusts; the Main Central Thrust

(MCT), the Main Boundary Thrust (MBT) and the Main Frontal Thrust (MFT). The MCT was the first intra-crustal thrust to break the Indian crust (Schelling, 1992). It separates the highly metamorphosed Higher Himalayan rock from the less metamorphosed Lesser Himalayan rocks. The MCT initiated around 22 Ma ago, was reactivated around 15 and 12 Ma, and again around 6.0 and 8.0 Ma (Harrison et al., 1998; Johnson et al., 2001). It is considered to be essentially inactive at present. The MBT is one of the major thrust systems which separates synorogenic sediments of the Siwalik Group from the Lesser Himalayan rocks. The MFT brought the Siwalik Group over the Gangetic Plain. The Himalaya sequences contain a long history of sedimentation, magmatism and tectonism related to the Himalayan orogeny (Valdiya, 1998).

3.2. Tectonic divisions of Nepal Himalaya

The Nepal Himalaya is divided into the five tectonic zones from north to south respectively (Gansser, 1964; Hagen, 1969) (Fig. 3.2) as following:

1. Tibetan-Tethys Zone
2. Higher Himalayan Zone

3. Lesser Himalayan Zone

4. Sub-Himalayan Zone (Siwalik / Churia Group)

5. Terai Zone

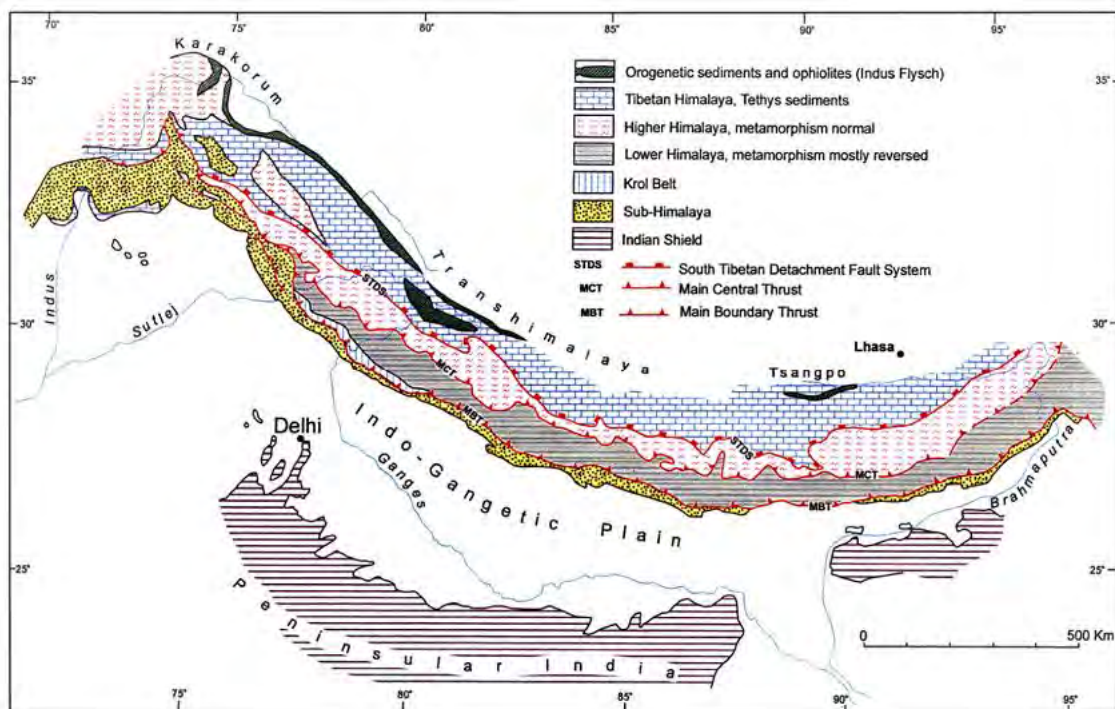


Fig. 3.1. Physiographic subdivisions of the Himalayan arc (after Gansser, 1964).

3.2.1. Tibetan-Tethys zone

Most of the great Himalayan peaks of the Nepal Himalayas including Mt. Everest, Mt. Manasalu, Mt. Annapurna and Mt. Dhaulagiri belong to the Tibetan-Tethys zone. The Tibetan-Tethys zone is the northernmost tectonic zone which is separated by

the Indus-Tangbo Suture Zone (ITS) in the north and the South Tibetan Detachment System (STDS) in the south. It consists of fossiliferous sedimentary rocks such as shales, sandstones and limestones ranging in age from Cambrian to Cretaceous (Colchen et al., 1986). The Tethyan sediments occur in several basins that cover almost the entire length of the northern margin of the Himalaya. This zone is well exposed around the Manang, Thakkhola and Dolpa areas of the western Nepal.

3.2.2. Higher Himalayan zone

The Higher Himalaya represents very steep topography and a snow-covered mountain chain. The Higher Himalayan zone is marked by the Main Central Thrust (MCT) in the south and the South Tibetan Detachment System (STDS) in the north. It is now generally accepted that the series of the north dipping STDS is a normal fault system (Burchfiel et al., 1992). Heim and Gansser (1939) firstly identified and described the Central Himalaya Crystalline zone in Kumaon Himalaya and then, mapped it along the entire Himalayan region. The Higher Himalaya is composed of high grade metamorphic rocks and granitic gneiss with mostly kyanite and sillimanite-bearing gneiss, schists, and migmatites. The crystalline rocks has been divided into four main units, as kyanite-sillimanite gneiss, pyroxenic marble and gneiss,

banded gneiss, and augen gneiss in ascending order (Bordet et al., 1972). Similarly, Le Fort (1975) divided this zone into three formations as Formation I, Formation II, and Formation III, in ascending order. Metamorphism occurred due to the intrusion of leucogranites after the collision of the continents as a result of the formation of the MCT (Le Fort, 1975). The thickness of this zone is about 10 km.

3.2.3. Lesser Himalayan zone

The Lesser Himalayan zone is 60 to 80 km wide and contains more than 30 km thick meta-sedimentary and metamorphic rocks. Mature, steep and rugged topography with gentle slopes and deeply dissected valleys of the Lesser Himalaya is still actively undercut by rivers. This zone consists of intermontane basins like the Kathmandu, Banepa and Pokhara basins. The Lesser Himalaya is tectonically situated between the Sub-Himalaya and the Higher Himalaya, and is separated by the Main Boundary Thrust (MBT) in the south and the Main Central Thrust (MCT) in the north. The Lesser Himalayan zone is folded and faulted, and is composed of unfossiliferous sedimentary and meta-sedimentary rocks like slate, phyllite, schist, quartzite, limestone, dolomite, with overriding crystalline nappes and klippen of the Higher Himalaya rock (Upreti, 1999). The age of this zone ranges from Precambrian to Eocene. Physiographically, the

Lesser Himalaya is divided into two zones i.e the Mahabharat Range and the Midland zone.

3.2.4. Sub-Himalayan zone (Siwalik or Churia Group)

The Sub-Himalayan zone is bounded between the Main Frontal Thrust (MFT) in the south and the Main Boundary Thrust (MBT) in the north. This zone runs from east to west and consists of Neogene fluvial sediments. The Sub-Himalayan zone is also known as the Siwalik Group (Churia Group). This zone is made up of fluvial deposits which were accumulated within the previous foreland basin in association with Himalayan uplift during the Middle Miocene to the Early Pleistocene (Gansser, 1964). The Lesser Himalaya metasedimentary rocks have been thrust southward over the Siwalik rocks along the MBT, and a large part of the Siwalik Group rocks were buried beneath the cover of the overthrust Lesser Himalaya rocks (Upreti, 1999). The thickness of the Siwalik Group varies from place to place, ranging from 4 to 6 km.

3.2.5. Terai zone

The Terai zone is the southernmost tectonic zone of Nepal Himalaya. It is a foreland basin originated due to the rise of the Himalaya, and also known as the

Indo-Gangetic Plain. This zone is separated from the Siwalik Group to the north by the Main Frontal Thrust (MFT). The Terai zone consists of the Pleistocene-Recent alluvium. The altitude of the Terai plain gradually increases from 100 m in the south to 200 m in the north (Upreti, 1999). The average thickness of alluvial is 1500 m (Valdiya 1998). The recent sediments represent the latest foreland basin, which is mainly derived from the Churia hills (Siwaliks) and also from the Lesser Himalaya by the river systems.

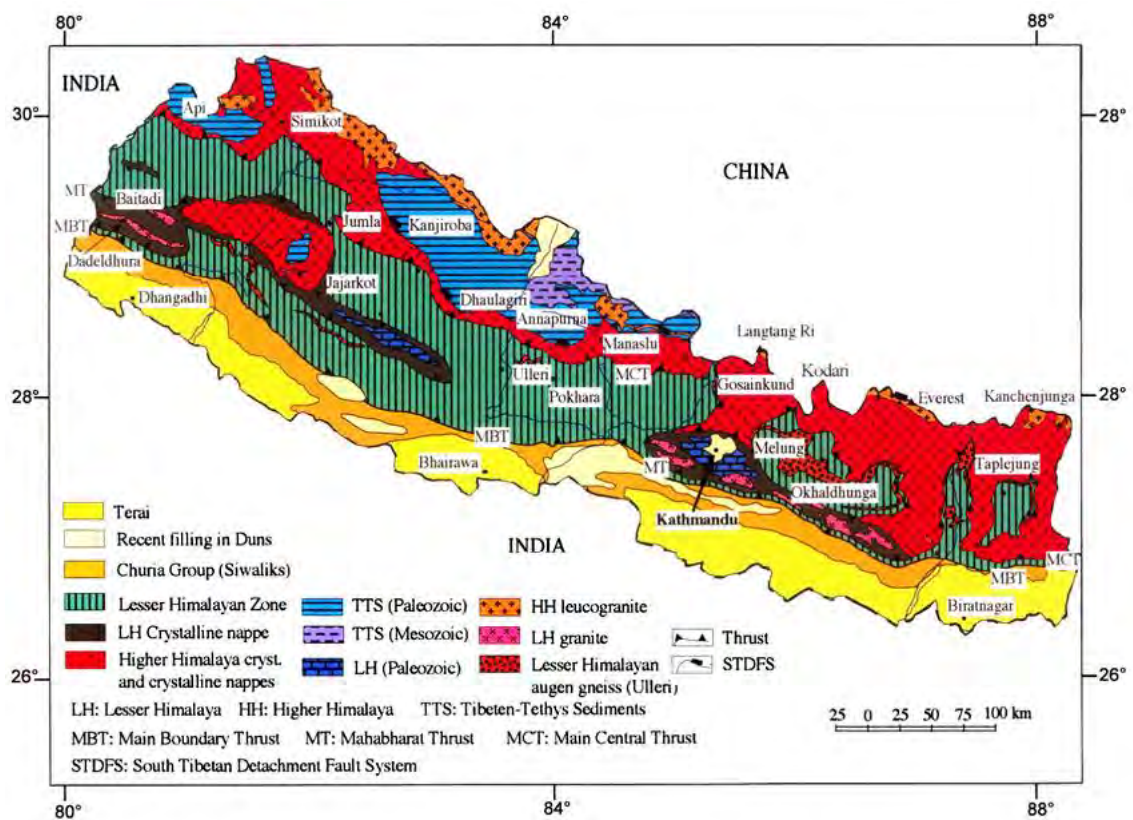


Fig. 3.2. Generalized geological map of the Nepal Himalaya (after Upreti and Le Fort, 1999).

3.3. Stratigraphy of the Siwalik Group, Nepal Himalaya

The Siwalik Group consists of 4 to 6 km thick fluvial sediments which extend more than 2000 km along the foothill regions of the whole Himalayan range. The sediments were supplied from the north, as a result of uplift as well as erosion of the Himalaya. The Siwalik Group is represented by coarsening upward succession.

A systematic study of the Siwalik Group began by the end of the nineteenth century. The Siwalik Group was initially studied lithologically in India and Pakistan and made tripartite subdivisions; the Lower, Middle and Upper Siwaliks, in ascending order (Medlicott, 1875; Pilgrim, 1913; Wadia, 1975 and others). The classification of the Siwalik Group of Nepal Himalaya is listed in Table 3.1.

Auden (1935) studied the Siwalik Group of central Nepal around Hetauda and Udaipur, and divided it into three units the Lower, Middle and Upper Siwaliks which was classified based on the lithology and increasing grain size. According to him, the Lower Siwalik consists of alternation of brown weathered sandstone and chocolate colored clays. The Middle Siwalik is composed of thick beds of sandstone with feldspar and mica, and the Upper Siwalik is comprised of conglomerates.

Glennie and Ziegler (1964) studied the Siwalik Group in Kali Ganga, Sarda River, Taptakunda, Koilabas, Butwal, Kaligandaki, Amlekhganj, Hetauda and

Saptakoshi areas. They divided the Siwalik Group into two units; the lower sandstone facies and the upper conglomerate facies. Sandstone facies corresponds to the Lower and Middle Siwaliks, and is composed of fine-grained sandstone, conglomerate and pebble bearing sandstone. The upper conglomerate facies composed of very coarse and massive conglomerate with few sandstones.

Hagen (1969) studied the Siwalik Group in various areas in the Nepal Himalaya. He followed the three-fold subdivision of the Siwalik Group. According to him, the Lower Siwalik is composed of siltstone, red shale facies with minor sandstones and pseudo-conglomerates. The Middle Siwalik comprised of sandstone and siltstone facies with minor conglomerates and red shale, and the Upper Siwalik consists of conglomerate facies.

Tokuoka et al. (1986, 1988, 1990) divided the Siwalik Group in the Arung Khola area into four formations; the Arung Khola, Binai Khola, Chitwan and Dcorali Formations in ascending order. They also recognized the Central Churia Thrust (CCT) which separates the Siwalik Group into southern and northern belts. The Arung Khola Formation is correlated with the Lower Siwalik and consists of moderately indurated fine-grained sandstone and variegated mudstone. The Binai Khola Formation consists of thick bedded, less indurated 'salt and pepper' sandstone and subordinate mudstone.

The 'salt and pepper' sandstone is characterized by significant amounts of a black mineral (biotite) scattered with white minerals such as quartz and feldspar. The Chitwan Formation comprised of conglomerate interbedded with sandstone and mudstone. The Deorali Formation is composed of boulder conglomerate.

Corvinus and Nanda (1994), and Dhital et al. (1995) studied the Siwalik Group in the Surai Khola area and divided it into the Bankas, Chor Khola, Surai Khola, Dobata and Dhan Khola Formations in ascending order. The Bankas Formation consists of bioturbated, variegated mudstone interbedded with fine-grained sandstone. The Chor Khola Formation is further divided into the Jungli Khola Member and Shivgarhi Member. The Jungli Khola Member consists of alternating beds of fine- to medium-grained, greenish-grey sandstone and variegated mudstone, whereas the Shivgarhi Member consists of medium- to coarse-grained grey sandstone interbedded with dark-grey, bioturbated mudstone. The Surai Khola Formation is composed of thick-bedded, coarse- to very coarse-grained 'salt and pepper' sandstones alternating with dark grey mudstone. The Dobata Formation is predominately mudstone with a minor amount of pebbly sandstone and conglomerate. Molluscan fossils are well preserved in the dark grey mudstones. The Dhan Khola Formation is composed of thick-bedded, cobble to pebble conglomerate interbedded with yellow mudstone in the

lower part, and boulder conglomerate interbedded with yellow-brown mudstone in the upper part.

Sah et al. (1994), and Ulak and Nakayama (1998) investigated the Siwalik Group of the Hetauda-Bakiya Khola area and divided it into the Rapti, Amlekhganj, Churia Khola and Churia Mai Formations, in ascending order. The Rapti Formation is further subdivided into lower, middle and upper members, and consists of fine- to medium-grained, grey sandstone interbedded with variegated, bioturbated mudstone and siltstone. Similarly, the Amlekhganj Formation is also subdivided into lower, middle and upper members. This formation is composed of thick-bedded, medium- to coarse-grained, 'salt and pepper' sandstone interbedded with dark grey mudstone. The Churia Khola Formation is characterized by unconsolidated, pebble- to cobble-sized, well-sorted, clast-supported conglomerate beds with reddish-brown sandstone and dark-grey mudstone. The Churia Mai Formation comprised of loose, poorly-sorted, boulder size conglomerate with subordinate pebble-cobble size, well-sorted gravel and grey sandstone and mudstone.

A petroleum exploration promotion project by the Department of Mine and Geology (DMG) (1994-2007) made a geological map of the Siwalik Group of Nepal Himalaya (Fig. 3.3) (Sharma et al., 2007). They also followed the tripartite subdivisions

of the Siwalik Group, but the Middle Siwalik was further divided into the Lower Middle Siwalik (MS1) and the Upper Middle Siwalik (MS2). The Lower Siwalik (LS) consists of the fine-grained sandstone interbedded with purple-red to greenish-grey mudstone, shale and siltstone. The Lower Middle Siwalik (MS1) consists of fine- to medium grained sandstone interbedded with siltstone and mudstone. The Upper Middle Siwalik (MS2) is composed of medium- to coarse-grained sandstone and pebbly sandstone interbedded with siltstone and mudstone. The Upper Siwalik (US) comprises of boulder cobble conglomerate with minor yellow, gery mudstone and siltstone.

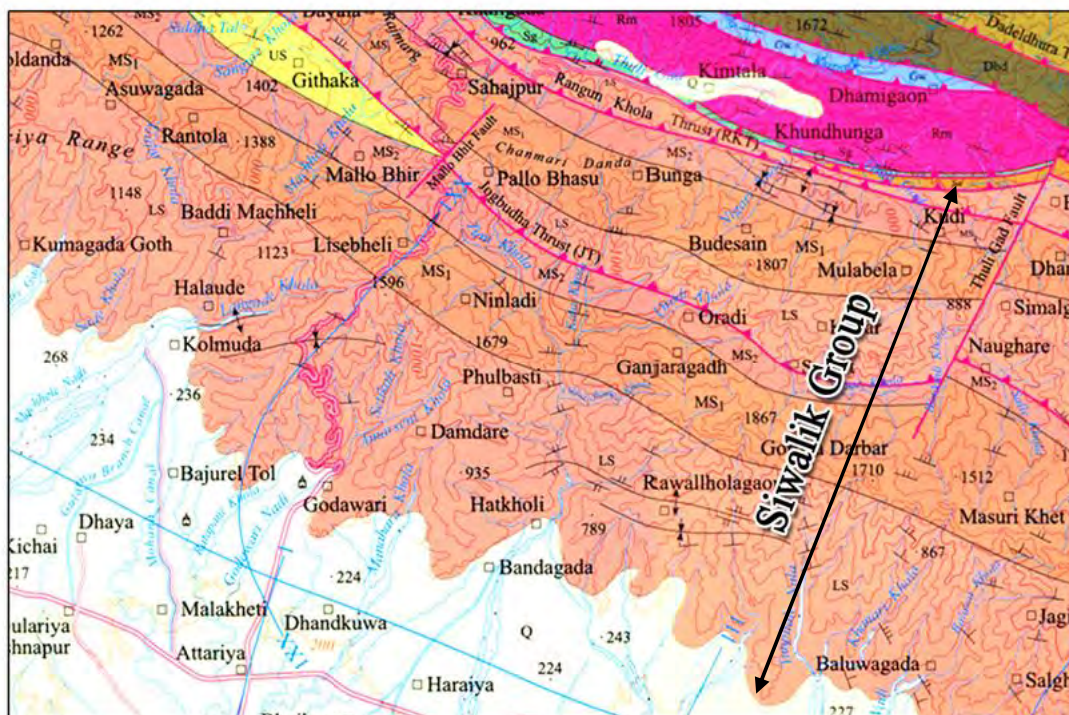


Fig. 3.3. Regional geological map of the far western Nepal (Sharma et al., 2007).

Auden (1935)	Glennie and Ziegler (1964)	Hagen (1969)	Sharma (1973)	Yoshida and Arita (1982), Tokuoka and Yoshida (1984)	Tokuoka et al. (1986, 1988)	Sah et al. (1994), Ulak and Nakayama (1998)	Corvinus and Nanda (1994), Dhital et al. (1995)	DMG (1987, 2003), Ojha et al. (2000), Robinson et al. (2006)	Sigdel et al. (2011)	Present Study
1	2	3	4	5	6	7	8	9	10	11
Upper Siwalik	Conglomerate Facies	Upper Siwalik	Upper Churia Group	Upper Siwalik	Deorali Formation	Churia Mai Formation	Dhan Khola Formation	Upper Siwalik	Panikhola Gaun Fm.	
Middle Siwalik		Middle Siwalik		Middle Siwalik	Chitwan Formation	Churia Khola Fm.	Dobata Formation			
Lower Siwalik	Sandstone Facies	Lower Siwalik	Lower Churia Group	Lower Siwalik	Binai Khola Formation	Amlekhganj Formation	Surai Khola Formation	Lower Siwalik	Chisapani Formation	Jagati Formation
		Lower Siwalik		Lower Siwalik	Lower Siwalik	Arung Khola Formation	Rapti Formation			
							Bankas Formation			

Table 3.1. Classification of the Siwalik Groups of the Nepal Himalaya. The colors denote the correlative successions and the numbers denote the study areas. 1) Udaipur Garhi-Anraha and Amlekhganj-Sanotar areas; 2) Kali Ganga, Sarda River, Taptakunda, Koilabas, Butwal, Kaligandaki, Amlekhganj, Hettauda and Saptakoshi areas. 3) Various areas in the Nepal Himalaya; 4) Dang, Koilabas, Butwal, Amlekhganj, Trijuga and Kankai River areas; 5) Surai Khola, Patharkot, Banganga, Butwal, Narayani River and Hettauda areas; 6) Arung Khola, Tinau Khola, Binai Khola areas; 7) Amlekhganj, Hettauda, Bakiya Khola areas; 8) Surai Khola area; 9) Far western Nepal around the Khutia Khola and other river sections; 10) Karnali River section; 11) Khutia Khola section.

Sigdel et al. (2011) studied the Siwalik Group in the Karnali River section, far western Nepal, and divided it into four formations; the Chisapani, Baka, Kuine and Panikhola Gaun Formations. The Chisapani Formation is equivalent to the Lower

Siwalik, and consists of greenish-grey, reddish-brown or variegated mudstone interbedded with fine- to medium-grained, grey sandstone. The Baka Formation is equivalent to the Middle Siwalik, and is composed of medium- to coarse-grained grey to light grey 'salt and pepper' sandstone and pebbly sandstone interbedded with greenish-grey mudstone. The Kuine Formation comprises of clast-supported and imbricated pebble to cobble conglomerates, whereas the Panikhola Gaun Formation consists of thick bedded, matrix-supported pebble, cobble and boulder conglomerates. The Kuine and Panikhola Gaun Formations are equivalent to the Upper Siwalik.

3.4. Regional geology of the far western Nepal Himalaya

The geology of the far western Nepal is mainly controlled by the major thrust systems (DeCelles et al., 2001; Robinson et al., 2006). These include the Main Frontal Thrust (MFT), Main Dun Thrust (MDT), Main Boundary Thrust (MBT), Dadeldhura Thrust (DT), Ramgarh Thrust (RT), Main Central Thrust (MCT) and South Tibetan Detachment System (STD) which separate the far western Nepal Himalaya in several tectonic units (Robinson et al., 2006).

The Siwalik Group of the far western Nepal is divided into the Lower, Middle and Upper Siwaliks (Quade et al., 1995; Mugnier et al, 1998; Ojha et al., 2000). The

Lower Siwalik consists of thick-bedded, variegated mudstone and siltstones and thin-bedded, fine-grained sandstones. The Middle Siwalik consists of thick-bedded, medium-grained 'salt and pepper' sandstone with mudstone, and the Upper Siwalik consists of conglomerate with intercalations of coarse-grained to pebbly sandstone and mudstone. The Main Dun Thrust (MDT) separates the Siwalik Group into southern and northern belts (DeCelles et al., 2001; Robinson et al., 2006). The age of the Siwalik Group in western Nepal ranges from 15.8 to 1 Ma, based on vertebrate fossils (West et al., 1975, 1991; Cornivus and Nanda, 1994) and paleomagnetic studies (Appel and Rossler, 1994; Gautam and Fujiwara, 2000; Ojha et al., 2000).

The northernmost boundary of the MFT is truncated by MBT overlying the Lesser Himalaya rocks. This zone consists of the Sangram, Galyang and Syangia Formations, the Lakharpata Group, and the Amile, Bhainskati and Dumri Formations. The northern boundary is marked by the Ranimata Formation, phyllite of the Galyang Formation, or dolomite of the Lakharpata Formation. The Ramgarh Thrust sheet is a synformal nappe of muscovite biotite garnet bearing schist, mylonite augen gneiss and Dadeldhura granite. The Dadeldhura synform is a remnant of an extensive thrust sheet which covered the entire Lesser Himalaya zone north of the nappe. The northern boundary of the Dadeldhura Thrust (DT) is marked by Lesser Himalayan rocks

consisting of steeply southward dipping asymmetric and imbricated folds of the Lower and Upper Nawakot units, overlain by Gondwana and tertiary units. The Main Central Thrust (MCT) marks the northern boundary of the Lesser Himalayan duplex, which lies in the medium to high grade schists and gneiss on top of the Lesser Himalayan schists and phyllite (DeCelles et al., 2001; Robinson et al., 2006).

CHAPTER FOUR

LITHOSTRATIGRAPHY

4.1. Introduction

The Siwalik Group has been traditionally classified as three units (Lower, Middle and Upper Siwaliks) (Auden, 1935; Hagen, 1969; Yoshida and Arita, 1982; Quade et al., 1995; DeCelles et al., 1998; Gautam and Fujiwara, 2000; Ojha et al., 2000; Robinson et al., 2006; Sharma et al., 2007) and with locally two-, four- or five- fold units is acceptable (Glennie and Ziegler, 1964; Sharma, 1973; Tokuoka et al., 1986, 1988; Sah et al., 1994; Corvinus and Nanda, 1994; Dhital et al., 1995; Ulak and Nakayama, 1998; Sigdel et al., 2011). The common three-fold classification starts in general with the mudstone-dominated Lower Siwalik, grading upward into the sandstone-dominated Middle Siwalik and the Upper Siwalik of the conglomerate-dominated sediments (Medlicott, 1875; Pilgrim, 1913; Wadia, 1975; Auden, 1935; Hagen, 1969; Yoshida and Arita, 1982; Quade et al., 1995; DeCelles et al., 1998; Upreti, 1999; Gautam and Fujiwara, 2000; Ojha et al., 2000; Robinson et al., 2006). The age of the Siwalik Group in the Nepal Himalaya ranges from 16 to 1 Ma, based on palcomagnetic studies (Tokuoka et al., 1986; Harrison et al., 1993; Appel and

Rosler, 1994; Gautam and Appel, 1994; Rosler et al., 1997; Gautam and Fujiwara, 2000; Ojha et al., 2000).

This chapter focuses on the lithostratigraphy of the Siwalik Group exposed along the Khutia Khola, far western Nepal. The Siwalik Group along the Khutia Khola was also classified based on the classical tripartite classification (Lower, Middle and Upper Siwaliks) (Ojha et al., 2000; Sharma et al., 2007). Ojha et al. (2000) made broad-scale description of lithology as well as the paleomagnetic polarity of the Siwalik Group sediments. Previous studies dealt stratigraphy of the Khutia Khola section (Quade et al., 1995; DeCelles et al., 1998; Ojha et al., 2000; Sharma et al., 2007), however their lithological information is limited. The present study proposes the lithostratigraphic classification based on the results of the high-resolution description of the Siwalik sediments along the Khutia Khola and its tributaries.

The distribution of the Siwalik Group of the Khutia Khola area is marked by the Main Frontal Thrust (MFT) to the south and the Main Boundary Thrust (MBT) to the north. In general the Main Dun Thrust (MDT) or Central Churia Thrust (CCT; Tokuoka et al., 1986) separates the Siwalik Group into the southern and northern belts (DeCelles et al., 1998; Robinson et al., 2006). In the study area, the Jogbudha Thrust (JT) equivalent to MDT/CCT and Rangun Khola Thrust (RKT) separate the Siwalik

Group into the southern, central and northern belts (Sharma et al., 2007). This study focuses on the rocks cropped out in the southern belt. The strata of the southern belt near the MFT are folded and show complicated geological structures (Fig. 4.1). The previous stratigraphic studies identified the Lower and Middle Siwaliks (Ojha et al., 2000; Sharma et al., 2007) and time interval ranges from 13.30 to 7.65 Ma according to magnetostratigraphy (Ojha et al., 2000). Around the Khutia Khola area, the Upper Siwalik may be masked by the JT, thrusting the central block onto the southern belt rock from the north.

4.2. Method

This study is based on geological traverses carried out along the Khutia Khola section on the southern belt of the Siwalik Group. The survey of rock units near the MFT were difficult due to thick cover of alluvial fan consisting of a series of terraces. Moreover, the area is covered by dense vegetation. Detailed lithological description has been given in this chapter based on the result of bed-by-bed data acquisition of the whole rock exposures along the river section producing a series of columnar sections. Description of lithological characteristics has also been followed by using the Munsell Color Chart (2000).

4.3. Lithostratigraphy

Two lithostratigraphic units, the Jagati and Kala Formations in ascending order has been proposed, which are equivalent to the Lower and Middle Siwaliks, respectively. The Upper Siwalik is not exposed in the study area. Each formation is subdivided into the lower, middle and upper members (Fig. 4.1).

4.3.1. Jagati Formation

4.3.1.1. Type Locality

The type locality of this formation is around Jagati Village.

4.3.1.2. Lithology

This unit is named after Jagati Village, one of the main villages located on the left bank of the Khutia Khola and is well exposed from Hatkholi Village in the south to the Gajari Khola in the north. The Jagati Formation is represented by bioturbated, variegated, reddish-brown, yellowish-brown, brown, yellow, yellowish-grey, grey to greenish-grey mudstones and very fine- to coarse-grained, brown, reddish-grey, light-grey, and grey to greenish-grey sandstones (Fig. 4.2 & 4.4). Thickness of the Jagati Formation is about 2110 m. In general, a sandstone unit grades upward into

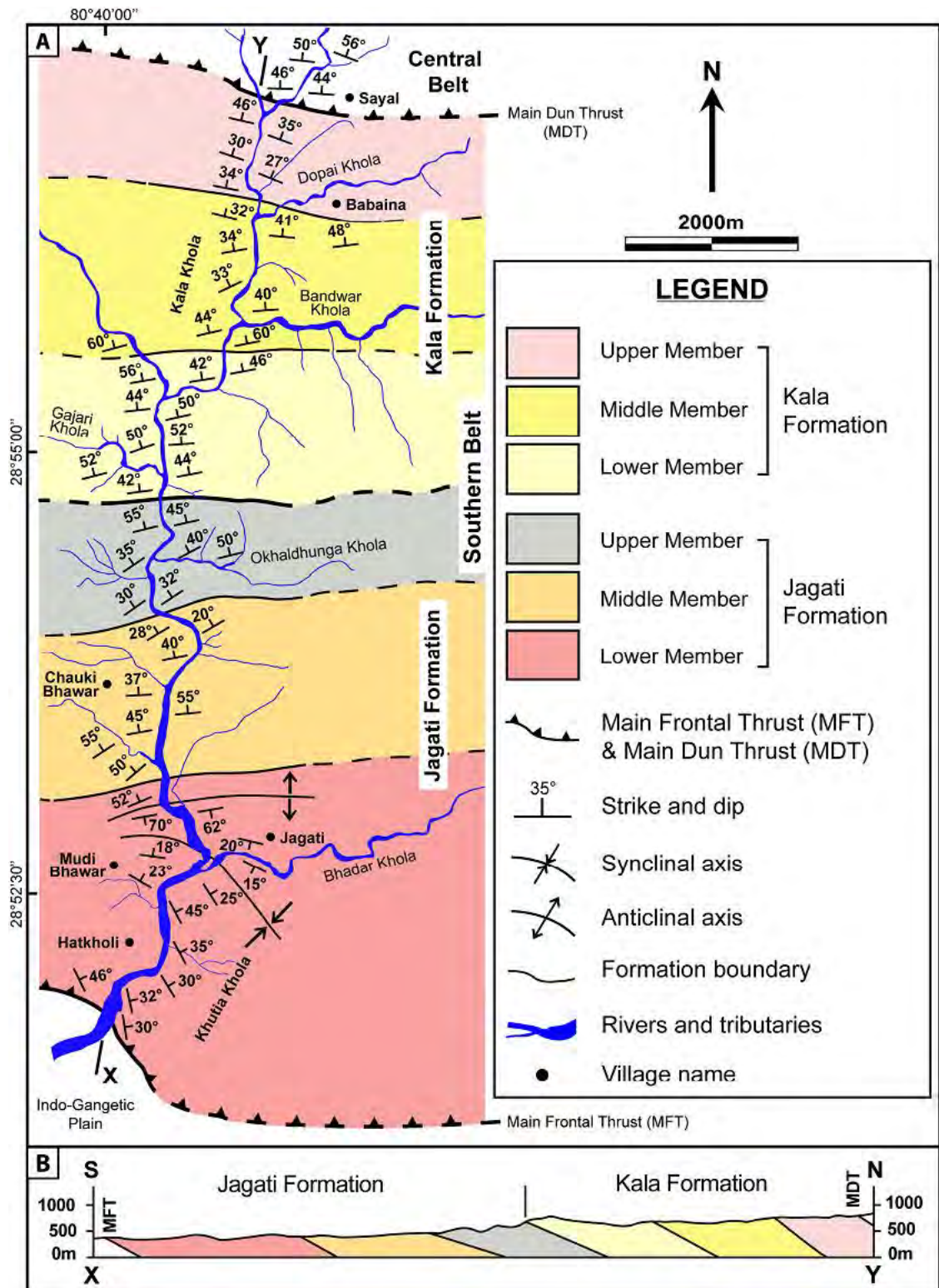


Fig. 4.1. (A) Geological map of the Siwalik Group along the Khutia Khola section. (B) Cross-section along X-Y (Adhikari and Sakai, 2015).

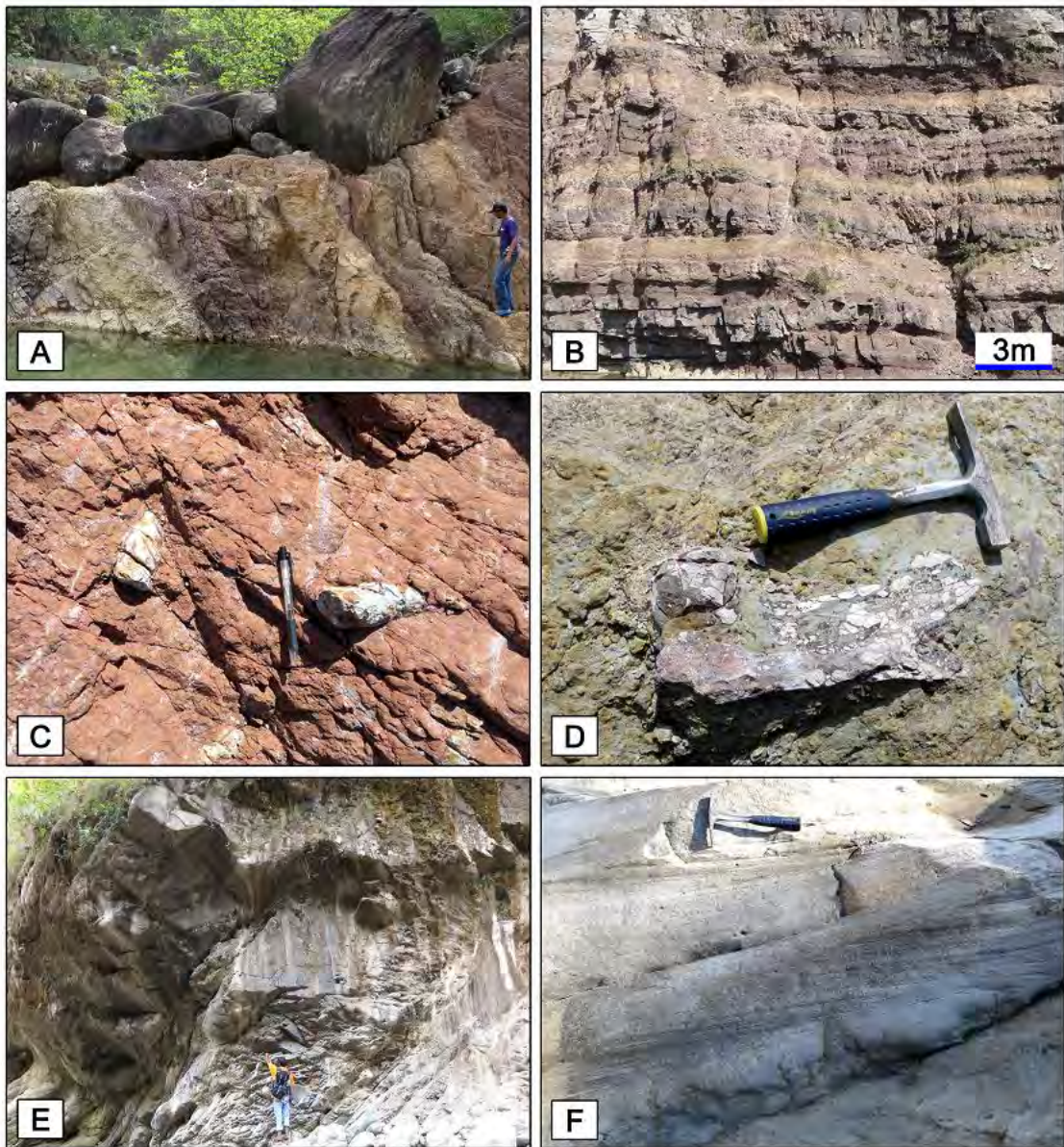


Fig. 4.2. Outcrop photographs of the Jagati Formation. A) Variegated mudstone alternating with fine-grained sandstone. B) Alternating sandstone and mudstone beds. C) Brown mudstone with bioturbation, rootlets and nodules. D) A vertebrate fossil found in mudstone. E) Very thick bedded sandstone near the boundary of the Jagati and Kala Formations. F) Cross-lamination in sandstone bed. (A in the lower member. B, C, D in the middle member. E, F in the upper member).

a mudstone unit to form an upward-fining succession. The Jagati Formation is further divided into the lower, middle and upper members based on dominant unit and, color and grain size. The boundary between the lower and middle members is marked by the appearance of interval exhibiting equal proportion of fine- to medium grained, greenish-grey to grey sandstones and variegated to reddish-brown paleosols. The first appearance of greenish-grey to grey mudstone is marked as the boundary between the middle and upper members.

4.3.1.2.1. Lower member

The lower member is well exposed around Hatkholi and Mudi Bhawar Village. The total thickness of this member is about 860 m. This member is represented by variegated, yellow (10YR 7/6), yellowish-brown (10YR 6/4), brown (7.5YR 5/4) to reddish-brown (2.5YR 3/4, 5RY 4/3) mudstones which are interbedded with very fine- to medium-grained, reddish-grey (2.5YR 6/1), light-grey (GLEY1 7/N, GLEY1 7/10GY, 2.5Y 7/1) to grey (GLEY1 6/N, 10YR 5/1, 5Y 6/1) sandstones (Fig. 4.2 A). In this member the proportion of mudstones is higher than sandstones (Fig. 4.4). Thickness of mudstone unit range from 0.2 to 10 m, whereas sandstone units range from 0.3 to 6 m. Some mudstones are thinly laminated containing plant fossils, whereas most of

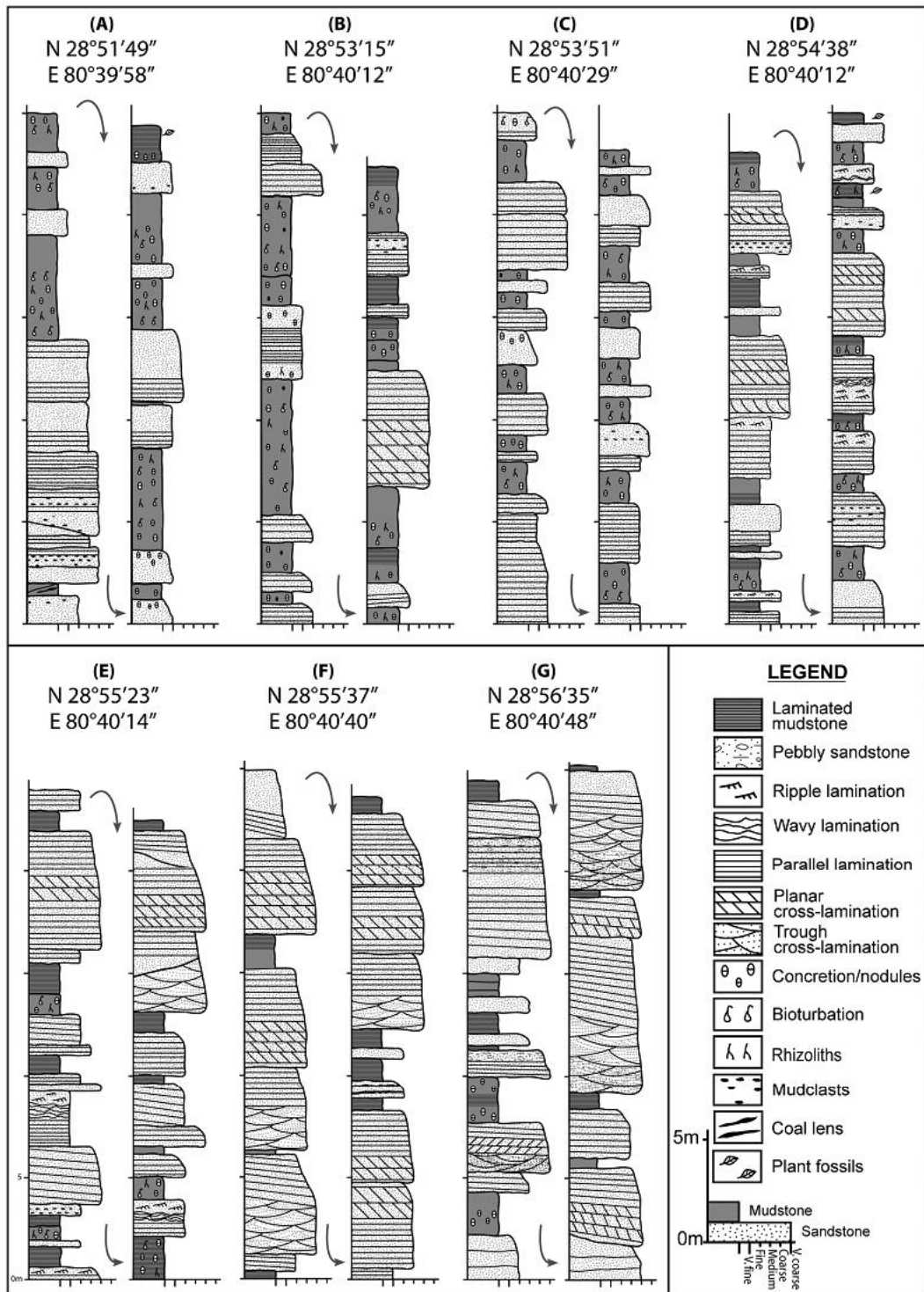


Fig. 4.3. Typical columnar sections. Jagati Formation (A and B, lower member; C, middle member; and, D upper member). Kala Formation (E, lower member; F, middle member; and, G, upper member).

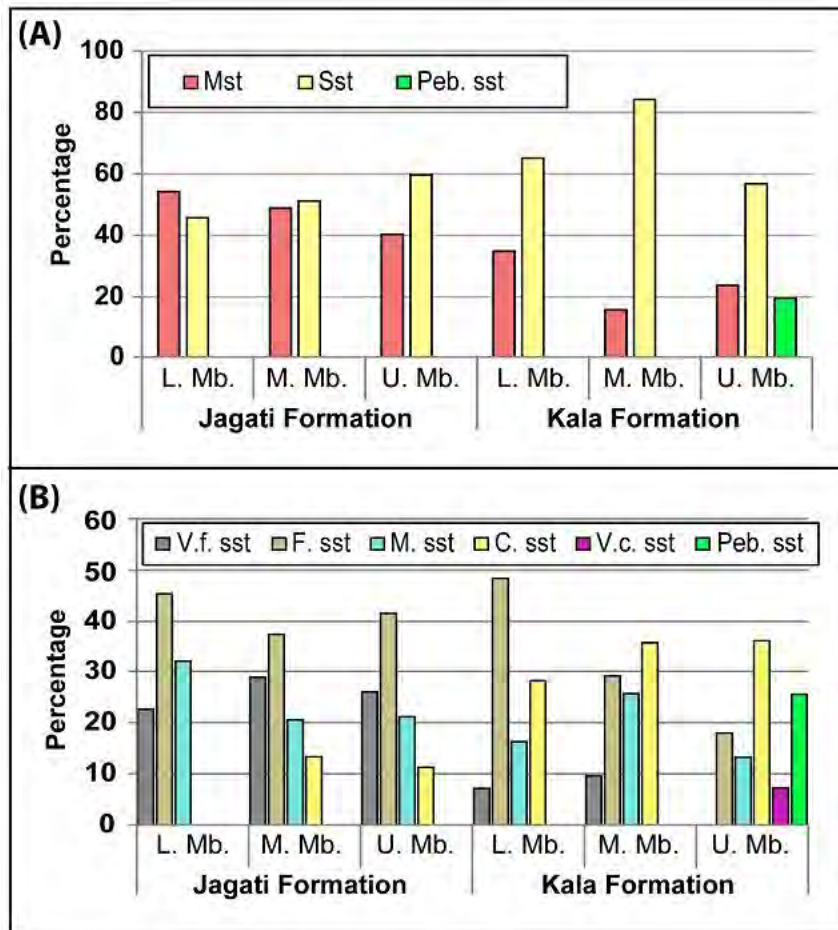


Fig. 4.4. The distribution of various rocks in the Khutia Khola area. A) Distribution of sandstones, mudstones and pebbly sandstones. B) Distribution of various sandstones. Abbreviation: Mst – mudstone, Sst – sandstone, Peb. sst – pebbly sandstone, V.f. sst – very fine grained sandstone, F. sst – fine grained sandstone, M. sst – medium grained sandstone, C. sst – coarse grained sandstone, V.c. sst – very coarse grained sandstone, L. Mb. – lower member, M. Mb. – middle member, U. Mb. – upper member.

the primary structures in mudstones are disturbed by burrows, rhizoliths, desiccation cracks, concretions and nodules, which are typical characteristics of paleosols (Fig. 4.3 A & B). The basal part of the sandstone beds contains parallel or planar

cross-laminations and some contain calcareous nodules, and are bioturbated in the upper part. The maximum thickness of fining upward succession is about 15 m.

4.3.1.2.2. Middle member

The middle member is well exposed around Jagati Village and has a total thickness of about 760 m. Fine- to coarse-grained, brown (7.5YR 4/4), light-grey (GLEY1 7/N, GLEY1 7/10GY) to grey (GLEY1 6/N, 10YR 5/1) sandstones and variegated, brown (7.5YR 5/4) to reddish-brown (2.5YR 3/4, 5RY 4/3) mudstones characterize this member (Fig. 4.2 B and 4.3 C). The proportion of the mudstones and sandstones is almost equal in this member (Fig. 4.4). Thickness of mudstone units range from 0.2 to 9 m, whereas sandstone units range from 0.2 to 7 m. Each sandstone tends to be thicker upward in this member. Parallel or planar cross-laminations are preserved in the basal part of the sandstone beds and in some cases mud and sand clasts are scattered in this part. The ripple laminations are also present in some of the upper part of the sandstone beds. The upper part of the sandstone beds is generally bioturbated and some contain calcareous nodules. In the lower part of this member, most of the mudstones show characteristics of palcosols (Fig. 4.2 C) as seen in the lower member and in the upper part thinly laminated mudstones are also present. Vertebrate and plant

fossils are preserved in mudstone beds (Fig. 4.2 D). The maximum thickness of fining-upward succession is about 16 m.

4.3.1.2.3. Upper member

The upper member is well exposed around Chauki Bhawar Village and along the Okhaldhunga Khola. Thickness of this member is about 490 m. The very fine- to coarse-grained, light-grey (GLEY1 7/N, GLEY1 7/10GY), grey (GLEY1 6/N, 5Y 6/1, 10YR 5/1) to greenish-grey (GLEY1 6/10GY) sandstones and variegated, reddish-brown (5YR 4/3), brown (7.5YR 5/4), yellowish-grey (5Y 6/2) to greenish-grey (GLEY2 6/5BG) mudstones represent this member (Fig. 4.3 D). The ratio of sandstones is greater than mudstones in this member (Fig. 4.4). Thickness of sandstone units range from 0.2 to 11 m (Fig. 4.2 E) and mudstone units range from 0.2 to 6 m. Trough and planar cross-lamination, parallel and ripple laminations are frequently observed in sandstone beds (Fig. 4.2 F). The finely laminated, greenish-grey mudstone are frequently occurred, whereas reddish-brown paleosols are less frequent than in the lower and middle members. Some reddish-brown mudstone beds containing bioturbations, rhizoliths, concretion and nodules grade upward into finely laminated

greenish-grey mudstone. Molluscan fossils are also found in some finely laminated mudstones. The maximum thickness of fining-upward sequences is about 14 m.

4.3.2. Kala Formation

4.3.2.1. *Type Locality*

Along Kala Khola, in exposures north of Gajari Khola up to the Sayal Village.

4.3.2.2. Lithology

This formation is well exposed from Gajari Khola in the south to Sayal Village in the north. Thickness of the Kala Formation is about 2050 m. This formation is represented by thin- to very thick-bedded, very fine- to very coarse-grained, light-grey, grey to greenish-grey sandstones and pebbly sandstones interbedded with reddish-brown, brown, grey, greenish-grey to dark-grey mudstones (Fig. 4.4 & 4.5). Biotite, quartz and feldspar are abundantly present in sandstones showing "salt and pepper" characteristic (c.g. Tokuoka et al., 1988; Dhital et al., 1995). The rock succession of this formation also exhibits fining-upward successions as in the Jagati Formation. This formation is further divided into the lower, middle and upper members. The first appearance of very thick-bedded (~15 m), medium-to coarse-grained "salt and

pepper" sandstones marks the base of the Kala Formation. The first appearance of thick- to very thick-bedded, medium- to very coarse-grained, light-grey to grey sandstones interbedded with grey, greenish-grey massive or finely laminated mudstones marks the boundary between the lower and middle members. The first pebbly sandstone demarks the boundary between the middle and upper member of this formation.

4.3.2.2.1. Lower member

The lower member is well exposed around Gajari Kholā and Amthala Village. The total thickness of this member is about 800 m. This member is characterized by presence of medium- to very thick-bedded, very fine- to coarse-grained, light-grey (GLE Y1 7/N, 2.5Y 7/1), grey (GLE Y1 6/N, 10YR 5/1, 5Y 6/1) to greenish-grey (GLE Y2 6/5BG) "salt and pepper" sandstones interbedded with finely laminated greenish-grey (GLE Y1 6/10GY, GLE Y2 6/5BG) mudstones or bioturbated, variegated, brown (7.5YR 5/4) to reddish-brown (5YR 4/3) mudstones (Fig. 4.3 E). In this member, the proportion of sandstones is higher than mudstones (Fig. 4.4). Thickness of sandstone units range from 0.3 to 15 m, whereas the thicknesses of mudstone units range from 0.2 to 5 m. The sandstone beds are characterized by trough and planar cross-lamination, parallel and ripple laminations (Fig. 4.5 A). The basal parts of some



Fig. 4.5. Outcrop photographs of the Kala Formation. A) Ripple lamination in sandstone. B) Coal lens. C) Thick sandstone beds. D) Finely laminated greenish-grey mudstone. E) Quartzite pebble-cobble in sandstone. F) Fractured zone around the MDT (between the southern and central belt of the Siwalik Group). (A, B in the lower member. C, D in the middle member. E, in the upper member).

sandstone beds are erosional and, mud and sand clasts are also scattered at the base. Bioturbations as well as concretions and nodules are less frequent in paleosols than those in the Jagati Formation. Some coal lenses (2 to 10 cm thick) (Fig. 4.5 B) and leaf impressions are also observed in this member. Fining upward succession is clearly seen in thick sandstone beds and the maximum thickness of fining-upward succession is about 17 m.

4.3.2.2. Middle member

The middle member is well exposed between the Bandwar Khola and Dopai Khola, and has a thickness of about 850 m. This member is composed of thick- to very thick-bedded, very fine- to coarse-grained, greenish-grey (GLEY1 6/10GY) to grey (GLEY1 6/N, 5Y 6/1, 10YR 5/1) "salt and pepper" sandstones interbedded with thin- to medium-bedded, reddish-brown (5YR 4/3), brown (7.5YR 5/4), yellowish-brown (10YR 7/6) to greenish-grey (GLEY2 6/5BG, GLEY1 6/10GY, GLEY1 4/N) mudstones (Fig. 4.3 F and 4.5 C). Black-colored mudstones (GLEY1 2.5/N), rich in organic matter, are also interbedded in this member. The proportion of sandstones is higher than mudstones (Fig. 4.4). Thickness of sandstone units range from 0.5 to 20 m, whereas mudstone units range from 0.2 to 3 m. The sandstone beds are thicker than the lower

member and the most part of this member is occupied by the sandstone-dominated units. Trough and planar cross-laminations and parallel lamination are commonly observed in thick sandstone beds, representing the lower part of the sandstone units. Mud and sand clasts are scattered within the lower part of some sandstone beds. The greenish-grey mudstones are finely laminated (Fig. 4.5 D), and brown mudstones are massive and contain calcareous concretions and nodules. Some mudstone units are characterized by the lower massive brown mudstone, the overlying finely laminated greenish-grey mudstone and the upper black mudstone. The maximum thickness of fining-upward sequences is about 25 m.

4.3.2.2.3. Upper member

The upper member is well exposed around Sayal Village and the total thickness is about 400 m. This member is characterized by thick- to very thick-bedded, fine- to very coarse-grained, greenish-grey (GLEY1 6/10GY) to grey (GLEY1 6/N, 5Y 6/1) "salt and pepper" sandstones and pebbly sandstones interbedded with reddish-brown (5YR 4/3), greenish-grey (GLEY2 6/5BG) to black (GLEY1 2.5/N) mudstones (Fig. 4.3 G). In this member the proportion of sandstones is higher than mudstones (Fig. 4.4). Thickness of sandstone units ranges from 0.4 to 21 m, whereas a

mudstone units range from 0.1 to 3 m. Fining upward succession is frequently observed in sandstone units. The lower part of the fining-upward succession consists of trough and planar cross-laminated sandstones with scattered pebbles which are followed by parallel laminated sandstones in the upper part. Gravel size tends to be larger and some cobble sized gravels also appear in the upper portion of this member (Fig. 4.5 E). Pebbles and cobbles are mainly composed of quartzite and sub-rounded to rounded in shape. In the upper most portion of this member few bands of conglomerates are sandwiched between the sandstone beds. Thinly laminated mudstones are frequently observed than palcosols. In some mudstone units the lower part is massive and the upper part is finely laminated. The upper horizon of some mudstone units is composed of black (GLEY1 2.5/N) organic rich materials. Bioturbations, rhizoliths as well as concretion and nodules are less frequent in palcosols than those in other members. The maximum thickness of fining-upward succession is about 21 m. The distribution of the upper member is punctuated by E-W extended Main Dun Thrust (MDT) (Fig. 4.5 F).

4.4. Correlation with magnetostratigraphic data

Ojha et al. (2000) analyzed the magnetostratigraphy from upper part of the Lower Siwalik to middle part of the Middle Siwalik in the area. They have shown two

possible correlations with Cande and Kent (1995)'s general magnetostratigraphy (Figures 6 and 7 in Ojha et al. (2000)). The age at the boundary between the Lower and Middle Siwaliks is 11.05 Ma in both cases (i.e. near the base of the C5n). They state that the correlation in Figure 6 in Ojha et al. (2000) is the more convincing correlation: the Figure 6 of Ojha et al. (2000)'s correlation is also used in the present study. Following their correlation, the rock units were dated from 13.30 to 7.65 Ma (Fig. 4.6).

Referring the base point (28°54'N; 80°40'E) of their study, the interval is equivalent to the portion from upper part of the middle member of the Jagati Formation up to the upper part of the middle member of the Kala Formation. Due to lack of detailed descriptions and lithological data of their study, tentative ages for boundaries of the middle and upper members of the Jagati Formation, and that of the lower and middle members of the Kala Formation are estimated on the basis of the thickness data. The measured thickness of the analyzed interval in Ojha et al. (2000) is slightly different with the thickness of the present study. The members' thickness were recalculated by taking the aspect ratio between the members' thickness and total thickness of this study with measurements of Ojha et al. (2000) for the estimation of the age between the member boundaries. As the result, the boundary age of the middle and upper members of the Jagati Formation is estimated to be around 12.7 Ma and the lower

4.5. Lithostratigraphy and comparison

This lithostratigraphic study corresponds with the previous studies of the Siwalik Group across the Nepal Himalaya. Our newly established lithostratigraphic units, the Jagati and Kala Formations permit regional correlation with other Siwalik successions in the Nepal Himalaya (Table 4.1). Lithologically, the Jagati and Kala Formations are correlatable with the Rapti and Amlekhganj Formations, respectively along the Hetauda-Bakiya Khola section in Central Nepal (Harrison et al., 1993; Sah et al., 1994, Ulak and Nakayama, 1998), the Arung Khola and Binai Khola Formations, respectively along the Arung Khola-Tinau Khola section in western Nepal (Tokuoka et al., 1986, 1990; Gautam and Appel 1994), the Bankas Formation and the Jungli Khola member of the Chor Khola Formation, and the Shivgarhi member of the Chor Khola Formation and the Surai Khola Formation, respectively along the Surai Khola section in West Central Nepal (Corvinus and Nanda 1994; Appel and Rosler 1994; Dhital et al., 1995), the Chisapani and Baka Formations, respectively along the Karnali River section in far western Nepal (Sigdel et al., 2011).

Age	Bakiya Khola¹ <i>Central Nepal</i>	Tinau Khola² <i>Western Nepal</i>	Surai Khola³ <i>West Central Nepal</i>	Karnali River⁴ <i>Far Western Nepal</i>	Khutia Khola⁵ <i>Far Western Nepal</i>		
(Ma)	Churia Mai Fm	Deorali Fm		Pani Khola Gaun Fm			
1			Dhan Khola Fm				
2	Churia Khola Fm	Chitwan Fm		Kuine Fm			
3		Upper mbr	Dobata Fm				
4	Amlekhganj Fm Upper mbr	Binai Khola Fm Middle mbr	Surai Khola Fm Upper mbr Middle mbr Lower mbr	Baka Fm Upper mbr Middle mbr Lower mbr	Kala Fm Upper mbr Middle mbr Lower mbr		
5							
6							
7							
8	Middle mbr	Lower mbr	Shivgarhi mbr		7.65 Ma Middle mbr		
9	Lower mbr		Chor Khola Fm		9.0 Ma Lower mbr		
10	Rapti Fm Upper mbr	Arung Khola Fm Upper mbr	Jungli Khola mbr		11.05 Ma Upper mbr		
11	Middle mbr	Middle mbr					
12	Lower mbr	Lower mbr	Bankas Fm	Chisapani Fm Upper mbr			
13				Middle mbr	Jagati Fm Upper mbr		
14				Lower mbr	12.7 Ma Middle mbr		
15					13.3 Ma Lower mbr		

Table 4.1. Classification of the Siwalik Group of the Nepal Himalaya and its correlation. The corresponding grey shades indicate the Upper, Middle and Lower Siwaliks. Numbers denote; 1) Hetauda-Bakiya Khola section, central Nepal (Sah et al., 1994; Ulak and Nakayama, 1998). 2) Tinau Khola section, western Nepal (Tokuoka et al., 1986). 3) Surai Khola section, west central Nepal (Dhital et al., 1995). 4) Karnali River section, far western Nepal (Sigdel et al., 2011). 5) Khutia Khola section (present study), far western Nepal, dated boundaries are denoted in white box and tentative age is denoted comparing measured thickness of this study with age data (Ojha et al., 2000).

CHAPTER FIVE

DEPOSITIONAL FACIES ANALYSIS

5.1. Introduction

The fluvial depositional systems in the Siwalik Group have been studied by several researchers in different sections of the Himalaya (Willis, 1993a, 1993b; Khan et al., 1997; Zaleha, 1997; Kumar et al., 2003; Tokuoka et al. 1986, 1990, 1994; Hisatomi and Tanaka, 1994; Nakayama and Ulak, 1999; Ulak and Nakayama, 2001). In Nepal Himalaya, the fluvial depositional systems of the Siwalik Group have reconstructed meandering and braided river systems in the Chatara-Barahakshetra area, east Nepal; Kankai river section, east Nepal; Hetauda-Bakiya Khola area, central Nepal; Tinau Khola section, west central Nepal; Surai Khola section, west Nepal; Karnali River section, far western Nepal from east to west respectively (Tokuoka et al., 1986; Nakayama and Ulak, 1999; Ulak and Nakayama, 2001; Ulak, 2004, 2009; Huyghe et al., 2005; Sigdel and Sakai, 2016). These studies show that the river style changes from a fine-grained meandering river system to a flood-flow dominated meandering river system, which is then followed by braided river systems.

The change in fine-grained meandering river system to a flood-flow dominated

meandering river system is inferred as the indicator of climate change due to increase in precipitation (Nakayama and Ulak, 1999). The age of this change is different among the different Siwalik sections in the Nepal Himalaya. River catchment size may be one of the possible cause of the diachronous facies change (Huyghe et al., 2005). Rivers with large catchment size could suppress the local fluctuation of water supply to river channel and respond only to the regional precipitation. In contrast, rivers with small catchments size could be sensitive to changes in precipitation induced by local uplift, as small increases in precipitation can change the channel characteristics (Sigdel and Sakai, 2016).

This chapter focuses on detail study of the depositional environment of the Siwalik Group along the Khutia Khola section, far western Nepal. Previous studies show that the Siwalik succession along the Khutia Khola section was deposited by small river system (DeCelles et al., 1998; Ojha et al., 2000). And, several studies along the Karnali River section (about 50 Km east of the study area) show that the Siwalik sediments were supplied by large river system, probably the palco-Karnali River (DeCelles et al., 1998; Huyghe et al., 2005; Szule et al., 2006; Sigdel and Sakai, 2016). The comparison of the studies on fluvial depositional environment between these areas can reveal the effect of local as well as regional climate change on different river

catchment sizes. Although, there have been some studies along the Khutia Khola section, however, no detail depositional facies information was available.

The aim of this study is to describe the depositional facies in detail and reconstruct the fluvial systems in the Siwalik Group along the Khutia Khola section and to compare the reconstructed fluvial systems with the Karnali River system to decipher the differences between climatic changes due to local as well as regional precipitation on different catchment basin sizes.

5.2. Methodology

The facies were classified based on lithology, bounding surfaces, internal sedimentary structures and textures. The lithofacies codes of Miall (1985, 1996) are used in this study. Thirty-eight representative columnar sections of individual facies were measured and detailed descriptions were done at good exposures along the Khutia Khola section (Fig. 5.1).

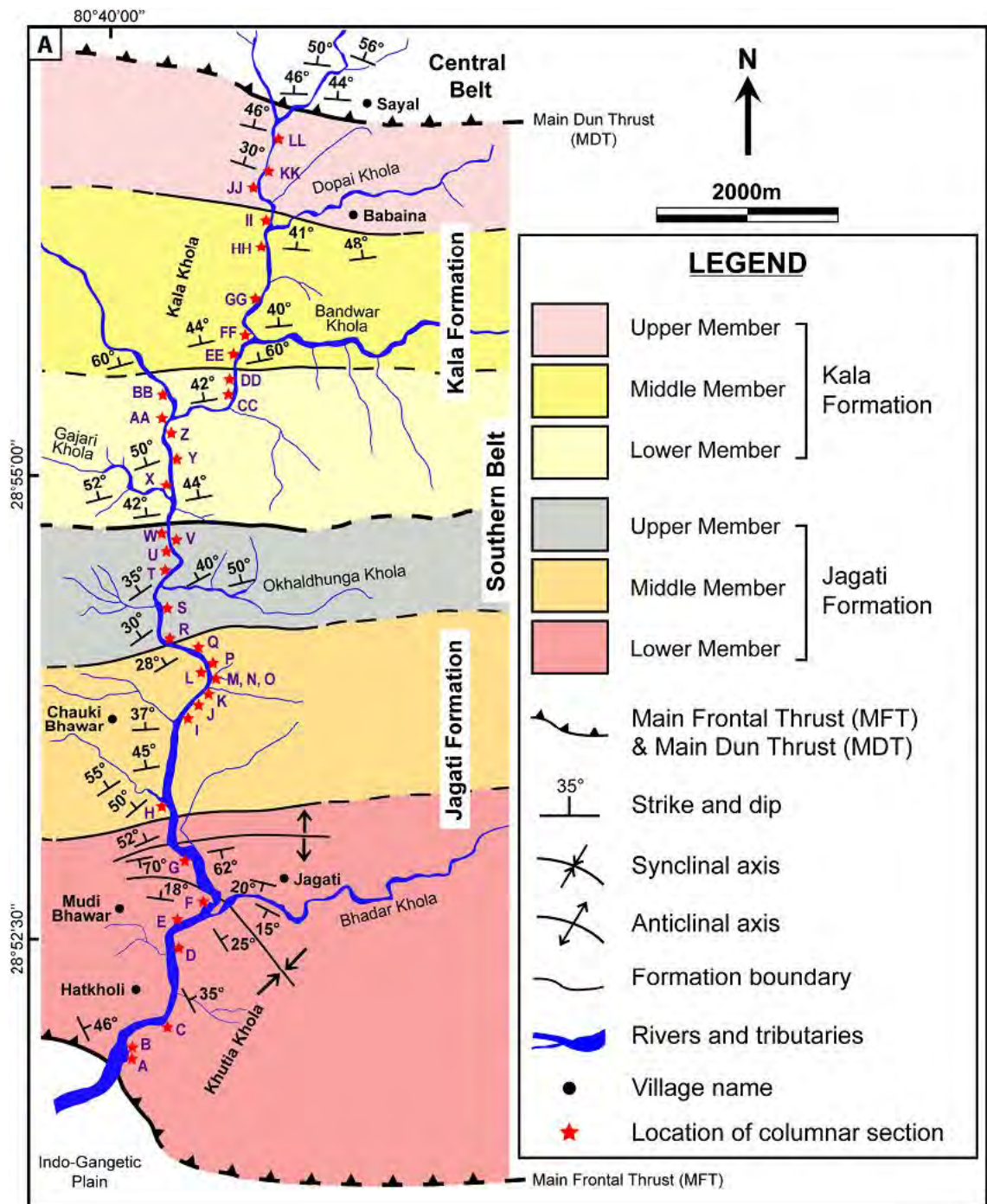


Fig. 5.1. A) Geological map of the Siwalik Group along the Khutia Khola section. Red stars with alphabet along the Khutia Khola section indicate the location of columnar sections.

5.3. Depositional facies

Eleven lithofacies were recognized from the Jagati and Kala Formations (Table 5.1, and Fig. 5.2 and 5.3). Three mudstone facies, F1, Fm and P were identified, occupying about 38% of the total succession. The thinly laminated mudstones (F1) are grey, greenish-grey to dark-grey and sometimes brown to reddish-brown in color (Fig. 5.2 A). The massive mudstones (Fm) are represented by grey to greenish-grey in color (Fig. 5.2 B). The palcosols (P) are variegated, yellow, yellowish-brown, brown to reddish-brown in color and contain burrows, rhizoliths, nodules and desiccation cracks (Fig. 5.2 C and D).

Sandstone facies occupy about 59% of the total successions and facies Sp, St, Sr, Sh, Sc and Sm were identified. These facies are brown, reddish-grey, light-grey, grey to greenish-grey in color. The Sp facies consists of fine- to very coarse-grained planar-cross-bedded sandstone (Fig. 5.2 E). The inclination of cross-beds ranges from 12 to 38°. The St facies consists of fine- to very coarse-grained trough-cross-bedded sandstone (Fig. 5.2 F). The Sr facies is characterized by very fine- to fine-grained, well-sorted sandstone with current or climbing ripples (Fig. 5.2 G). The facies Sh consists of very fine- to very coarse-grained horizontally laminated sandstones (Fig. 5.2 H). The Sc facies is characterized by very fine- to medium-grained, wavy or convolute


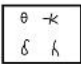

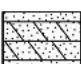


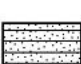

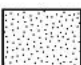

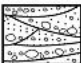
Facies	Symbol	Lithology & sedimentary structures	Interpretation
Fl <i>Laminated mudstone</i>		Thin, parallel or wavy laminated mudstone interbedded with very fine-grained sandstone; bed boundaries are planar or undulating; bioturbation and small rhizoliths are present in some beds; leaf impressions and plant fragments are observed in some beds; thickness: 0.2 to 3 m. 13% of total succession.	Deposited under low-energy conditions by suspension settling in overbank area during flood stage.
Fm <i>Massive mudstone</i>		Grey to greenish-grey massive mudstone; lower contact is gradual and upper contact is usually sharp; upper parts of some beds contain bioturbations, desiccation cracks, rhizoliths and nodules; thickness: 0.2 to 2.5 m. 7% of total succession.	Deposited by suspension in standing water or ponds in overbank areas.
P <i>Paleosol</i>		Variiegated, reddish-brown, red, brown to grey paleosols characterized with bioturbation, rhizoliths, desiccation cracks and nodules showing pedogenic features; lower and upper contacts are usually sharp; thickness: 0.2 to 6 m. 18 % of total succession.	Deposited originally as flood deposits; textures and structures indicate weathering under semi-arid or arid environment and chemical precipitation.
Sp <i>Planar-cross-bedded sandstone</i>		Fine- to very coarse-grained planar-cross-bedded sandstones; beds are lenticular or tabular; upper and lower contacts sharp and wavy, and upper contact sharp and flat; inclination of cross-beds ranges from 12 to 38°; thickness: 0.1 ~ 1.5 m. 10% of total succession.	Migration of straight crested dunes or bars deposited during periods of low water level or the waning stage of flood water towards the river banks.
St <i>Trough-cross-bedded sandstone</i>		Fine- to very coarse-grained sandstones; beds are lenticular or tabular and are stacked to form trough cross-bedded sets and cosets; lower contact is gradational, and the upper contact is sharp; granules are also present in some beds; thickness: 0.1 to 1.6 m. 6 % of total succession.	Migration of 3-D type dunes or megaripples under the low flow regime condition.
Sr <i>Ripple cross-laminated sandstone</i>		Very fine- to fine-grained ripple-cross-laminated sandstones interlaminated with thin mudstone layers; ripples are mainly current and climbing ripples; bioturbation and nodules are present near top of the beds which destroy boundary and internal structures; thickness: 0.5 to 3 m. 5% of total succession.	Deposited as ripples under lower flow regime condition by alternating traction and suspension processes.
Sh <i>Horizontally laminated sandstone</i>		Very fine- to coarse-grained, parallel laminated sandstones; lower contact is erosional and the upper contact is gradational with facies Sr or Fl; mud and sand clasts as well as bioturbation are also present in some beds; thickness: 0.2 to 4 m. 22% of total succession.	Deposited as plane bed with currents in the upper flow regime condition.
Sc <i>Convolute laminated sandstone</i>		Very fine- to medium-grained, convolute laminated sandstones; sometimes sand and mud clasts scattered on the surface; lower and upper contacts often sharp; thickness: 0.1 to 1.5 m. 7% of total succession.	Deformation structure developed by differential loading or dewatering process such as fluidization and liquefaction.
Sm <i>Massive sandstone</i>		Fine- to medium-grained massive sandstone; lower contact is gradational and the upper contact is sharp; mud and sand clasts are present in the lower part of some beds; bioturbation, rhizoliths, nodules and concretion are found near the top of some beds; thickness: 0.2 to 3.5 m. 9% of total succession.	Rapid deposition by heavy sediment load during floods or in sediment gravity flows from suspension; formed either as primary process or post depositional deformation.
Gh <i>Horizontally stratified gravel</i>		Medium- to very coarse-grained, gravely sandstone; extraformational clast mostly of quartzite; gravels are often distributed forming crude horizontal stratification; mostly clasts are normally graded; thickness: 0.2 to 2.0 m. 2% of total succession	Deposited as longitudinal bedforms under lower flow regime condition.
Gt <i>Trough-cross-bedded gravel</i>		Medium- to very coarse-grained, gravely sandstone; gravels are distributed forming trough- cross-bedding; thickness: 0.2 to 0.8 m. 1% of total succession	Deposited as transverse bedforms under lower flow regime condition.

Table 5.1. Description and interpretation of the depositional facies types found in the Khutia Khola section. For representative figures refer to Fig. 5.2. (lithofacies code after Miall, 1996 and interpretation (Allen, 1964; Turner 1980; Tucker, 1982; Miall, 1985, 1996; Collinson, 1996; Hjellbakk, 1997; Thomas et al., 2002; Capuzoo and Wetzcl, 2004; Bridge, 2006; Gahzi and Mountney 2009).

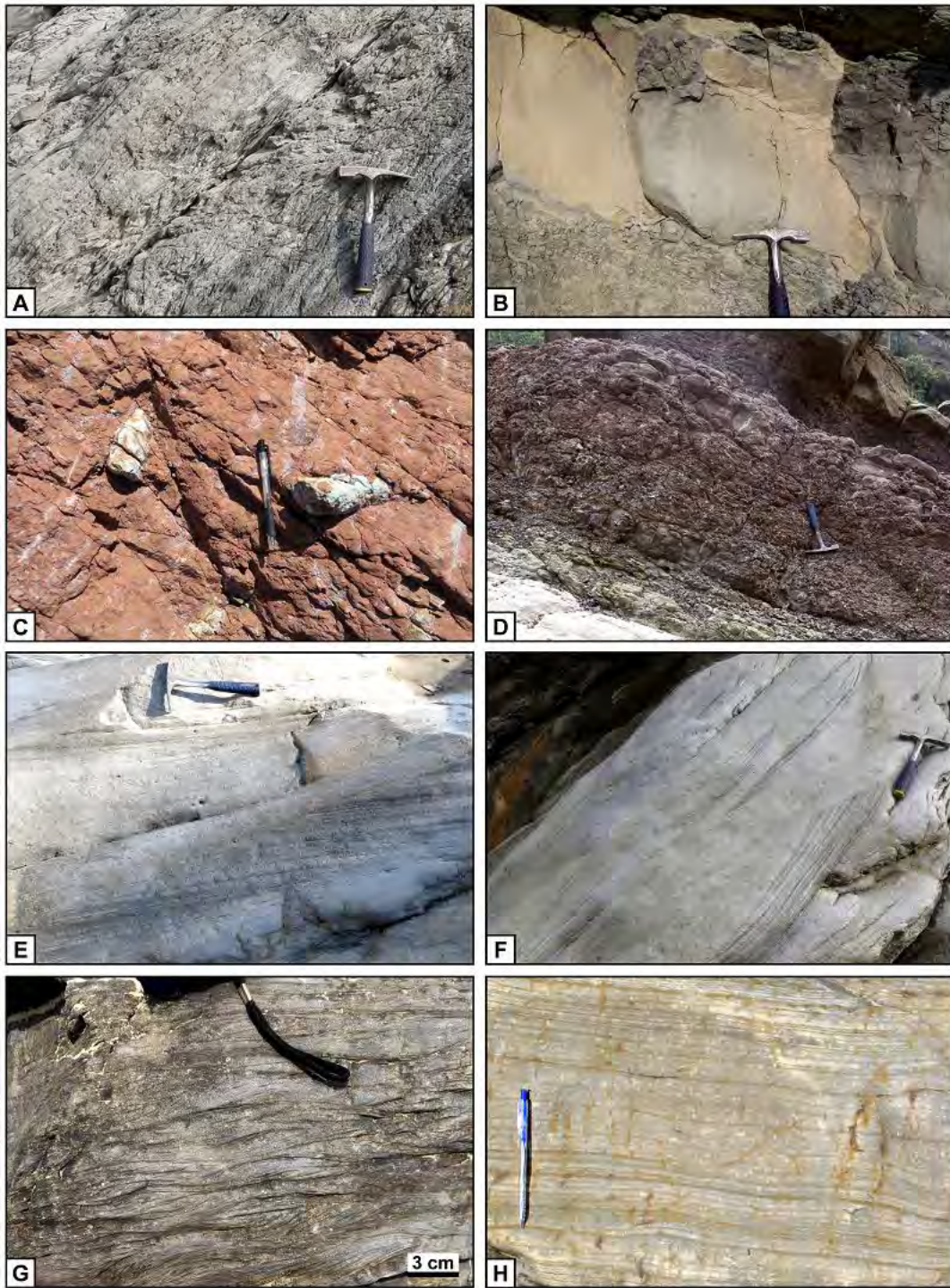


Fig. 5.2. Outcrop photographs of the lithofacies. A) Laminated mudstone (Fl). B) Massive mudstone (Fm). C and D) Palcosols with burrow and rhizoliths (P). E) Planar-cross-bedded sandstone (Sp). F) Trough-cross-bedded sandstone (St). G) Ripple cross-laminated sandstone (Sr). H) Horizontally laminated sandstone (Sh).

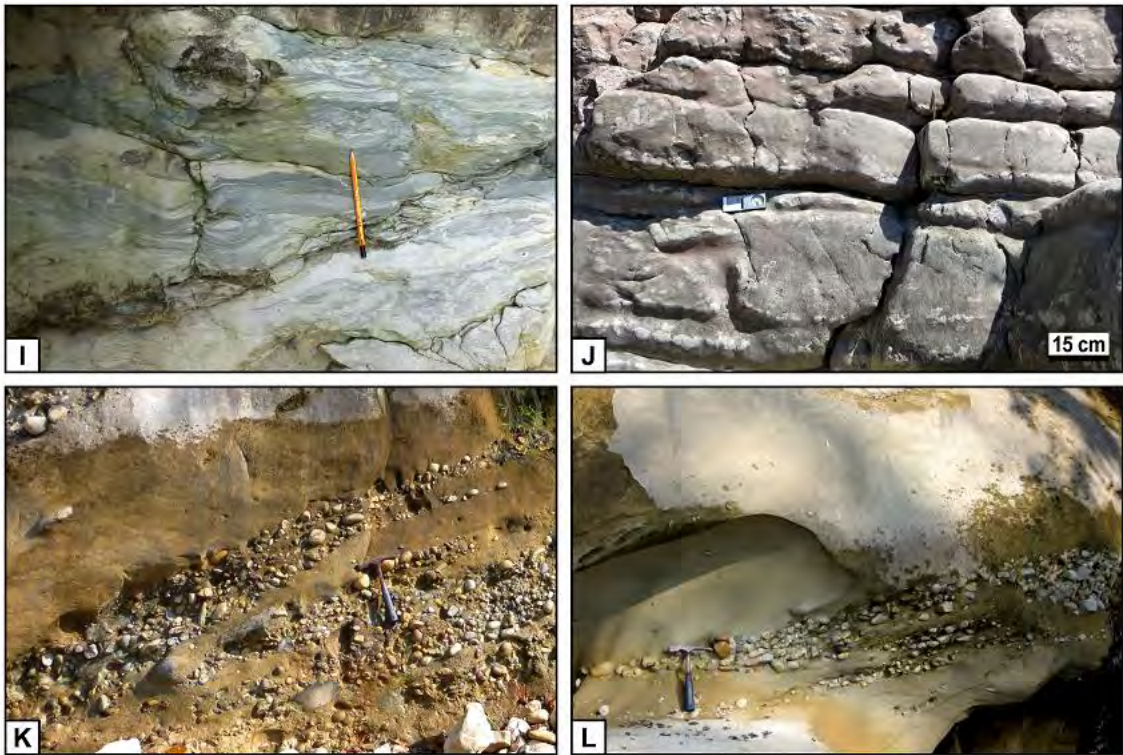


Fig. 5.2. cont. Outcrop photographs of the lithofacies. I) Convolute laminated sandstone (Sc). J) Massive sandstone (Sm). K) Horizontally stratified gravel (Gh). L) Trough-cross-bedded gravel (Gt).

laminated sandstones (Fig. 5.2 I). The Sm facies consists of fine- to medium-grained massive sandstones (Fig. 5.2 J). This sandstone facies contains burrows, rhizoliths and nodules are often present near the top of the bed.

Gravel facies consists of lithofacies Gh and Gt and represents about 3% of total succession. The Gh facies is characterized by medium- to very coarse-grained, gravely

sandstones in which gravels are horizontally-stratified (Fig. 5.2 K). In Gt facies gravels are distributed forming trough-cross-stratification and mostly show normal grading (Fig. 5.2 L). Most of the gravels are pebble sized (long axes, up to ~ 8 cm) and few are cobble sized (up to ~ 18 cm) too. The gravels are mainly composed of quartzite and sub-rounded to rounded in shape.

5.4. Architectural elements

Seven architectural elements were recognized from the Jagati and Kala Formations. The architectural elements codes of Miall (1985, 1996) are used in this study. Description and interpretation of individual architectural elements are provided in Table 5.2. perennial ephemeral

The channel (CH) elements are thin-to very thick-bedded sandstones with lenticular or tabular geometry. It consists of facies St and Sh, with subordinate sets of facies Sp and Sr in both formations, but in the upper member of the Kala Formation facies Gt and/or Gh are also present in the basal part of some beds (Fig. 5.3).

The lateral-accretion (LA) elements consist of thin-to medium-bedded, inclined (10 to 20°) sandstone units with lenticular geometry and show concave-up shape (Fig. 5.4 A). LA is characterized by facies Sp, St and Sr. This element is frequently observed

Element	Description	Facies Assoc.	Interpretation
CH <i>Channel</i>	Thin- to very thick-bedded sandstones with lenticular or tabular geometry; sometimes mud and sand clasts and/or gravels are distributed along the basal part of the thick sandstone beds; fining-upward trend is clearly observed; boundaries are sharp; bases are often irregular and truncate the underlying floodplain deposit; sometimes bioturbations are present near top of thin-to medium-bedded sandstones; thickness: 1 to 8 m.	Sr Sh St Sp Gh Gt	Vertically stacked thick- to very thick-bedded sandstones represent major (perennial) channel deposits and thin- to thick-bedded sandstones represent minor (ephemeral) channel deposits; presence of mud and sand clasts indicate the erosive flow of sediments, and gravels indicate the bedload migration during floods within the channel.
LA <i>Lateral-Accretion</i>	Fine- to very coarse-grained inclined sandstones with lenticular geometry and show concave-up shape; inclination ranges 10 to 20°; boundaries are sharp; sometimes mud and sand clasts or/and pebbles are present along the base; thickness: 1 to 4m.	Sr St Sp	Deposition in the point bars during the lateral migration of the meandering channel.
DA <i>Downstream-Accretion</i>	Medium- to very coarse-grained inclined sandstones with lenticular geometry and show convex-up shape; inclination <10°; boundaries are sharp; thickness: 0.5 to 2 m.	Sh St Sp	Deposition in the transverse bars during the downward migration of bars within the braided channel.
SB <i>Sandy Bedform</i>	Thin- to thick-bedded, fine-to very coarse-grained vertically stacked sandstones with wedge or sheet-like geometry; fining-upward trends are often observed; sometime mud drapes are preserved on the upper part; bed boundaries are almost sharp. thickness: 1 to 5 m.	Sr Sh St Sp	Sheet-like, thin-to medium-bedded sandstones with fining upward trend indicate the deposited in shallow channel-fill as crevasse splay channels, channel bars. or point bars.
CS <i>Crevasse Splay</i>	Thin- to medium-bedded, very fine- to medium-grained sandstones interbedded with very thin- to medium bedded finely laminated or massive mudstones with lenticular or sheet-like geometry; bed boundaries are flat or wavy; mostly beds are slightly inclined; bioturbation, rhizoliths and nodules are often present; coarsening-upward and fining-upward trends are observed; thickness: 0.5 to 4 m.	Fl Fm Sr Sc Sh	Alternation of slightly inclined thin-to medium bedded lenticular sandstones and mudstones represent the overbank sedimentation and accumulation in the proximal part of floodplain as crevasse splays deposits.
FF <i>Floodplain</i>	Thin- to very thick-bedded mudstones with sheet-like or tabular geometry; boundaries are mostly sharp and flat but some lower boundaries are wavy; variegated, reddish-brown to red paleosols (with bioturbation, rhizoliths, desiccation cracks and nodules) are major components; sometimes in a mudstone succession lower part consists of red paleosols, whereas the upper part consists of finely laminated greenish-grey mudstone; thickness: 0.2 to 10 m.	Fl Fm P	Thick mudstone beds and well-developed paleosols represent floodplain deposit; red paleosols indicate slow sedimentation rate, long-term exposure after deposition and frequent fluctuation in groundwater level; horizontally laminated greenish-grey Fl facies represent wetter climatic condition or deposition near the channel.
SL <i>Shallow Lake</i>	Thinly laminated or massive, reddish-brown, brown to drak-grey calcareous mudstones alternate with thinly bedded, very fine- to fine-grained sandstones with lenticular or sheet-like geometry; mudstones are 2 to 10 cm thick and sandstones are 2 to 6 cm thick; bioturbation, rhizoliths and nodules are occasionally present; sometimes load structures are present in finely laminated beds; thickness: 0.5 to 3 m.	Fl Fm Sh Sm Sc	Alternation of very thin- to thin-bedded, finely-laminated mudstones and very thin- to thin-bedded, very fine- to fine-grained sandstones represent deposition by suspension in standing water.

Table 5.2. Description and interpretation of the architectural elements found in the Khutia Khola section. Architectural element codes after Miall (1985, 1996) and interpretation after Allen (1964); Turner (1980); Tucker (1982); Miall (1985, 1996); Collinson (1996); Hjellbakk (1997); Thomas et al. (2002); Capuzoo and Wetzel (2004); Bridge (2006); Gahzi and Mountney (2009).

in the Jagati Formation than in the Kala Formation. The downstream-accretion (DA) elements consist of thin to thick-bedded, inclined ($< 10^\circ$) sandstone units with lenticular geometry and show concave-up shape (Fig. 5.4 B). DA is characterized by facies Sp, St and Sh. DA elements are commonly present in the Kala Formation. The lateral-accretion (LA) and downstream-accretion (DA) elements are present in comparatively thicker sandstone beds.

The sandy bedform (SB) elements consist of thin- to thick-bedded sandstone units with facies St, Sp, Sh and Sr and show wedge or sheet-like geometry (Fig. 5.4 C and D). SB elements are often present in both formations. The crevasse splay (CS) elements are characterized by thin-to medium-bedded, very fine- to medium-grained sandstones with facies Sh, Sc and Sr interbedded with very thin- to medium-bedded mudstones with facies Fl and Fm (Fig. 5.4 E). Beds are slightly inclined with lenticular or sheet-like geometry. CS elements are frequently observed in the Jagati Formation rather than in the Kala Formation.

The floodplain (FF) elements are characterized by thin- to very thick-bedded mudstone units with facies P, Fl and Fm (Fig. 5.4 E). The shallow lake (SL) elements are characterized by alternation of thinly-laminated calcareous mudstones with facies Fm or Fl and very thin- to thin-bedded, very fine-to fine-grained sandstones with facies

Sh, Sm or Sc (Fig. 5.4 F and G).

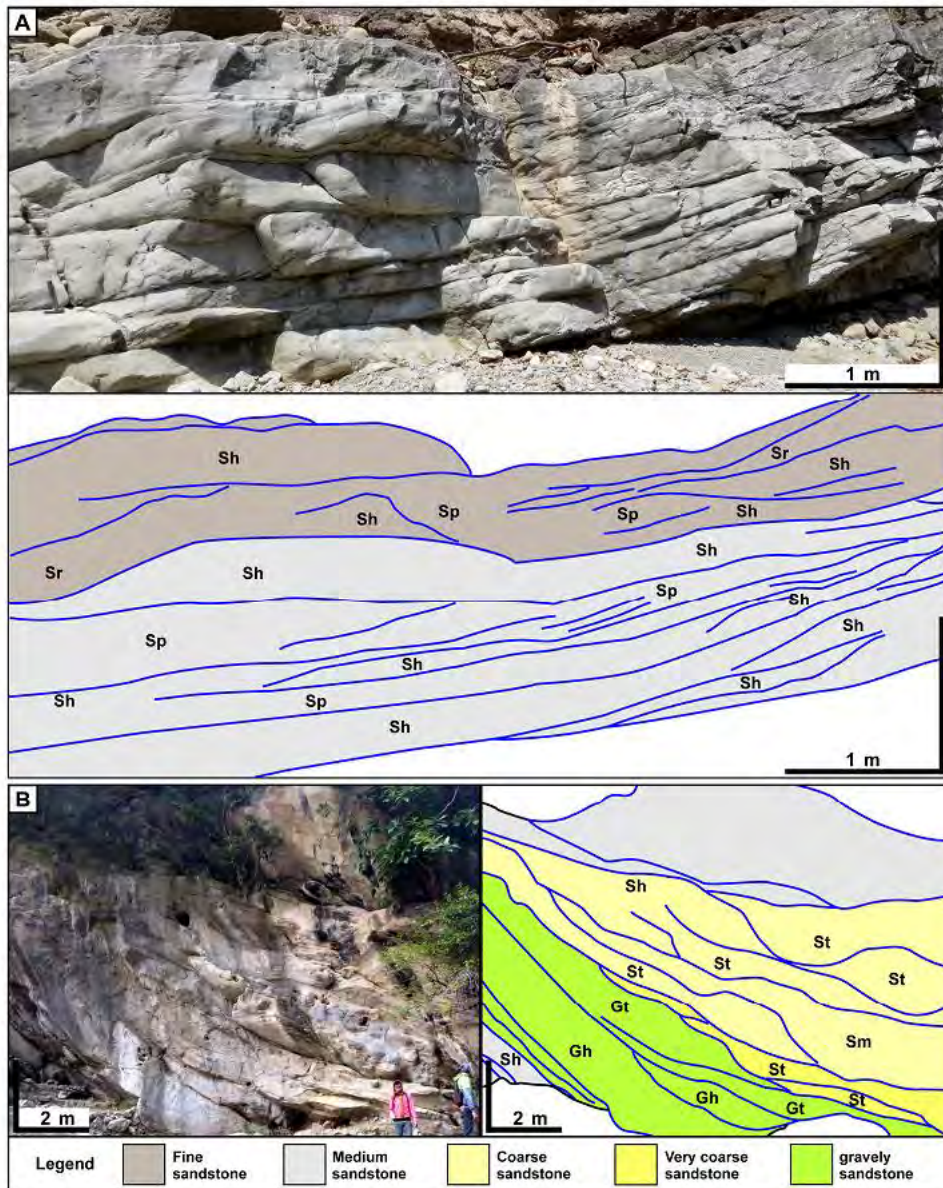


Fig. 5.3. Examples of channel deposit element, CH, (outcrops and sketches). A) Thin- to medium-bedded, fine- to medium-grained sandstone succession deposited as ephemeral (minor) channel deposit in middle member of the Jagati Formation. B) Medium- to very thick-bedded, medium- to very coarse-grained sandstones and gravelly sandstones deposited as perennial (major) channel deposit in upper member of the Kala Formation. In sketch blue lines indicate bed boundaries and abbreviations indicate facies (see Table 5.1).

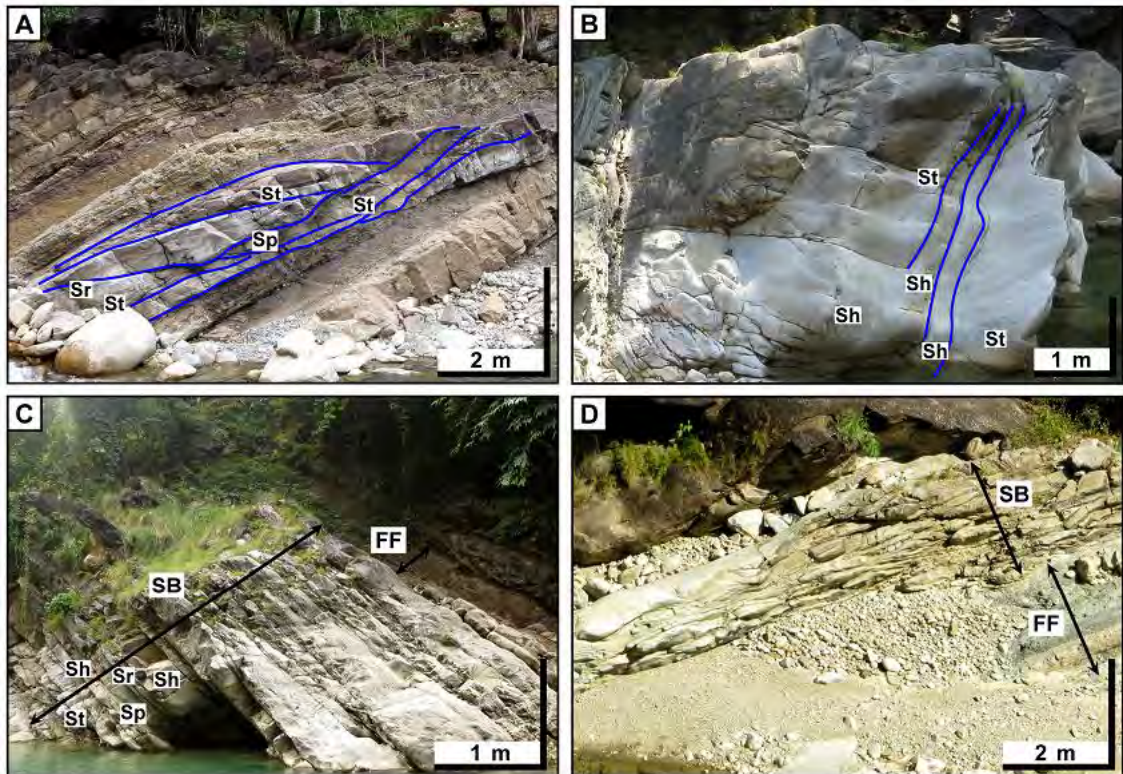


Fig. 5.4. Examples of different types of architectural elements. A) Lateral-accretion (LA) patterns in upper member of the Jagati Formation. B) Downstream-accretion (DA) pattern in lower member of the Kala Formation. C and D) Sandy bedform (SB) deposits in lower and middle members of the Kala Formation, respectively. E) Floodplain (FF) deposits and Crevasse splay (CS) deposits in middle member of the Jagati Formation. F and G) Shallow lake (SL) deposits in middle and upper members of the Jagati Formation, respectively. For facies abbreviations see Table 5.1.

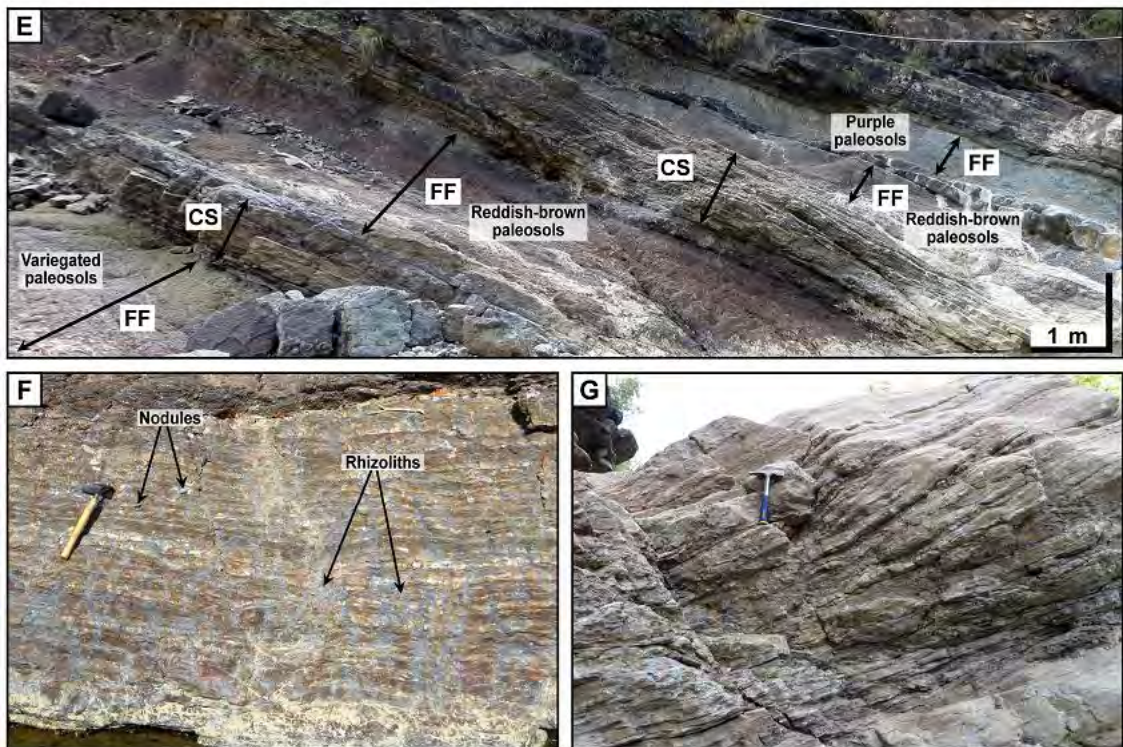


Fig. 5.4. cont. Examples of different types of architectural elements. E) Floodplain (FF) deposits and Crevasse splay (CS) deposits in middle member of the Jagati Formation. F and G) Shallow lake (SL) deposits in middle and upper members of the Jagati Formation, respectively. For facies abbreviations see Table 5.1.

5.5. Facies association

Four facies associations were recognized from the Jagati and Kala Formations on the basis of lithofacies, architectural elements and bed geometry. The individual facies associations and their corresponding depositional facies, architectural elements and lithostratigraphic units are summarized in Table 5.3.

5.5.1. Facies association 1 (FA1)

The facies association FA1 is found in the lower member and lower half of the middle member of the Jagati Formation, and has a total thickness of about 1280 m. The FA1 is represented by bioturbated mudstones (0.2–4 m; about 52%) interbedded with very fine-to medium-grained, calcareous sandstones (0.2–2 m; about 48%) (Fig. 5.5. A and H). The CH and LA elements are mostly fine-grained and less than 2 m thick with flat or undulating bases, on which mud clasts are scattered in some cases. Minor CH elements are frequently present and host the repeated Sh and laterally accreted Sp and St in this association. The Sh has an erosional base and is coarser than the underlying laterally accreted horizon in CH elements (Fig. 5.5). A set of CH and/or LA elements and muddy elements form an up to 15 m of upward-fining succession. The upper portion of the sandy elements contain burrows and calcareous nodules. The muddy elements are frequently interbedded with SB and CS elements. The FF and P elements are the most dominant in FA1. Some of LA elements contain rhizoliths and mud drapes in the upper horizon. Some coal lenses are also observed in very fine-grained sandstones. Paleosols are dominant in the lower member of the Jagati formation and proportion of sandstones increase in up section.

This facies association has characteristics similar to the fine-grained

meandering river system in other Siwaliks. A set of Sh and laterally-accreted horizon within CH element and a LA element show similarity to the typical meandering stream deposits (Miall, 1985, 1996; Collinson, 1996): the CH element here is made up of amalgamated meandering stream deposits. FF element with associated CS represents the proximal part of the floodplain deposit (Miall, 1996; Thomas et al., 2002). The relatively high proportion of FF compared to CH indicates a broad floodplain across which the channel meandered (Nakayama and Ulak, 1999). Increase in CH element in up-section suggest the change in depositional environment from a distal to a proximal setting with increase in discharge.

5.5.2. Facies association 2 (FA2)

The facies association FA2 is found in the upper half of the middle and upper members of the Jagati Formation, and has a total thickness of about 830 m. The FA2 is characterized by alternating very fine- to coarse-grained sandstones (0.2-4 m; about 61%) and bioturbated or finely laminated mudstones (0.2-5 m; about 39%) (Fig. 5.5). The CII and LA elements show similar characters to that of FA1, but contain coarser sediments and thicker beds. Minor CII elements are frequently observed than thicker major CII elements (ca. 5 m). The reddish-brown palcosols are the doiminant facies in

the FF element in the lower half of FA2, whereas the grey-to greenish-grey mudstones (F1 and Fm) are dominant in upper part. The SL element (0.5 - 3 m thick) is frequently observed. The SB and CS elements are observed in this association and the proportion of CS becomes higher in the upper part of this facies association. The SL elements characterized with a couplet of sst-mst alternation are also intercalated in this association.

Architectural elements CH and LA showing characteristics similar to those of FA1 suggest that they are of meandering river origin. Thicker sandstones with coarser grain-size in CH reflect the increase in river water discharge (cf. Ulak and Nakayama, 2001). The thick-bedded reddish-brown palcosols in FF are indicative of the long-term subaerial exposure after deposition (Nadon and Middleton, 1985; Reed, 1991; Sakai et al., 2010), whereas greenish-grey F1 and Fm facies, dominant in the upper part of FA2, indicate the water-logged conditions (Willis and Behrensmeyer, 1994; Quade et al., 1995; Reading, 2004), which is consistent with the appearance of SL element in this association. The SL elements characterized with a couplet of sst-mst alternation records inundation and desiccation events, respectively (cf. Zolcha, 1997; Sakai et al., 2010). Both the SB and CS indicate the occurrence of frequent flood flows (Birdge, 2006; Ghazi and Mountney, 2009) in FA2 (Nakayama and Ulak, 1999; Huyghe et al.,

2005). Therefore, FA2 represents meandering stream with frequent flood-related deposits more dominant than FA1, so this facies association is termed as "flood-flow dominated meandering river system" (cf. Nakayama and Ulak, 1999; Ulak and Nakayama, 2001).

5.5.3. Facies association 3 (FA3)

The facies association FA3 appears in the lower and middle members of the Kala Formation, and has a total thickness of about 1650 m. The FA3 consists of very fine- to coarse-grained sandstones (0.2-7 m; about 76%) interbedded with finely laminated or bioturbated mudstone (0.1-2 m; about 24%) (Fig. 5.5). Biotite, quartz and feldspar are abundantly present in sandstones showing "salt and pepper" characteristic (cf. Tokuoka et al., 1986; Dhital et al., 1995). Sandstone beds in FA3 are thicker and sediments are coarser than those in FA1 and 2. The CII elements mostly contain St facies at the basal part, which succeeded upward with facies Sp, Sh, Sr and Sm to form up to 20 m of fining-upward successions with the FF element. The bases of CII elements are commonly flat and erosional in some cases. The basal part of the CII elements contains mud and sand clasts (2-5 cm long). The DA and LA elements are often present. The FF elements are less frequent than those in FA1-FA2 and mostly

contains greenish-grey to grey Fl or Fm facies, whereas P facies are occasional. The black Fl facies, rich in organic matters are present in some of the upper horizon of FF elements. Thin-to thick-bedded SB elements are occasionally present.

Thicker CH elements indicate the increase in bedload and depth of channels (Allen, 1964; Collinson 1996) in FA3 than that of FA1-FA2. Frequently observed DA elements along with LA elements represent the braided stream deposits (cf. Allen, 1983; Miall, 1985, 1996; Bridge, 2006). The upstream part of braided bars commonly contains coarsening-upward trends (Einsele, 1992; Miall, 1996; Bridge 2003), and presence of such trends in FA3 also indicate the braided stream deposits. The predominance of greenish-grey Fl or Fm facies and preservation of organic matters in FF elements suggest the increase in water discharge or water logged condition (Willis and Behrensmeyer, 1994; Reading, 2004). Similarly, P facies in lesser amount also reflects the less exposure as well as wetter climatic condition in FA3 than the prior facies associations. Overall characteristics of FA3 resemble the "deep sandy braided river system" (cf. FA4 in Nakayama and Ulak 1999; Huyghe et al., 2005).

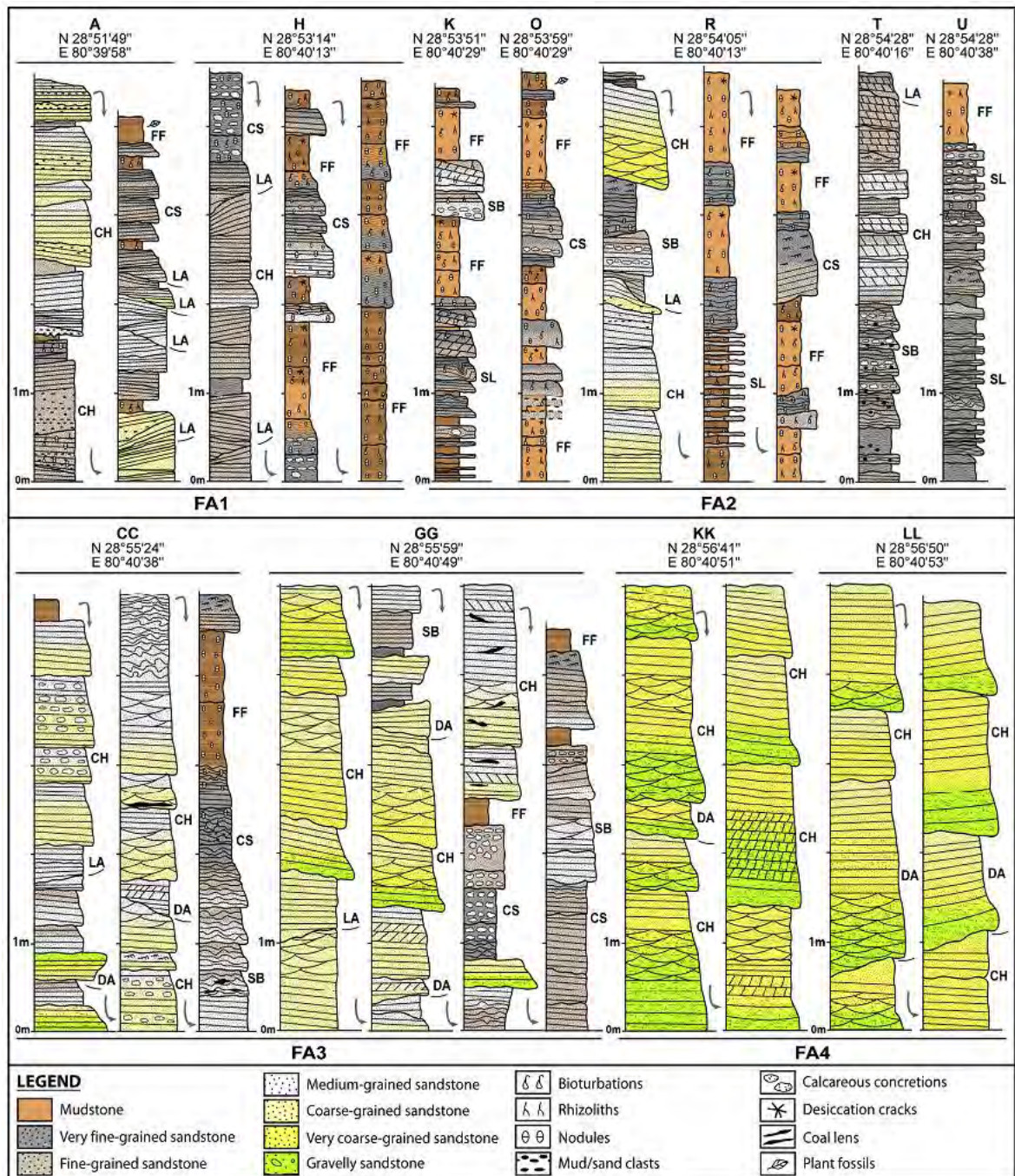


Fig. 5.5. Detail representative columnar sections of facies associations FA1, FA2, FA3 and FA4. Letters at the top (with latitude and longitude) indicate the location of the section in Fig 2. Refer to Table 5.1. for lithofacies symbols and refer to Table 5.2. for abbreviation of architectural elements.

5.5.4. Facies association 4 (FA4)

The facies association FA4 is found in the upper member of the Kala Formation, and has a total thickness of about 400 m. The FA4 is characterized by thick- to very thick-bedded, fine- to very coarse-grained "salt and pepper" sandstones (0.2-9 m; about 58%) and gravelly sandstones (about 19%) interbedded with finely laminated or massive mudstones (0.1-1 m; about 23%) (Fig. 5.5). The CH elements show up to 13 m of faint fining-upward trend from the basal St facies (locally Gt or Gh facies) through Sp and Sh facies into FF element. Some conglomerate beds containing Gh facies which represent CH elements are also observed in the upper most part of FA4. Gravel size tends to be larger up section and some are cobble. The DA elements are frequently observed and LA elements are less frequent than prior facies associations. Thin- to thick-bedded SB elements are occasionally found. The FF elements mostly contain greenish-grey to grey Fl or Fm facies and less amount of weakly developed P facies.

Thick CII elements and frequently observed DA elements indicate that FA4 also represents the braided stream deposits (cf. Miall, 1985, 1996; Bridge, 2006). The erosional bases indicate intermittent reworking of the sediments during lateral migration of bars within the channels (Olsen, 1988; Kumar and Nanda, 1989; Paredes et al., 2007). Presence of many gravels at the base of CII and some conglomerate beds indicate the

more proximal setting. Less thicker fining-upward successions reflect that the channels were shallower than those in FA3 and are similar to "shallow sandy braided river system" defined in previous studies (cf. FA5 in Nakayama and Ulak, 1999; Ulak and Nakayama, 2001; Huyghe et al., 2005).

Facies association	Lithofacies and architectural elements	Stratigraphic distribution
FA1 <i>Fine-grained meandering river system</i>	Dominant lithofacies: P, Fl, Fm, Sh, Sr Minor lithofacies: Sp, St, Sc, Sm Architectural elements: FF, CH, LA, CS, SB	Lower member and up to middle part of the middle member of the Jagati Formation (~ 1280 m)
FA2 <i>Flood-flow dominated meandering river system</i>	Dominant lithofacies: P, Fl, Sh, Sm, Fm, Sr, Sp Minor lithofacies: St, Sc Architectural elements: FF, CH, SL, LA, CS, SB	Upper part of the middle member and the upper member of the Jagati Formation (~ 830 m)
FA3 <i>Deep sandy braided river system</i>	Dominant lithofacies: Sh, Sp, St, Sr, P, Fl Minor lithofacies: Sm, Sc Architectural elements: CH, LA>DA, SB, FF	Lower and middle member of the Kala Formation (~ 1650 m)
FA4 <i>Shallow sandy braided river system</i>	Dominant lithofacies: St, Sp, Gt, Gh, Sh Minor lithofacies: Fl, Fm, P, Sr, Sm Architectural elements: CH, DA>LA, SB, FF	Upper member of the Kala Formation (~ 400 m)

Table 5.3. Facies associations recognized in the Siwalik Group, Khutia Khola section. Lithofacies and architectural element codes after Miall (1985, 1996). Refer Table 5.2 for lithofacies codes and refer Table 5.3 for architectural element codes.

5.6. Correlation with magnetostratigraphic data

Ojha et al. (2000) analyzed the magnetostratigraphy and the rock units were dated from 13.30 to 7.65 Ma in the Khutia Khola section. With reference of base point

(28°54'N; 80°40'E) of their study (due to lack of detail magnetostratigraphic data), boundaries between the facies associations were tentatively estimated by correlating stratigraphic thickness of this study with their study. The age of change from fine-grained meandering river system (FA1) to flood-flow dominated meandering river system (FA2) is inferred to be before 13.3 Ma, probably around 13.5 Ma. The age of change from meandering river system (FA1-FA2) to braided river system (FA3-FA4) is at around 11.0 Ma.

CHAPTER SIX

GEOCHEMICAL ANALYSIS

6.1. Introduction

The major and trace element analysis of sedimentary rocks has been widely used for the estimation on the influence of provenance and tectonic setting (Nesbitt and Young, 1982; Bhatia and Crook, 1986; Roser and Korsch, 1986, 1988; McLennan et al., 1993; Johnson, 1993; Condie, 1993 and others). The chemistry of clastic sedimentary rocks is affected by many physical factors such as diagenesis, sorting and weathering regime (Nesbitt and Young, 1984), although the composition of siliciclastic rocks predominantly reflects the nature and proportion of the detrital components and the provenance (Roser and Korsch, 1988).

The whole-rock geochemical composition of the Siwalik Group in the Nepal Himalaya was initially studied by Roser et al. (2002). They studied 206 sandstones and mudstones samples of the Siwalik succession in the Bakiya Khola area in central Nepal, and found that elemental abundances varied up section, due to decreasing carbonate content and possibly change in provenance. Similarly, Hossain et al. (2008) and Shimizu (2013) studied the sandstone and mudstone samples of the Siwalik Group in

the Surai Khola section, western Nepal and the Karnali River section, far western Nepal, respectively.

This study focuses on both sandstone and mudstone samples from the Siwalik Group along the Khutia Khola section, far western Nepal. This whole-rock geochemical analysis aims to identify the source of sediments, as well as sorting effect of sediments and weathering regime of the Siwalik sediments at the study area, and to compare the results with other Siwalik sections of the Nepal Himalaya.

6.2. Sample preparation

A total of 122 samples (55 mudstones and 67 sandstones) collected from the southern belt of the Khutia Khola section, far-western Nepal. All samples were prepared for analysis using the standard methods applied in the Department of Geoscience, Shimane University (Rosser et al., 1998).

Each sample was reduced to chips about 1-2 cm in diameter using a hammer and a manual hydraulic rock trimmer, and washed repeatedly in water. The washed samples were oven-dried in Pyrex beakers at 110°C for 24 hours. Roughly 100 grams of dried samples were crushed in a Rocklabs® tungsten carbide ring mill, with crushing times of about 20 – 30 seconds for the mudstones, and up to 60 seconds for the

sandstones. The mill was cleaned with ethanol between samples or if necessary, by crushing of a load of quartzose sand, followed by cleaning with ethanol.

Loss of ignition (LOI) value were determined by ignition of 8–10 grams of samples in ceramic crucibles in a muffle furnace at 1010°C for at least 3 hours (compared to normal ignition time of 2hrs). The longer time was adopted to ensure complete sublimation of carbonate. LOI was calculated from the difference between initial weight and the ignited weight of the samples, as well as, correction was also made for volatile loss from the crucibles. LOI values of the sandstones ranged from 1.2 to 28.9 wt% and the mudstones ranged from 2.9 to 28.0 wt% (Table 6.1). The ignited samples were manually reground in an agate pestle and mortar. They were then put in glass vials, and stored in a 110°C oven for at least 24 hours before preparation of the glass fusion beads used for the X-ray fluorescence (XRF) analysis.

6.3. XRF analysis

The glass fusion beads were prepared using an alkali flux consisting of 80% lithium tetraborate (Merck Spectromelt® A10) and 20% lithium metaborate (Merck Spectromelt® A20). The beads contained 1.8000 ± 0.0004 g of ignited sample and 3.6000 ± 0.0004 of flux (sample to flux ratio of 1:2). The beads were made in platinum

crucibles using an automatic bead sampler, with two static 120 second fusions, followed by fusion and rotation mixing for 360 seconds. Then, the samples were analyzed using the RIX 2000 XRF spectrometer (Rigaku Denki Co. Ltd.) at Shimane University, for major elements and fourteen trace elements (Ba, Ce, Cr, Ga, Nb, Ni, Pb, Rb, Sc, Sr, Th, V, Y and Zr). Analytical methods, instrumental conditions and calibration were essentially followed those described by Kimura and Yamada (1996). Calibrations for individual elements were confirmed by analysis at run time of nine standard rocks produced by the Geological Survey of Japan (GSJ).

6.4. Results

The bulk chemical compositions of individual samples are listed by formation in Table 6.1. The XRF data were normalized to 100% anhydrous (LOI-free) for all comparisons and plotting, and are listed on that basis in Table 6.1. Original anhydrous (as analyzed) total is also given along with hydrous loss of ignition values. Average chemical compositions by facies association and lithotype (sandstone and mudstone) are listed in Table 6.2.

6.4.1. Major elements

The most abundant major element is SiO_2 , which reaches a maximum of 91.09 wt% and as low as 38.24 wt% in sandstone (sst) and mudstone (mst), respectively (Table 6.1). The average SiO_2 content of the sandstones (average 77.19 wt%) in all facies associations (FA) are higher than values in average Upper Continental Crust (UCC) (66.00 wt%) and Post-Archean Australina Shale (PAAS) (62.80 wt%) of Taylor and McLennan (1985), whereas UCC and PAAS values are higher than the average SiO_2 content in the mudstones (except, FA1 and FA4 > PAAS). The next most abundant major element, Al_2O_3 , ranges from 3.57 to 11.53 wt% (average 6.76 wt%) in the sandstones and from 8.58 to 20.40 wt% (average 15.20 wt%) in the mudstones. The average contents of Al_2O_3 are lower than the UCC (15.20 wt%) and PAAS (18.90 wt%) values (except, FA4 mudstones; 19.47 wt%). Fe_2O_3 , MgO , CaO and K_2O are the four next most abundant major elements. Fe_2O_3 contents range from 1.15 to 4.03 wt% (average 2.18 wt%) in the sandstones and from 2.87 to 9.30 wt% (average 6.11 wt%) in the mudstones. Similarly, MgO contents range from 0.39 to 9.05 wt% (average 1.19 wt%) in the sandstones and from 0.91 to 15.96 wt% (average 2.90 wt%) in the mudstones. Abundances of CaO are very high in both lithotypes. CaO contents range from 0.11 to 44.93 wt% (average 10.67 wt%) in the sandstones and from 0.18 to 34.66

wt% (10.13 wt%) in the mudstones. The average values of CaO in all facies associations are higher than UCC (4.20 wt%) and PAAS (1.30 wt%) values (except FA4 mudstone; 1.18 wt%). K₂O contents are typically lower in the sandstones than in the mudstones. Contents range from 0.47 to 3.20 wt% (average 1.24 wt%) in the sandstones and from 1.17 to 6.05 wt% (average 3.75 wt%) in the mudstones. Concentrations of the four remaining major elements, TiO₂, MnO, Na₂O and P₂O₅, are all less than 1 wt%.

6.4.2. Trace elements

Seven elements (Ba, Ce, Cr, Rb, Sr, V and Zr) are present in concentrations near to or exceeding 100 ppm. Barium is the most abundant trace element and is typically lower in the sandstones than in the mudstones in all facies associations. Contents range from 106 to 361 ppm (average 214 ppm) in the sandstones and from 204 to 827 ppm (average 557 ppm) in the mudstones. Cerium, Cr, Rb and V contents in the mudstones are higher than in the sandstones. Concentrations of these elements are less than 300 ppm in all samples. Strontium contents are similar in both lithotypes, ranging from 17 to 375 ppm (average 105 ppm) in the sandstones and from 33 to 354 ppm (average 119 ppm) in the mudstones. Zirconium is present in significant concentrations. Zr contents range from 98 to 668 ppm (average 223 ppm) in the sandstones and from 75

to 393 ppm (206 ppm) in the mudstones. The seven remaining trace elements (Ga, Nb, Ni, Pb, Sc, Th and Y) are present in concentrations of less than 50 ppm. Most of these elements have higher values in the mudstones than in the sandstones.

Lost on ignition (LOI) values in the mudstones are higher than those in the sandstones of equivalent facies associations (except FA4, sst > mst). A number of key provenance and paleoweathering indicators (e.g. $\text{SiO}_2/\text{Al}_2\text{O}_3$, $\text{K}_2\text{O}/\text{Na}_2\text{O}$, Th/Sc, Zr/Sc, $\text{Al}_2\text{O}_3/\text{Na}_2\text{O}$, $\text{Al}_2\text{O}_3/\text{K}_2\text{O}$) show systematic shifts within lithotypes and facies associations, which indicate that stratigraphic shifts in geochemical composition occur within the Siwalik Group in the Khutia Khola section.

6.5. Element- Al_2O_3 covariations

Conventional variation diagrams of mudstones and sandstones from the Jagati and Kala Formations were plotted in pairs (FA1-FA2 and FA3-FA4) to examine the relationship between each element and Al_2O_3 contents. Al_2O_3 is used on the x-axis because it is a rough proxy of grain size, as sandstones usually have Al_2O_3 lower contents than siltstones and mudstones, which are typically richer in clays and poorer in quartz and feldspar (Roser, 2000).

6.5.1. Major elements

SiO₂ contents show very weak and scattered negative linear trends on the variation diagram, along which the sandstones are well separated from the mudstones (Fig. 6.1). Contents of Al₂O₃ increase as SiO₂ contents decrease, while the grain size becomes smaller. Sandstones in FA1-FA2 have higher values of SiO₂ than in FA3-FA4. Considering the high CaO contents of the Siwalik rocks and the constraints of constant sum, this trend is caused by carbonate dilution (Roser et al., 2002), and is a major problem in the interpretation of the Siwalik data, here and in other sections such as Bakiya Kholā (Roser et al., 2002) and Karnali River (Shimizu, 2013). Displacement towards the origin tends to be greater for sandstones than for mudstones, presumably due to greater porosity of the former. Na₂O contents also show a scattered negative correlation (Fig. 6.1). This is common in quartzofeldspathic sediments, due to relative concentration of Na-plagioclase (albite) in sandstones relative to mudstones due to hydrodynamic sorting (Roser, 2000). A few FA3 sandstones (KS-107, 110) show slightly higher values, but almost all analyzed samples contain <1 wt% Na₂O, which are very low compared to average values for UCC (3.70 wt%) and PAAS (1.20 wt%) (Taylor and McLennan, 1985). Probably, the lower contents of Na₂O is due to the carbonate dilution problem, the much lower values relative to PAAS and UCC suggest

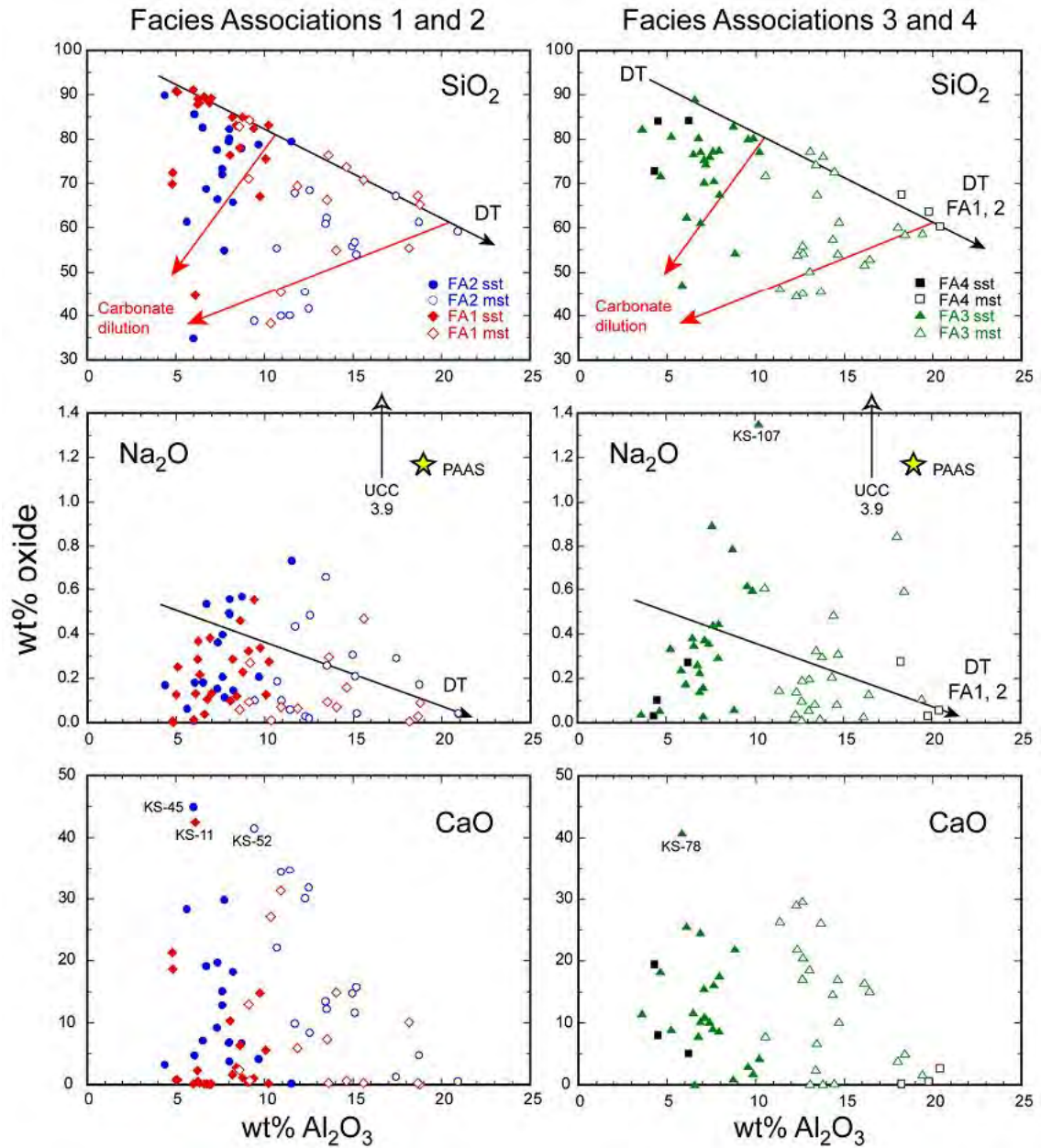


Fig. 6.1. Major element (Si, Na, Ca) – Al₂O₃ variation diagrams (anhydrous normalized basis) for the Siwalik Group sandstones (sst) and mudstones (mst) from the Khutia Khola section. Data from Table 6.1. Abbreviation: DT – indicative detrital trends (black line with arrow) drawn by eye, arrows in direction of fining. Red arrows (CA) – direction of displacement expected from dolomite addition. UCC - Upper Continental Crust value (Taylor and McLennan, 1985). PAAS - Post-Archean Australian shale value (Taylor and McLennan, 1985).

substantial loss of Na_2O from the Siwalik sediments relative to their source. The variation diagrams for CaO show the extent of the carbonate problem in the Siwalik sediments (Fig. 6.1). Abundances of CaO scatter upward to >40 wt% and high values are seen in both lithotypes.

The three ferromagnesian major elements (TiO_2 , Fe_2O_3 and MgO) show positive correlations with Al_2O_3 as is common in quartzofeldspathic sediments (Roser, 2000), though they show different patterns. The values in the mudstones are higher than in the sandstones. The FA1-FA2 TiO_2 detrital trend (DT) runs above the quartz dilution line (DL) from the most aluminous mudstone to the origin, where the diluents quartz and CaCO_3 would plot. Fe_2O_3 contents of FA1-FA2 and FA3-FA4 show quite similar trends, and the values of the sandstones are similar, but tendencies of the mudstones are scattered (Fig. 6.2). The FA1-FA2 DT lies below the DL, consistent with unmixing of quartz and feldspar, and also dilution from quartz and carbonate from clays. MgO contents show a flatter positive correlation and the sandstones and mudstones of both groups show a similar tendency, with mostly falling along a DT (Fig. 6.2). However, some of the sandstones and mudstones show a tendency to scatter upward away from the DT (red arrows in Fig. 6.2). This is probably due to sporadic carbonate addition, with deposition of more dolomitic carbonate cement during diagenesis.

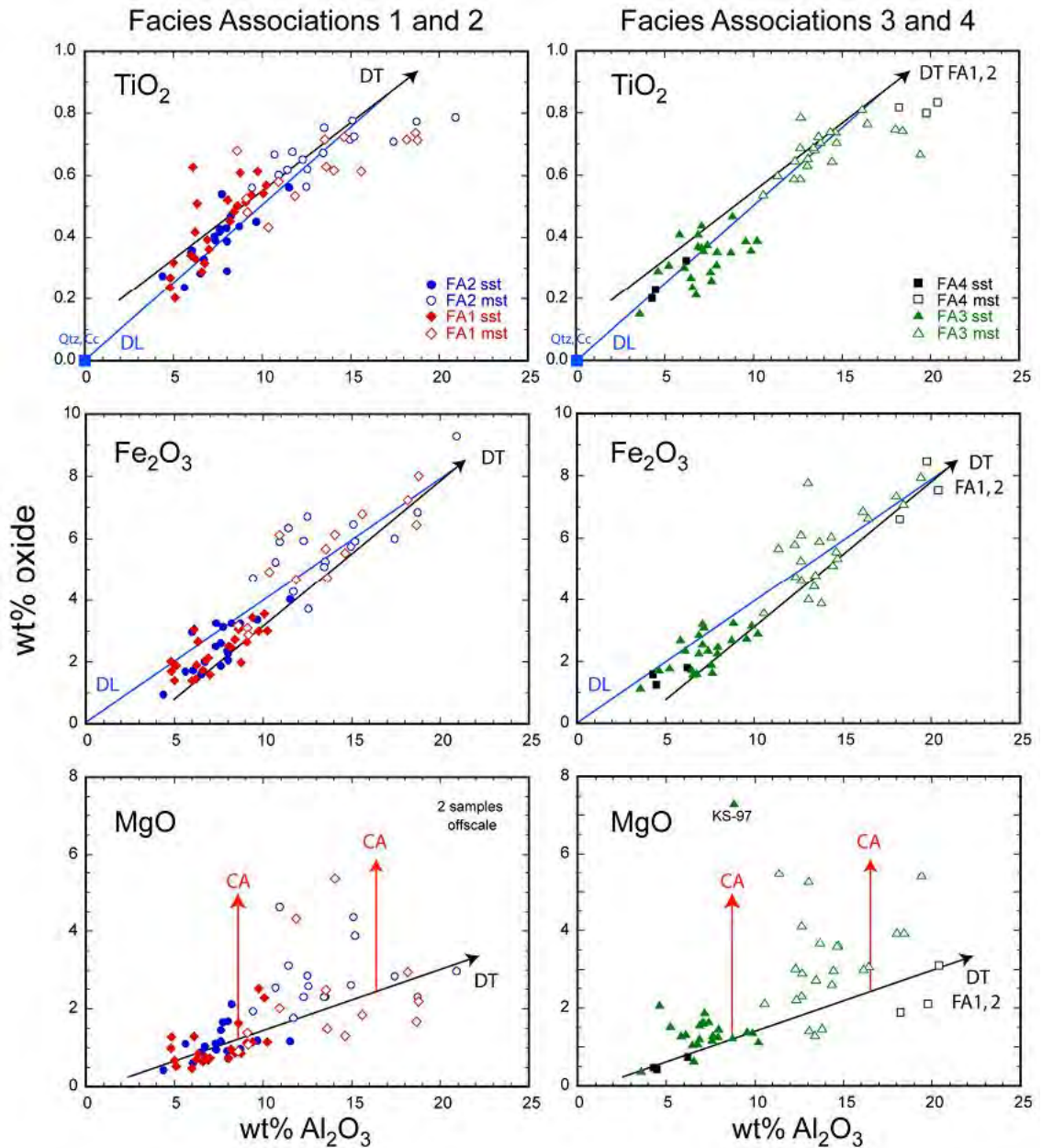


Fig. 6.2. Major element (Ti, Fe, Mg) – Al_2O_3 variation diagrams (anhydrous normalized basis) for the Siwalik Group sandstones (sst) and mudstones (mst) from the Khutia Khola section. Data from Table 6.1. Abbreviation: DT – indicative detrital trends (black line with arrow) drawn by eye. DL – dilution trend (blue line) expected from concentration of quartz or carbonate addition. Red arrows (CA) – direction of displacement expected from dolomite addition.

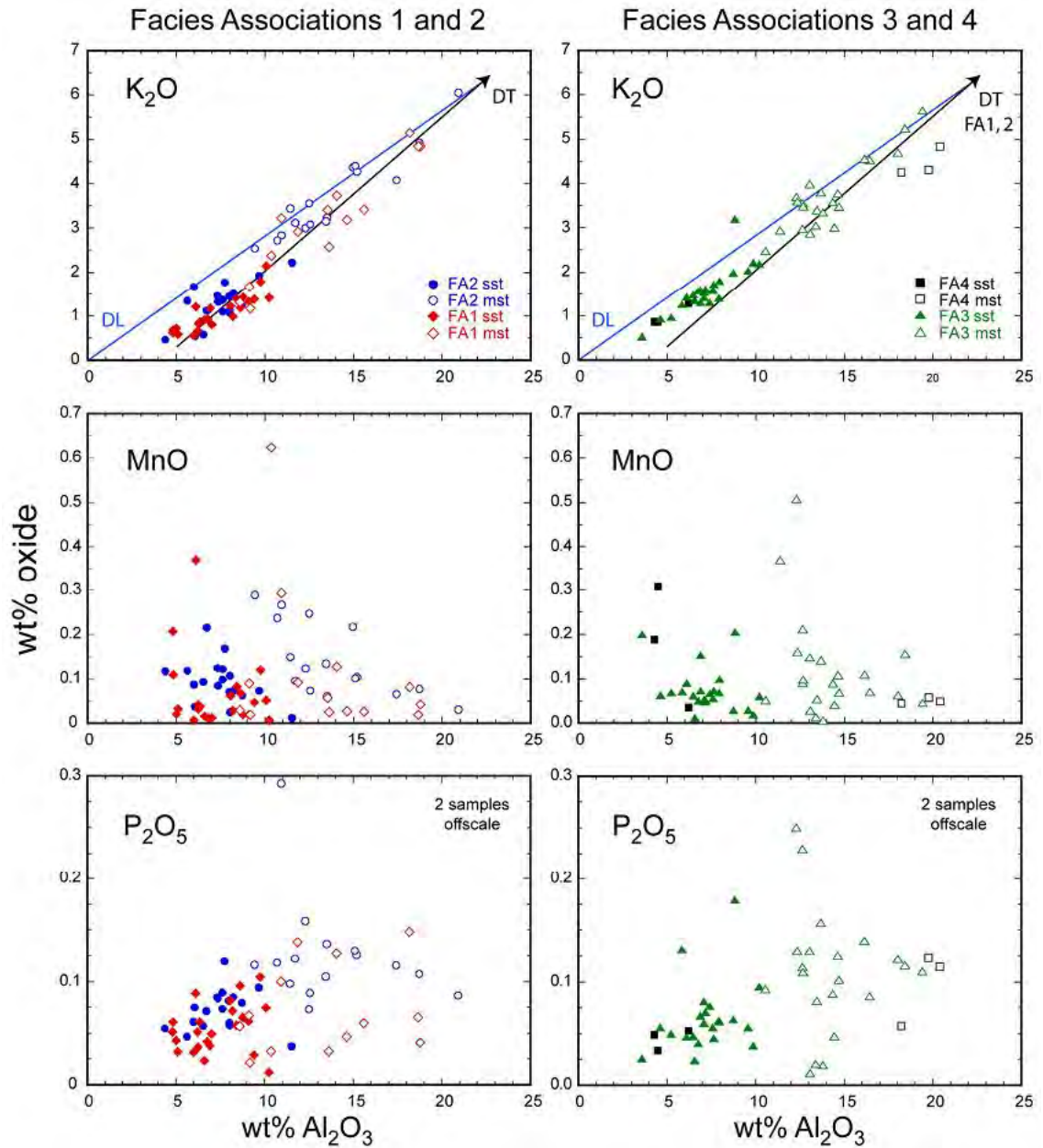


Fig. 6.3. Major element (K, Mn, P) – Al_2O_3 variation diagrams (anhydrous normalized basis) for the Siwalik Group sandstones (sst) and mudstones (mst) from the Khulia Khola section. Data from Table 6.1. Abbreviation: DT – indicative detrital trends (black line with arrow) drawn by eye. DL – dilution trend (blue line) expected from concentration of quartz or carbonate addition.

One mudstone in the FA1 has a higher value of just over 15 wt% MgO.

The three remaining major elements (K_2O , MnO and P_2O_5) show variable behavior. K_2O Contents define a quite clear positive correlation with a detrital trend (DT) lower than the dilution trend (DL) (Fig. 6.3). This suggests control of compositions by unmixing of quartz+feldspar and clays, and also dilution from quartz and carbonate from clays. No correlation is seen for MnO and P_2O_5 (Fig. 6.3). Most of the values are less than 0.3 wt% and are scattered. This is most probably due to the association of these elements with diagenetic carbonate.

6.5.2. Trace elements

The ten trace elements (Ba, Cr, Ni, V, Rb, Ga, Nb, Ce, Y and Th) show positive correlation and four trace elements (Pb, Sr, Sc and Zr) show weak correlations against Al_2O_3 . Barium, Cr, Ni, V, Rb and Ga show DT is lower than DL and intersect the x-axis at ~3-5 wt% Al_2O_3 which suggests hydrodynamic separation of quartz+feldspar and clays (Fig. 6.4, 6.5 and 6.6). The positive correlation suggests that much feldspar must have been destroyed in the Siwalik sediments and this is consistent with the QFL data of the Khutia Khola sandstones, which average $Q_{70}F_{7}L_{23}$ and $Q_{68}F_{10}L_{22}$ for the FA1-FA2 (Jagati Fm.) and FA3-FA4 (Kala Fm.), respectively. The FA3-FA4 mudstones

show higher and greater scatter values which is probably connected with K_2O content, and is related to the change in river environment, K-feldspar or biotite content, or the extent of K-metasomatism in individual samples during diagenesis.

Niobium, Ce and Y are all immobile incompatible trace elements which should reflect source variations very well (Taylor and McLennan, 1985) (Fig. 6.7). The plots of these elements show DT line is higher than DL and it intercepts the y-axis rather than the x-axis, which suggests a heavy mineral control (e.g. apatite, monazite). Scatter to higher values of the sandstones in FA1-FA2 than FA3-FA4 may be due to the change in the river environment, having greater opportunity to fractionate these elements by heavy mineral concentration in FA1-FA2, compared to FA3-FA4.

Thorium and Zr show curved correlations (Fig. 6.8). Thorium shows an inflected positive correlation, but the increase in Th abundances becomes small at higher Al_2O_3 contents. Zirconium contents have a very different distribution. The FA1-FA2 sandstones tend to be scattered to higher values compare to the values in the FA3-FA4 sandstones. This might be due to result of greater heavy mineral concentration (especially Zr) and mineralogical fractionation in the lower energy meandering river system in FA1-FA2 (Jagati Fm.), compared to the higher energy braided river system in FA3-FA4 (Kala Fm.).

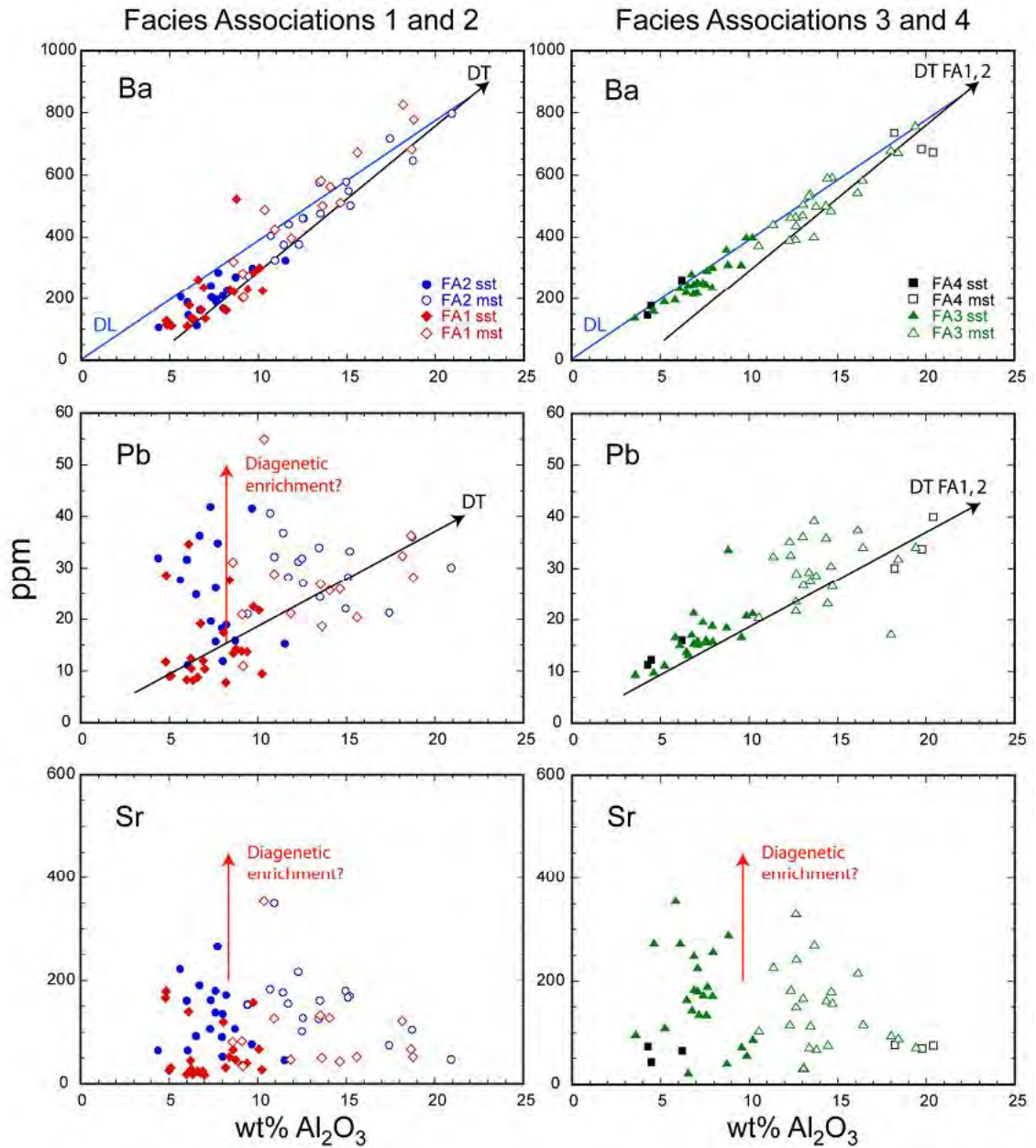


Fig. 6.4. Trace element (Ba, Pb, Sr) – Al₂O₃ variation diagrams (anhydrous normalized basis) for the Siwalik Group sandstones (sst) and mudstones (mst) from the Khutia Khola section. Abbreviation: DT – indicative detrital trends (black line with arrow) drawn by eye. DL – dilution trend (blue line) expected from concentration of quartz or carbonate addition. Red arrows – possible diagenetic enrichment.

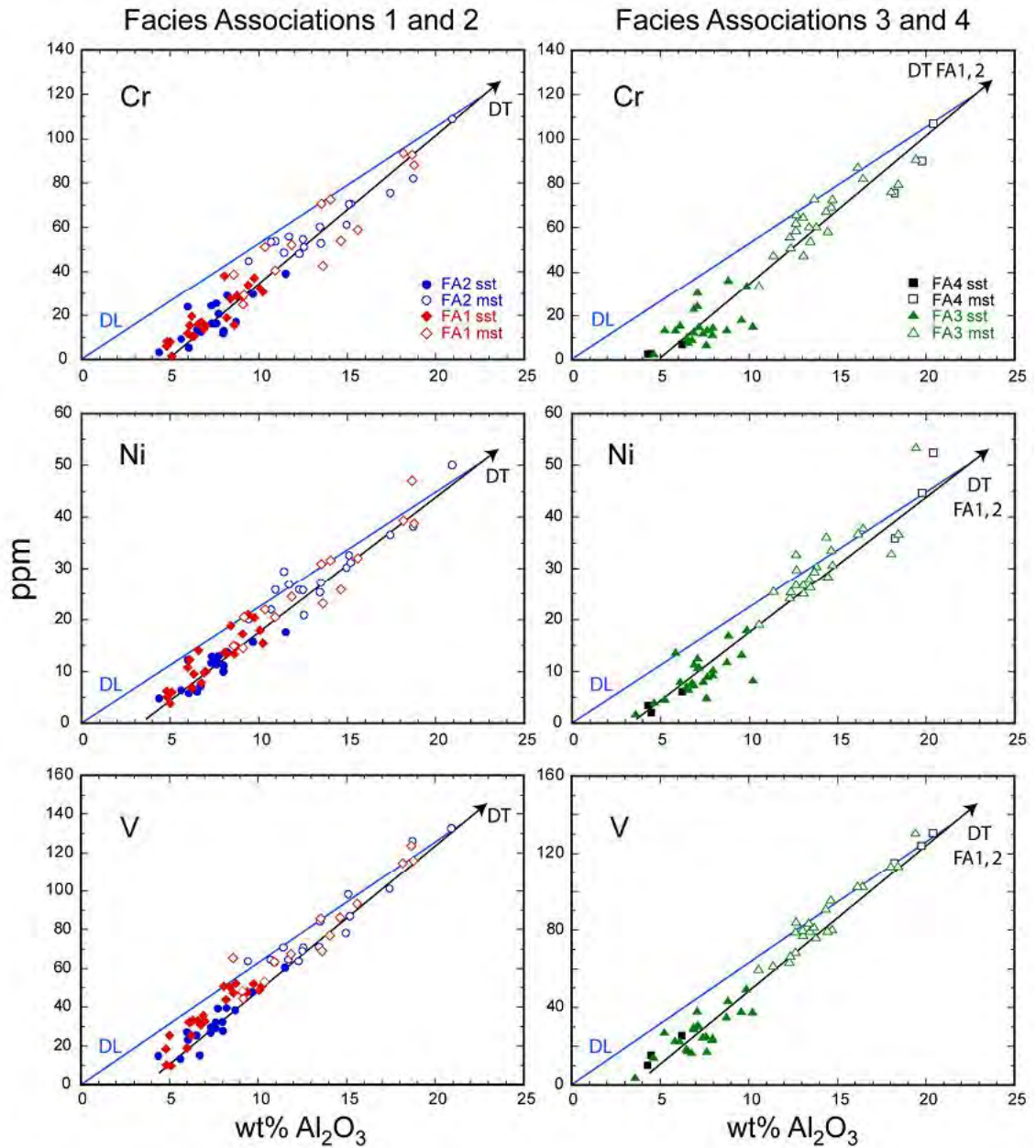


Fig. 6.5. Trace element (Cr, Ni, V) – Al_2O_3 variation diagrams (anhydrous normalized basis) for the Siwalik Group sandstones (sst) and mudstones (mst) from the Khulia Khola section. Data from Table 6.1. Abbreviation: DT – indicative detrital trends (black line with arrow) drawn by eye. DL – dilution trend (blue line) expected from concentration of quartz or carbonate addition.

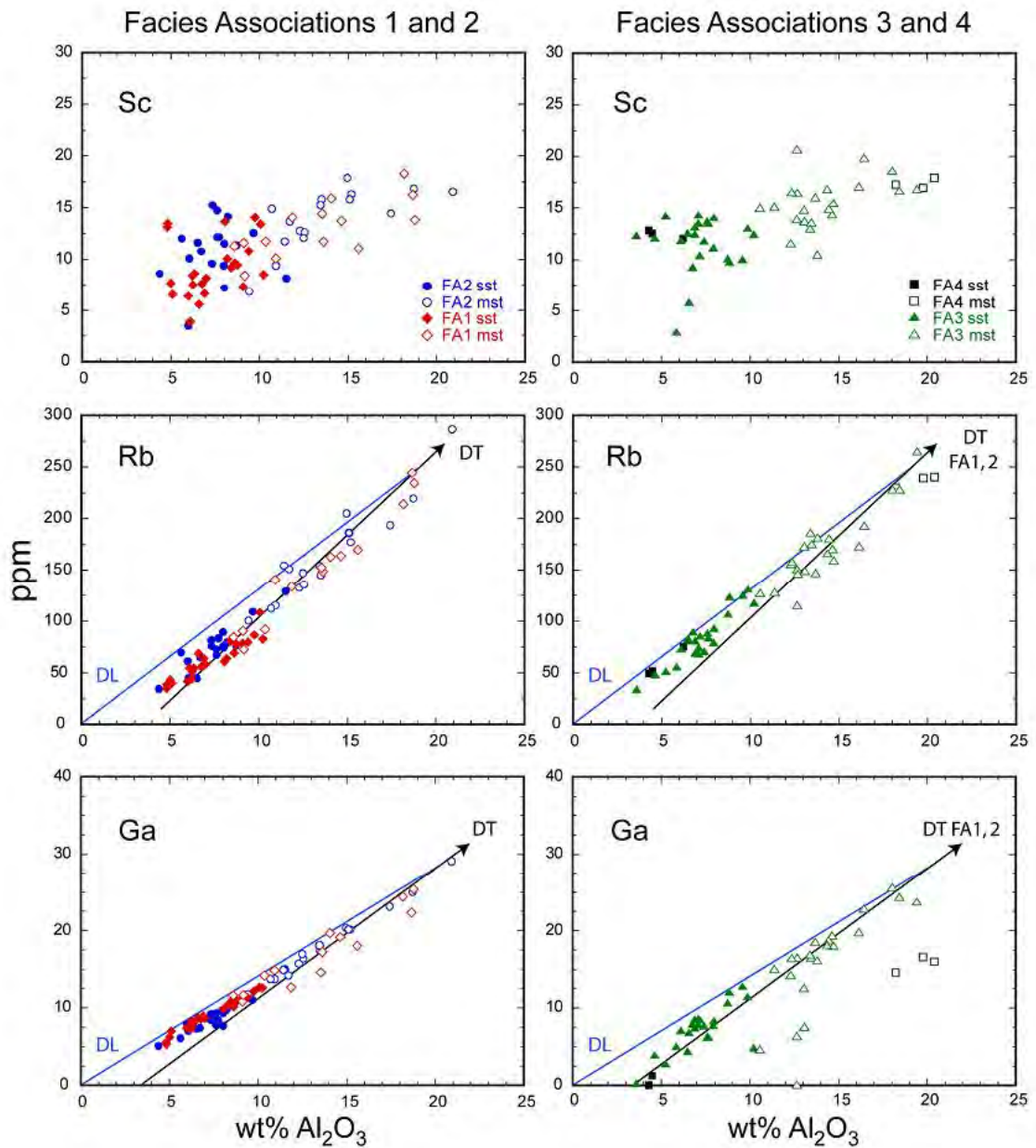


Fig. 6.6. Trace element (Sc, Rb, Ga) – Al₂O₃ variation diagrams (anhydrous normalized basis) for the Siwalik Group sandstones (sst) and mudstones (mst) from the Khutia Khola section. Data from Table 6.1. Abbreviation: DT – indicative detrital trends (black line with arrow) drawn by eye. DL – dilution trend (blue line) expected from concentration of quartz or carbonate addition.

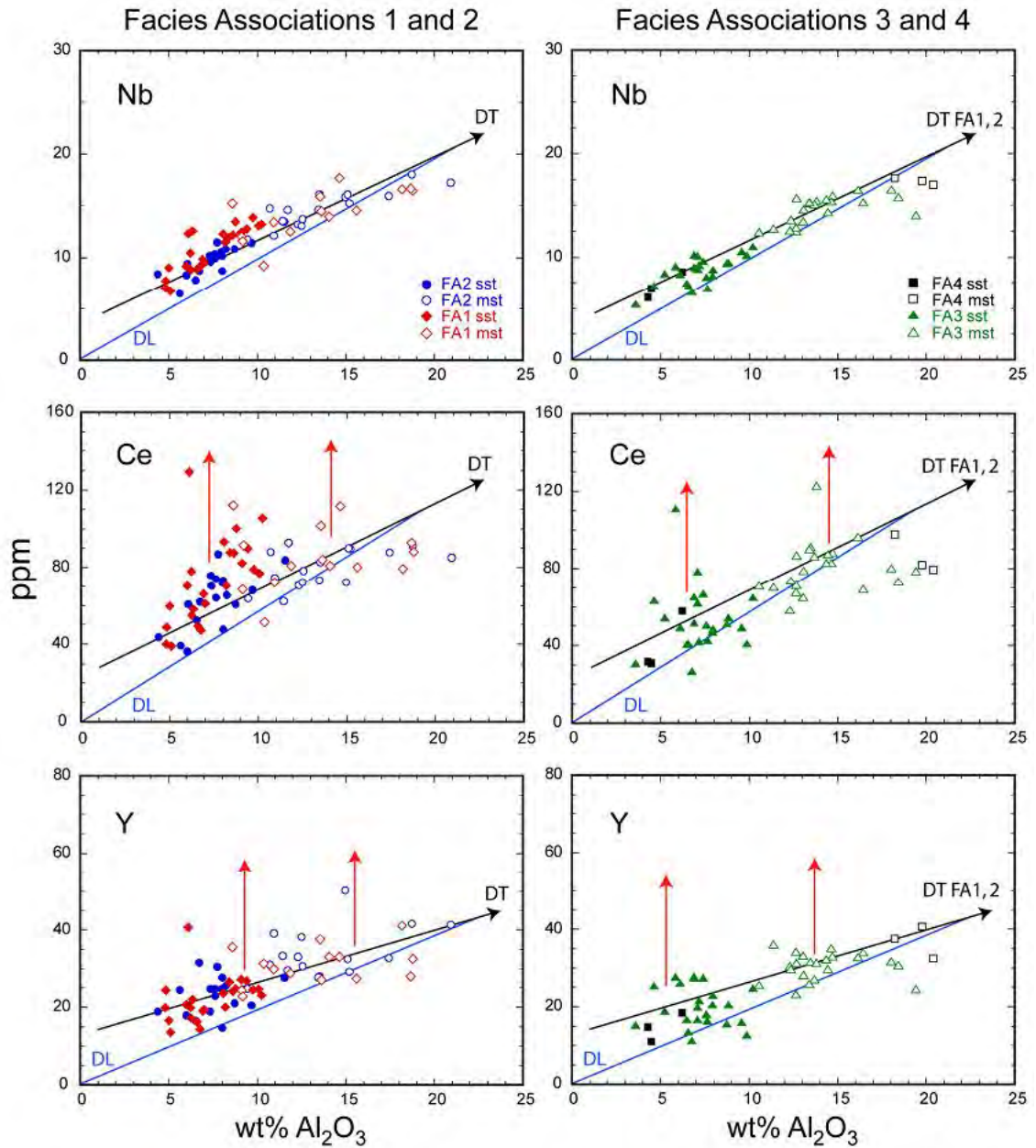


Fig. 6.7. Trace element (Nb, Ce, Y) – Al₂O₃ variation diagrams (anhydrous normalized basis) for the Siwalik Group sandstones (sst) and mudstones (mst) from the Khutia Khola section. Data from Table 6.1. Abbreviation: DT – indicative detrital trends (black line with arrow) drawn by eye. DL – dilution trend (blue line) expected from concentration of quartz or carbonate addition. Red arrows – possible heavy mineral enrichment.

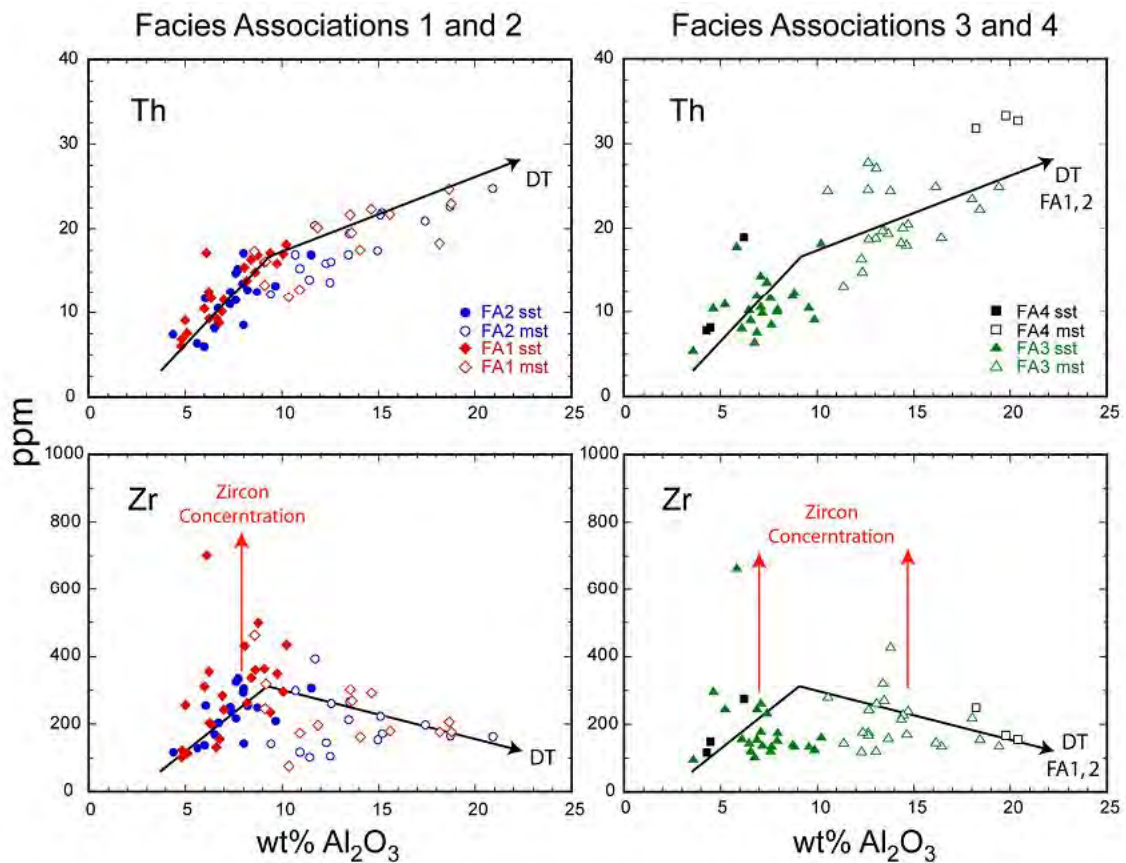


Fig. 6.8. Trace element (Th, Zr) – Al_2O_3 variation diagrams (anhydrous normalized basis) for the Neogene Siwalik Group sandstones (sst) and mudstones (mst) from the Khutia Khola section. Data from Table 6.1. Abbreviation: DT – indicative detrital trends (black line with arrow) drawn by eye, arrows in direction of fining. Red arrows – possible heavy mineral enrichment.

Lead, Sr and Sc show a scattered distribution (Fig. 6.4 and 6.6). The Pb contents in some FA2 sandstones have higher values, possibly due to diagenesis. FA3-FA4 sandstone contents are relatively consistent and the mudstones showing slight scatter to higher values suggest that it is most likely to be controlled by the abundances of clay minerals derived from the weathering of feldspar. The Sr plots bear some

resemblance to those for CaO, and so it is probably that the primary control on the abundance of this element is diagenesis. Scandium is generally regarded as an immobile element, which is transferred quantitatively from source to sediment, thus it is a good provenance indicator (Taylor and McLennan, 1985). Therefore, it should show regular trends with Al₂O₃, but in this case it does not. This is probably due to very high CaO contents.

The element- Al₂O₃ variation diagrams show that major and trace elements abundance in sandstones and mudstones are primarily controlled by sedimentary sorting. Elements Fe₂O₃, K₂O, Ba, Cr, Ni, V, Rb, and Ga show regular trends and suggest the control of compositions by sorting of quartz, feldspar and lithic fragments from clays. Some elements (CaO, MgO, Sr, and probably MnO, P₂O₅ and Pb) are strongly or moderately influenced by carbonate diagenesis. The elements TiO₂, Nb, Ce and Y show trends that cut the y-axis indicating consistency with heavy mineral concentration in the meandering river systems of FA1-FA2 (Jagati Fm.). The heavy mineral effect is less marked in the braided river systems of FA3-FA4 (Kala Fm.). Similarly, Zr and Th also show heavy mineral effects. Therefore, the bulk compositions of the Khutia Kholia sediments are a product of several processes, but fluvial style appears to exert a strong influence despite the very strong diagenetic geochemical overprint.

6.6. Geochemical classification

The geochemical classification of Herron (1988) is one of the useful tools for chemical classification of sediment type, which provides an important clue for estimating the origin of sediments. The Herron diagrams for FA1-FA2 and FA3-FA4 sediments show that samples are spread across the sublitharenite, litharenite (LA), wacke (WK) and shale fields (Fig. 6.9). Predominantly, the sandstones are classified as sublitharenite and litharenite fields, differentiating two lithotypes forming a cluster at the boundary. Similarly, the mudstones are also mostly classified as wackes and shales.

6.7. Comparison with UCC by lithotypes

Average values of both lithotypes in FA1-FA2 and FA3-FA4 were normalized against the average UCC composition of Rudnick and Gao (2005) to compare the bulk chemistry of sediments, and their relationship to other lithotypes (Fig. 6.10). It is considered that the Himalaya represent an upper continental crust (UCC) section, therefore the Siwalik sediments should have geochemical compositions similar to UCC, and hence show flat patterns on UCC_N spidergrams. However, there are some divergences from UCC, and each lithotype generally shows the same trend. The mudstone averages in general have patterns closer to the value of UCC than the

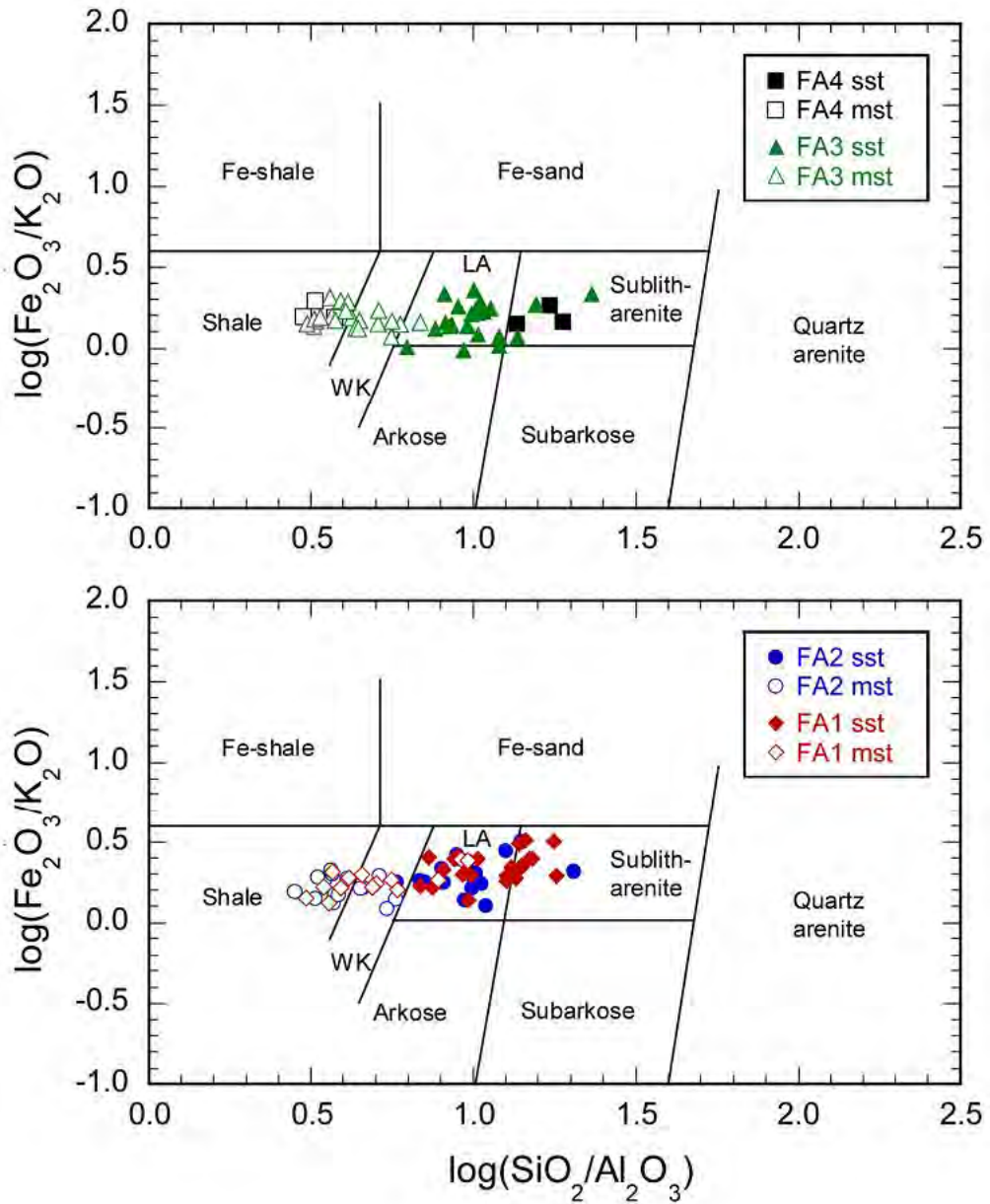


Fig. 6.9. Log ($\text{SiO}_2/\text{Al}_2\text{O}_3$) – log ($\text{Fe}_2\text{O}_3/\text{K}_2\text{O}$) geochemical classification diagram (Herron, 1988) for the Khutia Khola Siwalik Group sandstones and mudstones. Abbreviations: WK – wacke; LA – litharenite, sst – sandstone; mst – mudstone.

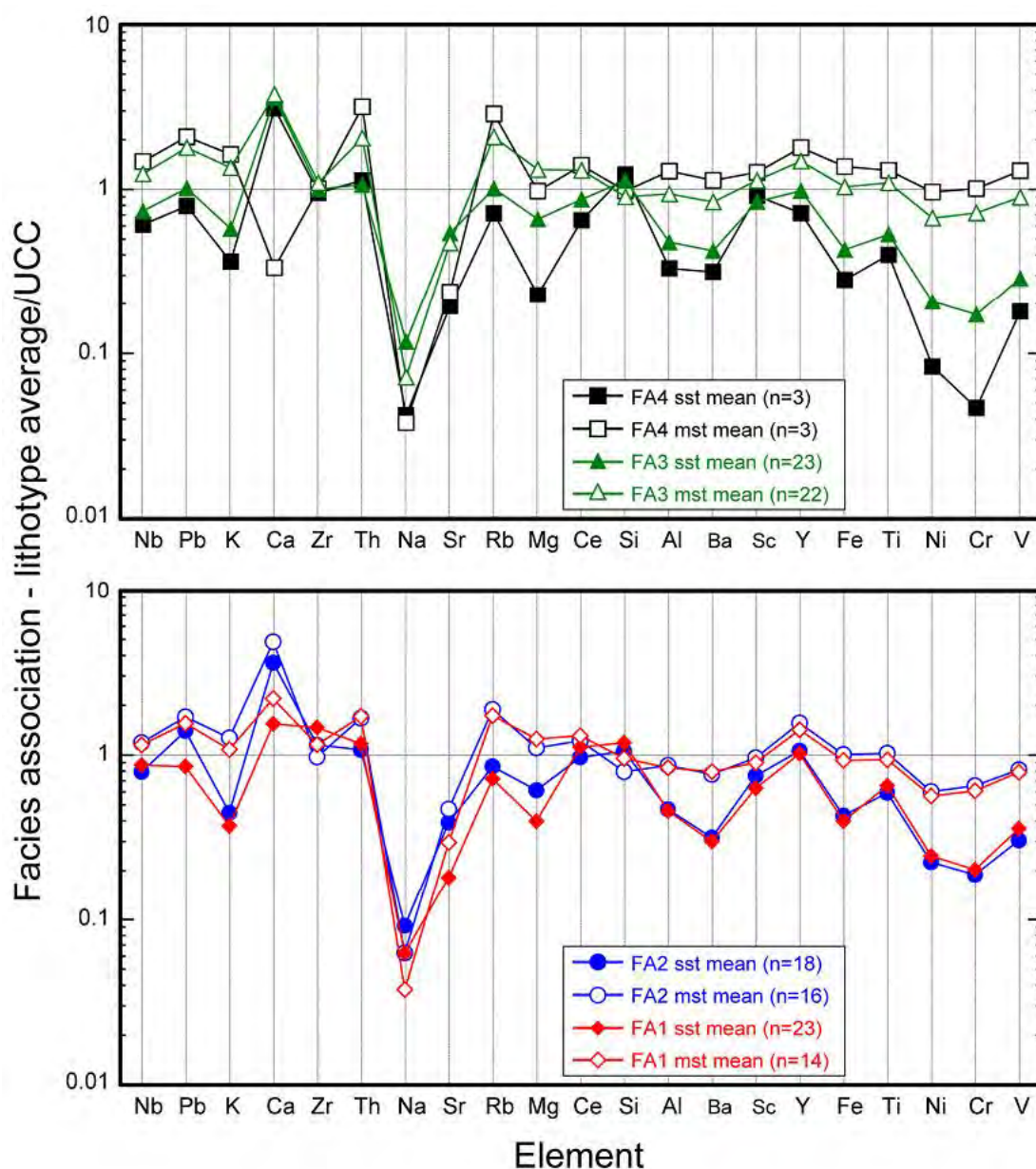


Fig. 6.10. UCC-normalized spidergrams of average sandstones and mudstones from the Siwalik Group, Khutia Khola section. Elements are arranged from left to right in order of increasing normalized abundances in average Mesozoic-Cenozoic greywacke (Condie, 1993), following the methodology of Dinelli et al. (1999). Major elements were normalized as oxides, trace elements as ppm. Abbreviations: sst – sandstone; mst – mudstone, n- number of samples. UCC (Upper Continental Crust) values from Rudnick and Gao (2005).

sandstones. On this graph, elements are roughly arranged from felsic elements on the left to ferromagnesian elements on the right according to the normalized value in average Cenozoic-Mesozoic greywacke (Condie, 1993). The patterns for depletion in the segment A1-V show the source is felsic. Separation of the sandstone and mudstone averages is produced by sorting. The patterns in FA1-FA2 and FA3-FA4 averages are remarkably similar, and no provenance change can be detected by using this method. Possibly, diagenetic carbonate has strongly affected these averages, and thus weakened any signals of source change based on them.

6.8. Provenance signatures by lithotypes

The oxide/ Al_2O_3 ratio provenance discriminant plot by Roser and Korsch (1988) clarifies the source rock based on major element compositions. The FA1-FA2 Khutia Kholā sediments are mostly plotted in P2 (intermediate) and P4 (quartzose) provenance fields and a few sandstones and mudstones fall in the P1 (mafic) field (Fig. 6.11). The FA3-FA4 sediments mainly fall in the quartzose field, with only a few sandstones and mudstones plotting in the P2 (intermediate) field.

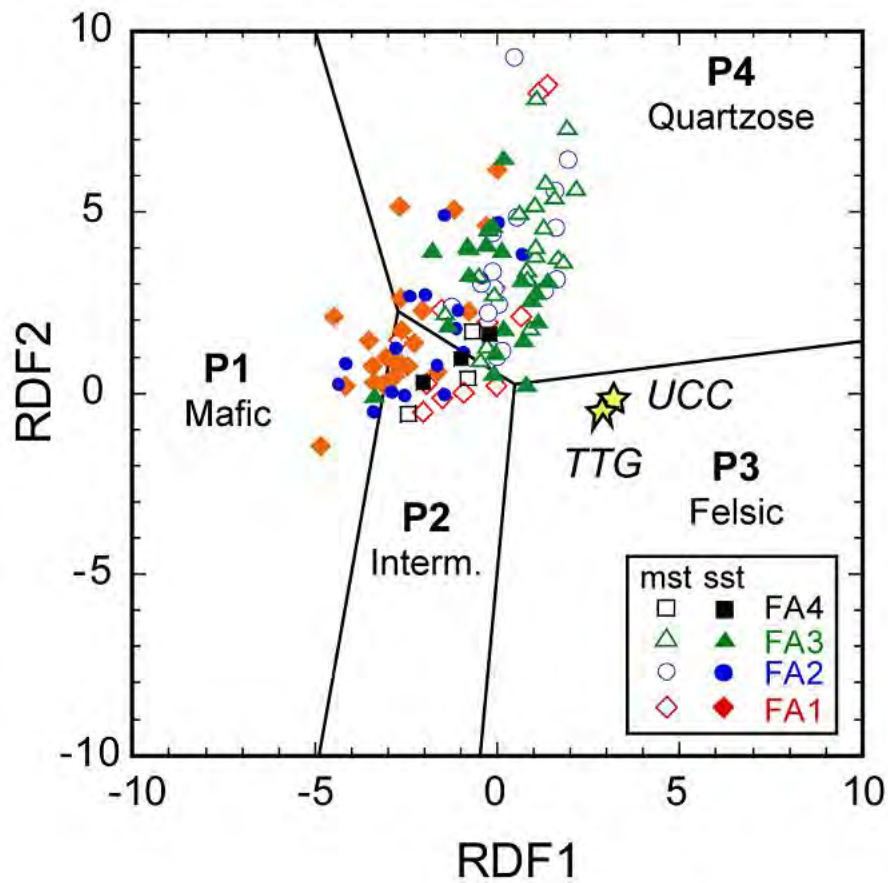


Fig. 6.11. Oxide/ Al_2O_3 ratio provenance discriminant (Roser and Korsch, 1988) for the Siwalik Group sandstones (sst) and mudstones (mst), Khutia Khola section. Stars: UCC – Upper Continental Crust (Taylor and McLennan, 1985); TTG – Phanerozoic TTG granodiorite (Condie, 1993). Abbreviations: Interm – Intermediate; RDF – ratio discriminant function. See Roser and Korsch (1988) for details of the calculation.

6.9. Weathering indices

Paleoweathering in source areas plays an important role in modifying the geochemical composition of derived sediments (Nesbitt and Young, 1984; Johnsson 1993; Fedo et al., 1995, and many others). Paleoweathering analysis may thus show the possible effect of change in monsoon conditions during Siwalik deposition.

A-CN-K plots (Nesbitt and Young, 1984) have three vertices, which are A = Al_2O_3 (representing weathering products such as kaolinite, gibbsite and chlorite), CN = $\text{CaO}^* + \text{Na}_2\text{O}$ (Plagioclase), and K = K_2O (K-feldspar). Such plots are also able to show the Chemical Index of Alteration (CIA) values. The CIA is used to evaluate the intensity of weathering conditions and the extent of destruction of feldspar, and is calculated using molecular proportions, using the equation: $\text{CIA} = [\text{Al}_2\text{O}_3 / (\text{Al}_2\text{O}_3 + \text{CaO}^* + \text{Na}_2\text{O} + \text{K}_2\text{O})] \times 100$; where CaO^* is the amount of CaO incorporated in the silicate fraction of the rock. The values are calculated in molar proportions to emphasize mineralogical relationships (Nesbitt and Young, 1984). Contents of CaO in the Khutia Khola Siwalik sediments are highly variable, with values in the mudstones ranging up to 34 wt%, and those in sandstones up to 44 wt%, due to secondary CaCO_3 . Fedo et al. (1995) proposed a correction for CaO contributions from non-silicate minerals, based on calculation of CaCO_3 content from CO_2 data for individual samples.

However, no correction could be made for carbonate CaO in this study, as no CO₂ data were available. The Khuita Khola Siwalik samples have been strongly modified by carbonate diagenesis, so thus added CaO drives samples down towards the CN apex in the A-CN-K plot. Consequently, no information can be gained about the original CIA ratios from the raw XRF analyses.

In an attempt to overcome this problem, approximate detrital CaO* values for each sample were calculated by assuming that CaO* values are equal to measured Na₂O content, following the method of McLennan (1993). This assumption rests on the fact that calcic and sodic feldspar weather at the same rate (Nesbitt and Young, 1984). The major element data were then re-normalized to sum to 100% to overcome the dilution effect of carbonate on all other components. The resulting CaO* values were then used to calculate approximate CIA ratios and to construct a modified A-CN-K plot (Fig. 6.12). On this plot the FA1-FA2 samples show the highest CIA values (>80), and cluster near the composition of illite. The FA3-FA4 samples generally show lower CIA, and are displaced to the right between illite and muscovite compositions. These features indicate higher weathering in the FA1-FA2 meandering river system, and supply of fresh detritus in the FA3-FA4 braided river system.

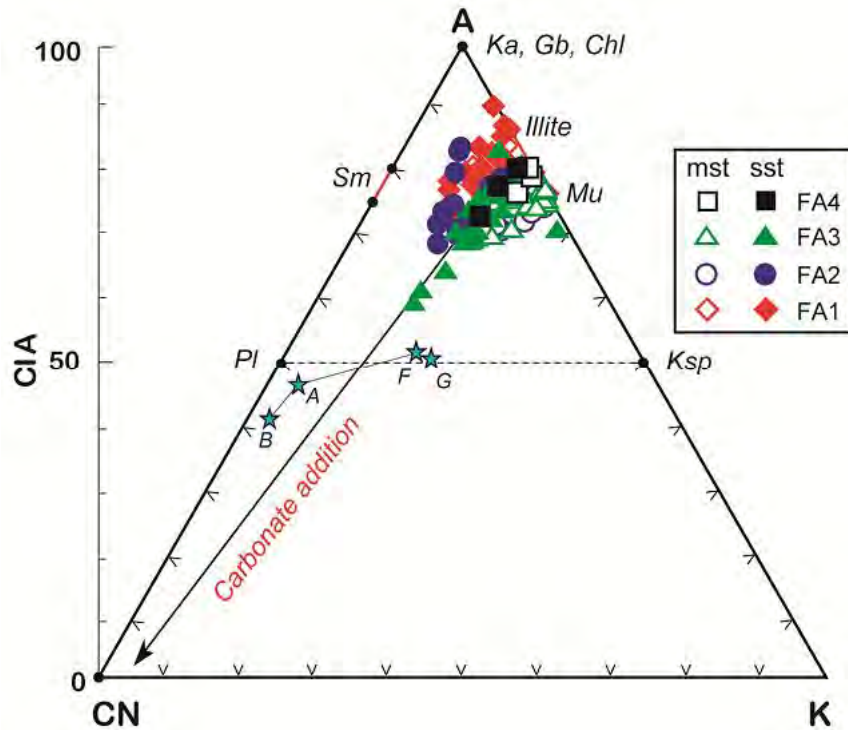


Fig. 6.12. A-CN-K plot (Nesbitt and Young, 1984) for the Siwalik Group sandstones (sst) and mudstones (mst), Khutia Khola section. CIA – Chemical Index of Alteration. Abbreviation: Stars rock averages: B- basalt; A- andesite; F- felsic volcanic rock, G- granite (Condic 1993). Minerals: Pl- plagioclase; Ksp- K-felspar, Sm- smectite; Mu- muscovite; Ka- Kaolinite; Gb- gibbsite; Chl- chlorite. Arrow lines show effect of carbonate addition.

Weathering intensity and approximate mineralogical composition of sediments can also be evaluated from the A-CNK-FM [$Al_2O_3 - (CaO^* + Na_2O + K_2O) - (Fe_2O_3 + MgO)$] (Nesbitt and Young, 1989) ternary plot (Fig. 6.13). Weathering paths are less predictable than those on the A-CN-K plot, due to the number of Fe-Mg phases that may occur, and their potentially variable compositions. An A-CNK-FM plot was

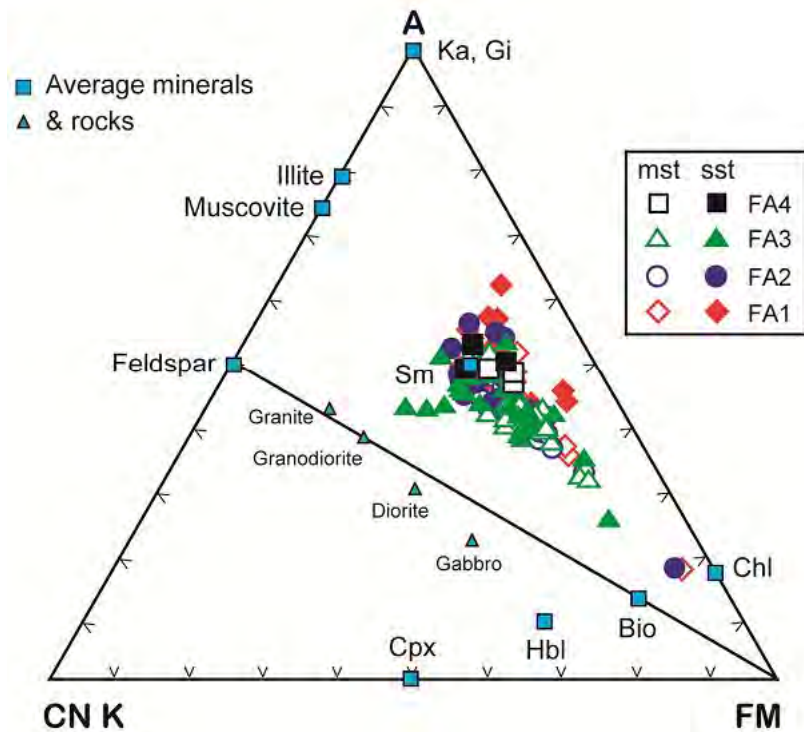


Fig. 6.13. A–CNK–FM plot (Nesbitt and Young, 1989) for the Siwalik Group sandstones (sst) and mudstones (mst), Khutia Khola section. A = Al_2O_3 , CNK = $\text{CaO}^* + \text{Na}_2\text{O} + \text{K}_2\text{O}$, FM = $\text{Fe}_2\text{O}_3\text{T} + \text{MgO}$, Mineral abbreviations: Ka = kaolinite, Gb = gibbsite, Sm = smectite, Chl = chlorite, Bio = biotite, Hbl = hornblende, Cpx = clinopyroxene.

constructed using the transformed data as described above, assuming CaO^* equals measured Na_2O . The Khutia Khola samples plot in a tight group above the Feldspar–FM tie-line, well above the compositions of pristine source rocks ranging from average gabbro through to granite (Fig. 6.13). This further illustrates the significant source weathering that has occurred. The FA1–FA2 samples cluster around smectite

composition, whereas FA3-FA4 sandstones and mudstones spread towards chlorite at lower A and greater FM. These contrasts again indicate more intense source weathering in the FA1-FA2 meandering river system, and influx of fresher detritus in FA3-FA4.

The MFW plot by Ohta and Arai (2007) can show provenance as well as the degree of source weathering. The MFW plot is based on the abundances of eight major elements (excluding MnO and P₂O₅), and multivariate statistical analyses and transformation to produce loadings for each element in individual samples. From these, values for three parameters are produced, namely M = mafic, F = felsic, and W = weathering products. These are combined on a ternary diagram, where fresh source rocks plot in an arc between M and F, depending on their composition. Weathered samples are displaced toward the W apex. As for the CIA calculation, CaO* was assumed to be equal to measured Na₂O content. The transformed data were then used to construct an M-F-W plot (Fig. 6.14). In this plot, the Khutia Khola samples cluster near the W apex (Fig. 6.14), indicative of significant source weathering. The data overall trend away from the primary source arc from a position between average TTG and felsic volcanic rock (FV), reflecting the evolved nature of the source. However, some FA3 sandstones plot closer to the source arc than FA1-FA2 equivalents. This indicates supply of fresh detritus in the braided river system (FA3-FA4), compared to the more

intense weathering in the meandering river system (FA1-FA2), as also shown by the A-CN-K systematics.

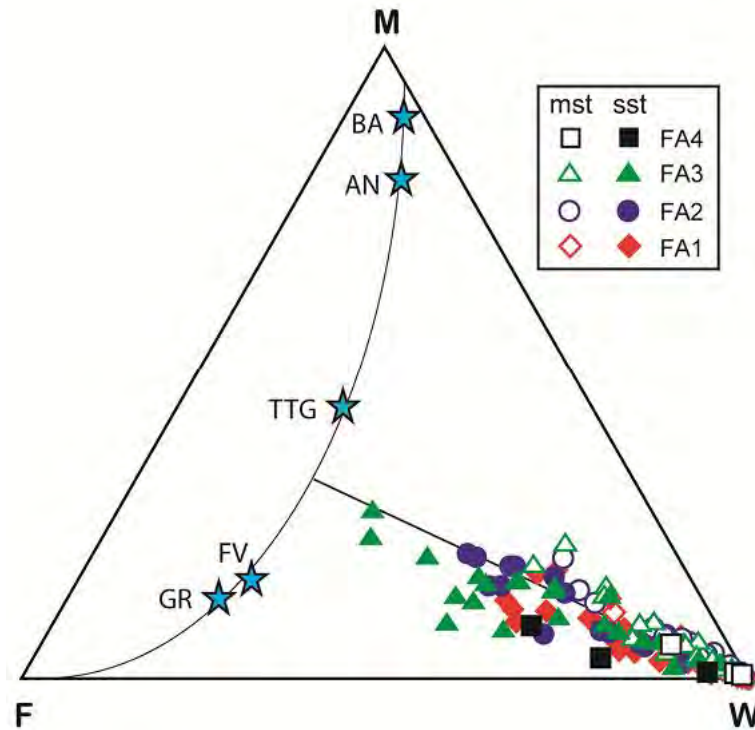


Fig. 6.14. M-F-W plot (Ohta and Arai, 2007) for the Siwalik Group sandstones (sst) and mudstones (mst), Khutia Kholā section, where M= mafic source, F = felsic source, and W = weathered material. Calculation procedure for the vertices is given in Ohta and Arai (2007). Curved line is the igneous rock trend. Stars are average values for Phanerozoic basalt (BA), andesite (AN), tonalite-trondhjemite-granodiorite (TTG), felsic volcanic rock (FV) and granite (GR) from Condie (1993). Arrow indicates weathering trend.

The SAM diagram (Kroonenberg, 1994) is a triangular diagram with the end members $S=SiO_2/20$, $A=(K_2O+Na_2O)$ and $M=(TiO_2+MgO+FeO)$, representing silica, alkalis and mafic components. SiO_2 and K_2O+Na_2O give a measure of felsic components (quartz and feldspar, respectively), whereas $TiO_2+MgO+FeO$ reflects mafic components including ferromagnesian minerals and matrix. Possible source rocks can be indicated by comparison with published average rock compositions, which form a primary igneous trend running from M towards the A–S edge (Fig. 6.15). Unmodified first-cycle sediments should therefore lie along this source evolution line. Modification by processes such as weathering and recycling increases SiO_2 contents, and samples then trend upwards towards the S apex as weathering or recycling progresses. Sorting effects are also evident, with sandstones usually having higher S values than associated mudstones due to quartz concentration. The original concept of the plot as developed by Kroonenburg (1994) was that it represents a geochemical version of QFL provenance plots.

A S-A-M plot for the Khutia Khola Siwalik data (Fig. 6.15) clearly shows the extent to which the sediment compositions have been modified by weathering, recycling and sorting. Mudstones are concentrated near the primary igneous trend near the composition of average andesite, and sandstones trend towards the S apex to values

reaching S_{70} . The S values in most of the FA1-FA2 sandstones are generally higher than in FA3-FA4 equivalents, which mainly cluster between S_{35} and S_{50} . This reflects the greater maturity and sorting fractionation of the sediments deposited in the meandering fluvial systems of FA1-FA2, and the influx of fresher detritus in the braided systems of FA3-FA4. The overall trend of the data indicate an average source composition near andesite, rather than the more felsic source indicated by the MFW plot (Fig. 6.14). This apparent discrepancy is most likely due to hydraulic concentration of Fe-Mg rich clays in the mudstones, as also suggested by the trend between smectite and chlorite on the A-CNK-FM plot (Fig. 6.13). The dolomitic component in diagenetic carbonate would also contribute to this shift of the finer-grained sediments towards the M apex.

The Ga/Rb- K_2O/Al_2O_3 binary plot devised by Roy and Roser (2013) also reflects weathering intensity associated with warm/wet and cold/dry climatic conditions. Increased weathering will produce higher Ga/Rb ratios and lower K_2O/Al_2O_3 ratios, and neither ratio should be greatly affected by carbonate diagenesis. On this plot, the Khutia Khola samples show extensive overlap, and ratios suggestive of moderate weathering (Fig. 6.16). However, FA1-FA2 samples clearly exhibit higher Ga/Rb ratios and lower K_2O/Al_2O_3 ratios than FA3-FA4 samples. This further supports the concept of higher weathering in the meandering river system, and influx of fresher

detritus in the braided river system.

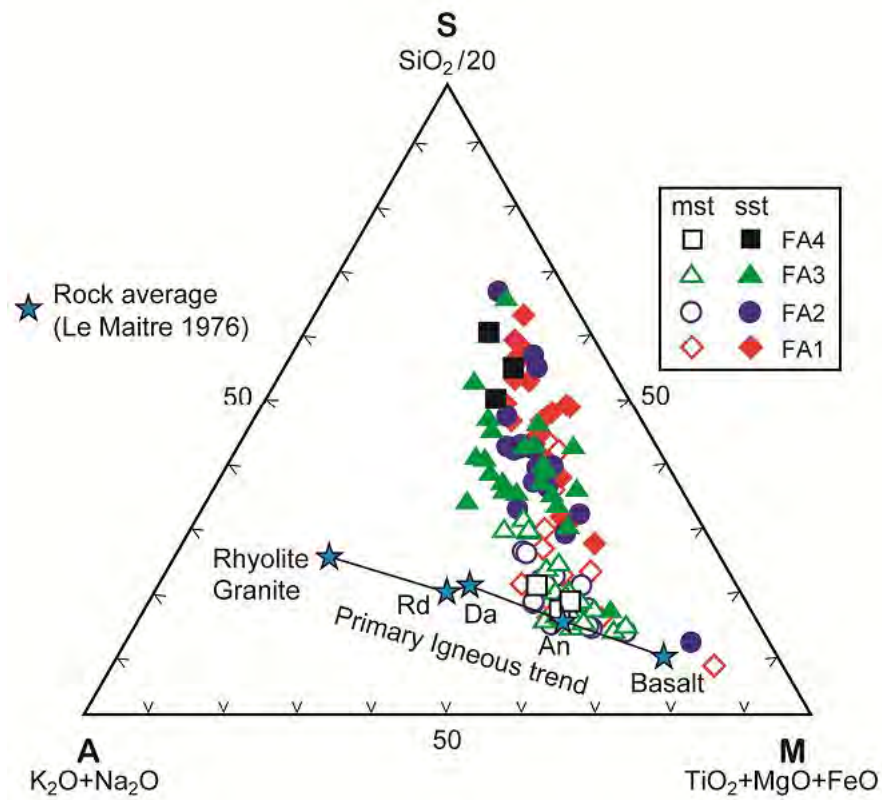


Fig. 6.15. S-A-M plot (Kroonenburg, 1994) for the Siwalik Group sandstones (sst) and mudstones (mst), Khutia Khola section. Rock average abbreviations: An = andesite, Da – dacite, Rd – rhyodacite. Rock averages from Le Maitre (1976).

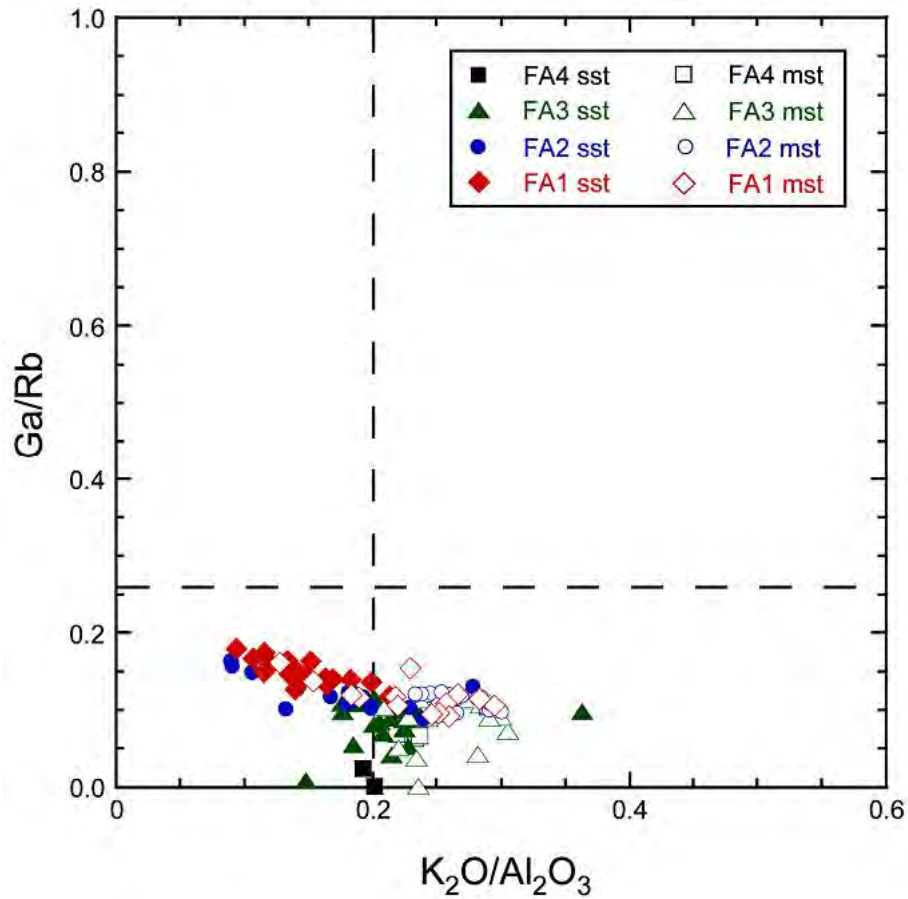


Fig. 6.16. Ga/Rb-K₂O/Al₂O₃ plot (Roy and Roser, 2013) for the Siwalik Group sandstones (sst) and mudstones (mst), Khutia Khola section.

6.10. Stratigraphic variation by lithotypes

Stratigraphic variations in selected elemental ratios by lithotype (sandstone and mudstone) were plotted to examine the possible effects of upward change in fluvial style, weathering intensity and provenance. The ratios used were chosen to avoid the effects of CaCO₃ dilution, by utilizing elements which are not contained within

authigenic calcite. Plots using the raw data for these two end members did not show clear trends, as shown by the examples $\text{SiO}_2/\text{Al}_2\text{O}_3$ and Basicity Index (Fig. 6.17), and also Th/Sc and $\text{Na}_2\text{O}/\text{Al}_2\text{O}_3$ (Fig. 6.18).

$\text{SiO}_2/\text{Al}_2\text{O}_3$ ratio is a well-known maturity indication as it reflects the ratio of quartz to feldspars plus clays. Therefore, the ratio can reflect recycling, the influence of weathering, and the extent of sand-mud fractionation. Using the raw data (Fig. 6.17) the mudstones typically have lower and more uniform $\text{SiO}_2/\text{Al}_2\text{O}_3$ ratios than the sandstones. As a result of higher clay contents and restricted grain size range in the former compared to the latter. The sandstones have very variable $\text{SiO}_2/\text{Al}_2\text{O}_3$ ratios (~7-20) as a result of higher quartz content and more variable grain size.

The Basicity Index (BI) gives a measure of the ratio of ferromagnesian minerals (e.g. olivine, pyroxene) versus quartz and feldspar (Kumon and Kiminami, 1994). Higher Basicity Index values indicate more mafic composition (Rosser et al., 2002). The Basicity Index is not totally independent of the effects of diagenesis in this section, however, as the dolomitic component in authigenic carbonate cements in individual samples would increase BI in samples rich in added carbonate. The raw data show the reverse pattern to $\text{SiO}_2/\text{Al}_2\text{O}_3$, with lower and more uniform ratios in the sandstones, and higher and more variable ratios in the mudstones (Fig. 6.17). No clear

vertical trends are apparent for either variable.

The immobile trace element ratio Th/Sc gives a good measure of average source composition, as it is not as affected by heavy mineral effects (e.g. zircon concentration) and sorting as the commonly-used companion Zr/Sc ratio. The Th/Sc plot based on raw data (Fig. 6.18) shows less contrast between sandstones and mudstones, with ratios in sandstones only slightly less than in the former than in the latter. Unlike $\text{SiO}_2/\text{Al}_2\text{O}_3$, and Basicity Index, there is a slight decline in ratios upward in both lithotypes, suggesting a slightly less geochemically evolved source with time, or the introduction of a mafic or ultramafic component in the higher stratigraphic levels. However, there is still considerable variability within each lithotype, with ratios frequently overlapping.

$\text{Na}_2\text{O}/\text{Al}_2\text{O}_3$ ratios are used as a proxy for the proportion of Na-rich detrital albite to Na-poor, Al-rich clay weathering products. High values of the $\text{Na}_2\text{O}/\text{Al}_2\text{O}_3$ ratio suggest some albite remains within the sample, and thus chemical weathering in the source was less. As for $\text{SiO}_2/\text{Al}_2\text{O}_3$, and Basicity Index, vertical variations in the raw $\text{Na}_2\text{O}/\text{Al}_2\text{O}_3$ ratios are considerable. Ratios in the sandstones are generally higher than in mudstones at the same stratigraphic level, consistent with survival of greater volumes of unaltered albite in the coarser sediments, and less in the mudstones and

siltstones. However, again there is no clear stratigraphic trend in the raw ratios.

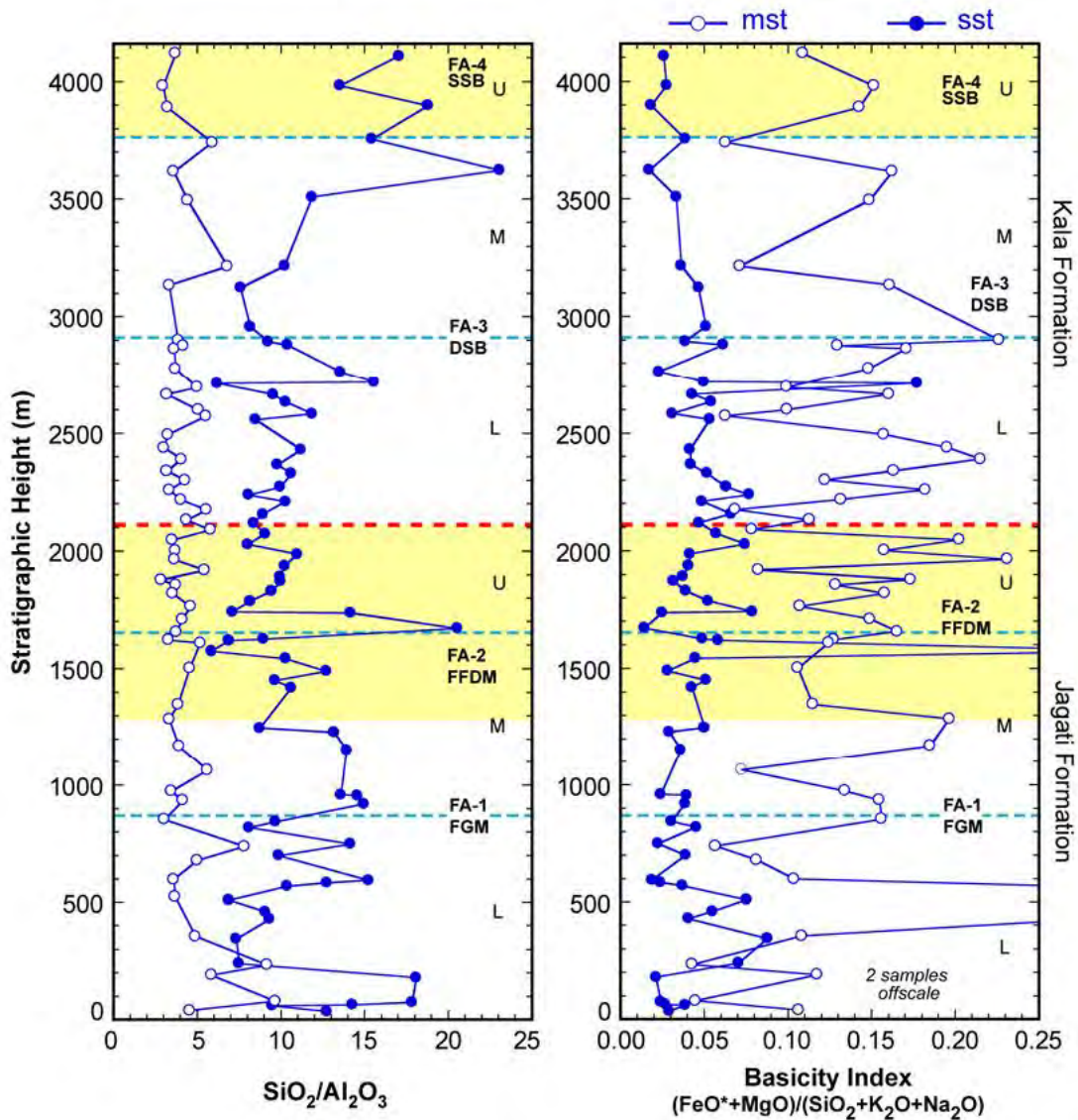


Fig. 6.17. Stratigraphic variation (*raw data*) in $\text{SiO}_2/\text{Al}_2\text{O}_3$ ratios and Basicity Index in the Khutia Khola Siwalik sandstones (sst) and mudstones (mst). Abbreviations: FA – facies association. FGM – fine-grained meandering; FFDM – flood-flow dominated meandering; SSB – shallow sandy braided; DSB – deep sandy braided. U – Upper; M – Middle; L – Lower.

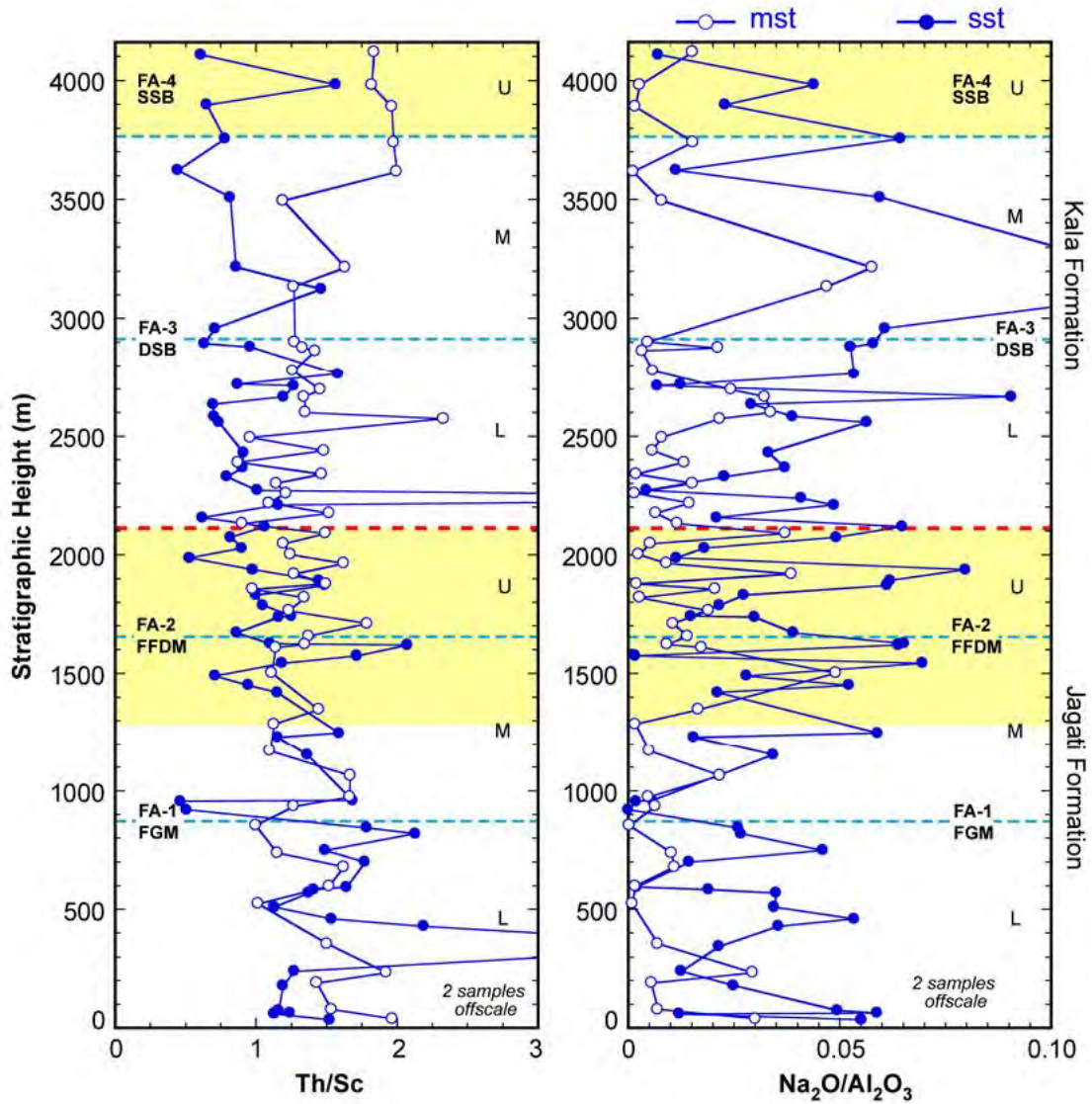


Fig. 6.18. Stratigraphic variation (*raw data*) in Th/Sc and Na₂O/Al₂O₃ ratios in the Khutia Khola Siwalik sandstones (sst) and mudstones (mst). Abbreviations: FA – facies association. FGM – fine-grained meandering; FFDM – flood-flow dominated meandering; SSB – shallow sandy braided; DSB – deep sandy braided. U – Upper; M – Middle; L – Lower.

The variability and lack of stratigraphic trend in the raw data plots for $\text{SiO}_2/\text{Al}_2\text{O}_3$, Basicity Index, and $\text{Na}_2\text{O}/\text{Al}_2\text{O}_3$ are attributed to variations in grain size of individual samples within each lithotype. Sorting effects within each lithotype thus contribute to “noise” within the data categories, potentially obscuring any trends resulting from contrasts in lithofacies, weathering intensity and provenance. To overcome this problem, the data were smoothed using a five-point moving average to reduce the variability of ratios with lithotypes due to grain size variations, as done by Roser et al. (2002) in the Bakiya Khola section. Values for the five lowermost samples in each lithotype are first averaged, with the next overlying sample then included in the moving average, while the lowermost sample is removed from the calculation.

The five-point moving averages for sandstone and mudstone averages in the modified $\text{SiO}_2/\text{Al}_2\text{O}_3$ ratio plot (Fig. 6.19) are well separated throughout the Khutia Khola section. The ratios of the sandstones are high in the lower part of FA1 and slightly decrease up-section, suggesting the effect of strong weathering, influence of the meandering river system and greater sorting fractionation in the lower part of the Jagati Formation. The sandstone moving average is relatively stable through the upper part of FA2 and the lower part of FA3, before increasing to higher ratios in FA4. This later increase is probably caused by coarsening of the sandstones in the upper part of the

braided system. However, the increase may also be partly due to the wider spacing of samples in this interval, and accidental sampling bias towards coarser samples in FA4. Similarly, the mudstone moving averages show a gentle decline from the lower to middle part of FA1, and similar pattern up to lower part of FA3 indicates the effects of strong weathering in the mudstones in the lower part of the Jagati Formation (Fig. 6.19); however, there is no great change after. The $\text{SiO}_2/\text{Al}_2\text{O}_3$ ratio trend thus seem to record higher weathering in the lower part, moderately stable conditions in the middle part, and supply of fresh sediments by braided river systems in the Kala Formation.

The five-point moving averages for Basicity Index in the sandstones are relatively constant in FA1, and increase slightly (~ 0.10) in the middle part of FA2, possibly due to higher content of mafic minerals such as biotite (Fig. 6.19). Afterward the sandstone data decline to lower (more felsic) values of < 0.05 . The mudstone data shows much clearer variation, with ratios similar to sandstones. The curve trends to higher ratios in the mudstones, reflecting the higher clay content of the finer grained sediments, and also suggesting the presence of more mafic minerals, including biotite and chlorite.

The moving averages of Th/Sc in both mudstones and sandstones show higher values in FA1 and decline slightly to lower ratio values to the upper part of the section

(Fig. 6.20). This indicates shift to slightly less felsic source upward, as also suggested by the trend for Basicity Index (Fig. 6.20). This shift could, however, also be produced by the introduction of a small amount of material with high geochemical contrast compared to the rest of the source, such as ultramafic detritus.

The moving average for $\text{Na}_2\text{O}/\text{Al}_2\text{O}_3$ in the mudstones shows no great change throughout the section, apart from a small increase in the upper part of FA3. The mudstone moving average ratios are lower than the sandstones, which suggests that the mudstones consist mainly of weathering products (Roser, 2000) (Fig. 6.20). The sandstones show a large compositional change. Values are low in FA1, suggesting higher source weathering. The values increase in FA2 and remain higher up-section, especially in the upper part of FA3, suggesting influx of fresher sediments in the braided systems in Kala Formation.

Stratigraphic plots of $\text{K}_2\text{O}/\text{Al}_2\text{O}_3$ can also be used as an index for the ratio of fresh K-feldspar to weathering products. Higher ratios in sandstones indicate less weathering. Similarly, Ga/Rb ratios are higher in intense weathering, and lower in weak weathering (Roy and Roser, 2013). A large difference is seen in the values of both plots of the mudstones and sandstone in lower part of the section (Fig. 6.21). In FA1, average $\text{K}_2\text{O}/\text{Al}_2\text{O}_3$ ratios are low and Ga/Rb ratios are high, suggesting the influence of strong

weathering in the meandering river system (Fig. 6.21). Increasing average K_2O/Al_2O_3 and decreasing Ga/Rb ratios stratigraphically upward reflect less weathering upsection and increased supply of voluminous fresh detritus due to uplift and erosion.

The stratigraphic variation ratio plots in the Khutia Khola section show some interesting geochemical features, even though the extensive carbonate diagenesis present causes complications. The ratios reflect more intense weathering and uniform source in the meandering river systems in FA1-FA2. The systematic changes evident in elemental ratios (Na_2O/Al_2O_3 , K_2O/Al_2O_3 and Ga/Rb) suggest response to change in fluvial style in FA3-FA4 (from meandering to braided river system). The geochemical changes identified in this study illustrate the complexity of the system controlling the composition of clastic sediments (c.g. Johnsson, 1993). They also show how change in provenance, influence of sorting and weathering, heavy mineral concentration and fluvial style are recorded as geochemical signals through stratigraphic sections.

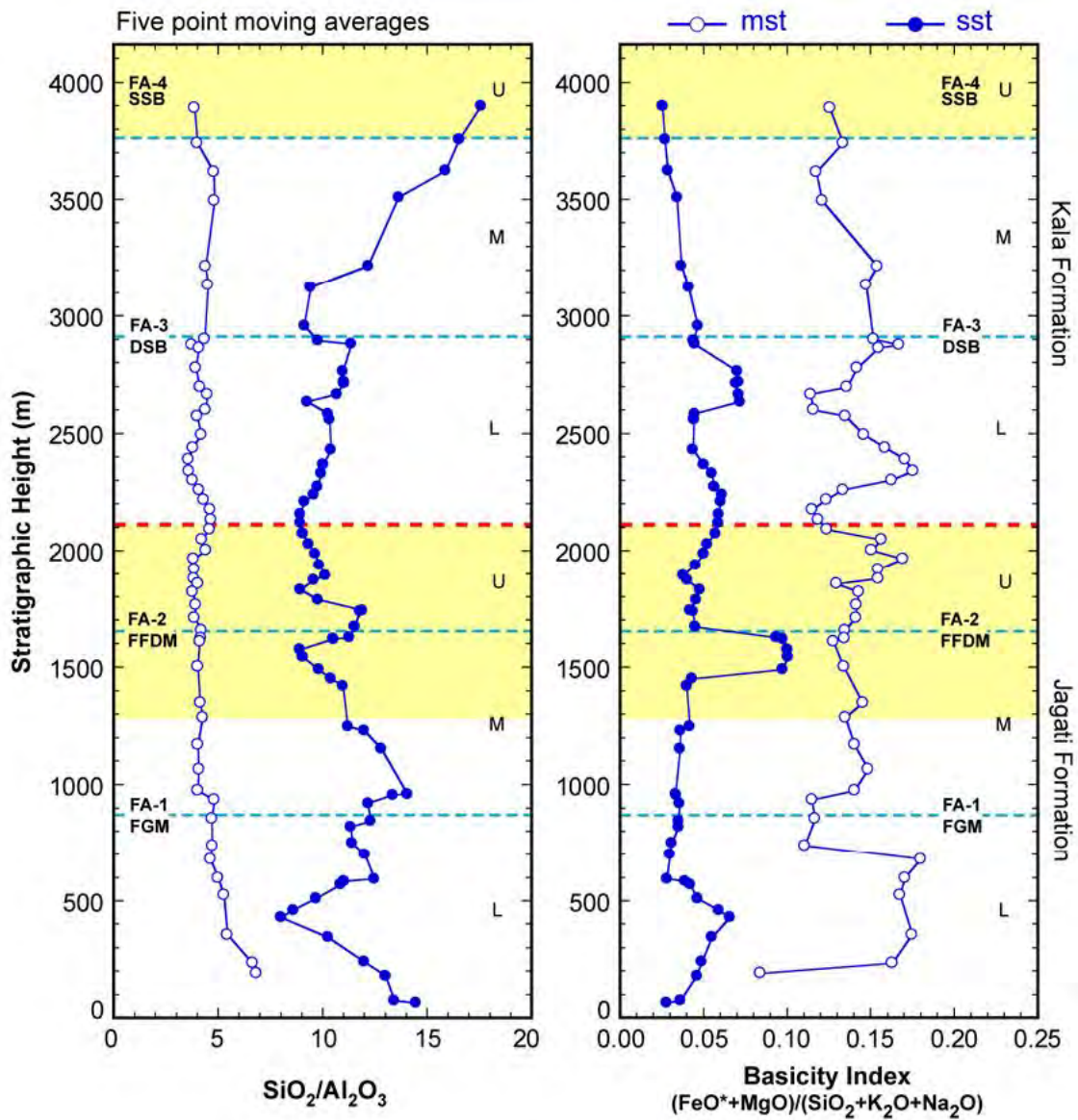


Fig. 6.19. Stratigraphic variation (*five-point moving averages*) in $\text{SiO}_2/\text{Al}_2\text{O}_3$ ratios and Basicity Index in the Khatia Khola Siwalik sandstones (sst) and mudstones (mst). Abbreviations: FA – facies association. FGM – fine-grained meandering; FFDM – flood-flow dominated meandering; SSB – shallow sandy braided; DSB – deep sandy braided. U – Upper; M – Middle; L – Lower.

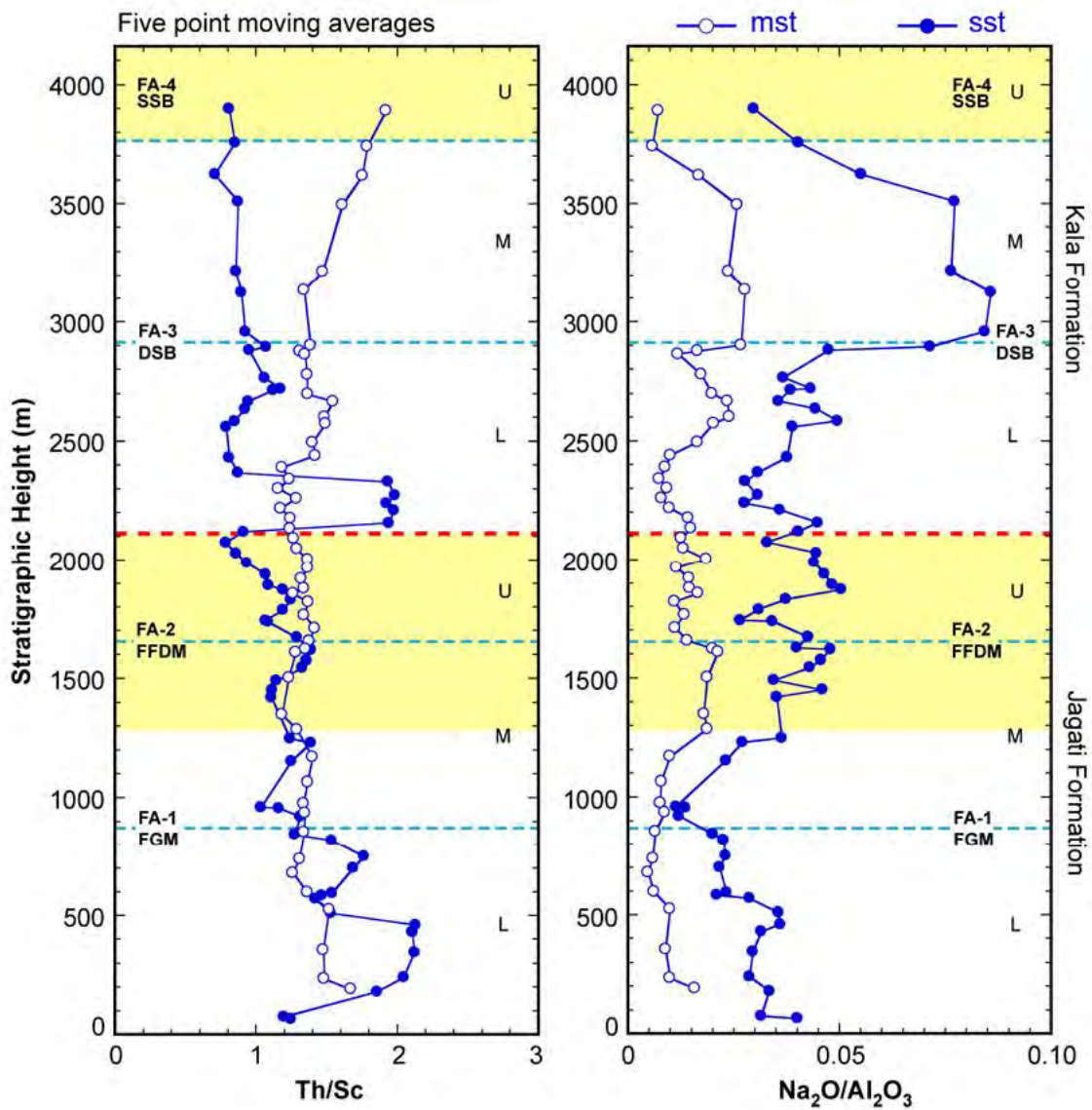


Fig. 6.20. Stratigraphic variation (*five-point moving averages*) in Th/Sc and Na₂O/Al₂O₃ ratios in the Khutia Khola Siwalik sandstones (sst) and mudstones (mst). Abbreviations: FA – facies association. FGM – fine-grained meandering; FFDM – flood-flow dominated meandering; SSB – shallow sandy braided; DSB – deep sandy braided. U – Upper; M – Middle; L – Lower.

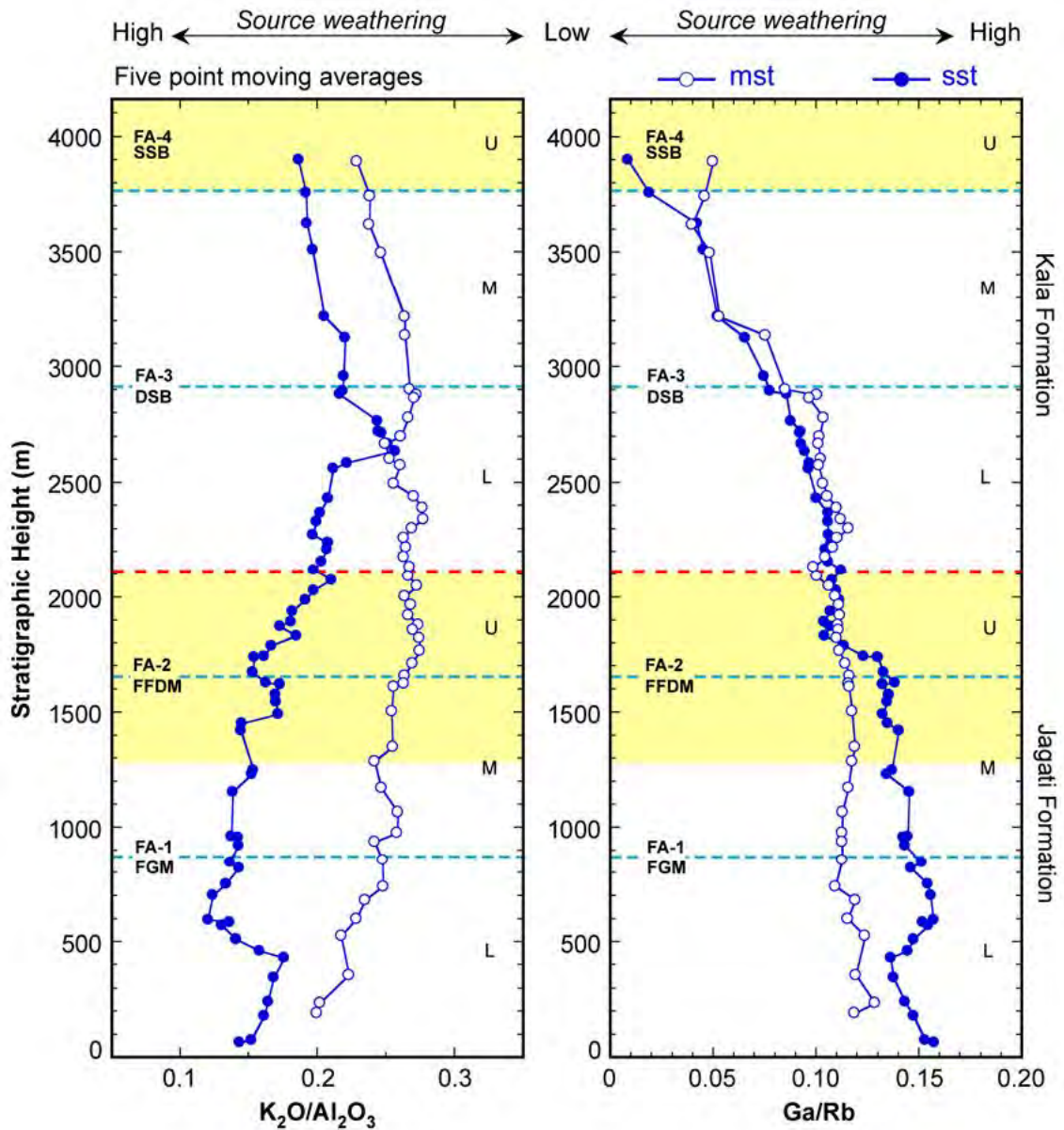


Fig. 6.21. Stratigraphic variation (*five-point moving averages*) in K_2O/Al_2O_3 and Ga/Rb ratios in the Khutia Khola Siwalik sandstones (sst) and mudstones (mst). Abbreviations: FA – facies association, FGM – fine-grained meandering; FFDM – flood-flow dominated meandering; SSB – shallow sandy braided; DSB – deep sandy braided. U – Upper; M – Middle; L – Lower.

Table 6.1. XRF analyses of Siwalik sandstones and mudstones from the Kala and Jagati Formations, Khutia Khola section, Nepal.

Major elements wt%, trace elements ppm, total iron as Fe₂O₃. Data are tabulated anhydrous normalized (major elements summing to 100.0 wt%). Original anhydrous analytical total (Total*) and hydrous loss on ignition (LOI) are listed at right. Abbreviations: SmN - sample number; Metre - stratigraphic height in metre; Lith - lithology: FS, M, CS, VCS - fine, medium, coarse, very coarse grained sandstone, respectively; Mst - mudstone; FA - Facies association; FA1 - fine-grained meandering; FA2 - flood-flow dominated meandering; FA3 - deep sandy braided; FA4 - shallow sandy braided.

(A) SANDSTONES

SmN	Metre	Lith	FA	SiO ₂	TiO ₂	Al ₂ O ₃	Fe ₂ O ₃	MnO	MgO	CaO	Na ₂ O	K ₂ O	P ₂ O ₅	Ba	Ce	Cr	Ga	Nb	Ni	Pb	Rb	Sc	Sr	Th	V	Y	Zr	Total*	LOI
-----	-------	------	----	------------------	------------------	--------------------------------	--------------------------------	-----	-----	-----	-------------------	------------------	-------------------------------	----	----	----	----	----	----	----	----	----	----	----	---	---	----	--------	-----

KALA FORMATION

Upper Member

KS-121	4108	CS	FA4	72.84	0.20	4.27	1.59	0.19	0.47	19.50	0.03	0.86	0.05	146	32	3	0	6	3	11	49	12.9	74	7.9	10	15	116	98.98	13.59
KS-120	3983	VCS	FA4	84.21	0.32	6.23	1.80	0.04	0.75	5.04	0.27	1.28	0.05	261	58	7	-3	9	6	16	75	12.1	65	18.9	26	18	275	99.46	5.02
KS-118	3898	CS	FA4	84.19	0.23	4.48	1.25	0.31	0.43	8.10	0.10	0.86	0.03	176	31	3	1	7	2	12	52	12.6	43	8.2	15	11	149	99.56	6.69

Middle Member

KS-116	3756	CS	FA3	80.72	0.31	5.23	1.79	0.07	1.54	8.99	0.34	0.97	0.05	192	54	14	3	8	5	11	51	14.3	111	11.1	27	19	248	99.22	7.59
KS-114	3623	CS	FA3	82.39	0.15	3.57	1.15	0.20	0.39	11.55	0.04	0.53	0.03	139	31	-2	0	5	2	9	34	12.4	97	5.5	4	15	98	99.77	8.95
KS-112	3510	CS	FA3	76.82	0.27	6.46	1.74	0.06	1.06	11.68	0.38	1.47	0.05	222	41	10	4	7	7	14	82	12.7	166	10.3	19	17	146	99.44	9.38
KS-110	3217	CS	FA3	77.37	0.29	7.57	1.91	0.06	1.19	9.10	0.89	1.58	0.06	248	51	7	6	8	5	16	89	13.8	136	11.8	26	18	123	99.61	8.21
KS-107	3125	CS	FA3	77.33	0.39	10.21	2.91	0.06	1.14	4.31	1.35	2.19	0.10	402	65	15	5	11	8	21	118	12.5	88	18.3	38	25	164	99.93	4.26
KS-106	2960	VCS	FA3	80.46	0.36	9.85	3.19	0.02	1.38	1.89	0.60	2.21	0.04	401	41	34	11	10	18	21	131	13.1	57	9.3	50	13	128	100.51	3.16

Lower Member

KS-104	2895	CS	FA3	70.67	0.26	7.65	1.66	0.07	1.31	16.17	0.44	1.72	0.05	294	43	14	6	7	9	16	84	13.6	191	8.6	18	16	136	99.61	12.37
KS-103	2880	CS	FA3	74.49	0.36	7.17	3.11	0.05	1.90	10.87	0.38	1.60	0.07	252	42	15	9	9	11	16	86	10.4	137	10.0	31	22	140	98.98	9.74
KS-99	2765	VCS	FA3	89.08	0.24	6.58	1.59	0.01	0.65	0.12	0.35	1.35	0.02	245	41	8	7	7	7	13	81	5.8	24	9.2	18	14	123	99.49	1.22
KS-98	2720	CS	FA3	71.89	0.29	4.62	1.72	0.06	2.09	18.29	0.06	0.93	0.06	164	64	3	4	7	4	10	48	12.1	274	10.5	15	25	298	97.79	14.03
KS-97	2714	FS	FA3	54.53	0.47	8.81	3.26	0.21	7.31	21.98	0.06	3.20	0.18	314	54	36	12	10	17	34	124	9.8	290	12.5	44	21	137	99.15	19.95

Table 6.1. (ctd). XRF analyses of Siwalik sandstones and mudstones from the Kala and Jagati Formations, Khutia Khola section, Nepal.

SANDSTONES (CTD)

KALA FORMATION (CTD)

Sm/N	Metre	Lith	FA	SiO ₂	TiO ₂	Al ₂ O ₃	Fe ₂ O ₃	MnO	MgO	CaO	Na ₂ O	K ₂ O	P ₂ O ₅	Ba	Ce	Cr	Ga	Nb	Ni	Pb	Rb	Sc	Sr	Th	V	Y	Zr	Total*	LOI		
Lower Member (ctd)																															
KS-94	2666	VCS	FA3	83.09	0.35	8.73	2.71	0.03	1.25	1.00	0.79	1.99	0.06	361	51	14	11	9	12	19	107	10.1	42	12.1	35	16	143	99.82	2.33		
KS-93	2635	CS	FA3	62.56	0.30	6.09	2.37	0.09	1.35	25.58	0.18	1.43	0.05	235	49	16	7	8	8	15	73	11.9	275	8.2	23	26	159	97.88	16.99		
KS-91	2585	VCS	FA3	80.46	0.21	6.78	1.62	0.05	1.09	7.92	0.26	1.56	0.04	281	27	9	8	7	8	17	89	9.3	145	6.5	17	11	104	98.53	7.20		
KS-89	2560	MS	FA3	67.65	0.36	7.96	2.49	0.10	1.48	17.65	0.45	1.80	0.06	304	49	15	8	9	10	16	93	14.1	258	10.4	25	23	178	97.98	13.25		
KS-86	2432	CS	FA3	77.25	0.41	6.90	2.28	0.07	1.23	10.26	0.23	1.30	0.07	217	65	13	7	10	7	16	69	13.2	185	12.1	29	27	247	98.55	8.86		
KS-84	2368	CS	FA3	77.66	0.31	7.93	2.28	0.07	1.27	8.71	0.29	1.40	0.06	238	47	12	8	8	9	19	79	11.2	173	10.1	24	21	155	98.57	8.08		
KS-82	2330	MS	FA3	75.52	0.37	7.10	2.57	0.05	1.68	10.95	0.16	1.53	0.06	256	62	25	9	9	11	16	74	13.6	182	10.8	31	17	182	99.07	9.89		
KS-80	2272	FS	FA3	70.44	0.44	7.08	3.24	0.05	1.63	15.59	0.03	1.42	0.08	221	79	31	8	10	13	15	68	14.4	226	14.5	39	20	264	98.38	12.67		
KS-78	2240	CS	FA3	47.25	0.41	5.85	2.71	0.07	1.30	40.78	0.24	1.25	0.13	199	111	14	5	9	14	17	56	3.0	357	17.9	23	28	668	98.45	9.41		
KS-76	2210	FS	FA3	76.15	0.38	7.40	2.37	0.07	1.66	10.23	0.36	1.30	0.08	254	67	12	8	10	8	20	71	11.8	174	13.7	25	27	236	98.81	23.38		
KS-74	2157	MS	FA3	61.34	0.37	6.89	2.87	0.15	1.58	24.64	0.14	1.59	0.42	249	52	24	9	9	11	21	81	12.5	251	7.7	30	28	157	98.01	16.61		
KS-72	2120	CS	FA3	80.13	0.39	9.57	2.75	0.03	1.40	3.02	0.62	2.03	0.06	312	49	18	13	11	13	17	125	10.0	74	10.6	38	16	136	99.67	4.25		

JAGATI FORMATION

Upper Member

KS-70	2075	MS	FA2	66.49	0.39	7.34	3.26	0.08	0.97	19.70	0.36	1.33	0.08	204	70	16	9	10	13	20	76	15.3	162	12.5	30	25	238	98.38	13.92
KS-68	2028	FS	FA2	65.86	0.47	8.21	3.24	0.07	2.12	18.27	0.15	1.52	0.09	228	65	29	10	11	14	19	80	14.2	172	12.8	40	26	254	98.52	14.23
KS-66	1988	CS	FA2	61.45	0.24	5.60	1.69	0.12	1.10	28.35	0.06	1.34	0.05	206	39	9	6	6	6	28	70	12.0	223	6.4	13	24	130	97.87	18.10
KS-64	1938	MS	FA2	68.79	0.33	6.72	2.01	0.22	1.04	19.15	0.54	1.13	0.07	163	62	13	7	9	7	36	65	10.8	191	10.6	15	32	204	98.31	13.77
KS-62	1893	MS	FA2	79.49	0.43	7.98	2.37	0.07	0.92	6.71	0.49	1.46	0.08	209	72	12	10	11	10	18	89	9.4	91	13.5	32	25	294	99.20	6.27
KS-60	1872	MS	FA2	80.13	0.39	8.02	2.06	0.11	0.73	6.94	0.49	1.07	0.06	168	73	12	8	10	10	18	76	11.5	135	17.1	28	28	305	98.89	6.75
KS-58	1830	FS	FA2	72.04	0.43	7.62	1.88	0.10	1.18	15.08	0.21	1.38	0.09	198	74	26	8	10	12	16	73	14.8	180	14.8	29	23	325	98.26	11.89
KS-56	1788	FS	FA2	78.84	0.45	9.66	3.37	0.07	1.19	4.19	0.21	1.92	0.09	298	68	30	11	11	16	42	109	12.6	77	13.2	48	21	208	98.93	5.3

Table 6.1. (ctd). XRF analyses of Siwalik sandstones and mudstones from the Kala and Jagati Formations, Khutia Khola section, Nepal.

**SANDSTONES (CTD)
JAGATI FORMATION (CTD)**

SmN	Metre	Lith	FA	SiO ₂	TiO ₂	Al ₂ O ₃	Fe ₂ O ₃	MnO	MgO	CaO	Na ₂ O	K ₂ O	P ₂ O ₅	Ba	Ce	Cr	Ga	Nb	Ni	Pb	Rb	Sc	Sr	Th	V	Y	Zr	Total*	LOI		
Upper Member (ctd)																															
KS-54	1743	MS	FA2	54.97	0.54	7.73	3.13	0.17	1.66	29.80	0.11	1.77	0.12	285	87	21	9	12	13	35	83	12.2	266	15.2	39	31	336	98.16	19.3		
KS-53	1738	MS	FA2	85.64	0.36	6.05	1.73	0.04	0.61	4.76	0.18	0.55	0.08	146	61	6	7	9	6	11	45	10.1	65	11.8	23	21	256	99.09	4.8		
KS-51	1672	CS	FA2	89.91	0.27	4.37	0.96	0.12	0.43	3.24	0.17	0.47	0.05	106	44	3	5	8	5	32	35	8.6	65	7.4	15	19	117	99.51	3.4		
KS-49	1628	FS	FA2	77.96	0.44	8.71	3.25	0.06	0.97	6.71	0.57	1.25	0.08	271	61	17	11	11	15	16	76	11.4	107	12.5	39	21	248	99.17	6.76		
Middle Member																															
KS-47	1620	FS	FA2	79.47	0.56	11.53	4.03	0.01	1.18	0.23	0.74	2.22	0.04	325	84	39	15	13	18	15	129	8.2	46	17.0	60	28	307	99.96	2.59		
KS-45	1574	FS	FA2	34.89	0.35	5.98	2.97	0.09	9.05	44.93	0.01	1.67	0.06	187	37	24	8	8	12	32	61	3.5	161	6.0	27	18	138	101.17	28.87		
KS-44	1545	CS	FA2	82.23	0.29	8.00	2.28	0.02	1.68	3.74	0.56	1.14	0.06	167	48	13	9	9	11	12	74	7.2	53	8.6	28	15	142	99.47	5.28		
KS-42	1490	MS	FA2	82.67	0.28	6.51	1.62	0.09	0.88	7.12	0.18	0.59	0.06	113	52	14	7	8	6	25	45	11.6	92	8.3	26	17	169	98.83	6.84		
KS-41	1450	FS	FA2	73.37	0.42	7.60	2.61	0.12	1.46	12.85	0.40	1.10	0.07	189	64	16	9	10	11	26	67	12.2	138	11.5	32	25	218	98.46	10.62		
KS-40	1419	FS	FA2	77.62	0.40	7.31	2.50	0.12	1.12	9.21	0.15	1.46	0.09	243	76	24	8	10	12	42	81	9.6	107	11.1	27	19	251	98.67	8.02		
KS-37	1250	FS	FA1	82.42	0.54	9.41	3.43	0.05	1.14	1.05	0.56	1.39	0.03	230	90	34	11	13	21	14	80	10.8	40	17.2	48	27	234	100.08	2.79		
KS-36	1230	CS	FA1	88.91	0.32	6.76	2.06	0.01	0.75	0.11	0.10	0.94	0.04	162	47	17	9	9	8	19	56	7.6	21	8.8	31	14	156	99.61	1.39		
KS-34	1155	CS	FA1	88.22	0.51	6.34	2.65	0.04	0.84	0.28	0.22	0.86	0.06	133	58	11	8	13	9	8	54	8.6	19	11.8	33	22	199	99.64	1.34		
KS-31	980	MS	FA1	89.60	0.29	6.59	1.73	0.02	0.64	0.14	0.04	0.92	0.02	262	49	16	9	9	14	9	69	5.6	24	9.4	33	16	132	99.99	1.55		
KS-30	955	CS	FA1	69.82	0.24	4.79	2.01	0.21	0.98	21.26	0.01	0.62	0.05	128	40	6	6	7	6	12	35	13.1	166	6.1	18	20	102	97.99	15.00		
KS-28	920	MS	FA1	72.42	0.27	4.84	1.70	0.11	1.28	18.64	0.00	0.68	0.06	115	49	8	5	8	5	29	39	13.5	179	6.8	10	24	122	98.02	13.81		
Lower Member																															
KS-26	845	FS	FA1	84.91	0.61	8.77	1.97	0.02	0.86	1.14	0.23	1.43	0.07	522	100	29	11	13	15	14	77	9.5	46	16.9	52	25	499	99.36	2.73		
KS-25	820	FS	FA1	83.07	0.57	10.25	3.00	0.01	1.14	0.25	0.27	1.42	0.01	226	106	31	13	13	15	9	83	8.5	27	18.1	51	23	434	100.03	3.50		
KS-24	750	MS	FA1	87.87	0.42	6.21	1.45	0.04	0.69	2.31	0.29	0.66	0.05	136	78	20	7	10	7	12	44	8.4	45	12.5	33	20	355	99.66	3.10		
KS-22	700	FS	FA1	83.15	0.48	8.41	2.71	0.08	0.86	2.75	0.12	1.38	0.06	229	88	27	11	12	19	28	81	9.2	52	16.4	50	27	337	99.78	4.16		

Table 6.1. (ctd). XRF analyses of Siwalik sandstones and mudstones from the Kala and Jagati Formations, Khutia Khola section, Nepal.

SANDSTONES (CTD)

JAGATI FORMATION (CTD)

SmN	Metre	Lith	FA	SiO ₂	TiO ₂	Al ₂ O ₃	Fe ₂ O ₃	MnO	MgO	CaO	Na ₂ O	K ₂ O	P ₂ O ₅	Ba	Ce	Cr	Ga	Nb	Ni	Pb	Rb	Sc	Sr	Th	V	Y	Zr	Total*	LOI		
Lower Member (ctd)																															
KS-19	595	CS	FA1	91.09	0.34	5.98	1.40	0.01	0.47	0.11	0.01	0.56	0.03	110	70	12	7	9	11	8	42	6.4	19	10.5	19	21	309	99.61	1.50		
KS-18	585	CS	FA1	89.18	0.36	7.00	1.58	0.01	0.74	0.14	0.13	0.81	0.05	134	61	15	9	10	10	10	58	8.2	17	11.5	33	19	242	100.01	1.84		
KS-17	570	CS	FA1	84.92	0.45	8.19	2.48	0.03	0.97	1.62	0.29	0.99	0.07	161	70	19	10	11	13	8	64	10.1	31	13.8	44	20	263	99.77	3.20		
KS-15	510	FS	FA1	67.06	0.61	9.75	2.98	0.12	2.52	14.73	0.34	1.79	0.10	285	79	37	12	14	20	22	87	14.1	157	15.9	52	25	348	98.64	13.13		
KS-14	460	FS	FA1	78.04	0.50	8.61	3.04	0.07	1.64	6.36	0.46	1.18	0.10	223	88	16	10	12	13	13	69	9.7	66	14.8	47	24	360	99.46	7.34		
KS-13	430	FS	FA1	84.52	0.51	9.08	2.64	0.02	1.13	0.39	0.32	1.33	0.06	202	82	28	11	12	17	14	78	7.3	36	16.0	48	27	364	99.86	2.38		
KS-11	345	FS	FA1	44.66	0.63	6.08	3.06	0.37	1.29	42.47	0.13	1.22	0.09	178	129	15	7	12	12	35	54	3.9	139	17.2	32	41	701	99.34	24.73		
KS-10	240	FS	FA1	75.60	0.54	10.08	3.55	0.05	2.28	5.55	0.13	2.15	0.07	300	77	32	13	13	18	22	108	13.4	67	17.1	49	25	295	99.51	7.41		
KS-7	180	MS	FA1	90.84	0.32	5.02	1.40	0.02	0.68	0.83	0.13	0.72	0.04	113	60	8	6	9	4	9	43	7.6	26	9.1	25	17	255	99.52	1.71		
KS-5	75	MS	FA1	90.61	0.20	5.09	1.87	0.03	0.52	0.80	0.25	0.59	0.03	112	39	1	7	7	6	9	40	6.5	32	7.6	10	14	113	100.18	1.75		
KS-4	65	MS	FA1	89.06	0.33	6.23	1.89	0.03	0.71	0.50	0.37	0.83	0.04	133	55	10	8	9	7	10	51	7.5	28	9.3	25	17	203	99.75	1.72		
KS-3	60	MS	FA1	76.42	0.52	8.06	2.50	0.06	0.74	10.30	0.10	1.23	0.08	166	93	38	10	12	14	17	61	13.7	119	15.4	51	24	430	98.73	9.26		
KS-1	35	MS	FA1	88.19	0.39	6.92	2.12	0.01	0.68	0.09	0.38	1.17	0.04	236	66	14	9	10	10	12	64	6.6	24	10.1	36	19	284	99.36	1.58		

(B) MUDSTONES

SmN	Metre	Lith	FA	SiO ₂	TiO ₂	Al ₂ O ₃	Fe ₂ O ₃	MnO	MgO	CaO	Na ₂ O	K ₂ O	P ₂ O ₅	Ba	Ce	Cr	Ga	Nb	Ni	Pb	Rb	Sc	Sr	Th	V	Y	Zr	Total*	LOI		
KALA FORMATION																															
Upper Member																															
KS-122	4119	Mst	FA4	67.57	0.82	18.23	6.61	0.04	1.90	0.24	0.28	4.26	0.06	736	98	76	15	18	36	30	230	17.3	77	31.8	115	37	249	99.41	4.75		

Table 6.1. (ctd). XRF analyses of Siwalik sandstones and mudstones from the Kala and Jagati Formations, Khutia Khola section, Nepal.

**MUDSTONES (CTD)
KALA FORMATION (CTD)**

SmN	Metre	Lith	FA	SiO ₂	TiO ₂	Al ₂ O ₃	Fe ₂ O ₃	MnO	MgO	CaO	Na ₂ O	K ₂ O	P ₂ O ₅	Ba	Ce	Cr	Ga	Nb	Ni	Pb	Rb	Sc	Sr	Th	V	Y	Zr	Total*	LOI		
Upper Member (ctd)																															
KS-119	3981	Mst	FA4	60.39	0.84	20.40	7.53	0.05	3.11	2.68	0.06	4.83	0.11	672	80	107	16	17	52	40	240	18.0	76	32.7	131	32	155	99.22	7.78		
KS-117	3890	Mst	FA4	63.71	0.80	19.77	8.46	0.06	2.11	0.62	0.03	4.32	0.12	685	82	90	17	17	45	34	239	17.0	70	33.3	124	41	169	99.28	5.93		
Middle Member																															
KS-115	3742	Mst	FA3	77.45	0.66	13.09	4.03	0.03	1.43	0.22	0.20	2.88	0.01	506	79	48	8	15	25	27	150	13.8	33	27.2	77	28	263	99.84	3.23		
KS-113	3617	Mst	FA3	45.35	0.69	12.63	6.13	0.09	2.33	29.66	0.02	2.98	0.11	394	71	62	0	13	33	22	115	14.0	332	27.9	79	23	178	99.67	20.50		
KS-111	3497	Mst	FA3	56.07	0.59	12.65	5.28	0.21	4.13	17.18	0.10	3.56	0.23	468	68	59	6	13	27	24	151	20.7	151	24.7	69	34	170	98.83	15.18		
KS-109	3215	Mst	FA3	72.02	0.54	10.57	3.58	0.05	2.13	7.92	0.61	2.48	0.09	375	71	34	5	12	19	21	127	15.1	105	24.6	60	26	282	99.18	8.22		
KS-108	3135	Mst	FA3	60.21	0.75	18.03	7.36	0.06	3.95	3.97	0.85	4.69	0.12	680	80	77	26	17	33	17	229	18.6	96	23.6	113	32	220	100.26	6.63		
Lower Member																															
KS-105	2903	Mst	FA3	50.26	0.63	13.04	7.80	0.15	5.27	18.68	0.06	3.98	0.13	472	65	65	13	13	27	36	174	14.8	168	19.0	80	33	122	100.06	17.09		
KS-102	2878	Mst	FA3	61.44	0.71	14.70	5.36	0.07	3.64	10.19	0.31	3.48	0.10	595	88	73	18	16	31	27	159	15.5	158	20.6	81	33	242	98.97	11.46		
KS-101	2865	Mst	FA3	44.67	0.59	12.31	5.82	0.51	3.04	29.09	0.04	3.70	0.25	393	58	56	14	13	24	35	156	11.6	117	16.5	64	31	122	99.79	20.04		
KS-100	2778	Mst	FA3	54.31	0.74	14.63	5.58	0.11	3.60	17.04	0.09	3.78	0.13	488	83	70	19	15	34	31	171	14.4	182	18.2	96	35	173	99.18	15.20		
KS-96	2698	Mst	FA3	67.67	0.68	13.46	4.82	0.05	2.75	6.76	0.33	3.40	0.08	541	91	54	16	15	26	28	175	13.6	114	19.9	80	32	274	99.08	8.09		
KS-95	2668	Mst	FA3	58.63	0.75	18.42	7.11	0.16	3.95	5.05	0.60	5.24	0.12	675	73	80	24	16	37	32	229	16.7	90	22.3	114	31	157	99.47	7.85		
KS-92	2600	Mst	FA3	72.93	0.65	14.43	5.14	0.04	2.98	0.28	0.49	3.02	0.05	594	87	59	19	14	29	23	181	14.9	78	20.2	80	30	231	99.54	3.78		
KS-90	2575	Mst	FA3	76.23	0.71	13.80	3.92	0.01	1.49	0.18	0.30	3.35	0.02	503	123	61	16	15	30	29	182	10.6	69	24.6	76	31	431	99.43	2.94		
KS-88	2495	Mst	FA3	53.09	0.77	16.43	6.66	0.07	3.08	15.15	0.13	4.53	0.09	585	69	82	23	15	38	34	193	19.9	118	19.0	103	34	138	99.70	13.36		
KS-87	2440	Mst	FA3	58.92	0.67	19.41	7.97	0.05	5.44	1.68	0.11	5.65	0.11	761	79	91	24	14	54	34	265	16.9	73	25.0	131	25	138	100.01	6.79		
KS-85	2390	Mst	FA3	46.27	0.60	11.36	5.69	0.37	5.49	26.42	0.15	2.94	0.71	442	70	48	15	13	26	32	128	15.2	228	13.2	62	36	146	99.92	20.57		
KS-83	2341	Mst	FA3	51.80	0.81	16.14	6.89	0.11	3.00	16.51	0.03	4.56	0.14	544	96	88	20	17	37	38	173	17.1	217	25.0	103	33	148	99.34	14.84		
KS-81	2302	Mst	FA3	54.51	0.79	12.68	4.66	0.10	2.91	20.57	0.19	3.49	0.11	439	87	66	16	16	30	29	147	16.5	243	18.8	84	31	246	98.75	16.18		

Table 6.1. (ctd). XRF analyses of Siwalik sandstones and mudstones from the Kala and Jagati Formations, Khutia Khola section, Nepal.

MUDSTONES (CTD)

KALA FORMATION (CTD)

SmN	Metre	Lith	FA	SiO ₂	TiO ₂	Al ₂ O ₃	Fe ₂ O ₃	MnO	MgO	CaO	Na ₂ O	K ₂ O	P ₂ O ₅	Ba	Ce	Cr	Ga	Nb	Ni	Pb	Rb	Sc	Sr	Th	V	Y	Zr	Total*	LOI		
Lower Member (ctd)																															
KS-79	2260	Mst	FA3	45.72	0.73	13.67	5.92	0.14	3.70	26.13	0.02	3.81	0.16	402	86	73	19	15	30	39	147	16.1	272	19.5	82	27	162	99.79	19.75		
KS-77	2219	Mst	FA3	57.60	0.74	14.34	6.06	0.09	2.62	14.66	0.21	3.58	0.09	504	83	68	18	16	36	36	167	16.9	163	18.4	91	32	218	98.69	12.84		
KS-75	2176	Mst	FA3	74.43	0.69	13.40	4.46	0.01	1.32	2.53	0.09	3.06	0.02	535	90	61	17	15	28	29	186	13.0	73	19.8	84	26	323	99.39	4.74		
KS-73	2132	Mst	FA3	54.05	0.65	12.34	4.77	0.16	2.24	21.92	0.14	3.60	0.13	465	74	51	16	14	26	33	158	16.5	184	14.9	67	30	179	98.93	16.18		

JAGATI FORMATION

Upper Member

KS-71	2092	Mst	FA2	67.93	0.68	11.71	4.28	0.10	1.77	9.87	0.44	3.12	0.12	440	93	56	14	15	27	28	151	13.7	156	20.4	64	30	393	98.71	9.07
KS-69	2047	Mst	FA2	40.10	0.62	11.42	6.35	0.15	3.11	34.66	0.06	3.44	0.10	374	62	49	15	14	29	37	155	11.7	177	14.0	71	33	102	100.62	22.61
KS-67	2003	Mst	FA2	45.47	0.65	12.28	5.93	0.12	2.31	30.04	0.03	3.01	0.16	377	71	48	16	13	26	31	133	12.8	217	15.9	64	33	144	99.60	20.34
KS-65	1964	Mst	FA2	40.03	0.60	10.94	5.90	0.27	4.63	34.41	0.10	2.84	0.29	326	75	54	14	12	26	32	115	9.4	350	15.3	63	39	117	100.52	23.82
KS-63	1920	Mst	FA2	68.44	0.62	12.54	3.71	0.07	2.58	8.36	0.48	3.09	0.09	461	78	51	16	14	21	27	136	12.6	127	16.1	71	31	261	98.85	9.20
KS-61	1878	Mst	FA2	59.27	0.79	20.93	9.30	0.03	2.96	0.55	0.04	6.05	0.09	797	85	109	29	17	50	30	286	16.5	48	24.8	133	41	163	99.63	4.92
KS-59	1857	Mst	FA2	55.88	0.71	14.97	5.75	0.22	2.61	14.75	0.31	4.37	0.43	579	72	61	20	16	30	22	205	17.9	180	17.4	78	50	152	99.03	12.52
KS-57	1820	Mst	FA2	54.00	0.73	15.19	5.92	0.10	3.88	15.73	0.04	4.28	0.13	502	89	71	20	15	31	33	178	16.3	171	21.9	87	29	171	99.59	14.66
KS-55	1765	Mst	FA2	62.25	0.75	13.51	5.25	0.06	2.31	12.24	0.26	3.23	0.14	475	83	53	17	16	27	24	145	15.8	161	19.5	84	28	265	98.99	11.50
KS-52	1710	Mst	FA2	38.82	0.56	9.43	4.72	0.29	1.94	41.48	0.10	2.55	0.12	275	64	45	12	12	20	21	101	6.8	154	12.2	64	25	141	100.17	24.77
KS-50	1658	Mst	FA2	56.86	0.78	15.09	6.46	0.10	4.36	11.60	0.21	4.41	0.13	548	90	70	20	16	33	28	186	15.8	167	21.7	98	32	222	99.12	12.62

Middle Member

KS-48	1622	Mst	FA2	61.32	0.77	18.72	6.84	0.08	2.31	4.74	0.17	4.92	0.11	646	91	82	25	18	38	36	220	16.8	105	22.7	126	42	165	99.76	7.65
KS-46	1610	Mst	FA2	55.45	0.67	10.70	5.23	0.24	2.55	22.14	0.19	2.72	0.12	404	88	54	14	15	22	41	112	14.9	183	17.0	65	31	299	98.79	16.83

Table 6.1. (ctd). XRF analyses of Siwalik sandstones and mudstones from the Kala and Jagati Formations, Khutia Khola section, Nepal.

**MUDSTONES (CTD)
JAGATI FORMATION (CTD)**

SmN	Metre	Lith	FA	SiO ₂	TiO ₂	Al ₂ O ₃	Fe ₂ O ₃	MnO	MgO	CaO	Na ₂ O	K ₂ O	P ₂ O ₅	Ba	Ce	Cr	Ga	Nb	Ni	Pb	Rb	Sc	Sr	Th	V	Y	Zr	Total*	LOI		
Middle Member (ctd)																															
KS-43	1502	Mst	FA2	61.02	0.67	13.45	5.08	0.13	2.30	13.42	0.66	3.15	0.10	576	73	60	18	15	25	34	154	15.3	125	17.0	71	28	213	99.24	11.77		
KS-39	1348	Mst	FA2	67.22	0.71	17.43	6.00	0.07	2.84	1.25	0.29	4.08	0.12	718	88	76	23	16	37	21	194	14.5	75	20.9	101	33	198	99.80	5.28		
KS-38	1287	Mst	FA2	41.68	0.56	12.49	6.71	0.25	2.85	31.80	0.02	3.56	0.07	461	72	55	17	13	26	32	147	12.1	102	13.6	69	38	105	100.22	21.55		
KS-35	1170	Mst	FA1	54.93	0.62	14.05	6.13	0.13	5.36	14.86	0.07	3.74	0.13	561	81	73	20	14	32	26	163	15.9	128	17.5	77	33	161	99.21	14.98		
KS-33	1065	Mst	FA1	76.35	0.63	13.61	4.71	0.02	1.49	0.27	0.30	2.58	0.03	500	84	43	17	14	23	19	149	11.7	50	19.5	69	27	269	99.91	3.18		
KS-32	975	Mst	FA1	65.21	0.71	18.79	8.01	0.04	2.19	0.08	0.09	4.84	0.04	778	88	88	25	16	39	28	234	13.8	52	23.0	116	33	176	99.85	4.02		
KS-29	935	Mst	FA1	45.34	0.58	10.93	6.11	0.29	2.02	31.32	0.07	3.23	0.10	424	72	41	15	13	21	29	141	10.1	127	12.8	63	30	173	99.79	20.48		
Lower Member																															
KS-27	855	Mst	FA1	55.46	0.72	18.17	7.24	0.08	2.95	10.08	0.01	5.15	0.15	827	79	93	24	17	39	32	214	18.3	121	18.3	115	41	175	99.44	10.70		
KS-23	740	Mst	FA1	71.08	0.52	9.10	3.08	0.09	1.38	12.93	0.09	1.67	0.07	282	68	25	11	12	14	21	91	11.6	83	13.3	48	24	246	98.43	10.73		
KS-21	680	Mst	FA1	73.73	0.72	14.65	5.53	0.03	1.31	0.64	0.16	3.19	0.05	510	112	54	19	18	26	26	164	13.7	44	22.3	86	33	292	100.17	3.74		
KS-20	600	Mst	FA1	67.26	0.74	18.66	6.44	0.02	1.68	0.27	0.03	4.85	0.07	682	93	93	22	17	47	36	244	16.3	67	24.7	124	28	206	99.75	4.26		
KS-16	525	Mst	FA1	38.24	0.43	10.36	4.91	0.62	15.96	27.06	0.01	2.38	0.03	488	52	51	14	9	22	55	92	11.7	354	11.9	53	31	75	101.55	28.02		
KS-12	355	Mst	FA1	66.33	0.71	13.53	5.67	0.06	2.47	7.30	0.09	3.41	0.43	581	101	71	15	16	31	27	153	14.4	132	21.7	86	38	302	98.76	8.52		
KS-9	235	Mst	FA1	84.20	0.48	9.16	2.87	0.02	1.08	0.73	0.27	1.17	0.02	204	91	29	12	12	20	11	73	8.4	34	16.2	44	23	318	99.86	2.75		
KS-8	190	Mst	FA1	69.47	0.53	11.87	4.67	0.09	4.32	5.92	0.06	2.92	0.14	396	81	52	13	13	24	21	134	14.1	48	20.1	67	29	197	98.97	9.22		
KS-6	80	Mst	FA1	82.86	0.68	8.58	3.17	0.03	0.91	2.33	0.06	1.32	0.06	320	112	39	12	15	15	31	85	11.3	81	17.3	65	35	461	99.79	4.28		
KS-2	40	Mst	FA1	70.85	0.61	15.60	6.79	0.03	1.85	0.32	0.47	3.42	0.06	672	80	59	18	15	32	20	170	11.0	52	21.7	93	27	180	99.66	3.23		

Table 6.2. Average compositions of the Siwalik sandstones and mudstones from the Khutia Khola area, by facies association (data from Table 6.1).

Facies As. Code N	Sandstones					Mudstones					Total Average	UCC	PAAS
	FA1	FA2	FA3	FA4	Average	FA1	FA2	FA3	FA4	Average			
	FGM	FFDM	DSB	SSB		FGM	FFDM	DSB	SSB				
	23	18	23	3		14	16	22	3				
<i>Major elements (wt%)</i>													
SiO ₂	81.76	72.88	73.71	80.42	77.19	65.81	54.73	58.80	63.89	60.81	69.00	66.00	62.80
TiO ₂	0.43	0.39	0.33	0.25	0.35	0.62	0.68	0.69	0.82	0.70	0.53	0.50	1.00
Al ₂ O ₃	7.32	7.50	7.22	4.99	6.76	13.36	13.80	14.16	19.47	15.20	10.98	15.20	18.90
Fe ₂ O ₃	2.31	2.50	2.36	1.55	2.18	5.38	5.84	5.68	7.54	6.11	4.14	4.98	7.22
MnO	0.06	0.09	0.07	0.18	0.10	0.11	0.14	0.12	0.05	0.11	0.10	0.10	0.11
MgO	1.02	1.57	1.60	0.55	1.19	3.21	2.83	3.20	2.37	2.90	2.05	2.20	2.20
CaO	5.73	13.39	12.67	10.88	10.67	8.15	17.94	13.26	1.18	10.13	10.40	4.20	1.30
Na ₂ O	0.21	0.31	0.38	0.14	0.26	0.13	0.21	0.23	0.12	0.17	0.22	3.90	1.20
K ₂ O	1.08	1.30	1.58	1.00	1.24	3.13	3.68	3.72	4.47	3.75	2.49	3.40	3.70
P ₂ O ₅	0.05	0.07	0.08	0.05	0.06	0.10	0.14	0.14	0.10	0.12	0.09	0.20	0.16
<i>Trace elements (ppm)</i>													
Ba	195	206	261	194	214	516	497	516	698	557	385	550	650
Ce	73	63	54	40	57	85	80	81	86	83	70	64	80
Cr	19	18	16	4	14	58	62	65	91	69	42	35	110
Ga	9	9	7	1	7	17	18	16	16	17	12	17	20
Nb	11	10	9	7	9	14	15	15	17	15	12	25	2
Ni	12	11	9	4	9	28	29	31	44	33	21	20	55
Pb	15	25	17	13	17	27	30	30	35	30	24	20	20
Rb	62	74	83	59	70	150	164	171	237	180	125	112	160
Sc	9	11	12	13	11	13	14	16	17	15	13	11	16
Sr	60	130	170	60	105	98	156	148	74	119	112	350	200
Th	13	12	11	12	12	19	18	21	33	23	17	11	15
V	36	31	27	17	28	79	82	85	123	92	60	60	150
Y	22	23	20	15	20	31	34	31	37	33	27	22	27
Zr	293	230	190	180	223	231	195	207	191	206	215	190	210
LOI (wt%)	5.52	10.46	10.08	8.43		9.15	14.32	12.03	6.15				
<i>Ratios</i>													
SiO ₂ /Al ₂ O ₃	11.16	9.72	10.21	16.10		4.93	3.97	4.15	3.28				
K ₂ O/Na ₂ O	5.12	4.19	4.20	7.40		24.57	17.32	16.18	36.61				
Th/Sc	1.39	1.08	0.95	0.93		1.43	1.30	1.35	1.87				
Zr/Sc	32.11	21.20	16.45	14.37		17.72	13.96	13.33	10.96				
Al ₂ O ₃ /Na ₂ O	34.64	24.18	19.18	36.95		104.81	65.01	61.65	159.45				
Al ₂ O ₃ /K ₂ O	6.77	5.78	4.56	4.99		4.27	3.75	3.81	4.36				

Abbreviations: FA1 - fine-grained meandering (FGM); FA2 - flood-flow dominated meandering (FFDM); FA3 - deep sandy braided (DSB); FA4 - shallow sandy braided (SSB). UCC (Upper Continental Crust) values from Taylor and McLennan (1985). PAAS (Post-Archean Australian shale) values from Taylor and McLennan (1985).

CHAPTER SEVEN

PETROGRAPHICAL ANALYSIS

7.1. Introduction

Petrography of sandstone deciphers the nature of the source rocks (Pettijohn, 1975; Folk, 1980; Blatt et al., 1980), tectonic setting of the source area (Dickinson, 1970, 1985; Crook, 1974; Basu et al., 1975; Dickinson and Suczek, 1979; Ingersoll and Suczek, 1979; Dickinson et al., 1983) and climatic condition during sedimentation (Suttner et al., 1981; Suttner and Dutta, 1986; Weltje, 1994, 2002; Weltje et al., 1998). At the same time, weathering conditions in the source area also control the sediments composition (Critelli et al., 1997). In tectonically active area, source rock type determines sediment composition (Dickinson, 1970; Dickinson et al., 1983) however, climate and relief play important roles in determining the final composition of sediments in tectonically less active area (Basu, 1976; Suttner et al., 1981). Such methods have been used by several researches for study of the Siwalik sandstones to reveal the provenance and tectonic history of the Himalaya (cf. Hisatomi, 1990; Tokuoka et al., 1986, 1988; Critelli and Ingersoll, 1994; Dhital et al., 1995; DeCelles et al., 1998; Tamrakar et al., 2003; Sigdel and Sakai, 2013; Tamrakar and Syangbo, 2014)

This chapter focuses on the sandstone petrography of the Neogene Siwalik Group in the Khutia Khola section of Nepal Himalaya in detail, and determine the provenance, paleoclimate and tectonic settings of these fluvial successions.

7.2. Methodology

Modal compositions of 67 Siwalik Group sandstone samples from the Khutia Khola section were studied using standard thin-section petrographic analysis and framework modal analysis was quantified using the Gazzi-Dickinson method (Dickinson, 1970; Ingersoll et al., 1984; Dickinson, 1985). A total of 500 grains were counted per thin section by using a Swift point counter with horizontal grid spacing 0.3 mm to avoid individual grains being counted more than once. The main categories of grains identified include monocrystalline quartz (Qm), polycrystalline quartz (Qp), plagioclase (P), K-feldspar (K), sedimentary lithic (Ls), carbonate lithic (Lc), metamorphic lithic (Lm), volcanic lithic (Lv) and chert. In addition biotite, muscovite, chlorite, calcite cement, other cements, heavy minerals, altered minerals, accessory minerals, matrix and opaque were also included in point count. The detrital modes were recalculated to 100% and the parameters were plotted on ternary diagrams, Q-F-L and Q-F-R for classification (Pettijohn, 1975; Folk, 1980) and, Qt-F-L, Qm-F-L, Qp-Lv-Ls,

Qm-P-K and Lm-Lv-Ls for determination of provenance (Dickinson et al., 1983; Dickinson, 1985; Ingersoll and Suczek, 1979). Similarly, for determination of climatic indexes bivariate log/log diagram of $Q_p/F+R$ Vs $Q_t/F+R$, bivariate log-ratio diagram of Q/F Vs Q/R (Suttner and Dutta, 1986; Weltje et al., 1998) and ternary Q-F-R diagram (Suttner et al., 1981) were plotted. The framework parameters used in this study are listed in Table 7.1 and recalculated detrital framework compositions (%) with other calculations are listed in Table 7.2.

Table 7.1. Framework parameters used in this study.

Symbol	Definition
Qm	Monocrystalline quartz
Qp	Polycrystalline quartz
Q	Total quartz grains (Qm + Qp)
Qt	Total quartz grains (Qm + Qp) + chert
P	Plagioclase
K	K-feldspar
F	Total feldspar (P + K)
Ls	Sedimentary lithic fragment
Lm	Metamorphic lithic fragment
Lv	Volcanic lithic fragment
L	Total lithic fragments (Ls + Lm + Lv)
Lt	L + Qp + chert
R	Total lithic fragments (L) + chert

7.3. Results

7.3.1. Jagati Formation (Meandering river system- FA1-FA2)

Forty-one samples were obtained from the Jagati Formation, seventeen from the lower member, twelve from the middle member and twelve from the upper member were analyzed (Table 7.2). The Jagati Formation sandstones are mostly matrix-poor, moderately to well-sorted and grains are sub-angular to rounded. Quartz is the dominant detrital constituent (average 57%) and monocrystalline quartz is more abundant than polycrystalline quartz (Qm:Qp ratio 65:35) (Fig. 7.1 A). The abundance of quartz is slightly increased from the lower member (58%) to the middle member (60%) and is decreased in the upper member (55%). Lithic fragments are the second most abundant detrital constituent overall, and sedimentary (Ls = 56%) and metamorphic (Lm = 43%) lithic fragments are much more abundant than volcanic (Lv = 1%) lithic fragments (Fig. 7.1 C and D). The lithic fragments constituent range from a low 12% in KS-1 to a high 27% in KS-30. The sedimentary lithic fragments are mainly shale, siltstone, sandstone, carbonate and chert (Fig. 7.1 B) whereas metamorphic lithic fragments are phyllitic and quartz-mica schists and quartzite. Feldspar is the least abundant among QFL and overall range is 2.6 to 8.4%. Feldspars are mainly plagioclase, orthoclase and microcline. The average abundance of feldspar is approximately similar in the lower (5.5%) and

middle members (5.0%) but slightly higher in the upper member (6.4%). In most samples K-feldspar (K) and plagioclase (P) are approximately subequal, with P:K ratio 53:47, 48:52 and 46:54 in the lower, middle and upper members, respectively. Of the total frameworks in the Jagati Formation, mica ranges from 1.8 to 12.2% (average 5.2%) and overall mica contents are 6.2%, 3.5% and 5.6% in the lower, middle and upper members, respectively. In most samples muscovite (M) content is higher than biotite (B) with an overall M:B ratio 57:43. Carbonate intraclast is another significant constituent which ranges from 0.4 to 12.6% in the Jagati Formation. Cement is differentiated into calcite and other cements and overall ratio is 79:21. Trace amounts of a number of heavy minerals also occurs which ranges from 0.2 to 4.2% (average 1.8%), include opaque, zircon, kyanite, sillimanite, garnet, etc.

7.3.2. Kala Formation (Braided river system- FA3-FA4)

Of the 26 samples analyzed for the Kala Formation, seventeen were from the lower member, six from the middle member, and three from the upper member (Table 7.2). The Kala Formation sandstones are moderately to well-sorted, grains are sub-angular to sub-rounded and mostly matrix supported, but grain supported sandstones also occur. Again, quartz is the dominant detrital constituent (average 53%)

with Qm:Qp ratio 64:36. The abundance of quartz increases from the lower member (51%) through middle (55%) to upper (57%) members. Lithic fragments range from 11 to 23% (average 17%), with the average composition of Ls = 53, Lm = 43 and Lv = 4. The sedimentary lithic fragments constituent decrease up section whereas metamorphic and volcanic lithic fragments constituent increase up section from lower to upper member. Metamorphic lithic fragments are dominantly quartz-mica schist, phyllite and quartzite whereas sedimentary lithic fragments content mudstone, siltstone and carbonate. Feldspar content ranges from 5 to 10% and is slightly higher in the Kala Formation (average 7.7%) than in the Jagati Formation (average 5.5%). The average constituent of feldspar are approximately similar in all three members (lower = 7.9%, middle = 7.3% and upper = 8.0%). In most samples K-feldspar (K) content is slightly higher than plagioclase (P) with P:K ratio 48:52, 48:52 and 50:50 in the lower, middle and upper members, respectively. The amount of mica present ranges from 2.0 to 10.8% (average 5.8%) and overall mica contents are 5.5%, 6.8% and 5.5% in the lower, middle and upper members, respectively. Muscovite (M) contents is higher than biotite (B) also in the Kala Formation with an overall M:B ratio 55:45. The average carbonate content is 4.3% but few samples show higher abundance (up to 14.4%, KS-78). The overall ratio of calcite cement and other cements is 74:26. Heavy minerals and opaque minerals

are in minor amount which ranges from 0.6 to 4.6% but overall content is higher than the Jagati Formation (average 2.9%).

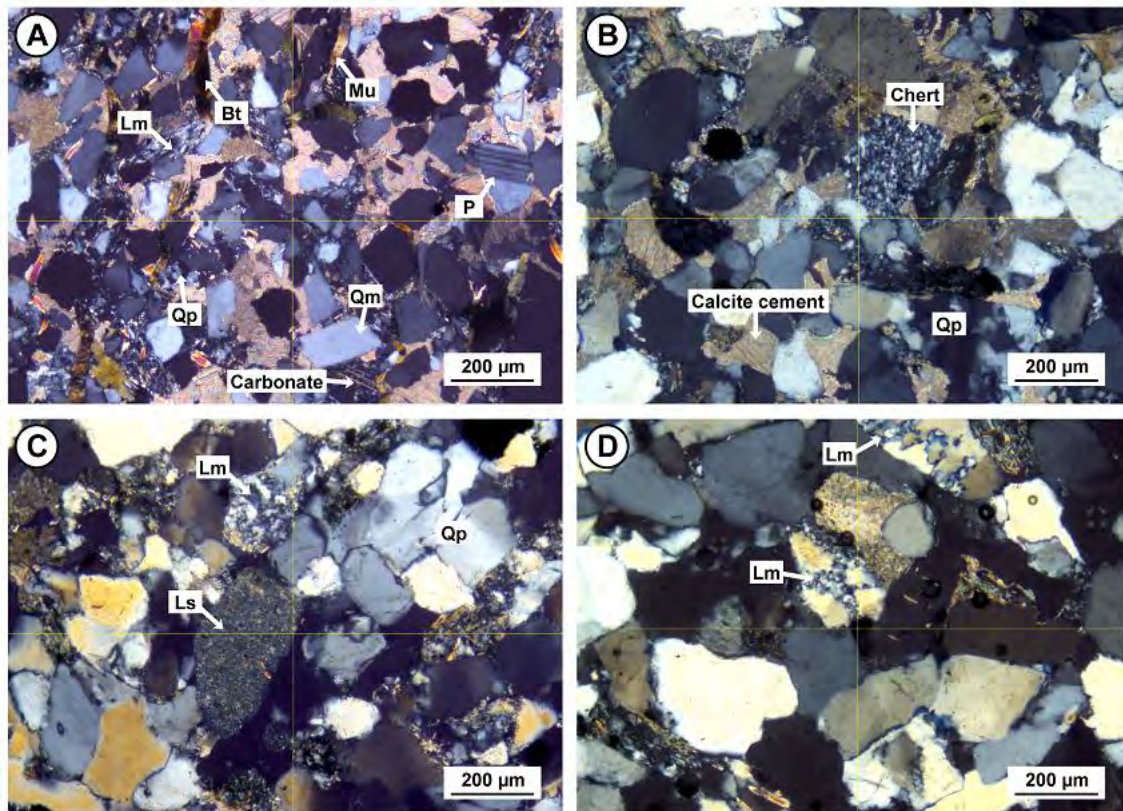


Fig. 7.1: Photomicrographs of sandstones from the Jagati and Kala Formations. (A) Qp (polycrystalline quartz), Qm (monocrystalline quartz), P (plagioclase), Bt (biotite), Mu (muscovite), Lm (metamorphic lithic fragment), and carbonate. (B) Chert, calcite cement and Qp (polycrystalline quartz). (C) Lm (metamorphic lithic fragment, Ls (sedimentary lithic fragment, and Qp (polycrystalline quartz). (D) Lm (metamorphic lithic fragment).

7.4 Sandstone classification

Major detrital components, quartz, feldspar and lithic fragments, have been recalculated as 100% for Q-F-L ternary diagrams. Plot in the Q-F-L diagram proposed by Pettijohn (1975) shows that the sandstones are sub-litharenites (70%) and lithic arenites (30%) (Fig. 7.2 A). Similarly, plot in the Q-F-R diagram proposed by Folk (1980) shows that most of the sandstones are litharenites (42%) and feldspathic litharenites (45%), with fewer sub-litharenites (13%) (Fig. 7.2 B). The average modal composition of the Jagati Formation is $Q_{70}F_7L_{23}$ and that of the Kala Formation is $Q_{68}F_{10}L_{22}$. The overall average composition is $Q_{70}F_8L_{22}$. The Kala sandstones show slightly higher content of feldspar and high quartz/feldspar ratio (average 10.9) is maintained throughout the formation whereas this ratio is slightly less (average 7.0) in the Jagati Formation.

The Khutia Khola sandstone classification (Q-F-L plot) were compared with the Siwalik sections in the Karnali River (Sigdel and Sakai, 2013), Surai Khola (Dhital et al., 1995), Arung Khola (Tokuoka et al., 1986) and Samari River (Tamrakar and Syangbo, 2014) areas from west towards east in the Nepal Himalaya (Fig. 5). The Karnali River sandstones are classified as litharenite and sub-litharenite, and contain the low amount of feldspar. The Surai Khola and Arung Khola sandstones have the highest

amount of feldspar and lithic fragments and are classified as litharenite and feldspathic litharenite, and some as lithic arkose. Similarly, the Samari River sandstones are classified as litharenite through to lithic arkose and contains higher amount of feldspar and quartz than the Khutia Khola sandstones. These Q-F-L diagrams show that the compositions are similar among these Siwalik sections.

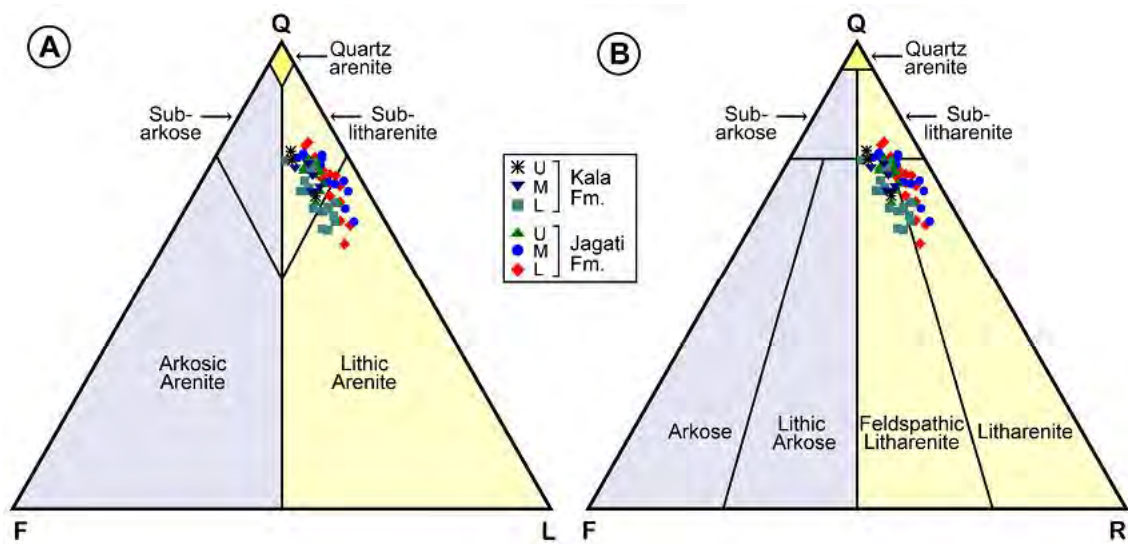


Fig 7.2: Ternary diagram for sandstone composition based on schemes proposed by A) Pettijohn (1975); Q-F-L (quartz, feldspar, lithic fragments), and B) Folk (1980); Q-F-R (quartz, feldspar, rock fragments).

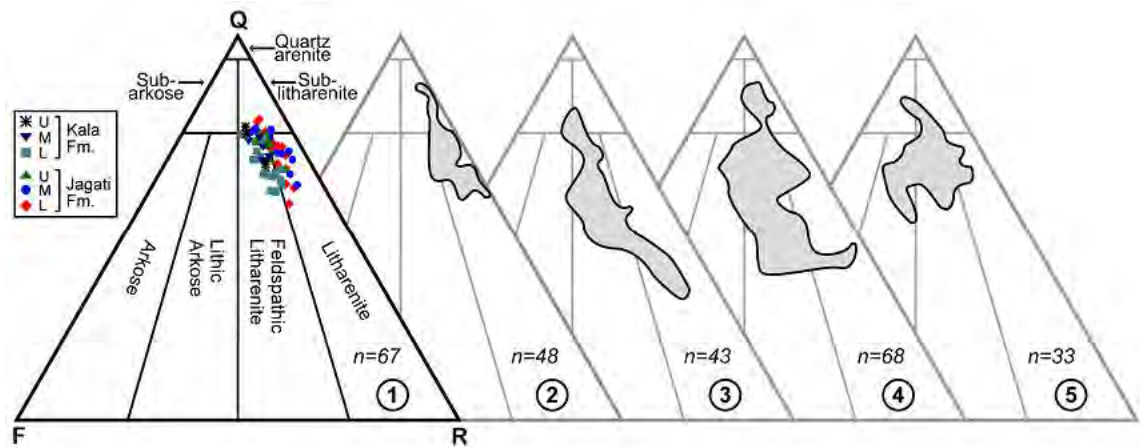


Fig: 7.3. Comparison of sandstones classification from different sections of the Siwalik Group, Nepal (after Folk, 1980). (1) The Khutia Khola section, far western Nepal (present study). (2) The Karnali River section, far western Nepal (Sigdel and Sakai, 2013). (3) The Surai Khola area, mid western Nepal (Dhital et al., 1995). (4) The Arung Khola area, west central Nepal (Tokuoka et al., 1986). (5) The Samari River area, central Nepal (Tamrakar and Syangbo, 2014). Standard plot: Q-F-R (Quartz, feldspar, rock fragments). ‘n’ is number of samples.

7.5 Provenance and tectonic setting

The ternary diagram analyses (Q-F-L, Q-F-R, and Qt-F-L) resulted that the composition of Jagati and Kala Formations’ sandstones were plotted almost in the same regions. Garzanti et al. (2007) analyzed the present river sand along the Marsyandi River systems in the western Nepal Himalaya. They revealed the changes in petrographical composition of sands from the Tethys Himalaya to the Lesser Himalayan

regions: from the lithic fragment rich sand to the quartz and feldspar rich sand towards downstream (Fig. 3 in Garzanti et al., 2007). The simple comparison with their result suggests the Siwalik sandstones of the Khutia Khola section were contributed mainly from the Lesser Himalaya. As the source of the Lesser Himalaya, these sandstones are rich in quartz grains and poor in rock or lithic fragments which suggest the Kushma (quartzite) and Ranimata (phyllite) Formations, consisting of the Ramgarh Thrust Sheet (DeCelles et al., 2001) are the highly possible source with taking the period of the thrusts activity to the north of our study area (cf. DeCelles et al., 2001; Hyughe et al., 2005). The sub-rounded to rounded minor chert grains may indicate the water discharge system at that time extended to the Trans-Himalayan region. The obtained compositional data and the sediment source indicated by the sediment grains are, thus, consistent.

Careful comparison of two formations' plots implies that the Jagati Formation sandstones are plotted in the area very slightly toward the Q-R or L axes: the Kala Formation sandstones are slightly richer in feldspar grains. This may be due to the contribution of sand grains from the Higher Himalaya origin. This result matches with the apparent changes in sandstone characteristics: the appearance in "salt and pepper" sandstone in the Kala Formation.

The provenance discrimination plots of Dickinson et al. (1985) show that all the Khutia Khola Siwalik sandstones fall in the recycled orogenic field of the Qt-F-L plot, and in the transitional recycled field of the Qm-F-Lt plot (Fig. 7.4). The plots on the diagram were concentrated along the Qt-L and Qm-Lt lines within the recycled orogenic and transitional recycled areas in the recycled orogen block provenances showing that bulk compositions do not vary significantly within the section. The Qp-Lv-Ls diagram suggests that the Khutia Khola sandstone specimens fall in the field of the collision suture and fold-thrust belt source (Dickinson et al., 1985) (Fig. 7.5 A). The Khutia Khola sandstone composition plots in the Lm-Lv-Ls diagram also suggest the suture zone as their provenance (Ingersoll and Suezck, 1979) (Fig. 7.5 C), which is quite consistent with the tectonic setting of the Himalayas. However, the Qm-P-K diagram indicated that the Khutia Khola sandstones' provenance as the continental block with increased maturity (Dickinson et al., 1985) (Fig. 7.5 B), which is not consistent with the tectonic setting due to the rich monocrystalline quartz. The abundance in monocrystalline quartz may reflect the presence of granitic and volcanic rocks in the source area (Young, 1976): the Dadeldhura granite (Szulc et al., 2006; Bernet et al., 2006) may have contributed on such result in the present case.

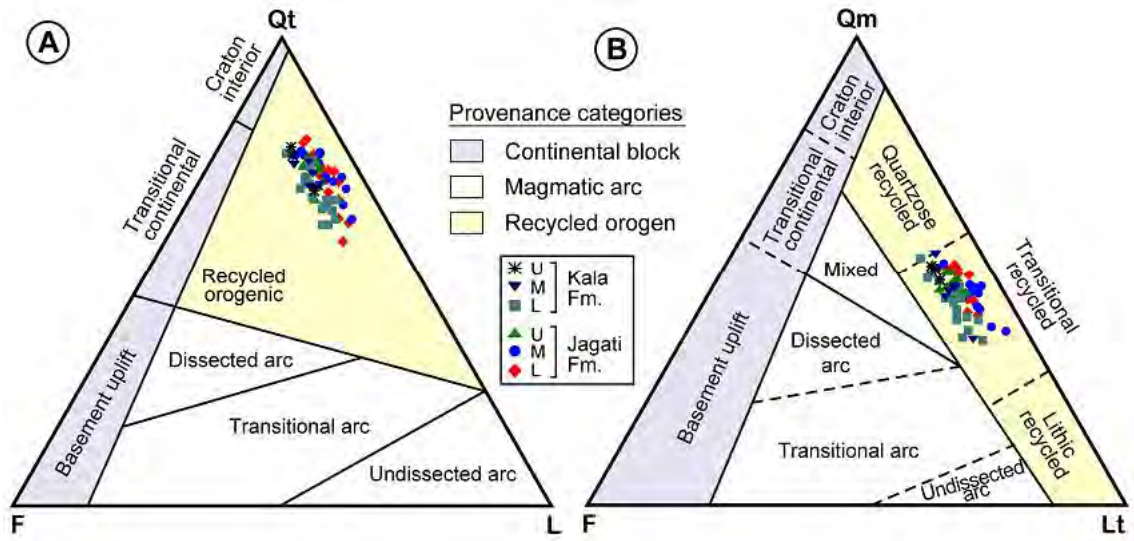


Fig: 7.4. Ternary diagram for provenance discrimination (after Dickinson et al., 1983). A) Qt-F-L (Quartz, feldspar, lithic fragments). B) Qm-F-Lt (Monocrystalline quartz, feldspar, total lithic grains).

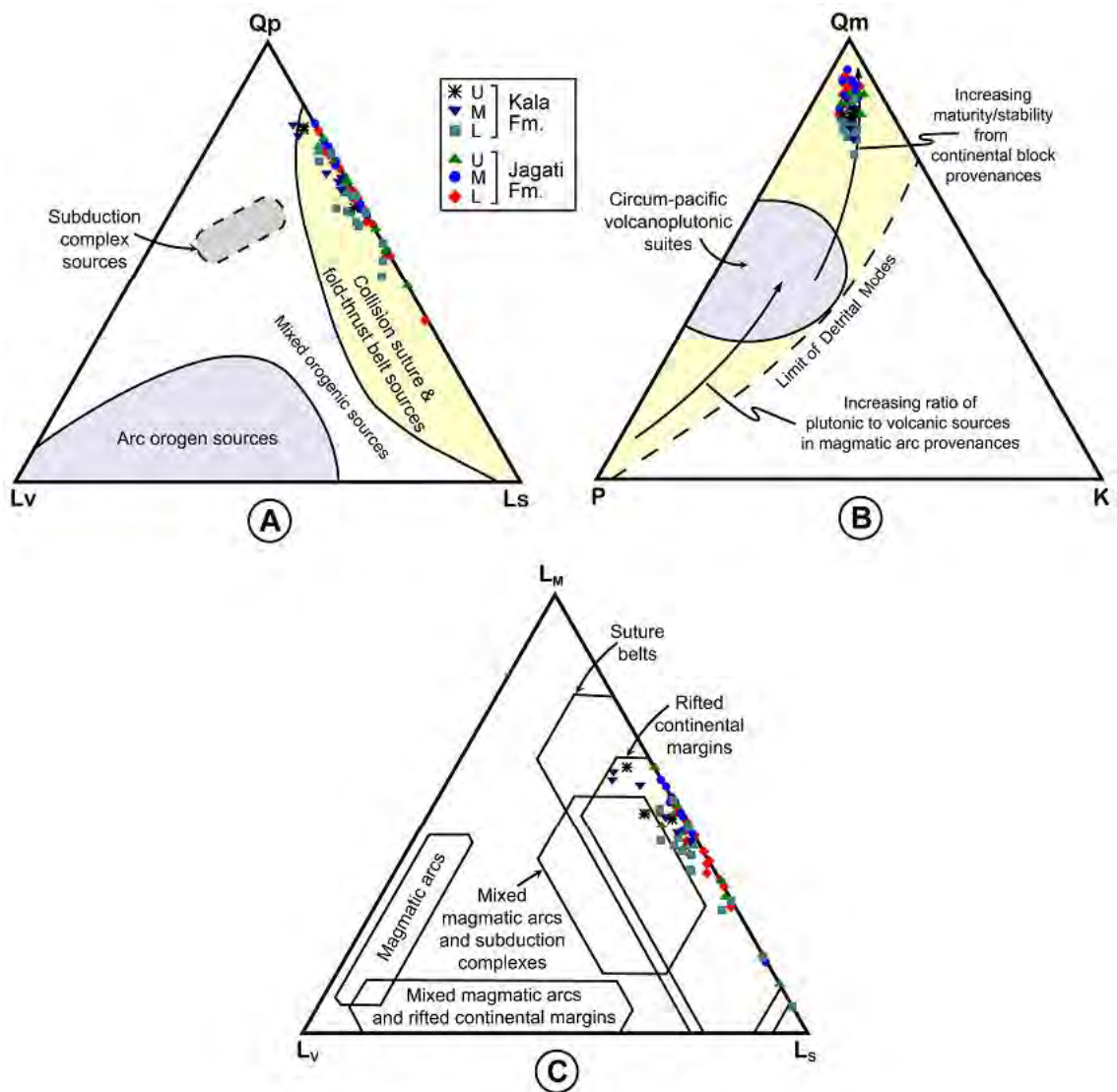


Fig: 7.5. Ternary diagram for provenance discrimination. (A) Qp-Lv-Ls (Polycrystalline quartz, volcanic lithic fragment, sedimentary lithic fragment) and (B) Qm-P-K (Monocrystalline quartz, plagioclase, K-feldspar) (after Dickinson, 1985). (C) Lv-Ls-Lm (Volcanic lithic fragment, sedimentary lithic fragment, metamorphic lithic fragment) (after Ingersoll and Suczek, 1979).

7.6 Climatic indexes

A biavariant log/log plot based on polycrystalline quartz to feldspar plus rock fragments against ratio of total quartz to feldspar allows discrimination on climatic control (Suttner and Dutta, 1986). The diagram suggests semi-humid to humid climate during the sedimentation of the Khutia Khola sandstones (Fig. 7.6 A). Tamrakar and Syangbo (2014) have also suggested the semi-humid to humid climate for the Siwalik sandstones in their study area. Plots in the Q-F-R diagram of Suttner et al. (1981) suggest the source of these sandstones is metamorphic rock and sediments were derived under humid climatic condition (Fig. 7.6 B). The Q-F-R diagram by Kundu et al. (2012) have also suggested humid climate for the Siwalik sandstones in Tista valley, India. However, the diagrams (Fig. 7.6 A and B) are defined for first-cycle sediments and do not discriminate between tectonic settings but can discriminate humid or arid climatic (desert) condition of the source rocks (Suttner et al., 1981; Suttner and Dutta, 1986). On these diagrams the Siwalik sediments reflect the semi-humid and humid climatic condition during sedimentation, the reason is that these sediments were always influenced by fluvial system. The Siwalik sandstones are rich in quartz and poor in feldspar content which also reflects that the climate was almost wet and humid for all the time to cause significant feldspar weathering. The Khutia Khola sandstones contain

altered to less-altered, angular to sub-angular feldspars which also indicate burial under humid climatic condition (Basu et al., 1975; Pettijohn et al., 1987).

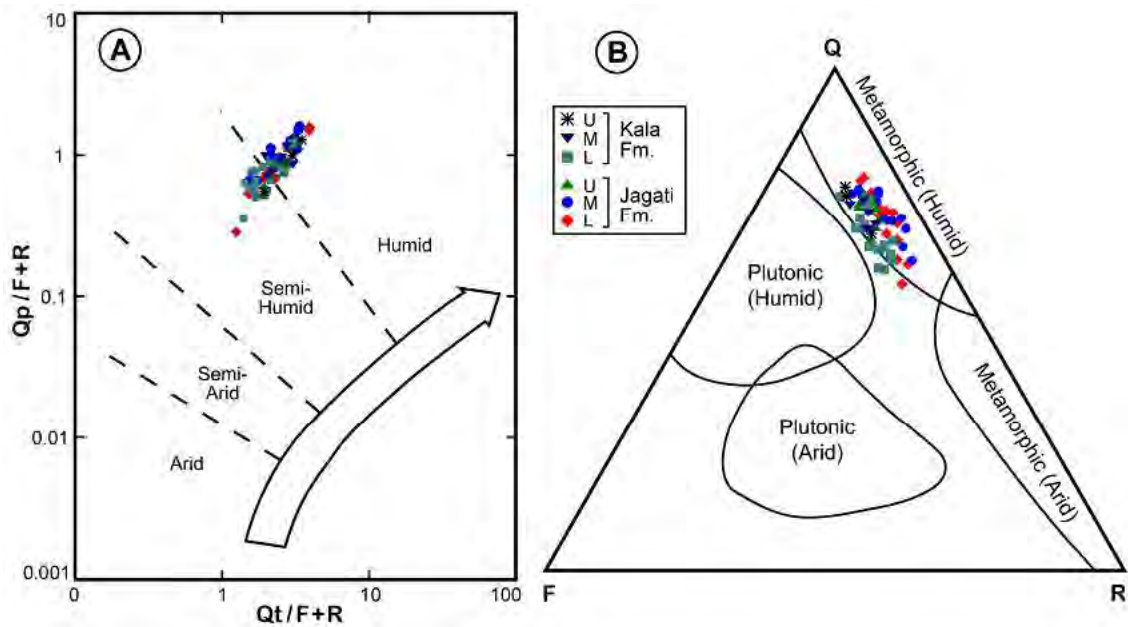
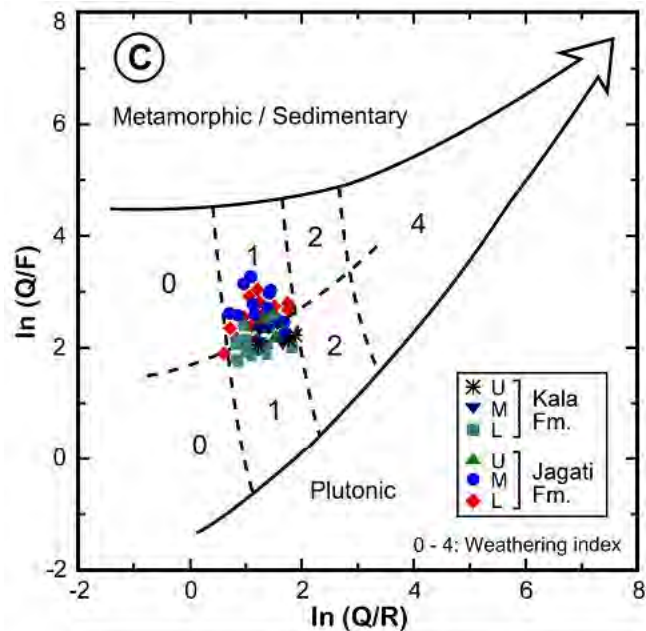


Fig: 7.6. (A) Bivariant log/log plot of $Qp/(F+R)$ (polycrystalline quartz to feldspar plus rock fragments) against $Qt/(F+R)$ (total quartz to feldspar plus rock fragments) (after Suttner and Dutta, 1986). (B) Ternary Q-F-R (quartz, feldspar, rock fragments) diagram for the effect of source rock on the composition as a function of climate (after Suttner et al., 1981).

Weltje et al. (1998) proposed a diagram to determine the climatic conditions and the relief in which clastic sediments are deposited. This diagram was constructed by



SEMI-QUANTITATIVE WEATHERING INDEX		PHYSIOGRAPHY (relief)		
		High (mountains) 0	Moderate (hills) 1	Light (plains) 2
climate (precipitation)	(semi-) arid and mediterranean	0	0	0
	temperate subhumid	1	1	2
	tropical humid	2	2	4

Fig: 7.7. Bivariant log-ratio plot of Q/F (quartz to feldspar) against Q/R (quartz to rock fragments) (after Weltje et al., 1998). Field 1-4 refer to the semi-quantitative weathering indices defined on the basis of relief and climate as indicated in the table.

means of current observations in various basins and compares the relationship of the $\log(Q/F)$ or $\log(Q/R)$, where Q stands for the quartz content, F for the feldspar content and R for the rock-fragment content (Weltje, 1994). The use of both logratios in a single diagram allows the distinction of parent rock type, weathering history and palcotopography (Weltje et al., 1998). On this diagram, all the Khutia Khola samples

plot in the field of weathering index 1, some are near the boundary between weathering index 0 and 1 (Fig. 7.7). Most of the samples from the Jagati Formation fall towards metamorphic and sedimentary parentage and the samples from the Kala Formation fall near the boundary between metamorphic/sedimentary and plutonic parentage. These indices indicate that the sediments were mainly derived from high mountains (Higher Himalaya) and moderate hills (Lesser Himalaya) (Fig. 7.7). Sigdel and Sakai (2013) have also suggested similar result for the Siwalik sandstones in the Karnali River section.

7.7 Stratigraphic variation in petrographic modes

Stratigraphic variations in petrographic modes were plotted to examine the change in mineral distribution against stratigraphy. Carbonate grains are slightly increased from the upper member of the Jagati Formation to lower part of the lower member of the Kala Formation (Fig. 7.8 A). This increase was possibly due to the Lesser Himalaya (Chirouze et al., 2012). The increment of carbonate grains resembles with the change in river system from FA1 to FA2 which is around 13.5 Ma. Sigdel and Sakai (2013) also found similar trend of carbonate distribution in the Karnali River section. The feldspar grains remain unchanged in the lower part but the proportion

increase from the upper member of the Jagati Formation and continue up to the lower member of the Kala Formation (Fig. 7.8 B). The increase in feldspar grains (mainly K-feldspar) in sandstones indicates erosion of granitic rocks which are mainly derived from Dadeldhura granite (DeCelles et al., 1998). Mica grains do not change significantly but slightly increase upsection in the Kala Formation (Fig. 7.8 C), which indicate that both muscovite and biotite grains are abundant in upsection (cf. Decelles et al., 1998). The Siwalik Group in the west central Nepal also showed increase in mica content in stratigraphic upsection (Tokuaka et al., 1986; Hisatomi, 1990). The presence of 'salt and pepper' sandstones in the Kala Formation show increase in feldspar and mica grains after 11.0 Ma and it indicates dominant supply from the Higher Himalayan source in the Middle Siwalik (Sigdel and Sakai, 2013). The $Qp/(F+R)$ and $Qt/(F+R)$ ratios are slightly decreased in stratigraphic upsection with the average values 0.9 and 2.4 for the Jagati Formation, and 0.7 and 2.1 for the Kala Formation, respectively (Table 3), which suggest diminishing compositional maturity of sandstones toward stratigraphic up section (Suttner and Dutta, 1986) (Fig. 7.8 D and E).

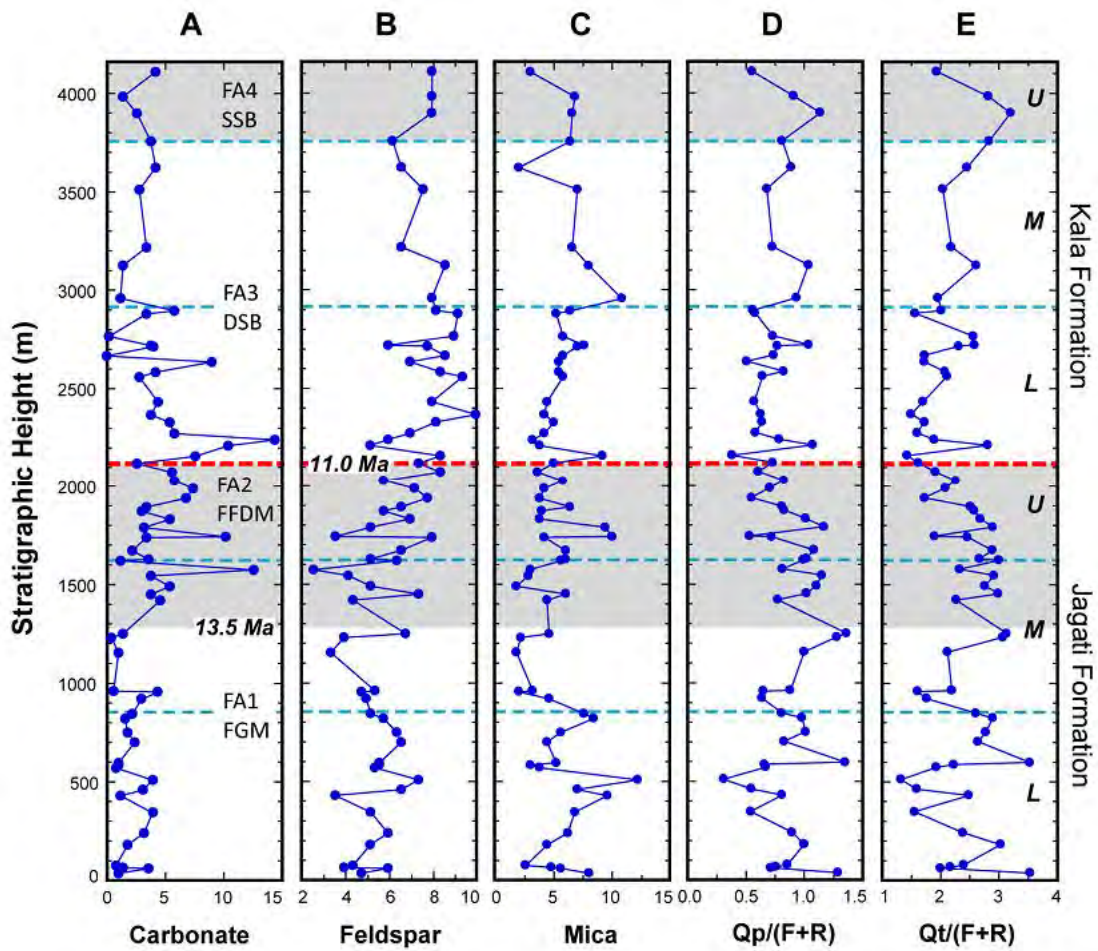


Fig: 7.8. Plots showing the stratigraphic variations. (A) Carbonate. (B) Feldspar. (C) Mica. (D) $Q_p/(F+R)$ (Polycrystalline quartz to feldspar plus rock fragments). (E) $Q_t/(F+R)$ (Total quartz to feldspar plus rock fragments). Age is denoted with reference of Ojha et al. (2000). Abbreviation: L - lower member, M - middle member, U - upper member, FA- facies association, FGM- fine-grained meandering river system, FFDM- flood-flow dominated meandering river system, DSB- Deep sandy braided river system, SSB- shallow sandy braided river system.

This petrographic results combining with other previous study in the Siwalik Group, we can conclude that the Khutia Khola sediments were mainly derived from the Higher and Lesser Himalaya because no significant changes were observed in the mineralogical composition within the whole section. Presence of low- to high-grade metamorphic lithic fragments even in the lower part of the Jagati Formation reflect that the Lesser as well as Higher Himalayas provided sediments from the beginning. The unstable tectonic setting and uplift of the Higher Himalaya is reflected with the higher content of muscovite and biotite showing 'salt and pepper' sandstones in the Kala Formation. The increased in biotite detritus from the Higher Himalayan source initiated after 11.0 Ma around the Khutia Khola section and the appearance of 'salt and pepper' sandstones is comparable with the other Siwalik sections but the timing of appearance is earlier in the Khutia Khola section. The timing of appearance of the Middle Siwalik with 'salt and pepper' sandstone is around 9.6 Ma in the nearby Karnali River section in the far western Nepal (Sigdel et al., 2011; Sigdel and Sakai, 2013) and around 8.5 to 9.5 Ma in the western and central Nepal (Nakayama and Ulak, 1999; Ulak and Nakayama, 2001). Comparing our petrographical study with Karnali River section (Sigdel and Sakai, 2013) together with other studies (Quade et al., 1995; DeCelles et al., 1998; Huyge et al., 2001, 2005; Szule et al., 2006; Bernet et al., 2006) from other Siwalik

sections suggest the lateral continuity in tectonic uplift of the Himalaya, but an earlier starting in western Nepal at about 12-9 Ma (DeCelles et al., 1998; Robinson et al., 2001; Huyghe et al., 2005). The earlier appearance of the Middle Siwalik around the Khutia Khola section than in nearby Karnali River section could possibly be related with the activation as well as proximity of the Ramgarh and Dadeldhura Thrusts in the Lesser Himalaya (Foldout 1a. in DeCelles et al., 2001).

Table 7.2. Recalculated framework (%) and other parameters for the Jagati and Kala Formations, Khutia Khola section.

Abbreviation: SmN - sample number; r: Metre - stratigraphic height in metre; Lith - lithology: FS, M, CS, VCS - fine, medium, coarse, very coarse grained sandstone, respectively; FA - Facies association; FA1 - fine-grained meandering; FA2 - flood-flow dominated meandering; FA3 - deep sandy braided; FA4 - shallow sandy braided; for other parameters refer to Table 2.

KALA FORMATION

SmN	Meter	Lith	FA	QtFL %			QFL %			QmFLt %			QmPK %			LsLmLv %			QplvLs %			Quartz %			Feld %		logratio		$\frac{\alpha}{\beta} \pm \frac{\gamma}{\delta}$
				Qt	F	L	Q	F	L	Qm	F	Lt	Qm	P	K	Ls	Lm	Lv	Qp	Lv	Ls	Qm	Qp	P	K	$\frac{\alpha}{\beta}$	$\frac{\gamma}{\delta}$		
Upper Member																													
KS-121	4108	CS	FA4	67.7	10.1	22.2	67.1	10.3	22.6	47.0	10.1	42.9	82.3	8.4	9.3	48.9	48.9	2.3	62.5	1.7	35.8	71.3	28.7	47.5	52.5	1.9	1.1	0.6	1.9
KS-120	3983	VCS	FA4	75.1	10.4	14.5	74.8	10.5	14.7	50.0	10.4	39.6	82.8	9.9	7.3	33.9	60.7	5.4	80.7	2.6	16.7	67.7	32.3	57.5	42.5	2.0	1.6	0.9	2.8
KS-118	3898	CS	FA4	76.7	9.9	13.4	76.6	10.0	13.5	49.1	9.9	40.9	83.2	7.6	9.2	42.6	50.0	7.4	80.1	2.9	16.9	64.5	35.5	45.0	55.0	2.0	1.7	1.1	3.2
Middle Member																													
KS-116	3756	CS	FA3	74.2	8.1	17.7	74.2	8.1	17.8	52.9	8.1	39.1	86.8	7.3	6.0	51.5	45.6	2.9	68.6	1.7	29.7	71.5	28.5	54.8	45.2	2.2	1.4	0.8	2.8
KS-114	3623	CS	FA3	71.8	8.4	19.8	71.6	8.4	19.9	45.4	8.4	46.2	84.4	7.1	8.5	55.1	43.6	1.3	69.7	0.7	29.7	63.9	36.1	45.5	54.5	2.1	1.3	0.9	2.5
KS-112	3510	CS	FA3	68.7	9.8	21.5	68.2	10.0	21.8	44.8	9.8	45.3	82.0	8.5	9.5	38.6	56.6	4.8	70.5	3.3	26.2	66.8	33.2	47.4	52.6	1.9	1.1	0.7	2.0
KS-110	3217	CS	FA3	69.3	8.3	22.4	69.1	8.4	22.5	45.7	8.3	46.0	84.7	7.0	8.4	47.2	49.4	3.4	66.9	2.2	30.9	66.7	33.3	45.5	54.5	2.1	1.1	0.7	2.2
KS-107	3125	CS	FA3	73.4	10.9	15.7	73.1	11.0	15.9	43.7	10.9	45.4	80.0	9.8	10.2	32.3	58.1	9.7	81.3	4.3	14.4	60.4	39.6	48.8	51.2	1.9	1.5	1.0	2.6
KS-106	2960	VCS	FA3	69.0	10.2	20.8	68.1	10.4	21.4	34.8	10.2	55.1	77.4	10.7	11.9	31.7	59.8	8.5	79.0	4.5	16.6	52.5	47.5	47.5	52.5	1.9	1.2	0.9	2.0
Lower Member																													
KS-104	2895	CS	FA3	66.8	11.2	20.0	68.2	11.5	20.4	48.2	11.2	40.5	81.1	10.6	8.3	54.8	41.1	4.1	61.3	2.7	36.0	72.1	27.9	56.1	43.9	1.8	1.2	0.6	2.0
KS-103	2880	CS	FA3	66.1	11.3	22.6	64.2	11.9	23.8	38.3	11.3	50.4	77.2	9.9	12.9	53.3	46.7	0.0	65.2	0.0	34.8	62.9	37.1	43.5	56.5	1.7	1.0	0.6	1.6
KS-99	2765	VCS	FA3	75.2	11.4	13.4	74.3	11.8	13.9	51.4	11.4	37.2	81.9	8.5	9.7	45.3	50.9	3.8	75.7	1.9	22.4	71.5	28.5	46.7	53.3	1.8	1.7	0.7	2.6
KS-98	2720	CS	FA3	72.6	8.1	19.2	72.5	8.2	19.3	43.1	8.1	48.8	84.1	7.4	8.5	49.3	43.7	7.0	72.8	3.4	23.8	59.8	40.2	46.7	53.3	2.2	1.3	1.0	2.6
KS-97	2714	FS	FA3	70.1	10.5	19.4	70.0	10.5	19.5	46.6	10.5	42.9	81.6	10.8	7.5	56.9	40.3	2.8	66.7	1.6	31.8	66.8	33.2	59.0	41.0	1.9	1.3	0.8	2.3
KS-94	2666	VCS	FA3	70.3	10.3	19.4	68.1	11.1	20.8	36.4	10.3	53.3	77.9	11.3	10.8	46.9	53.1	0.0	74.8	0.0	25.2	57.4	42.6	51.2	48.8	1.8	1.2	0.7	1.7
KS-93	2635	CS	FA3	65.6	8.9	25.6	64.8	9.1	26.2	44.6	8.9	46.6	83.4	8.1	8.5	69.3	27.7	3.0	50.3	2.0	47.6	70.4	29.6	48.6	51.4	2.0	0.9	0.5	1.7
KS-91	2585	VCS	FA3	69.0	10.3	20.7	68.5	10.5	21.0	40.6	10.3	49.0	79.7	9.2	11.1	70.2	29.8	0.0	64.9	0.0	35.1	60.2	39.8	45.2	54.8	1.9	1.2	0.8	2.1
KS-89	2560	MS	FA3	66.1	12.3	19.6	68.1	12.3	19.6	47.3	12.3	40.5	79.4	11.4	9.2	56.0	42.7	1.3	64.8	0.8	34.4	69.6	30.4	55.3	44.7	1.7	1.3	0.6	2.1
KS-86	2432	CS	FA3	64.3	10.1	25.6	63.9	10.2	26.0	42.0	10.1	48.0	80.7	10.1	9.2	43.1	50.0	6.9	62.2	5.2	32.6	66.5	33.5	52.5	47.5	1.8	0.9	0.6	1.7
KS-84	2368	CS	FA3	60.4	12.2	27.4	60.2	12.3	27.5	34.7	12.2	53.1	74.0	12.0	14.1	58.9	36.6	4.5	59.2	2.9	37.9	58.0	42.0	46.0	54.0	1.6	0.8	0.6	1.5
KS-82	2330	MS	FA3	63.8	10.6	25.6	63.6	10.6	25.7	39.8	10.6	49.6	79.0	9.7	11.3	52.5	42.4	5.1	61.5	3.4	35.1	62.9	37.1	46.3	53.7	1.8	0.9	0.6	1.7
KS-80	2272	FS	FA3	61.8	9.2	29.1	61.7	9.2	29.1	39.0	9.2	51.8	81.0	8.7	10.3	52.3	44.1	3.6	58.1	2.7	39.2	63.4	36.6	45.7	54.3	1.9	0.7	0.6	1.6
KS-78	2240	CS	FA3	65.5	7.3	27.3	65.5	7.3	27.3	38.4	7.3	54.3	84.0	7.4	8.5	83.0	17.0	0.0	54.4	0.0	45.6	58.7	41.3	46.7	53.3	2.2	0.9	0.8	1.9
KS-76	2210	FS	FA3	73.7	7.3	19.0	73.7	7.3	19.0	45.5	7.3	47.2	86.2	5.8	7.9	94.1	5.9	0.0	61.2	0.0	38.8	61.7	38.3	42.3	57.7	2.3	1.4	1.1	2.8

Table 7.2. (ctd). Recalculated framework (%) and other parameters for the Jagati and Kala Formations, Khutia Kholia section.

KALA FORMATION (Lower Member) (ctd)																													
SrnN	Meter	Lith	FA	QtFL %			QFL %			QmFLt %			QmPK %			LsLmLv %			QplvLs %			Quartz %		Feld %		Iogratio		$\frac{\sigma}{\sigma}$	$\frac{\sigma}{\sigma}$
				Qt	F	L	Q	F	L	Qm	F	Lt	Qm	P	K	Ls	Lm	Lv	Qp	Lv	Ls	Qm	Qp	P	K	$\frac{\sigma}{\sigma}$	$\frac{\sigma}{\sigma}$		
KS-74	2157	MS	FA3	60.4	11.2	28.3	59.8	11.4	28.8	43.0	11.2	45.7	79.3	9.4	11.3	58.5	36.8	4.7	46.8	4.0	49.2	73.2	26.8	45.2	54.8	1.6	0.7	0.4	1.4
KS-72	2120	CS	FA3	63.3	8.9	27.8	62.8	9.0	28.2	34.1	8.9	57.1	79.3	8.9	11.7	48.3	49.1	2.6	66.3	1.7	32.0	55.0	45.0	43.2	56.8	1.9	0.8	0.7	1.6
Mean				68.7	9.9	21.5	68.2	10.0	21.8	43.3	9.9	46.8	81.3	9.1	9.7	52.9	43.5	3.7	66.4	2.2	31.5	64.4	35.6	48.4	51.6	1.9	1.2	0.7	2.1
SD				4.7	1.4	4.6	4.7	1.5	4.6	5.2	1.4	5.4	3.0	1.6	1.8	14.3	12.6	2.7	9.0	1.5	9.3	5.7	5.7	4.6	4.6	0.2	0.3	0.2	0.5
JAGATI FORMATION																													
<i>Upper Member</i>																													
KS-70	2075	MS	FA2	65.7	10.9	23.4	65.7	10.9	23.4	44.9	10.9	44.2	80.5	10.2	9.3	65.6	34.4	0.0	57.6	0.0	42.4	68.4	31.6	52.4	47.6	1.8	1.0	0.6	1.9
KS-68	2028	FS	FA2	69.4	7.6	23.0	69.4	7.6	23.0	44.0	7.6	48.4	85.3	9.1	5.6	54.5	42.0	3.4	65.5	2.0	32.4	63.4	36.6	62.1	37.9	2.2	1.1	0.8	2.3
KS-66	1988	CS	FA2	68.3	9.0	22.7	68.1	9.0	22.9	44.6	9.0	46.4	83.3	7.4	9.3	89.0	11.0	0.0	53.2	0.0	46.8	66.1	33.9	44.4	55.6	2.0	1.1	0.7	2.1
KS-64	1938	MS	FA2	64.4	9.3	26.3	64.0	9.4	26.6	43.3	9.3	47.4	82.3	8.6	9.1	68.2	30.9	0.9	52.5	0.6	46.9	68.3	31.7	48.7	51.3	1.9	0.9	0.5	1.7
KS-62	1893	MS	FA2	71.5	8.2	20.3	71.5	8.2	20.3	48.5	8.2	43.3	85.6	7.0	7.4	52.4	47.6	0.0	68.4	0.0	31.6	67.8	32.2	48.5	51.5	2.2	1.3	0.8	2.5
KS-60	1872	MS	FA2	72.0	6.9	21.1	72.0	6.9	21.1	48.8	6.9	44.3	87.7	6.0	6.4	48.3	51.7	0.0	69.5	0.0	30.5	67.8	32.2	48.3	51.7	2.4	1.2	0.8	2.6
KS-58	1830	FS	FA2	72.8	9.4	17.7	72.8	9.4	17.7	45.4	9.4	45.2	82.8	6.4	10.8	56.1	42.4	1.5	72.9	0.7	26.4	62.4	37.6	37.1	62.9	2.0	1.4	1.0	2.7
KS-56	1788	FS	FA2	74.3	6.5	19.1	74.3	6.5	19.1	44.3	6.5	49.1	87.1	4.5	8.4	47.4	47.4	5.3	74.8	2.5	22.6	59.7	40.3	34.6	65.4	2.4	1.4	1.2	2.9
KS-54	1743	MS	FA2	65.5	6.7	27.7	65.5	6.7	27.7	47.2	6.7	46.1	87.5	3.5	9.0	82.4	17.6	0.0	44.5	0.0	55.5	72.0	28.0	27.8	72.2	2.3	0.9	0.5	1.9
KS-53	1738	MS	FA2	72.6	9.5	17.9	72.2	9.7	18.2	50.4	9.5	40.1	84.1	6.8	9.2	52.0	45.3	2.7	68.0	1.6	30.5	70.8	29.2	42.5	57.5	2.0	1.4	0.7	2.5
KS-51	1672	CS	FA2	74.8	7.8	17.5	74.6	7.8	17.5	46.5	7.8	45.8	85.7	7.8	6.5	45.9	50.0	4.1	76.1	1.9	21.9	62.5	37.5	54.5	45.5	2.3	1.5	1.1	2.9
KS-49	1628	FS	FA2	73.3	7.0	19.8	73.1	7.0	19.9	44.9	7.0	48.1	86.6	6.2	7.2	39.2	60.8	0.0	78.2	0.0	21.8	61.8	38.2	46.2	53.8	2.4	1.3	1.0	2.7
<i>Middle Member</i>																													
KS-47	1620	FS	FA2	75.0	7.8	17.2	75.0	7.8	17.2	50.2	7.8	42.0	86.6	6.3	7.1	42.3	57.7	0.0	77.3	0.0	22.7	67.0	33.0	46.9	53.1	2.3	1.5	1.0	3.0
KS-45	1574	FS	FA2	70.3	3.4	26.4	70.2	3.4	26.4	45.5	3.4	51.1	93.0	3.8	3.2	84.0	16.0	0.0	52.5	0.0	47.5	65.0	35.0	53.8	46.2	3.0	1.0	0.8	2.3
KS-44	1545	CS	FA2	75.2	4.8	20.0	75.0	4.8	20.2	45.1	4.8	50.1	90.4	4.1	5.5	55.7	43.2	1.1	72.1	0.6	27.4	60.6	39.4	42.9	57.1	2.7	1.3	1.2	2.9
KS-42	1490	MS	FA2	73.4	6.1	20.5	73.4	6.1	20.5	44.1	6.1	49.9	87.9	4.7	7.4	47.7	52.3	0.0	75.0	0.0	25.0	60.0	40.0	38.5	61.5	2.5	1.3	1.1	2.8
KS-41	1450	FS	FA2	74.9	9.6	15.5	74.9	9.6	15.5	49.4	9.6	41.1	83.8	7.0	9.2	55.0	45.0	0.0	75.0	0.0	25.0	65.9	34.1	43.2	56.8	2.1	1.6	1.0	3.0
KS-40	1419	FS	FA2	69.5	5.4	25.1	69.5	5.4	25.1	45.8	5.4	48.8	89.4	3.8	6.7	54.9	45.1	0.0	63.2	0.0	36.8	66.0	34.0	36.4	63.6	2.5	1.0	0.8	2.3
KS-37	1250	FS	FA1	75.8	8.0	16.2	75.8	8.0	16.2	43.0	8.0	49.1	84.3	9.7	6.0	46.4	53.6	0.0	81.4	0.0	18.6	56.7	43.3	61.8	38.2	2.3	1.5	1.4	3.1
KS-36	1230	CS	FA1	75.6	4.6	19.8	75.6	4.6	19.8	43.9	4.6	51.5	90.5	4.3	5.2	50.0	50.0	0.0	76.1	0.0	23.9	58.2	41.8	45.0	55.0	2.8	1.3	1.3	3.1

Table 7.2. (ctd). Recalculated framework (%) and other parameters for the Jagati and Kala Formations, Khutia Kholra section.

JAGATI FORMATION (Middle Member) (ctd)

SmN	Meter	Lith	FA	QtFL %			QFL %			QimFLt %			LsLmLv %			QpLvLs %			Quartz %		Feld %		logratio		$\frac{\sum \text{Feld}}{\sum \text{Qtz}}$	$\frac{\sum \text{Feld}}{\sum \text{Qtz}}$			
				Qt	F	L	Q	F	L	Qm	F	Lt	Qm	P	K	Ls	Lm	Lv	Qp	Lv	Ls	Qm	Qp	P			K	$\frac{\sum \text{Feld}}{\sum \text{Qtz}}$	$\frac{\sum \text{Feld}}{\sum \text{Qtz}}$
KS-34	1155	CS	FA1	68.0	3.7	28.3	68.0	3.7	28.3	36.0	3.7	60.3	90.6	6.1	3.3	52.7	45.7	1.6	67.6	0.9	31.5	52.9	47.1	64.7	35.3	2.9	0.9	1.0	2.1
KS-31	960	MS	FA1	70.3	6.3	23.4	69.8	6.4	23.8	41.1	6.3	52.6	86.7	4.9	8.4	44.0	56.0	0.0	72.8	0.0	27.2	59.9	40.1	37.0	63.0	2.4	1.1	0.9	2.2
KS-30	955	CS	FA1	61.7	5.9	32.4	61.7	5.9	32.4	36.8	5.9	57.3	86.3	6.3	7.4	46.6	52.6	0.8	61.8	0.6	37.6	59.7	40.3	45.8	54.2	2.4	0.6	0.6	1.6
KS-28	920	MS	FA1	64.5	6.0	29.5	64.3	6.0	29.7	40.7	6.0	53.3	87.2	7.1	5.6	50.8	49.2	0.0	60.6	0.0	39.4	63.8	36.2	56.0	44.0	2.4	0.8	0.6	1.8
Lower Member																													
KS-26	845	FS	FA1	72.5	6.3	21.2	72.4	6.3	21.2	49.9	6.3	43.8	88.7	5.2	6.1	55.2	44.8	0.0	65.7	0.0	34.3	69.0	31.0	46.2	53.8	2.4	1.2	0.8	2.6
KS-25	820	FS	FA1	74.6	7.1	18.3	74.5	7.1	18.4	49.1	7.1	43.8	87.4	7.8	4.8	50.7	49.3	0.0	73.0	0.0	27.0	66.1	33.9	62.1	37.9	2.4	1.4	1.0	2.9
KS-24	750	MS	FA1	74.0	7.6	18.4	73.9	7.6	18.5	46.8	7.6	45.6	86.1	6.5	7.4	48.7	50.0	1.3	74.3	0.7	25.0	63.7	36.3	46.9	53.1	2.3	1.4	1.0	2.8
KS-22	700	FS	FA1	73.0	7.7	19.3	72.9	7.7	19.4	49.8	7.7	42.6	86.6	6.9	6.5	65.1	34.9	0.0	64.5	0.0	35.5	68.6	31.4	51.5	48.5	2.3	1.3	0.8	2.6
KS-19	595	CS	FA1	77.9	6.6	15.5	77.9	6.6	15.5	48.1	6.6	45.3	88.0	6.9	5.2	48.5	51.5	0.0	79.9	0.0	20.1	61.7	38.3	57.1	42.9	2.5	1.6	1.4	3.5
KS-18	585	CS	FA1	70.1	6.3	23.7	69.8	6.3	23.9	48.4	6.3	45.3	88.6	6.1	5.3	51.9	48.1	0.0	62.6	0.0	37.4	70.2	29.8	53.6	46.4	2.4	1.1	0.7	2.2
KS-17	570	CS	FA1	66.0	6.3	27.7	66.0	6.3	27.7	42.8	6.3	50.9	87.2	7.1	5.7	58.8	41.2	0.0	58.6	0.0	41.4	65.0	35.0	55.6	44.4	2.4	0.9	0.7	1.9
KS-15	510	FS	FA1	57.0	10.0	33.0	57.0	10.0	33.0	43.5	10.0	46.5	81.3	9.6	9.1	70.5	28.7	0.8	36.5	0.7	62.8	76.3	23.7	51.4	48.6	1.7	0.5	0.3	1.3
KS-14	460	FS	FA1	61.9	8.4	29.7	61.7	8.4	29.8	40.4	8.4	51.3	82.8	10.9	6.3	66.7	33.3	0.0	51.6	0.0	48.4	65.7	34.3	63.6	36.4	2.0	0.7	0.5	1.6
KS-13	430	FS	FA1	71.6	4.3	24.2	71.5	4.3	24.2	48.1	4.3	47.6	91.9	5.0	3.2	52.9	46.1	1.0	64.1	0.7	35.3	67.4	32.6	61.1	38.9	2.8	1.1	0.8	2.5
KS-11	345	FS	FA1	60.9	7.0	32.2	60.9	7.0	32.2	39.7	7.0	53.4	85.1	7.5	7.5	60.8	38.3	0.8	51.6	0.7	47.7	65.2	34.8	50.0	50.0	2.2	0.6	0.5	1.6
KS-10	240	FS	FA1	70.7	7.2	22.1	70.6	7.2	22.2	44.0	7.2	48.8	85.9	7.5	6.6	60.9	39.1	0.0	66.3	0.0	33.7	62.5	37.5	53.3	46.7	2.3	1.2	0.9	2.4
KS-7	180	MS	FA1	75.4	6.0	18.6	75.3	6.0	18.7	50.3	6.0	43.7	89.4	3.3	7.3	53.1	46.9	0.0	71.5	0.0	28.5	67.0	33.0	30.8	69.2	2.5	1.4	1.0	3.0
KS-5	75	MS	FA1	72.0	5.2	22.8	71.6	5.3	23.1	45.4	5.2	49.4	89.7	6.1	4.2	54.2	43.8	2.1	66.3	1.3	32.5	64.3	35.7	59.1	40.9	2.6	1.1	0.9	2.4
KS-4	65	MS	FA1	69.4	4.6	26.0	69.1	4.6	26.2	44.6	4.6	50.8	90.7	5.1	4.2	61.9	36.3	1.8	59.1	1.1	39.8	65.1	34.9	55.0	45.0	2.7	1.0	0.8	2.2
KS-3	60	MS	FA1	67.5	7.3	25.2	67.2	7.4	25.4	43.0	7.3	49.6	85.4	8.3	6.3	55.3	43.7	1.0	62.6	0.6	36.8	64.5	35.5	56.7	43.3	2.2	1.0	0.7	2.0
KS-1	35	MS	FA1	78.4	5.9	15.7	78.3	5.9	15.8	49.5	5.9	44.6	89.4	5.8	4.9	56.3	40.6	3.1	75.3	1.3	23.4	63.5	36.5	54.2	45.8	2.6	1.6	1.3	3.5
Mean				70.5	6.9	22.5	70.4	6.9	22.6	45.3	6.9	47.8	86.8	6.5	6.7	56.2	43.0	0.8	65.9	0.5	33.7	64.7	35.3	49.4	50.6	2.3	1.2	0.9	2.4
SD				4.9	1.7	4.8	4.9	1.7	4.9	3.6	1.7	4.2	2.9	1.9	1.9	10.8	10.7	1.3	10.1	0.7	10.2	4.4	4.4	9.1	9.1	0.3	0.3	0.2	0.5

CHAPTER EIGHT

The Middle Bengal Fan turbidites

8.1. Introduction

The Bengal Fan is the world's largest submarine fan and the Himalaya is main source of the sediments in this basin (Curry and Moore, 1971; Emmel and Curry, 1981; Cochran, 1990). Sediments originated from the Himalayas are transported through the Ganges and Brahmapurta rivers from the central and eastern Himalayas, and the southern part of the Tibetan plateau to the Bengal Basin. These Himalayan sediments passing through delta and shelf canyon, and the sediments supplying by turbidity currents in the Middle Bengal Fan show grain sizes variations (France-Lanord et al., 2016). These sediments contain a record of the erosion and the uplift of the Himalayas (Curry and Moore, 1971).

International Ocean Discovery Program (IODP) Expedition 354 to 8°N in the Bay of Bengal drilled seven-sites, 320 km long transect across the Bengal Fan (Fig. 8.1) (cf. France-Lanord et al., 2016). The submarine fan near the sea floor in the study area consists of channel and levee complexes. The evolution of the channel and levee complexes is the function of external forces such as climatic changes which may be

related to sea-level changes, and tectonics as well as autogenic processes such as shifting of submarine channels. Sedimentation process is expected to be changed even within a single channel-levee complex due to buildup of the levee through time which leads to the changes in grain size distribution.

This chapter focuses on the grain size distribution and statistic parameters of turbidite beds from two sites; U1450 (811 m deep) and U1451 (1181 m deep) of IODP Expedition 354. Two holes were drilled in each site; Holes A and B.

The deepest point of the Hole U1450A was 688 meter below sea floor (mbsf) and Hole U1450B depth ranges from 608 to 812 mbsf. The lower limit of the Hole U1451A was 582 mbsf and Hole U1451B depth ranges from 542 to 1181 mbsf. The sediments obtained during the Expedition 354 dominantly consists turbidite beds with thickness between a few centimeters and 2 m or more. The grain size analyses of the sediments from these two holes allow the study of the long-term changes in turbidites and their grain-size variations in the Middle Bengal Fan.

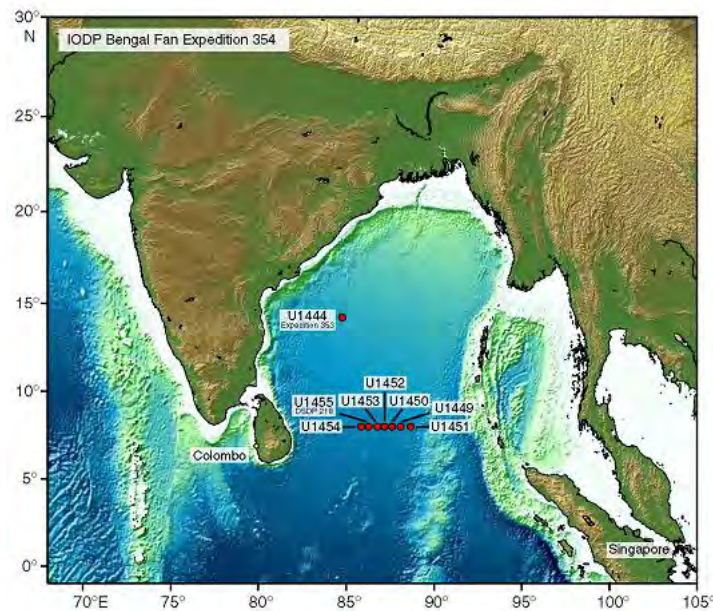


Fig. 8.1. Location of Expedition 354 drill sites (France-Lanord et al., 2016).

8.2. Samples

A total of 311 samples were collected, ninety-six were from Hole U1450A, and twenty-four were from Hole U1450B, one hundred samples were from Hole U1451A, and ninety-one were from Hole U1451B. Sediment specimens were collected from the base, middle and top horizons of sandy part and upper muddy horizon of the well-preserved turbidite beds (Fig. 8.2).

8.2.1. Sample preparation and analysis

Sediment samples of approximately 0.1 g of dry weight were placed in a glass vials and mixed with 10% hydrogen peroxide (H₂O₂) solution. Then the sample is kept



Fig. 8.2. Representative examples of turbidites. A) 354-U1450A-30F-2, 48-81 cm. B) 354-U1450A-42F-1, 25-58 cm. C) 354-U1451A-7H-2, 84-116 cm. D) 354-U1451A-10F-1, 93-126 cm.

for more than twenty-four hours to decompose the organic matters contained in the sample. For complete disaggregation of the sediment, an ultrasonic probe was used for approximately 30 seconds before analyzing the sample in the laser-analyzer. The grain size analysis was performed by laser diffraction method using SALD 3000s (Shimadzu

Corp.: range of measureable size, $0.3\mu\text{m} - 3\text{ mm}$). 2% of Sodium hexametaphosphate (NaPO_3)₆ solution was used as dispersant for the samples in the laser-analyzer. For each sample at least five times of measurement were taken to confirm reproducibility and then all results were averaged to obtain the final value. After analysis of each sample, laser analyzer was cleaned two times with tap water and finally one time with filter water.

8.2.2. Data processing

Grain size parameters, mean (M_z), standard deviation (σ), skewness (SK) and kurtosis (K_G) as well as sand, silt and clay weight percentage were calculated for all samples using phi-scale according to methods of Folk and Ward (1957). The results are tabulated in Table 8.1.

Graphical mean, standard deviation, skewness and kurtosis were plotted against the depth to understand the vertical variation of these parameters. Similarly, relative wt % of sand, silt and clay were plotted on the ternary diagram by Shepard (1954) to understand the textural characteristic of sediments. Frequency distribution curves were drawn from number percent of grain sizes to obtain the grain size distribution patterns.

Frequency curves of the different horizons of a turbidite bed were compared to understand the variation in grain size distribution along the bed.

Following mathematical calculations (Folk and Ward, 1957) were applied in this study;

$$1) \text{ Mean } (M_z) = (\phi_{16} + \phi_{50} + \phi_{84}) / 3$$

$$2) \text{ Standard deviation } (\sigma) = \{(\phi_{84} - \phi_{16}) / 4\} + \{(\phi_{95} - \phi_5) / 6.6\}$$

$$3) \text{ Skewness } (SK) = \{(\phi_{16} + \phi_{84} - 2\phi_{50}) / 2(\phi_{84} - \phi_{16})\} + \\ \{(\phi_5 + \phi_{95} - 2\phi_{50}) / 2(\phi_{95} - \phi_5)\}$$

$$4) \text{ Kurtosis } (K_G) = (\phi_{95} - \phi_5) / \{2.44 (\phi_{75} - \phi_{25})\}$$

8.3. Results

Graphical grainsize parameters of each hole were plotted against depth to understand the vertical variations in these parameters. Results of both sites have been described below separately.

8.3.1. Holes U1450 A & B

The mean (M_z) values of grain size range from 2.53 to 8.28 phi with an average

value of 5.36 phi. The mean values denote that the major class is of silt-size particles and show slightly coarsening upward trend (Fig. 8.3. A and E). A few samples show low values which represent fine sand-size particles. The standard deviation (σ) values range from 0.95 to 2.27 phi with an average of 1.58 phi. Most of the samples are poorly sorted and a few samples are moderately sorted or very poorly sorted (Fig. 8.3. B and F). The skewness (SK) values range from -0.06 to + 0.49 with an average of 0.15. Most of the samples fall in the symmetrical and positively skewed category except four samples fall in very positively skewed category (Fig. 8.3. C and G). The kurtosis (K_G) values range from 0.76 to 2.05 with an average of 1.09. Most of samples show mesokurtic and leptokurtic distributions except four samples show very leptokurtic distributions (Fig. 8.3. D and H).

8.3.2. Holes U1451 A & B

The mean(M_z) values of grain size show that the major class is of silt-size particles and few are in fine sand-size particles (Fig. 8.4. A and E). The mean values range from 1.69 to 8.02 phi with an average value of 5.63 phi. The standard deviation (σ) show almost all samples are poorly sorted except two samples are moderately sorted and one sample is well sorted (Fig. 8.4. B and F). The values range from 0.38 to 2.29

phi with an average value of 1.58 phi. The skewness (SK) values range from -0.12 to +0.45 with an average of 0.17. Most of the samples are distributed in the symmetrical and positively skewed category except nine samples fall in very positively skewed category (Fig. 8.4. C and G). The kurtosis (K_G) values range from 0.78 to 1.40 with an average of 1.08. Most of samples show mesokurtic and leptokurtic distributions except five samples show platykurtic distributions (Fig. 8.4. D and H).

8.4. Textural classification of sediments

The ternary plot of sand-silt-clay by Shepard (1954) provides the textural classification of the sediment based on grain size. Sediment specimens from the base, middle and top horizons, and upper muddy horizon of the well-preserved turbidite beds were plotted separately in the diagram (Fig. 8.5 and 8.6). Most of the samples from the base, middle and top horizons are clustered near the line joining silt and sand, and the samples from upper muddy horizons are clustered near the line joining silt and clay. The diagrams show that sediments are mostly sandy silt, silty sand and clayey silt, and few are silt and sand.

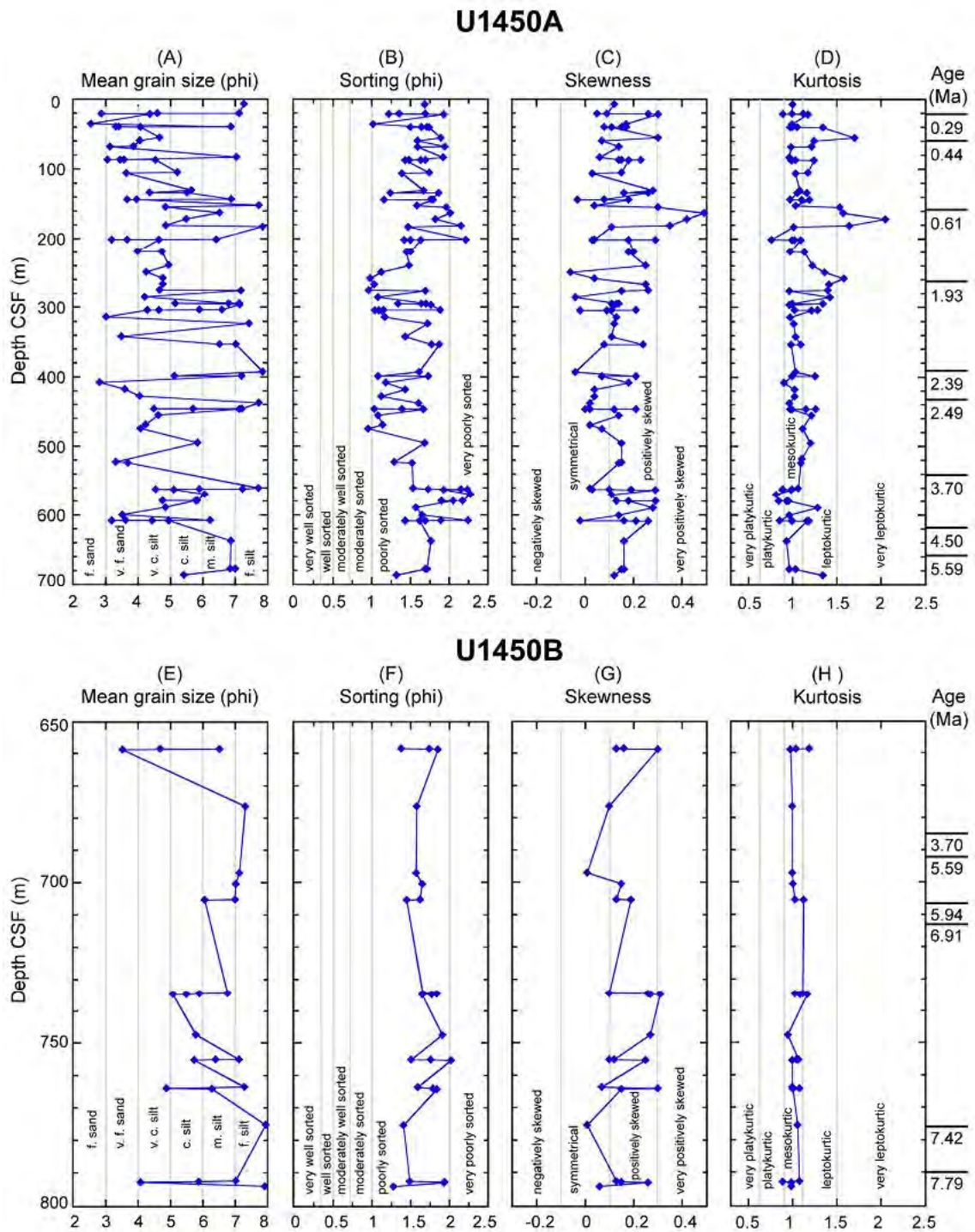


Fig. 8.3. Depth variation of textural components of site U1450 sediments. A) Mean grain size, B) Standard deviation (sorting), C) Skewness, and D) Kurtosis. Age after France-Lanord et al. (2016). Calculation methods are after Folk and Ward (1957). Abbreviation: CSF – core depth below seafloor.

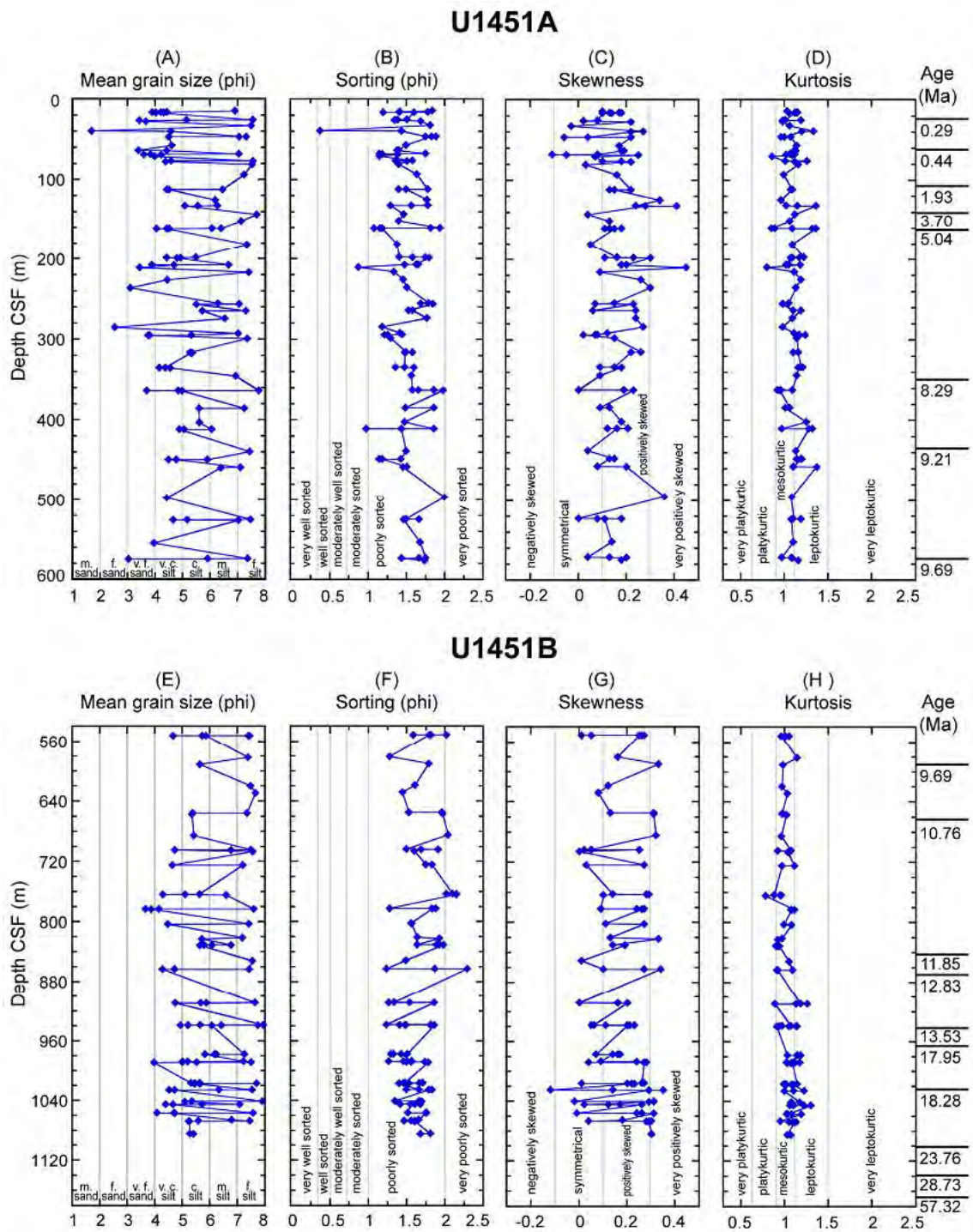


Fig. 8.4. Depth variation of textural components of site U1451 sediments. A) Mean grain size, B) Standard deviation (sorting), C) Skewness, and D) Kurtosis. Age after France-Lanord et al. (2016). Calculation methods are after Folk and Ward (1957). Abbreviation: CSF – core depth below seafloor.

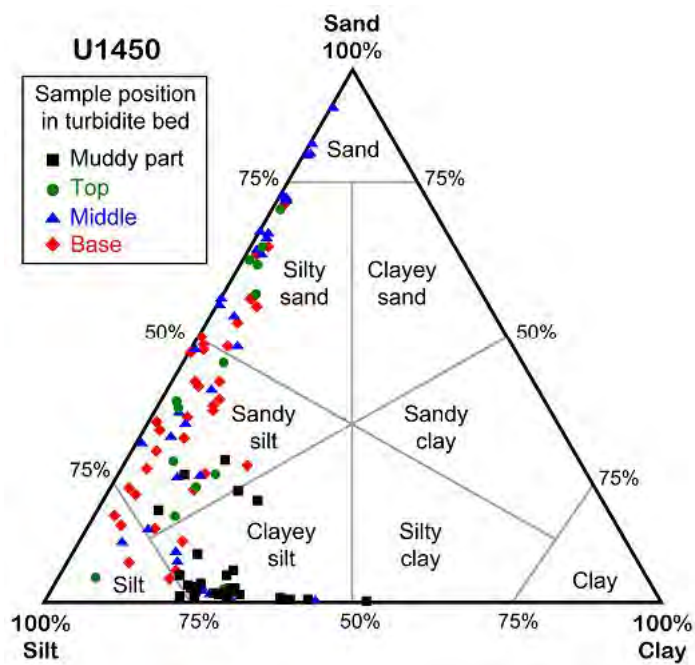


Fig. 8.5. Ternary plots of sand-silt-clay of site U1450 (after Shepard, 1954).

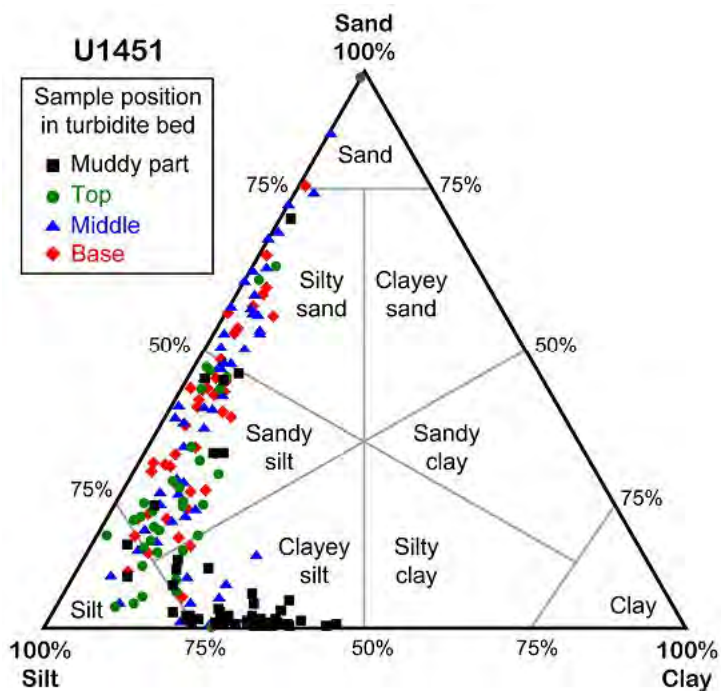


Fig. 8.6. Ternary plots of sand-silt-clay of site U1451 (after Shepard, 1954).

8.5. Frequency curve

Frequency distribution curve shows the pictorial representation of weight percentage of different fractions of sediments and is used to describe the nature of sediments. Frequency curves of the different horizons of turbidite beds were compared to understand the variation in grain size distribution along the bed. Altogether 20 turbidite beds from site U1450 and 46 turbidite beds from site U1451 were studied. Frequency distribution curves show that three types of beds are mainly present; normally graded, inversely graded and homogeneous (massive) beds (Fig 8.6). The samples from site U1450 show inversely graded beds are dominant in site U1450 and thicker massive beds are dominant in site U1451.

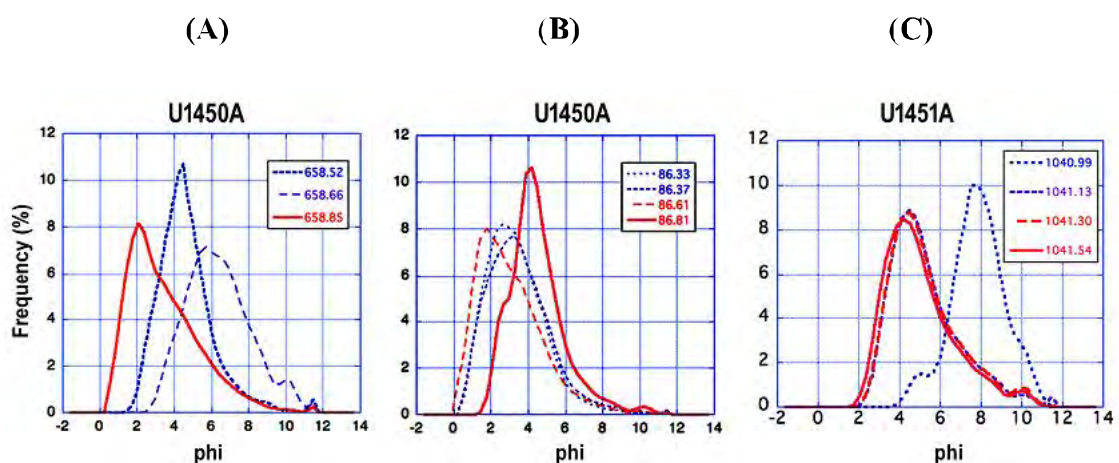


Fig. 8.7. Frequency curve plots against grain size (phi) showing different bed types. (A) Normally graded bed (U1450A). (B) Inversely graded bed (U1450A). (C) Massive (homogeneous) bed (U1451A).

8.6. Comparison of the Siwalik Group sediments and the Bengal Fan turbidites

The grain size parameters of the turbidites in the Middle Bengal Fan do not show any significant variations along the stratigraphic depth and age. In the instance, the variation in the grain size in the Middle Bengal Fan turbidites cannot be correlated with lithological changes in the Khutia Khola section of the Siwalik Group, probably because the change around 13.5 Ma was not strong enough to cause the sediment characteristics from the far western Himalaya to be transmitted to the Ganges River mouth.

Table 8.1. Grain size analysis data of Itoic U1450A (IODP Bengal Fan Expedition 354)

Abbreviation: S.No. - serial number; Type- drilling type; H- half-length advanced piston corer, F- full-length advanced piston corer, X- extended core barrel, R- rotary core barrel; CSF- core depth below seafloor; M_z- mean, σ - sorting, SK- skewness, KG- kurtosis; F- fine (muddy part of turbidite bed); T- turbidite bed, H- hemipelagic bed; D.gr.- dark gray, Gr.- gray, G. gr.- greenish gray, L. gr. - light gray; similar color indicates the single bed.

S.No.	Core	Type	Sect.	Top offset (cm)	Bottom offset (cm)	Top depth CSF (m)	Bottom depth CSF (m)	Sand (%)	Silt (%)	Clay (%)	M _z	σ	SK	KG	Position	Turbi/Hemi	Color
1	1	H	5	64	69	6.64	6.69	1.44	69.89	28.66	7.26	1.68	0.12	1.00	F. top	T	D. gr.
2	4	F	1	2	3	20.22	20.23	1.64	71.74	26.62	7.11	1.69	0.09	0.99	F. top	T	D. gr.
3	4	F	1	11	12	20.31	20.32	37.64	59.84	2.53	4.58	1.35	0.05	1.12	Top	T	D. gr.
4	4	F	1	30	31	20.50	20.51	83.99	14.83	1.04	2.85	1.22	0.26	0.89	Middle	T	D. gr.
5	4	F	1	95	96	21.15	21.16	55.86	37.61	6.53	4.35	1.93	0.36	1.17	Base	T	D. gr.
6	7	F	1	47	52	34.77	34.82	92.77	6.90	0.33	2.53	1.02	0.17	0.99	Middle	T	D. gr.
7	8	F	1	12	13	39.12	39.13	2.83	74.39	22.77	6.86	1.71	0.15	0.99	F. base	T	D. gr.
8	8	F	1	18	19	39.18	39.19	73.72	24.69	1.36	3.30	1.50	0.17	1.05	Top	T	D. gr.
9	8	F	1	50	51	39.50	39.51	67.95	29.85	1.65	3.39	1.64	0.08	0.97	Middle	T	D. gr.
10	8	F	1	84	85	39.84	39.85	52.73	42.36	4.91	4.06	1.74	0.11	1.34	Base	T	D. gr.
11	11	F	1	133	134	54.53	54.54	41.37	50.96	7.67	4.65	1.89	0.36	1.70	Base	T	D. gr.
12	12	F	1	79	80	58.69	58.70	53.65	42.43	3.92	4.04	1.59	0.07	1.24	Middle	T	D. gr.
13	14	F	1	2	3	67.42	67.43	57.96	36.78	5.26	3.84	1.94	0.14	1.21	Top	T	D. gr.
14	14	F	1	33	34	67.73	67.74	74.37	23.32	1.38	3.12	1.59	0.14	0.98	Base	T	D. gr.
15	17	F	1	106	112	82.66	82.72	5.67	66.42	27.91	7.03	1.92	0.06	0.96	F. middle	T	D. gr.
16	18	F	1	2	3	86.32	86.33	70.35	28.30	1.12	3.43	1.48	0.15	0.98	F. top	T	D. gr.
17	18	F	1	6	7	86.36	86.37	66.49	31.18	1.91	3.55	1.63	0.14	1.03	Top	T	D. gr.
18	18	F	1	30	31	86.60	86.61	74.62	22.92	1.53	3.04	1.69	0.23	0.99	Middle	T	D. gr.
19	18	F	1	50	51	86.80	86.81	41.60	54.95	3.45	4.52	1.43	0.18	1.24	Base	T	D. gr.
20	22	H	1	43	47	104.93	104.97	26.10	66.15	7.75	5.21	1.74	0.15	1.17	Top	T	D. gr.
21	22	H	1	96	97	105.46	105.47	65.65	32.78	1.58	3.62	1.39	0.03	1.03	Base	T	D. gr.
22	27	F	2	54	55	130.27	130.28	17.18	72.93	9.90	5.63	1.67	0.28	1.08	F. top	T	D. gr.
23	28	F	1	62	63	133.52	133.53	47.46	50.69	1.85	4.34	1.24	0.16	1.16	Base	T	D. gr.
24	28	F	1	84	89	133.74	133.79	23.86	65.38	10.77	5.50	1.86	0.26	1.05	F. top	T	D. gr.

Table 8.1. (ctd). Grain size analysis data of I/Oc U1450A (IODP Bengal Fan Expedition 354)

S.No.	Core	Type	Secl.	Top offset (cm)	Bottom offset (cm)	Top depth CSF (m)	Bottom depth CSF (m)	Sand (%)	Silt (%)	Clay (%)	M _z	σ	SK	KG	Position	Turbi/Hemi	Color
25	30	F	1	67	68	143.07	143.08	3.40	73.06	23.55	6.87	1.76	0.08	0.97	F. top	T	D. gr.
26	30	F	1	103	104	143.43	143.44	69.40	30.37	0.04	3.65	1.16	-0.03	1.10	Middle	T	D. gr.
27	30	F	1	132	133	143.72	143.73	57.18	37.87	4.95	3.94	1.79	0.18	1.19	Base	T	D. gr.
28	32	F	1	20	25	152.10	152.15	0.35	61.51	38.14	7.72	1.58	0.04	1.03	F. top	T	D. gr.
29	32	F	2	77	78	154.17	154.18	36.89	54.45	8.66	4.83	1.96	0.32	1.53	Base	T	D. gr.
30	34	F	1	107	108	162.47	162.48	4.34	77.88	17.77	6.50	2.01	0.49	1.57	Base	T	D. gr.
31	36	F	1	77	78	171.67	171.68	13.68	75.46	10.86	5.48	1.82	0.42	2.05	Base	T	D. gr.
32	38	F	1	43	44	180.83	180.84	38.17	52.63	9.20	4.84	2.15	0.35	1.64	Base	T	D. gr.
33	38	F	2	100	105	182.93	182.98	0.26	60.81	38.94	7.84	1.47	0.11	1.01	F. middle	T	D. gr.
34	42	F	2	34	35	201.19	201.20	18.85	55.99	25.17	6.41	2.21	0.04	0.76	F. top	T	D. gr.
35	42	F	2	52	53	201.37	201.38	64.15	34.43	1.01	3.65	1.42	0.03	0.99	Top	T	Gr.
36	42	F	2	63	68	201.48	201.53	75.93	22.88	1.19	3.17	1.50	0.29	1.02	Middle	T	D. gr.
37	42	F	2	75	76	201.60	201.61	40.68	54.92	4.40	4.63	1.63	0.18	1.09	Base	T	D. gr.
38	46	F	1	102	107	219.42	219.47	58.92	39.10	1.99	3.97	1.50	0.20	0.97	F. middle	T	D. gr.
39	46	F	1	123	124	219.63	219.64	35.33	60.69	3.98	4.73	1.45	0.18	1.13	Middle	T	D. gr.
40	50	F	2	46	52	239.31	239.37	30.79	64.17	5.05	4.94	1.48	0.25	1.22	Middle	T	D. gr.
41	52	F	3	13	14	249.30	249.31	46.88	52.94	0.17	4.24	1.12	-0.06	1.36	Base	T	D. gr.
42	54	F	2	32	33	258.03	258.04	21.20	75.99	2.81	4.75	0.98	0.04	1.58	Base	T	D. gr.
43	56	F	1	97	98	266.87	266.88	24.97	71.03	3.99	4.75	1.03	0.25	1.41	Base	T	D. gr.
44	58	F	1	21	22	275.61	275.62	28.32	67.87	3.81	4.66	0.96	0.26	1.40	Base	T	D. gr.
45	58	F	2	37	43	276.43	276.49	1.25	71.14	27.60	7.17	1.69	0.15	0.96	F. top	T	Gr.
46	60	F	1	38	39	285.28	285.29	50.13	49.67	0.20	4.19	1.08	-0.04	1.42	Base	T	D. gr.
47	62	F	1	2	3	294.42	294.43	3.04	75.34	21.62	6.79	1.70	0.13	0.99	F. top	T	D. gr.
48	62	F	1	26	27	294.66	294.67	1.33	72.62	26.05	7.12	1.64	0.14	1.00	Middle	T	D. gr.
49	62	F	1	32	33	294.72	294.73	20.06	75.54	4.40	5.14	1.34	0.11	1.34	Base	T	D. gr.
50	62	F	2.0	42	47	296.27	296.32	2.05	70.04	27.91	7.13	1.76	0.12	0.96	Top	T	D. gr.

Table 8.1. (ctd). Grain size analysis data of I/Olc U1450A (IODP Bengal Fan Expedition 354)

S.No.	Core	Type	Sect.	Top offset (cm)	Bottom offset (cm)	Top depth CSF (m)	Bottom depth CSF (m)	Sand (%)	Silt (%)	Clay (%)	M _z	σ	SK	KG	Sample Description	Turbi/ Hemi	Color
51	64	F	1	3	4	303.93	303.94	8.72	70.89	20.38	6.58	1.88	0.11	1.02	F. top	T	D. gr.
52	64	F	1	9	10	303.99	304.00	4.42	89.72	5.86	5.89	1.15	0.21	1.28	Top	T	D. gr.
53	64	F	1	22	23	304.12	304.13	29.52	69.72	0.76	4.63	1.04	-0.02	1.21	Middle	T	D. gr.
54	64	F	1	32	33	304.22	304.23	48.47	50.06	1.48	4.27	1.09	0.09	1.21	Base	T	Gr.
55	66	F	1	85	86	314.25	314.26	83.79	15.63	0.58	3.00	1.17	0.13	0.97	Middle	T	D. gr.
56	68	F	1	71	76	323.61	323.66	1.17	67.64	31.19	7.42	1.72	0.12	1.01	F. top	T	D. gr.
57	72	F	1	45	46	342.35	342.36	69.15	29.14	1.71	3.47	1.43	0.11	1.03	Middle	T	D. gr.
58	74	F	2	52	54	353.38	353.40	5.68	76.04	18.28	6.51	1.77	0.24	1.09	Base	T	Gr.
59	74	F	2	54	56	353.40	353.42	5.03	67.98	26.99	7.01	1.87	0.08	0.98	F. top	H	D. gr.
60	82	F	3	63	68	392.88	392.93	0.19	57.10	42.71	7.84	1.61	-0.04	1.03	F. middle	H	D. gr.
61	84	F	1	49	50	399.19	399.20	16.24	80.89	2.87	5.12	1.08	0.21	1.25	Base	T	D. gr.
62	84	F	1	51	57	399.21	399.27	2.29	68.79	28.92	7.19	1.73	0.07	0.99	F. top	T	D. gr.
63	86	F	1	52	53	408.72	408.73	85.94	13.60	0.46	2.80	1.18	0.18	0.90	Middle	T	D. gr.
64	88	F	1	80	81	418.50	418.51	66.05	32.74	1.21	3.58	1.43	0.04	1.02	Middle	T	D. gr.
65	90	F	1	92	93	428.12	428.13	55.67	43.88	0.44	4.03	1.12	0.04	1.02	Middle	T	D. gr.
66	92	F	2	1	2	438.21	438.22	0.41	60.03	39.56	7.72	1.60	0.02	0.96	F. middle	H	G. gr.
67	94	F	1	8	9	446.28	446.29	1.76	69.01	29.22	7.20	1.66	0.00	0.97	F. top	T	G. gr.
68	94	F	1	19	20	446.39	446.40	11.04	82.12	6.84	5.68	1.39	0.21	1.15	Middle	T	D. gr.
69	94	F	1	29	30	446.49	446.50	33.84	65.25	0.91	4.48	1.03	0.02	1.26	Base	T	D. gr.
70	94	F	1	50	55	446.70	446.75	1.28	72.27	26.45	7.12	1.67	0.12	0.99	Middle	T	D. gr.
71	96	F	1	37	38	456.07	456.08	32.42	65.21	2.37	4.62	1.08	0.14	1.21	Base	T	D. gr.
72	98	F	3	125	126	469.45	469.46	47.26	52.16	0.58	4.22	1.14	0.02	1.01	Middle	T	D. gr.
73	100	F	1	51	52	475.21	475.22	57.06	42.85	0.09	4.07	0.95	0.07	1.11	Middle	T	D. gr.
74	104	F	2	45	50	495.65	495.70	13.31	76.70	9.98	5.83	1.68	0.15	1.20	Middle	T	D. gr.
75	110	F	1	79	84	522.99	523.04	75.53	23.20	1.25	3.30	1.29	0.15	1.00	Middle	T	D. gr.
76	110	F	3	20	21	524.49	524.50	65.29	32.14	2.57	3.67	1.52	0.14	1.09	Middle	T	D. gr.
77	119	F	1	73	79	561.03	561.09	0.55	61.51	37.94	7.71	1.53	0.02	1.06	F. top	T	D. gr.

Table 8.1.1. (ctd). Grain size analysis data of Iloc U1450A (IODP Bengal Fan Expedition 354)

S.No.	Core	Type	Sect.	Top offset (cm)	Bottom offset (cm)	Top depth CSF (m)	Bottom depth CSF (m)	Sand (%)	Silt (%)	Clay (%)	M _z	σ	SK	KG	Position	Turbi/Hemi	Color
78	120	X	2	10	11	562.42	562.43	2.48	67.76	29.76	7.22	1.73	0.03	0.99	F. top	T	D. gr.
79	120	X	2	20	21	562.52	562.53	23.71	60.33	15.96	5.88	2.15	0.10	0.89	Top	T	D. gr.
80	120	X	2	55	56	562.87	562.88	47.18	44.50	7.07	4.53	2.23	0.19	0.88	Middle	T	D. gr.
81	120	X	2	93	94	563.25	563.26	36.05	54.64	9.30	5.10	1.93	0.29	0.98	Base	T	D. gr.
82	121	X	CC	52	53	570.42	570.43	25.75	54.34	19.91	6.05	2.27	0.11	0.81	Base	H	D. gr.
83	122	X	1	50	51	580.10	580.11	26.61	57.35	16.04	5.82	2.17	0.13	0.84	F. top	T	D. gr.
84	122	X	1	58	59	580.18	580.19	44.76	48.51	6.73	4.74	1.90	0.29	0.93	Top	T	D. gr.
85	122	X	1	77	78	580.37	580.38	24.11	62.14	13.75	5.77	2.05	0.18	0.95	Base	T	D. gr.
86	123	X	1	47	48	589.87	589.88	34.71	59.67	5.63	4.83	1.57	0.28	1.28	Base	T	D. gr.
87	124	F	2	55	56	600.93	600.94	65.25	32.15	2.60	3.50	1.65	0.14	0.96	Middle	T	D. gr.
88	126	F	1	5	6	608.55	608.56	20.61	58.28	21.11	6.22	2.24	-0.02	0.85	F. top	T	D. gr.
89	126	F	1	13	14	608.63	608.64	62.91	33.58	2.84	3.60	1.89	0.16	0.99	Top	T	D. gr.
90	126	F	1	35	36	608.85	608.86	75.93	23.00	0.50	3.17	1.43	0.21	0.99	Middle	T	D. gr.
91	126	F	1	60	61	609.10	609.11	48.32	46.39	5.29	4.42	1.69	0.26	1.18	Base	T	D. gr.
92	126	F	1	66	70	609.16	609.20	33.14	60.62	6.24	4.93	1.62	0.26	1.16	Middle	T	D. gr.
93	132	X	1	64	68	638.34	638.38	1.95	74.37	23.68	6.86	1.76	0.16	0.93	F. middle	H	D. gr.
94	136	X	2	42	46	678.39	678.43	2.34	75.11	22.55	6.84	1.71	0.16	0.96	F. middle	H	D. gr.
95	136	X	2	50	51	678.47	678.48	2.32	73.57	24.11	6.99	1.69	0.15	1.03	Middle	T	D. gr.
96	137	X	1	94	95	687.24	687.25	14.45	80.74	4.81	5.40	1.32	0.12	1.34	Base	T	D. gr.

Table 8.1. (ctd). Grain size analysis data of I/Olc U1450B (IODP Bengal Fan Expedition 354)

S.No.	Core	Type	Sect.	Top offset (cm)	Bottom offset (cm)	Top depth CSF (m)	Bottom depth CSF (m)	Sand (%)	Silt (%)	Clay (%)	M _z	σ	SK	KG	Sample Description	Turbi/Hemi	Color
1	7	R	2	41	42	658.51	658.52	36.26	60.23	3.51	4.67	1.39	0.16	1.18	Top	T	D. gr.
2	7	R	2	55	56	658.65	658.66	7.22	75.13	17.65	6.50	1.75	0.13	1.03	Middle	T	D. gr.
3	7	R	2	74	75	658.84	658.85	66.84	29.96	2.67	3.50	1.86	0.30	0.97	Base	T	D. gr.
4	9	R	1	29	33	676.29	676.33	0.54	69.90	29.56	7.31	1.59	0.10	0.99	Middle	T	D. gr.
5	11	R	2	3	5	696.92	696.94	1.10	72.83	26.07	7.12	1.58	0.01	0.99	Middle	H	G. gr.
6	11	R	5	79	84	700.33	700.38	1.74	73.89	24.37	7.01	1.66	0.15	1.00	Middle	T	D. gr.
7	12	R	1	5	6	705.15	705.16	1.87	74.71	23.42	6.99	1.63	0.13	1.02	Top	T	D. gr.
8	12	R	1	17	18	705.27	705.28	7.23	82.89	9.88	6.04	1.46	0.19	1.12	Base	T	D. gr.
9	15	R	1	24	25	734.44	734.45	4.75	75.74	19.51	6.75	1.67	0.10	1.11	F. top	T	Gr.
10	15	R	1	37	38	734.57	734.58	15.76	70.91	13.33	5.88	1.85	0.26	1.02	Top	T	Gr.
11	15	R	1	51	52	734.71	734.72	23.17	66.93	9.90	5.47	1.78	0.27	1.08	Middle	T	Gr.
12	15	R	1	59	60	734.79	734.80	30.71	62.23	7.07	5.07	1.66	0.31	1.16	Base	T	Gr.
13	16	R	3	110	115	747.36	747.41	21.09	65.33	13.58	5.78	1.92	0.27	0.94	Base	T	Gr.
14	17	R	2	46	47	754.93	754.94	0.93	75.33	23.74	7.11	1.52	0.12	1.06	F. top	T	D. gr.
15	17	R	2	54	55	755.01	755.02	9.28	74.31	16.41	6.39	1.77	0.10	1.04	Middle	T	Gr.
16	17	R	2	63	65	755.10	755.12	23.48	63.06	13.46	5.72	2.03	0.25	0.99	Middle	T	Gr.
17	18	R	1	20	21	763.50	763.51	0.65	70.18	29.17	7.28	1.60	0.07	0.99	F. top	T	D. gr.
18	18	R	1	56	57	763.86	763.87	39.57	53.20	7.23	4.86	1.80	0.30	1.07	Middle	T	Gr.
19	18	R	1	78	79	764.08	764.09	11.19	72.18	16.63	6.28	1.85	0.15	1.00	Base	T	Gr.
20	19	R	3	67	69	775.18	775.20	0.13	56.04	43.83	7.94	1.42	0.01	1.05	Middle	H	G. gr.
21	21	R	1	20	21	792.60	792.61	0.78	77.61	21.61	7.01	1.50	0.13	1.07	F. top	T	D. gr.
22	21	R	1	29	30	792.69	792.70	21.47	64.59	13.94	5.86	1.95	0.15	0.88	Top	T	Gr.
23	21	R	1	50	51	792.90	792.91	56.97	37.95	4.63	4.06	1.94	0.26	0.98	Base	T	Gr.
24	21	R	2	19	21	794.09	794.11	0.01	47.78	52.21	8.28	1.29	0.06	0.98	F. middle	T	D. gr.

Table 8.1. (ctd). Grain size analysis data of I/Olc U1451A (IODP Bengal Fan Expedition 354)

S.No.	Core	Type	Sect.	Top offset (cm)	Bottom offset (cm)	Top depth CSF (m)	Bottom depth CSF (m)	Sand (%)	Silt (%)	Clay (%)	M _z	σ	SK	KG	Position	Turbi/Hemi	Color
1	2	H	6	53	58	14.53	14.58	5.29	70.12	24.58	6.91	1.84	0.10	1.03	Middle	T	D. gr.
2	3	H	1	13	14	16.13	16.14	42.69	54.22	3.08	4.44	1.42	0.17	1.15	Top	T	D. gr.
3	3	H	1	40	41	16.40	16.41	50.31	47.39	2.30	4.21	1.41	0.13	1.15	Middle	T	D. gr.
4	3	H	1	48	49	16.48	16.49	55.54	37.08	3.27	3.90	1.78	0.18	1.05	Base	T	D. gr.
5	3	H	1	58	59	16.58	16.59	46.59	51.47	1.94	4.32	1.20	0.14	1.13	Top	T	D. gr.
6	3	H	1	93	94	16.93	16.94	53.94	42.99	3.07	4.04	1.60	0.10	1.12	Base	T	D. gr.
7	4	H	2	24	25	25.74	25.75	0.05	65.68	34.27	7.57	1.51	0.08	1.01	F. top	T	D. gr.
8	4	H	2	29	30	25.79	25.80	22.15	73.36	4.49	5.15	1.39	0.08	1.19	Top	T	D. gr.
9	4	H	2	117	118	26.67	26.68	71.13	27.98	0.90	3.43	1.35	0.02	0.98	Middle	T	D. gr.
10	4	H	3	56	57	27.56	27.57	64.48	33.01	2.30	3.67	1.69	0.22	0.98	Middle	T	D. gr.
11	5	H	3	77	82	32.67	32.72	2.70	61.68	35.63	7.49	1.81	-0.03	1.06	F. top	T	D. gr.
12	7	H	1	6	7	39.76	39.77	98.86	1.14	0.00	1.69	0.38	0.27	1.33	Top	T	D. gr.
13	7	H	1	56	57	40.26	40.27	40.92	55.57	3.51	4.58	1.44	0.22	1.20	Base	T	D. gr.
14	8	H	1	40	46	46.70	46.76	1.86	66.65	31.49	7.32	1.75	0.04	1.00	F. top	T	D. gr.
15	8	H	1	49	50	46.79	46.80	5.94	64.54	29.53	7.06	1.89	-0.06	0.96	F. top	T	D. gr.
16	8	H	1	55	56	46.85	46.86	47.15	47.34	5.37	4.50	1.83	0.22	1.07	Middle	T	D. gr.
17	10	F	2	64	65	57.61	57.62	39.65	56.52	3.82	4.61	1.50	0.17	1.14	Base	T	D. gr.
18	11	F	3	55	60	63.85	63.90	73.03	24.61	1.80	3.40	1.40	0.19	1.11	F. middle	H	D. gr.
19	11	F	3	61	62	63.91	63.92	44.60	52.49	2.91	4.42	1.38	0.18	1.13	base	H	Gr.
20	12	F	3	36	37	68.27	68.28	3.20	71.18	25.62	7.05	1.75	0.08	1.06	F. top	T	Gr.
21	12	F	3	60	61	68.51	68.52	62.06	37.93	0.00	3.84	1.15	-0.11	1.12	Middle	T	D. gr.
22	12	F	3	100	101	68.91	68.92	69.71	30.23	0.06	3.59	1.19	-0.05	1.02	Middle	T	D. gr.
23	12	F	4	19	20	69.31	69.32	52.92	44.07	3.01	4.22	1.39	0.25	1.09	Base	T	D. gr.
24	13	F	2	7	8	71.26	71.27	56.78	43.20	0.01	3.99	1.15	0.07	0.86	Base	T	D. gr.
25	14	F	2	102	103	76.92	76.93	0.47	65.54	33.99	7.57	1.58	0.10	1.01	Top	T	Gr.
26	14	F	2	112	113	77.02	77.03	36.61	60.09	3.31	4.59	1.36	0.18	1.26	Middle	T	D. gr.
27	14	F	3	46	47	77.87	77.88	48.11	48.55	3.34	4.39	1.51	0.22	1.12	Base	T	D. gr.
28	15	F	2	71	75	81.31	81.35	0.93	67.86	31.21	7.53	1.40	0.03	1.16	F. middle	H	G. gr.
29	18	F	1	94	99	94.14	94.19	0.96	71.11	27.93	7.24	1.64	0.16	0.99	F. middle	H	G. gr.

Table 8.1. (ctd). Grain size analysis data of Iloc U1451A (IODP Bengal Fan Expedition 354)

S.No.	Core	Type	Sect.	Top offset (cm)	Bottom offset (cm)	Top depth CSF (m)	Bottom depth CSF (m)	Sand (%)	Silt (%)	Clay (%)	M _z	σ	SK	KG	Sample Description	Turbi/Hemi	Color
30	22	H	1	52	53	112.52	112.53	6.37	76.12	17.51	6.46	1.78	0.22	1.09	Top	T	D. gr.
31	22	H	1	61	62	112.61	112.62	44.39	52.96	2.65	4.42	1.40	0.13	1.07	Middle	T	D. gr.
32	22	H	1	70	71	112.70	112.71	42.78	54.04	3.18	4.50	1.50	0.15	1.09	Base	T	D. gr.
33	23	H	5	16	21	125.99	126.04	7.47	76.18	16.35	6.19	1.77	0.34	0.96	F. base	H	D. gr.
34	24	H	2	21	22	132.71	132.72	8.53	75.09	16.38	6.27	1.78	0.24	1.02	Top	T	D. gr.
35	24	H	2	29	34	132.79	132.84	15.21	75.03	9.76	5.56	1.57	0.41	1.15	Middle	T	D. gr.
36	24	H	2	34	35	132.84	132.85	19.66	75.69	4.65	5.09	1.30	0.28	1.36	Base	T	D. gr.
37	25	H	3	50	55	144.00	144.05	0.55	63.32	36.13	7.70	1.47	0.04	1.12	F. middle	H	G. gr.
38	26	H	3	36	40	152.35	152.39	0.32	76.94	22.73	7.13	1.40	0.13	1.06	F. middle	H	G. gr.
39	27	H	2	2	3	161.02	161.03	10.37	69.15	20.48	6.41	1.94	0.13	0.85	F. top	T	G. gr.
40	27	H	2	14	15	161.14	161.15	13.73	71.47	14.80	6.07	1.82	0.18	0.89	Top	T	G. gr.
41	27	H	2	24	25	161.24	161.25	37.52	60.78	1.70	4.52	1.16	0.15	1.32	Middle	T	G. gr.
42	27	H	2	26	31	161.26	161.31	57.50	42.14	0.36	4.05	1.08	0.11	1.09	Middle	T	G. gr.
43	27	H	2	31	32	161.31	161.32	42.99	55.77	1.25	4.42	1.19	0.15	1.36	Base	T	G. gr.
44	29	H	3	62	67	181.35	181.40	0.31	73.03	26.66	7.34	1.38	0.05	1.09	F. middle	H	D. gr.
45	31	F	1	103	104	198.53	198.54	14.52	79.73	5.75	5.49	1.41	0.16	1.22	F. top	T	Gr.
46	31	F	1	115	116	198.65	198.66	32.30	62.11	5.59	4.93	1.58	0.23	1.17	Middle	T	D. gr.
47	31	F	1	125	126	198.75	198.76	44.78	50.98	4.24	4.42	1.75	0.11	1.09	Base	T	D. gr.
48	31	F	2	30	35	199.30	199.35	41.55	51.62	6.83	4.80	1.80	0.30	1.07	Middle	T	D. gr.
49	33	F	1	41	42	207.41	207.42	2.43	78.69	18.88	6.68	1.63	0.20	1.02	F. top	T	D. gr.
50	33	F	1	74	75	207.74	207.75	59.84	37.39	2.77	3.89	1.66	0.18	1.05	Middle	T	D. gr.
51	33	F	1	109	110	208.09	208.10	36.29	59.88	3.84	4.70	1.48	0.18	1.18	Base	T	D. gr.
52	33	F	4	12	17	210.91	210.96	76.07	23.93	0.00	3.44	0.88	0.45	0.80	Middle	T	D. gr.
53	35	F	1	27	32	216.77	216.82	0.32	71.86	27.82	7.42	1.34	0.09	1.11	T. fine	H	D. gr.
54	37	F	1	30	35	226.30	226.35	46.57	49.53	3.90	4.45	1.46	0.26	1.19	Middle	T	D. gr.
55	39	F	1	71	76	236.21	236.26	77.57	18.83	3.07	3.11	1.51	0.30	1.13	Middle	T	D. gr.
56	43	F	1	95	99	255.45	255.49	10.04	74.32	15.64	6.30	1.79	0.15	1.05	F. base	H	D. gr.
57	43	F	2	65	66	256.65	256.66	2.29	71.37	26.34	7.07	1.69	0.07	0.98	T. fine	T	D. gr.
58	43	F	2	74	75	256.74	256.75	24.27	65.22	10.51	5.51	1.85	0.23	0.98	Base	T	D. gr.

Table 8.1. (ctd). Grain size analysis data of I/Olc U1451A (IODP Bengal Fan Expedition 354)

S.No.	Core	Type	Sect.	Top offset (cm)	Bottom offset (cm)	Top depth CSF (m)	Bottom depth CSF (m)	Sand (%)	Silt (%)	Clay (%)	M _z	σ	SK	KG	Sample Description	Turbi/ Hemi	Color
59	45	F	1	90	92	264.90	264.92	1.81	70.36	27.83	7.31	1.53	0.06	1.10	T. fine	T	D. gr.
60	45	F	1	95	97	264.95	264.97	13.31	77.27	9.42	5.72	1.58	0.24	1.19	Base	T	Gr.
61	47	F	1	110	115	274.60	274.65	5.38	76.05	18.57	6.54	1.77	0.24	1.09	Base	T	D. gr.
62	49	F	2	115	119	285.27	285.31	88.69	11.04	0.24	2.53	1.19	0.27	0.98	Middle	T	D. gr.
63	51	F	1	35	39	292.85	292.89	0.96	78.42	20.62	7.03	1.42	0.12	1.11	Middle	T	D. gr.
64	51	F	2	113	114	295.13	295.14	19.88	75.06	5.06	5.32	1.45	0.08	1.17	Top	T	D. gr.
65	51	F	2	128	129	295.28	295.29	63.91	35.56	0.53	3.80	1.26	0.07	1.13	Middle	T	D. gr.
66	51	F	2	144	145	295.44	295.45	66.97	31.90	1.13	3.74	1.22	0.02	1.24	Base	T	D. gr.
67	52	F	2	75	80	299.45	299.50	0.23	74.33	25.44	7.36	1.30	0.15	1.14	Middle	H	D. gr.
68	56	F	1	46	47	316.66	316.67	21.66	71.92	6.42	5.28	1.50	0.26	1.16	F. top	T	D. gr.
69	56	F	1	58	59	316.78	316.79	21.93	70.98	7.09	5.36	1.58	0.22	1.10	Middle	T	D. gr.
70	56	F	1	69	70	316.89	316.90	20.40	73.61	5.99	5.31	1.48	0.22	1.16	Base	T	D. gr.
71	60	F	1	29	30	335.49	335.50	46.18	51.13	2.69	4.38	1.48	0.15	1.19	Top	T	D. gr.
72	60	F	1	40	41	335.60	335.61	52.85	45.62	1.53	4.16	1.36	0.09	1.21	Middle	T	D. gr.
73	60	F	1	58	59	335.78	335.79	43.02	53.10	3.88	4.55	1.60	0.18	1.16	Base	T	D. gr.
74	62	F	1	89	93	345.59	345.63	4.21	75.13	20.66	6.94	1.57	0.09	1.14	Middle	H	G. gr.
75	66	F	1	3	4	363.73	363.74	0.97	59.35	39.68	7.78	1.58	0.00	1.09	T. fine	T	D. gr.
76	66	F	1	13	14	363.83	363.84	62.45	35.19	2.12	3.70	1.66	0.19	0.92	Top	T	D. gr.
77	66	F	1	30	31	364.00	364.01	39.01	54.35	6.61	4.84	1.86	0.19	0.96	Middle	T	D. gr.
78	66	F	1	46	47	364.16	364.17	38.69	52.82	8.48	4.98	1.98	0.23	0.95	Base	T	D. gr.
79	70	F	3	81	83	386.01	386.03	0.61	73.00	26.39	7.25	1.49	0.09	1.06	T. fine	H	D. gr.
80	70	F	3	84	86	386.04	386.06	22.58	67.05	10.37	5.60	1.86	0.13	1.01	Top	H	D. gr.
81	74	F	2	36	41	403.56	403.61	13.81	78.67	7.52	5.61	1.48	0.18	1.25	Middle	T	D. gr.
82	76	F	1	62	63	411.82	411.83	11.80	73.12	15.08	6.06	1.86	0.25	0.97	T. fine	T	D. gr.
83	76	F	1	70	71	411.90	411.91	16.40	82.01	1.59	5.05	0.98	0.12	1.32	Top	T	D. gr.
84	76	F	1	84	85	412.04	412.05	29.35	66.51	4.14	4.89	1.44	0.16	1.28	Base	T	D. gr.
85	82	F	1	8	12	439.78	439.82	1.25	68.31	30.44	7.45	1.50	0.04	1.13	Middle	H	D. gr.
86	84	F	1	19	20	449.39	449.40	8.85	82.75	8.40	5.90	1.43	0.15	1.14	F. top	T	Gr.
87	84	F	1	29	30	449.49	449.50	39.52	59.26	1.22	4.49	1.15	0.15	1.19	Middle	T	Gr.

Table 8.1.1. (ctd). Grain size analysis data of Iolc U1451A (IODP Bengal Fan Expedition 354)

S.No.	Core	Type	Sect.	Top offset (cm)	Bottom offset (cm)	Top depth CSF (m)	Bottom depth CSF (m)	Sand (%)	Silt (%)	Clay (%)	M _z	σ	SK	KG	Position	Turbi/ Hemi	Color
88	84	F	1	38	39	449.58	449.59	29.47	68.45	2.09	4.77	1.19	0.13	1.20	Base	T	Gr.
89	86	F	1	65	67	459.35	459.37	1.19	75.30	23.51	7.11	1.51	0.08	1.10	base	T	Gr.
90	86	F	1	67	69	459.37	459.39	4.17	83.83	11.99	6.40	1.46	0.20	1.37	Top	T	Gr.
91	94	F	1	76	81	497.46	497.51	52.68	40.01	7.28	4.43	2.00	0.36	1.03	Middle	T	Gr.
92	100	F	1	23	24	525.43	525.44	1.33	66.74	31.93	7.47	1.50	0.00	1.10	F. top	T	Gr.
93	100	F	1	47	48	525.67	525.68	26.33	66.80	6.87	5.17	1.67	0.18	1.19	Top	T	Gr.
94	100	F	1	66	67	525.86	525.87	28.14	69.20	2.65	4.66	1.11	0.08	1.40	Base	T	Gr.
95	100	F	1	90	95	526.10	526.15	1.07	77.18	21.75	7.04	1.47	0.11	1.08	F. top	T	Gr.
96	106	F	1	85	90	554.55	554.60	57.19	39.27	3.54	3.95	1.68	0.14	1.10	Middle	T	Gr.
97	111	X	1	30	31	574.00	574.01	1.08	65.77	33.15	7.37	1.75	0.04	0.97	F. top	T	D. gr.
98	111	X	1	56	57	574.26	574.27	13.47	75.46	11.08	5.92	1.67	0.13	1.08	Top	T	D. gr.
99	111	X	1	72	73	574.42	574.43	78.76	19.30	0.99	3.03	1.44	0.20	1.09	Base	T	D. gr.
100	111	X	3	85	90	577.39	577.44	32.35	60.80	6.85	4.93	1.74	0.18	1.16	Top	T	D. gr.

Table 8.1. (ctd). Grain size analysis data of Iolc U1451B (IODP Bengal Fan Expedition 354)

S.No.	Core	Type	Sect.	Top offset (cm)	Bottom offset (cm)	Top depth CSF (m)	Bottom depth CSF (m)	Sand (%)	Silt (%)	Clay (%)	M _z	σ	SK	KG	Porosity (%)	Turbi/Hemi	Color
1	3	X	1	27	30	551.97	552.00	45.57	46.78	7.64	4.66	2.02	0.26	1.05	F. top	T	Gr.
2	3	X	1	30	33	552.00	552.03	0.27	66.89	32.84	7.42	1.59	0.01	1.00	Top	T	Gr.
3	3	X	1	31	32	552.01	552.02	0.61	66.95	32.44	7.45	1.59	0.05	1.01	Top	T	Gr.
4	3	X	1	37	38	552.07	552.08	19.70	68.27	12.03	5.72	1.82	0.27	0.96	Middle	T	Gr.
5	3	X	1	43	45	552.13	552.15	16.22	70.92	12.86	5.86	1.80	0.25	0.96	Base	T	Gr.
6	6	X	1	107	112	581.87	581.92	0.01	73.98	26.01	7.39	1.28	0.16	1.14	Top	T	Gr.
7	7	X	CC	7	13	591.21	591.27	21.48	67.04	11.48	5.64	1.79	0.33	0.98	Base	T	Gr.
8	11	X	1	30	35	619.90	619.95	0.10	67.29	32.62	7.48	1.61	0.12	0.97	F. top	T	D. gr.
9	12	X	1	0	5	629.30	629.35	0.07	64.20	35.73	7.67	1.45	0.08	1.03	F. top	T	Gr.
10	16	R	1	6	7	655.66	655.67	0.26	69.96	29.79	7.36	1.53	0.13	0.97	F. middle	T	Gr.
11	16	R	1	18	19	655.78	655.79	31.13	57.86	11.01	5.37	1.96	0.31	0.98	Top	T	Gr.
12	16	R	2	60	65	657.48	657.53	31.08	57.95	10.98	5.35	1.97	0.31	1.02	F. top	T	Gr.
13	19	R	1	66	70	685.66	685.70	31.23	56.49	12.28	5.42	2.04	0.32	0.96	F. top	T	Gr.
14	21	R	1	13	14	704.73	704.74	0.71	67.22	32.06	7.49	1.50	0.05	1.07	F. top	T	D. gr.
15	21	R	1	25	26	704.85	704.86	7.51	67.99	24.50	6.77	1.91	0.02	0.92	Middle	T	D. gr.
16	21	R	1	48	49	705.08	705.09	41.77	52.69	5.54	4.71	1.69	0.25	1.07	Base	T	D. gr.
17	21	R	2	125	135	707.20	707.30	1.26	63.21	35.54	7.57	1.60	0.00	1.04	F. top	T	D. gr.
18	23	R	1	90	95	725.10	725.15	44.23	49.86	5.91	4.64	1.75	0.27	1.11	F. top	T	D. gr.
19	23	R	1	97	102	725.17	725.22	4.02	65.36	30.62	7.20	1.83	0.03	0.97	F. middle	T	D. gr.
20	27	R	1	50	51	763.70	763.71	27.46	59.07	13.47	5.63	2.10	0.14	0.88	Top	T	D. gr.
21	27	R	1	70	71	763.90	763.91	53.21	39.72	7.06	4.29	2.15	0.29	0.96	Middle	T	D. gr.
22	27	R	1	90	91	764.10	764.11	37.72	52.22	10.06	5.10	2.02	0.28	0.95	Base	T	D. gr.
23	27	R	2	32	36	764.91	764.95	12.95	60.56	26.49	6.60	2.15	0.10	0.78	Middle	T	D. gr.
24	29	R	1	49	50	782.99	783.00	0.30	67.85	31.85	7.60	1.28	0.09	1.11	F. top	T	D. gr.
25	29	R	1	58	59	783.08	783.09	64.86	31.47	3.67	3.65	1.88	0.24	1.07	Top	T	Gr.
26	29	R	1	80	81	783.30	783.31	56.02	38.83	5.15	4.14	1.83	0.27	1.11	Middle	T	Gr.
27	29	R	1	99	100	783.49	783.50	61.25	34.66	4.09	3.87	1.84	0.26	1.08	Base	T	Gr.
28	31	R	1	77	79	802.67	802.69	0.23	68.24	31.53	7.43	1.56	0.11	0.99	F. top	T	D. gr.
29	31	R	2	40	42	803.32	803.34	47.26	48.40	4.34	4.47	1.57	0.27	1.08	Middle	T	D. gr.

Table 8.1. (ctd). Grain size analysis data of I/Olc U1451B (IODP Bengal Fan Expedition 354)

S.No.	Core	Type	Secl.	Top offset (cm)	Bottom offset (cm)	Top depth CSF (m)	Bottom depth CSF (m)	Sand (%)	Silt (%)	Clay (%)	M _z	σ	SK	KG	Position	Turbi/Hemi	Color
30	33	R	1	13	18	821.43	821.48	0.85	71.43	27.72	7.19	1.64	0.13	0.97	F. top	T	D. gr.
31	33	R	2	29	34	822.66	822.71	22.02	64.16	13.83	5.71	1.93	0.33	0.92	Top	T	D. gr.
32	34	R	1	17	18	831.17	831.18	1.75	76.95	21.30	6.77	1.64	0.14	0.91	F. top	T	D. gr.
33	34	R	1	23	24	831.23	831.24	16.42	67.86	15.73	6.08	1.93	0.14	0.92	Top	T	Gr.
34	34	R	1	30	31	831.30	831.31	21.13	65.95	12.92	5.79	1.89	0.19	0.90	Middle	T	Gr.
35	34	R	1	38	39	831.38	831.39	24.84	62.62	12.55	5.64	1.98	0.19	0.94	Base	T	Gr.
36	36	R	CC	13	16	851.88	851.91	0.64	65.03	34.34	7.55	1.49	0.01	1.05	F. middle	T	D. gr.
37	37	R	3	35	36	863.02	863.03	0.19	72.62	27.19	7.44	1.24	0.10	1.09	F. middle	T	D. gr.
38	37	R	3	48	50	863.15	863.17	44.70	49.14	6.17	4.72	1.87	0.27	0.91	Top	T	D. gr.
39	37	R	3	59	60	863.26	863.27	56.22	36.19	7.59	4.27	2.29	0.34	0.92	Base	T	D. gr.
40	42	R	1	6	7	908.96	908.97	0.62	65.56	33.82	7.64	1.34	0.00	1.18	F. top	T	D. gr.
41	42	R	1	14	15	909.04	909.05	10.98	79.24	9.78	5.87	1.54	0.20	1.13	Top	T	Gr.
42	42	R	1	19	20	909.09	909.10	9.13	85.02	5.85	5.68	1.27	0.16	1.26	Middle	T	Gr.
43	42	R	1	28	29	909.18	909.19	42.43	51.74	5.83	4.74	1.86	0.20	0.89	Base	T	Gr.
44	45	R	2	6	7	938.90	938.91	0.14	55.72	44.14	8.01	1.24	0.06	1.07	F. middle	T	D. gr.
45	45	R	2	14	15	938.98	938.99	21.60	67.45	10.95	5.65	1.82	0.20	0.97	Top	T	Gr.
46	45	R	2	33	34	939.17	939.18	24.15	69.95	5.90	5.21	1.49	0.23	1.13	Middle	T	Gr.
47	45	R	2.0	43	44	939.27	939.28	31.24	64.15	4.60	4.93	1.48	0.21	1.14	Base	T	Gr.
48	45	R	2.0	46	47	939.30	939.31	0.26	61.84	37.89	7.75	1.41	0.05	1.05	F. top	T	D. gr.
49	45	R	2.0	57	58	939.41	939.42	8.71	73.43	17.85	6.42	1.81	0.11	0.94	Middle	T	Gr.
50	45	R	2.0	77	78	939.61	939.62	14.50	70.14	15.36	6.07	1.86	0.20	0.91	Base	T	Gr.
51	50	R	1.0	94	95	977.94	977.95	0.78	71.94	27.28	7.26	1.51	0.07	1.03	F. top	T	D. gr.
52	50	R	1.0	99	100	977.99	978.00	3.62	87.08	9.30	6.23	1.30	0.17	1.14	Top	T	L. gr.
53	50	R	1.0	109	110	978.09	978.10	4.38	86.32	9.30	6.18	1.33	0.16	1.15	Middle	T	L. gr.
54	50	R	1.0	126	127	978.26	978.27	10.14	81.98	7.88	5.83	1.43	0.14	1.18	Base	T	Gr.
55	51	R	1.0	95	96	987.65	987.66	0.86	71.67	27.47	7.23	1.57	0.09	1.02	F. top	T	D. gr.
56	51	R	1.0	98	99	987.68	987.69	19.27	76.49	4.23	5.19	1.27	0.24	1.17	Top	T	Gr.

Table 8.1. (ctd). Grain size analysis data of I/Olc U1451B (IODP Bengal Fan Expedition 354)

S.No.	Core	Type	Secl.	Top offset (cm)	Bottom offset (cm)	Top depth CSF (m)	Bottom depth CSF (m)	Sand (%)	Silt (%)	Clay (%)	M _z	σ	SK	KG	Position	Turbi/Hemi	Color
57	51	R	1.0	111	112	987.81	987.82	29.02	66.06	4.92	5.01	1.46	0.24	1.12	Base	T	Gr.
58	51	R	2.0	52	53	988.57	988.58	0.41	66.40	33.19	7.51	1.50	0.04	1.03	F. top	T	D. gr.
59	51	R	2.0	60	61	988.65	988.66	17.94	73.82	8.24	5.52	1.56	0.27	1.10	Top	T	Gr.
60	51	R	2.0	73	74	988.78	988.79	35.68	57.22	7.10	5.00	1.74	0.28	1.07	Middle	T	Gr.
61	51	R	2.0	105	106	989.10	989.11	60.15	35.98	3.87	3.97	1.78	0.27	1.09	Base	T	Gr.
62	54	R	1.0	60	61	1016.40	1016.41	20.84	72.67	6.49	5.31	1.48	0.26	1.14	Top	T	Gr.
63	54	R	1.0	89	90	1016.69	1016.70	18.99	70.62	10.39	5.64	1.71	0.27	0.99	Middle	T	Gr.
64	54	R	1.0	116	117	1016.96	1016.97	19.50	71.24	9.25	5.61	1.67	0.20	1.01	Base	T	Gr.
65	54	R	2.0	3	5	1017.01	1017.03	0.05	61.79	38.16	7.70	1.46	0.01	1.02	F. top	T	D. gr.
66	54	R	2.0	19	20	1017.17	1017.18	14.31	77.39	8.30	5.66	1.53	0.23	1.08	Top	T	Gr.
67	54	R	2.0	30	31	1017.28	1017.29	17.30	75.90	6.81	5.47	1.48	0.22	1.10	Middle	T	Gr.
68	54	R	2.0	44	45	1017.42	1017.43	16.50	77.69	5.81	5.43	1.40	0.23	1.10	Base	T	Gr.
69	55	R	1.0	4	5	1025.64	1025.65	4.65	59.48	35.87	7.54	1.66	-0.12	1.22	F. top	T	D. gr.
70	55	R	1.0	11	12	1025.71	1025.72	5.42	81.98	12.60	6.33	1.50	0.14	1.10	Top	T	Gr.
71	55	R	1.0	27	28	1025.87	1025.88	49.88	43.88	6.24	4.52	1.83	0.35	1.00	Middle	T	Gr.
72	55	R	1.0	45	46	1026.05	1026.06	44.17	49.67	6.16	4.72	1.79	0.29	1.00	Base	T	Gr.
73	57	R	2.0	28	30	1040.97	1040.99	0.17	54.32	45.51	8.02	1.35	-0.02	1.17	F. base	T	D. gr.
74	57	R	2.0	43	44	1041.12	1041.13	25.10	66.40	8.51	5.34	1.67	0.31	1.08	Top	T	Gr.
75	57	R	2.0	60	61	1041.29	1041.30	25.77	65.56	8.66	5.33	1.70	0.31	1.07	Middle	T	Gr.
76	57	R	2.0	84	85	1041.53	1041.54	32.19	60.43	7.38	5.09	1.70	0.29	1.08	Base	T	Gr.
77	58	R	1.0	28	29	1045.28	1045.29	1.92	76.37	21.71	7.08	1.42	0.02	1.10	F. top	T	D. gr.
78	58	R	1.0	31	32	1045.31	1045.32	17.27	73.39	9.33	5.72	1.68	0.12	1.06	Top	T	D. gr.
79	58	R	1.0	45	46	1045.45	1045.46	46.23	49.46	4.31	4.39	1.61	0.17	1.22	Middle	T	Gr.
80	58	R	1.0	46	47	1045.46	1045.47	39.38	55.38	5.24	4.66	1.55	0.26	1.30	Middle	T	Gr.
81	59	R	2.0	23	24	1056.52	1056.53	0.46	63.95	35.59	7.58	1.52	-0.01	1.04	F. top	T	Gr.
82	59	R	2.0	26	27	1056.55	1056.56	42.56	51.26	6.18	4.69	1.76	0.24	1.08	Top	T	Gr.
83	59	R	2.0	51	52	1056.80	1056.81	56.44	39.37	4.19	4.08	1.75	0.26	1.02	Middle	T	Gr.
84	59	R	2.0	81	82	1057.10	1057.11	42.52	50.80	6.68	4.73	1.75	0.31	1.19	Base	T	Gr.
85	60	R	2.0	75	76	1066.31	1066.32	1.85	76.67	21.48	6.79	1.66	0.18	0.95	F. middle	T	D. gr.

Table 8.1.1. (ctd). Grain size analysis data of I/Olc U1451B (IODP Bengal Fan Expedition 354)

S.No.	Core	Type	Sect.	Top offset (cm)	Bottom offset (cm)	Top depth CSF (m)	Bottom depth CSF (m)	Sand (%)	Silt (%)	Clay (%)	M _z	σ	SK	KG	Depth	Turbi/Hemi	Color
86	60	R	3.0	44	45	1067.49	1067.50	0.56	68.01	31.43	7.46	1.47	0.04	1.05	F. top	T	D. gr.
87	60	R	3.0	57	58	1067.62	1067.63	15.57	75.50	8.93	5.58	1.56	0.30	1.13	Top	T	D. gr.
88	60	R	3.0	72	73	1067.77	1067.78	26.59	66.02	7.38	5.23	1.61	0.28	1.09	Middle	T	D. gr.
89	60	R	3.0	88	89	1067.93	1067.94	25.82	66.69	7.49	5.25	1.60	0.29	1.11	Base	T	D. gr.
90	62	R	1.0	81	82	1084.71	1084.72	29.90	60.68	9.42	5.28	1.81	0.30	1.03	Top	T	G. gr.
91	62	R	1.0	120	121	1085.10	1085.11	23.75	67.39	8.87	5.40	1.68	0.30	1.07	Middle	T	Gr.

Chapter Nine

DISCUSSION

9.1 Fluvial setting

This study identified four facies associations from the Siwalik Group along the Khutia Khola section; fine-grained meandering river system (FA1), flood-flow dominated meandering river system (FA2), deep (FA3) and shallow (FA4) sandy braided river systems. The detailed facies analyses of the Khutia Khola section resulted that ephemeral stream deposits (up to 3 m) are frequently present and perennial stream deposits (ca. 5 m) are few in meandering river system (FA1 and FA2), whereas perennial stream deposits are common in braided river system (FA3 and FA4). Overall, mudstone facies and very fine- to- fine-grained sandstone facies, as well as thinner sandstone successions are dominant in FA1-FA2 and mudstone facies are frequent even in FA3-FA4 along the Khutia Khola section than in other neighboring sections (Karnali River section to the east (Gautam and Fujiwara, 2000; Hyughe et al., 2005; Sigdel et al., 2011) and Budar-Jogbudha area to the west (Dhital, 2015)). Frequency of thick sandstone beds of perennial stream deposits are less in FA3-FA4 intervals than in the Karnali River section (cf. Sigdel and Sakai, 2016). These characteristics indicate that

the fluvial facies of the Khutia Khola section is of a smaller river system. Comparison of the petrographical and geochemical studies between the Khutia Khola and the Karnali River sections show no significant changes which indicate that the Khutia Khola section may probably located at the western margin of the paleo-Karnali River system (particularly perennial meandering stream deposit) or may represent the interfluvial setting of major river systems.

9.1.1 Significance in change from FA1 to FA2

The previous fluvial facies studies of the Siwalik Group in the Nepal Himalaya revealed the same order of the appearance in fluvial facies; fine-grained meandering river system, flood-flow dominated meandering river system, deep sandy braided river system, shallow sandy braided river system, gravelly braided river system and debris-flow dominated braided river system (Nakayama and Ulak, 1999; Ulak and Nakayama, 2001; Huyghe et al., 2005). As mentioned above, the Khutia Khola section hosts the first four systems. Nakayama and Ulak (1999) emphasized the appearance of the flood-flow dominated meandering river system (FA2 of the present study) as a proxy of climate change, implying increase in water discharge. The timing in appearance of the flood-flow dominated meandering river system is, however, different

among the Siwalik sections: 13.5 Ma in the Karnali River section (Sigdel and Sakai, 2016), 9.5 Ma in the Surai Khola section (Nakayama and Ulak, 1999), 10.0 Ma in the Tinau Khola section (Ulak and Nakayama, 2001), and 10.5 Ma in the Bakiya Khola section (Nakayama and Ulak, 1999).

Huyghe et al. (2005) interpreted the difference in timing of the facies change was due to the catchment size of each river system. The sediments of the Paleo-Karnali River system are represented by thicker fluvial channel fill deposits (Gautam and Fujiwara, 2000; Huyghe et al., 2005; Sigdel and Sakai, 2016), implying the presence of a large river system with wide catchment basin (cf. Huyghe et al, 2005). Huyghe et al. (2005) speculated the water discharge from the large catchment system affected on the earlier facies change than in the other Siwalik sections. Theoretically, a large river system from a large catchment basin is not sensitive against the local climate change for the river channel features (channel size, style and so on). However, in the Khutia Khola (sediments from a small catchment basin) the estimated timing of the shift from FA1 to FA2 is almost same with that of the Karnali River section, i.e. 13.5 Ma: This indicates that the catchment effect seems to have been very small on the appearance of the flood-flow dominated meandering river system (Table 9.1). The 3-4 M.y. earlier appearance of the flood-flow dominated river system in far western Nepal could not be

responsible only for the catchment size, but local tectonics in Himalayas, having resulted in the local mountain up-building with increase precipitation. As discussed in Sigdel and Sakai (2016), the earlier uplift in the far western Nepal Himalaya is the reasonable explanation for the facies change from FA1 to FA2. Several other studies have identified the earlier uplift and exhumation of the Himalaya in western Nepal (DeCelles et al., 1998; Huyge et al., 2001, 2005; Bernet et al., 2006; Chirouze et al., 2012).

9.1.2 Significance in change from meandering to braided river system

The timing of change from meandering river system (FA1-FA2) to braided river system (FA3-FA4) is around 11.0 Ma along the Khutia Khola section and around 9.6 Ma along the Karnali River section (Sigdel and Sakai, 2016) which is 1.6 Ma later than the Khutia Khola section. This change occurred slightly later in the other Siwalik sections in the Nepal Himalaya: 6.5 Ma in the Surai Khola section (Nakayama and Ulak, 1999), 8.2 Ma in the Tinau Khola section (Ulak and Nakayama, 2001) and 9.0 Ma in the Bakiya Khola section (Nakayama and Ulak, 1999). The earlier appearance of braided river system with the Higher Himalayan detrital grains in the Khutia Khola section indicates the earlier uplift of the source area and promoted enhanced erosion even in the small river system in the far western Nepal. The appearance of the Higher Himalayan

detritus in the braided river system also coincides with the increase in uplift rate of the Himalaya in western Nepal at about 12-9 Ma (DeCelles et al., 1998; Robinson et al., 2001; Huyghe et al., 2005). the earlier appearance of the braided river system in the Khutia Khola than in the nearby Karnali River section could possibly be related with the proximity and activity of the Ramgarh and Dadeldhura Thrusts in the Lesser Himalaya (Foldout 1a. in DeCelles et al., 2001).

Around the Khutia Khola area, the Upper Siwalik representing gravelly braided river system and debris-flow dominated braided river system (Table 9.1) are not present, which may be masked by the Jogbudha Thrust (JT) thrusting the central block of the Siwalik section onto the southern belt rock from the north (Ojha et al., 2000; Adhikari and Sakai, 2015).

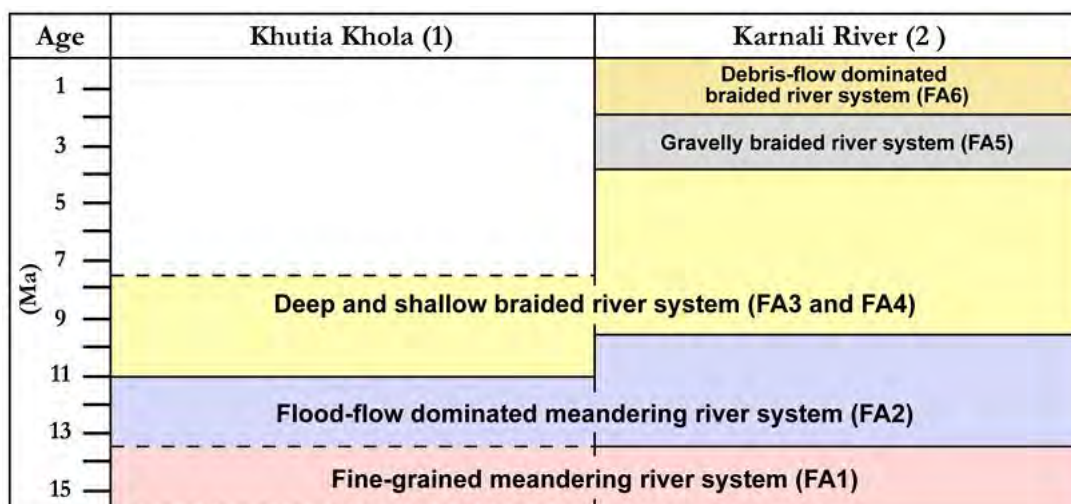


Table 9.1 . Comparison of the fluvial systems; 1) Present study, dotted line represents the age (Ojha et al., 2000) boundary. 2) Karnali River section (Sigdel and Sakai, 2016).

9.2 Geochemical variation

Comparison of the petrographical and geochemical dataset showed some variation in sediment composition between Jagati (FA1-FA2; meandering river system) and Kala (FA3-FA4; braided river system) Formations. These variations are mainly related to the source lithology, change in fluvial style and weathering intensity.

9.2.1 Source lithology

The provenance discrimination plot by Roser and Korsch (1988) shows that the source of the Khutia Khola samples are mostly plotted in quartzose (P4) and intermediate (P2), and a few samples in mafic (P1) provenance fields (Fig. 9.1) (detail description in chapter Six). The (Qt-F-L) provenance discrimination plot by Dickinson et al. (1983) shows the recycled orogenic provenance field for all the Khutia Khola sandstones (Fig. 9.2) (detail description in chapter Seven). The comparison of these results with the Karnali River section and the Bakiya Khola section show that the provenances of the Siwalik Group along the Khutia Khola and the Karnali River sections are similar, but are a little different from those in the Bakiya Khola section. This reflects some differences lie in source composition among the Siwalik Groups.

The ternary diagrams among the Siwalik Groups in the Nepal Himalaya show

similar composition, but slightly different one from the Siwaliks of the Potwar Plateau (Pakistan) (Fig. 9.2). The detritus derived from volcanic source in their hinterland are the possible cause of the compositional variation in the Potwar Siwalik sediments (Critelli and Ingersoll 1994). The fluvial facies characteristics between the Khutia Khola and Karnali River sections are different, but the sandstone compositions are similar with each other. The Karnali River sandstones are slightly rich in lithic fragments, which may reflect wider catchment in the Paleo-Karnali River system (Hyughe et al., 2005), which might have been expanded deep in the Himalaya into the Tethys and Trans Himalayan zones. The Surai Khola and Bakiya Khola sandstones show relatively higher content of feldspar and lithic fragments than the Khutia Khola and the Karnali River sandstones. These compositional variations are possibly due to the different in source lithology in the Lesser Himalaya, such as the Agra Granite and the Palung Granite in west-central, and Amarpur Granite and Kabeli Granite in eastern Nepal.

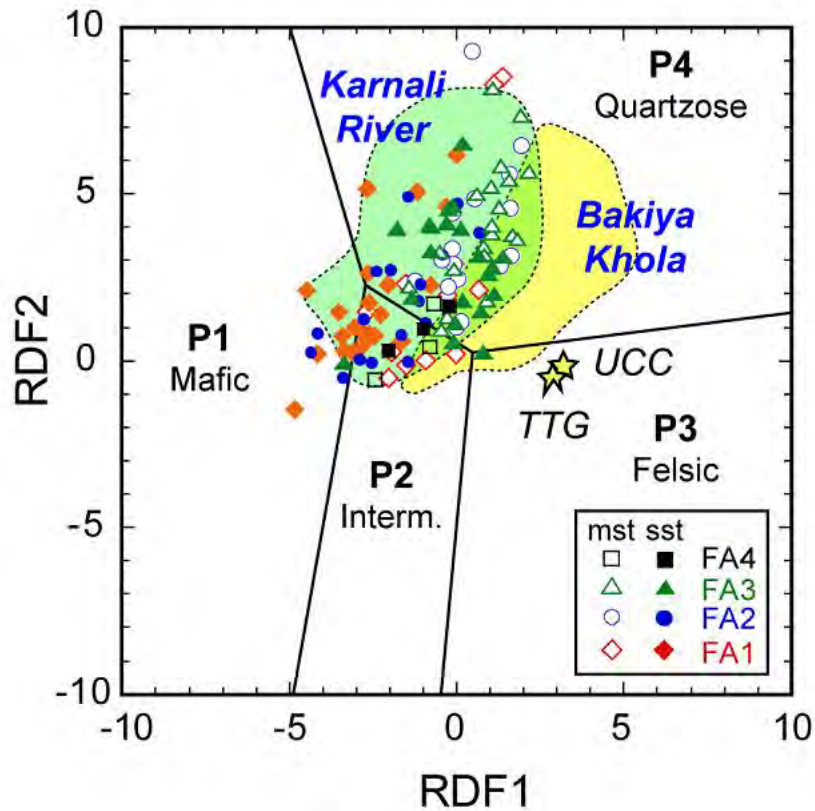


Fig. 9.1. Oxide/ Al_2O_3 ratio provenance discriminant (Roser and Korsch, 1988) for the Siwalik Group sandstones (sst) and mudstones (mst), Khutia Khola section and comparison with the Karnali River and Bakiya Khola sections. Dotted light green field, the Karnali River Siwalik sediments (data from Shimizu, 2013) and dotted light yellow field, the Bikaya Khola Siwalik sediments (data from Roser et al., 2002). Stars: UCC – Upper Continental Crust (Taylor and McLennan, 1985); TTG – Phanerozoic TTG granodiorite (Condic, 1993). Abbreviations: Interm – Intermediate; RDF – ratio discriminant function. See Roser and Korsch (1988) for details of the calculation.

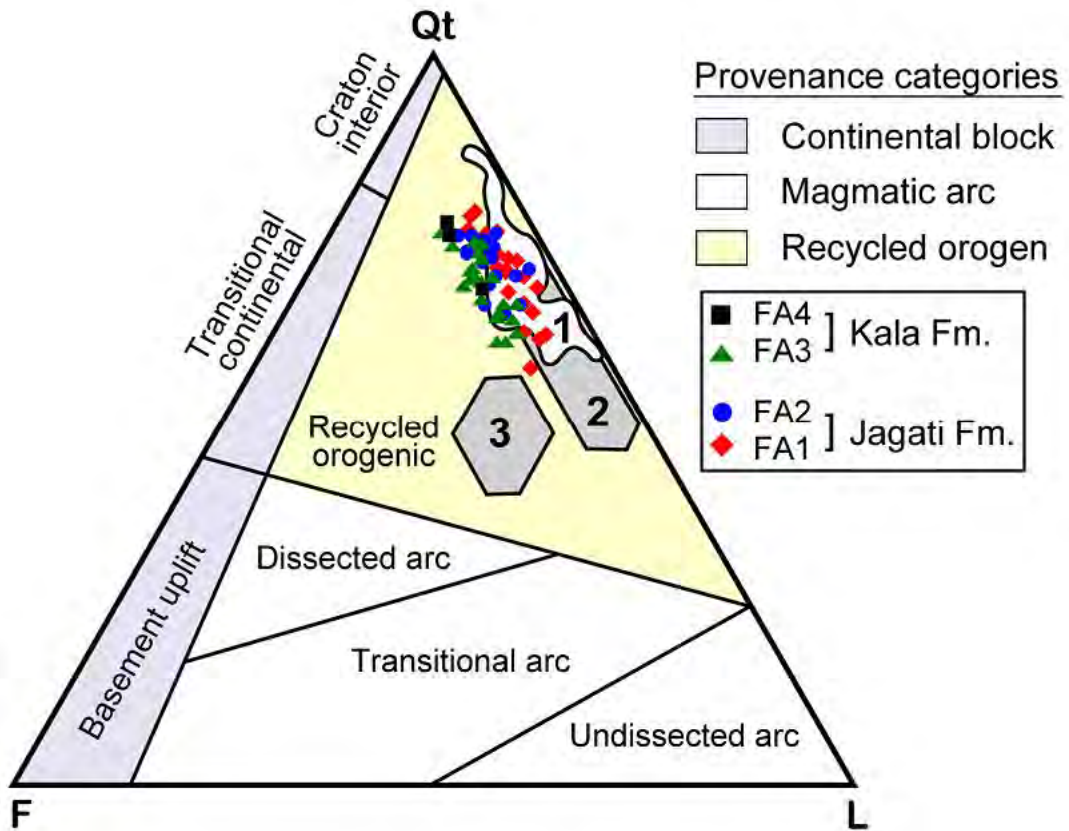


Fig: 9.2. Qt-F-L (Quartz, feldspar, lithic fragments) Ternary diagram for provenance discrimination (after Dickinson et al., 1983). Field 1 = Karnali River section, far western Nepal (modified from Sigdel and Sakai, 2013), Field 2 = Surai Khola section, western Nepal and Bakiya Khola section, central Nepal, and Field 3 = Potwar Plateau, Pakistan (modified from Critelli and Intersoll 1994).

9.2.2 Change in fluvial style and weathering intensity

The $\text{SiO}_2/\text{Al}_2\text{O}_3$ ratio plot against stratigraphy shows the values of sandstones and mudstones are well separated and reflect higher weathering and influence of meandering river system in the lower part, moderately stable conditions in the middle part, and supply of fresh sediments by braided river system in the Kala Formation (Fig. 9.3A) (detail description in chapter Six). Weathering indices A-CN-K plot (Fig. 6.12), A-CNK-FM plot (Fig. 6.13), M-F-W plot (Fig. 6.14), S-A-M plot (Fig. 6.15) and $\text{Ga/Rb-K}_2\text{O/Al}_2\text{O}_3$ plot (Fig. 6.15) also indicate higher weathering in the FA1-FA2 meandering river system, and supply of fresh detritus in the FA3-FA4 braided river system.

Comparing the Khutia Khola plot with the Karnali River and Bakiya Khola plots, show the similar trends of plots among these Siwalik sections (Fig. 9.3). The distribution of sandstones and mudstones are distinctly separated in all sections. The similar trend among the three different Siwalik sections reflects that the geochemical variations are controlled by fluvial systems.

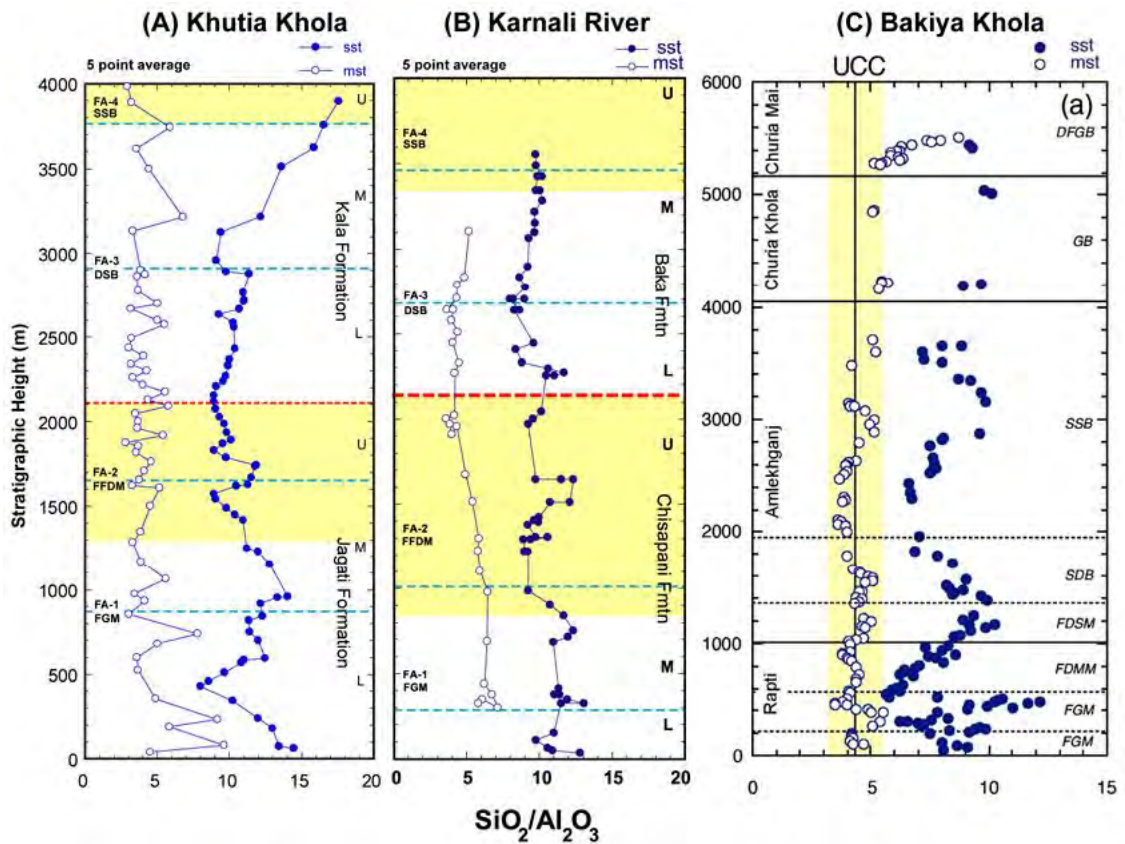


Fig. 9.3. Comparison of the stratigraphic variation in $\text{SiO}_2/\text{Al}_2\text{O}_3$ of different Siwalik sections. A) Khutia Khola section (present study). B) Karnali River section (Shimizu, 2013). C) Bakiya Khola section (Roser et al., 2002). Abbreviations: sst – sandstone, mst – mudstone. FA – facies association. FGM – fine-grained meandering; FFDM – flood-flow dominated meandering; SSB – shallow sandy braided; DSB – deep sandy braided. U – Upper; M – Middle; L – Lower.

9.3. Climate change

9.3.1 Siwalik sedimentation and correlation with other studies along the Khutia

Khola section

The Siwalik group sediments along the Khutia Khola section were initially deposited by fine-grained meandering river system (FA1) (Fig. 9.4). The frequently present thick-bedded red paleosols on flood plains indicate dry period which may have been caused by high evaporation and chemical weathering. The Main Central Thrust (MCT), Dadelhura Thrust (DT) and Ramgarh Thrust (RT) were active during that time and the Higher Himalayan ranges were the main source of sediment supply in the Siwalik Group (DeCelles et al., 1998). During that time, the height of the Himalaya may not have been sufficient to block the northward moving wind, thus no significant and regular precipitation occurred in the far western part of Nepal Himalaya (cf. Huyghe et al., 2005; Sigdel and Sakai; 2016).

Around 13.5 Ma (prior to 13.3 Ma, Ojha et al., 2000) (Fig. 9.4), the river system was changed with increase in precipitation (flood-flow dominated meandering river system, FA2). The presence of amalgamated fine-grained sandstone and seasonal lake deposits reflect the increase in precipitation and change in climate from drier to wetter condition. The increase in precipitation was due to orographic precipitation related

to the uplift of the Higher and Lesser Himalayas (Sigdel and Sakai, 2016). During the time (13 ~ 10.5 Ma), the Dadeldhura thrust (DT) was active which led the uplift of the Lesser Himalaya (Decelles et al., 1998; Huyghe et al., 2005). The continuous under-thrusting along the MCT caused the Higher Himalayan uplift (Harrison et al., 1998). During that time, the Higher and Lesser Himalayas were the source of sediment in the Siwalik Group.

At around 11.0 Ma, the fluvial facies show change from meandering river system (fine-grained facies) to braided river system (coarse-grained 'salt and pepper' sandstones) (FA3-FA4). Presence of thicker and coarse sandstone beds compare to the lower portion show the increase in sediment supply in the braided river system. Abrupt increased in sedimentation rate from 0.32 mm/yr to 0.47 mm/yr at around 10.95 Ma along the Khutia Khola also reflect the change in river system (Fig. 9.4 D) (Ojha et al., 2000). Similar change in sediment accumulation rates for other Siwalik Group was interpreted by Burbank et al. (1996). The Lesser Himalayan Duplex became active around 11 Ma (Decelles et al. 1998), and petrographical studies also show that the Khutia Khola sandstones in the Kala Formation are rich in quartz grain and poor in lithic fragments which suggest the possible source as the Kushma (quartzite) and Ranimata (phyllite) Formations, consisting the Ramgarh Thrust Sheet in the Lesser

Himalaya (cf. DeCelles et al., 2001; Huyghe et al., 2005). The presence 'salt and pepper' sandstone show that the sediments were also supplied from the Higher Himalaya in the braided river system.

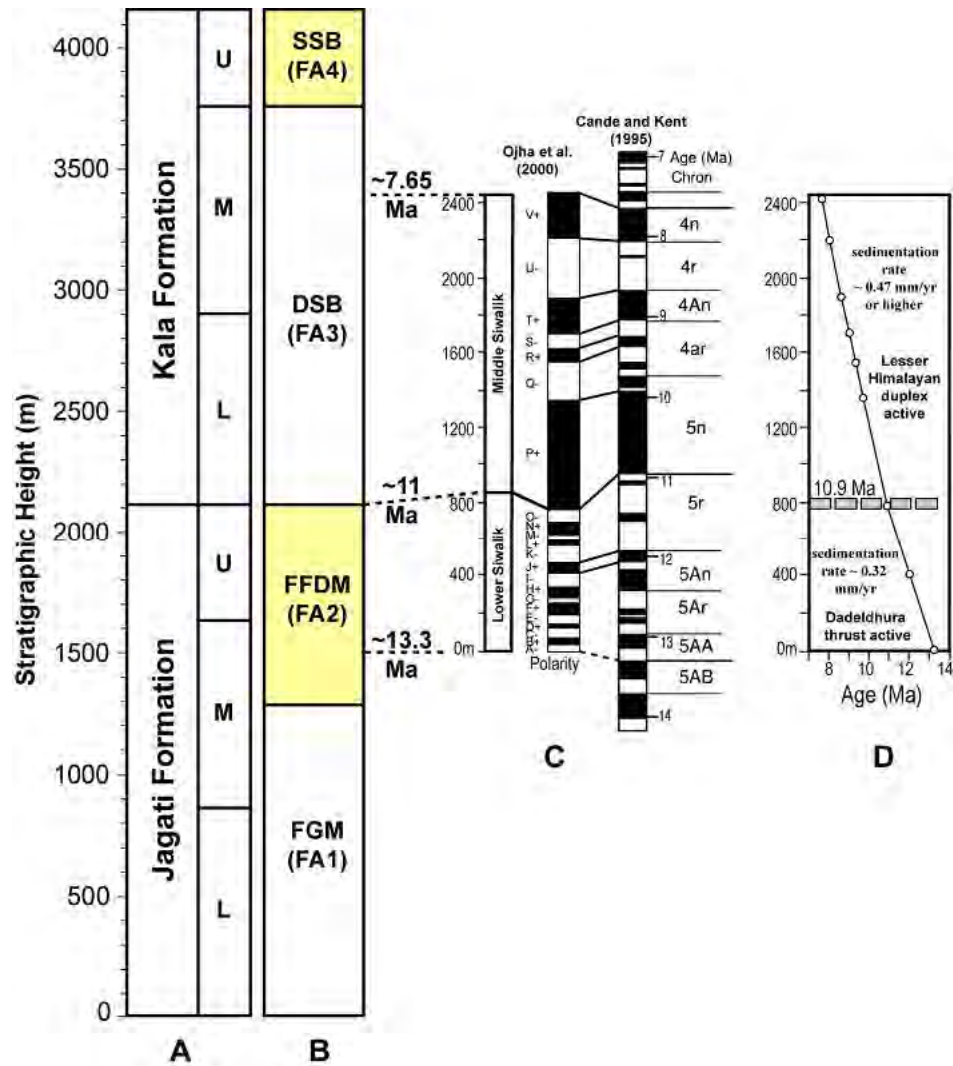


Fig. 9.4. Correlation of present study with Ojha et al. (2000) study along the Khutia Khola section. A) Lithostratigraphy and B) Depositional facies analysis (present study). C) Magnetostratigraphy and D) Sediment accumulation rates study (Ojha et al., 2000). Abbreviations: FA- facies association. FGM – fine-grained meandering; FFDM – flood-flow dominated meandering; SSB – shallow sandy braided; DSB – deep sandy braided. U- Upper member; M – Middle member; L – Lower member.

9.3.2. Comparative studies on paleoclimate and Himalayan tectonics

The monsoon intensification in the South Asia has led by the Tibetan-Himalayan uplift (Ruddiman and Kutzbach, 1989; Raymo and Ruddiman, 1992) and it was initiated between 12 and 9 Ma (Amano and Taira, 1992). The foreland sedimentary record suggests a gradual increase in Himalayan erosion from 24 to 18 Ma which indicate the time of strengthening monsoons and thereafter the erosion rate started to decrease (Szulc et al., 2006). A variety of environmental indicators suggest that the East Asian monsoon was established around 24 Ma, reached a peak around 15 Ma and remained high until around 10.5 Ma (Clift et al., 2008). Based on 'abrupt uplift model', Prell and Kutzbach (1992) suggested the rapid uplift began at around 10 Ma. The uplift of the Himalaya affected the monsoon precipitation, in particular, Indian Summer Monsoon (ISM) and resulted the changes in fluvial system (Nakayama and Ulak, 1999). Burbank et al. (1996) showed that almost all the Siwalik sections recorded acceleration in sedimentation and increase in subsidence rate at around 11 Ma.

Several studies on the Siwalik Group for the implication of climatic changes and tectonics of Himalaya have revealed the difference in timing of climate change. The plant fossils studies around the Surai Khola section (Awasthi et al., 1994) and the Tinau Khola section (Konomatsu et al., 1997) in Western Nepal showed the inception of

deciduous monsoonal forest after 9.5 Ma and 7.5 Ma, respectively. Carbon isotope studies of paleosols from also reflect the difference in time of climatic changes which show shifting from C3 plants (trees and shrubs, cool growth season) to C4 plants (shrubs and grass, warm growth season) at around 7.0 Ma in the Surai Khola, around 10.0 Ma in the Tinau Khola, around 7.0 Ma in the Bakiya Khola and around 7.0 Ma in Pakistan (Quade et al., 1989, 1995; Tanaka et al., 1997) (Fig. 9.5 E). The Oxygen isotope studies on bivalve fossils showed that the monsoon initiated prior to 10.7 Ma (Dettman et al. (2001). Sedimentary and petrographic studies indicate an increase in precipitation in the Himalayan region at around 10.5 Ma due to major uplift (Zalcha, 1997; Kumar et al., 2003). The fluvial facies studies (discussed above) showed the difference in timing of monsoon intensification in the different Siwalik section in the Nepal Himalaya: at around 13.5 to 9.5 Ma (Nakayama and Ulak, 1999; Ulak and Nakayama, 2001; Sigdel and Sakai, 2016).

The Himalaya is main source of sediment in the Bengal Fan and several studies have linked the climatic changes recorded in the basin sediments and the tectonics in the source area. Geochemical studies of the Bengal Fan sediments reflect the history of Himalayan erosion and showed a short dry period around 16.5 to 15.0 Ma, and followed by high precipitation until about 10 Ma (Clift et al., 2008) (Fig 9.5 C). Other studies on

sediment accumulation rate (Gartner, 1990), clay mineralogy (Bouquillon et al., 1990), carbon isotope study (France-Lanord and Derry, 1994) of the sediments from ODP holes 717 and 718, Bengal Fan show major change occurred from 7.4 Ma (Fig. 9.5 A, B and D). Besides the Bengal Fan studies, geochemical studies in the Indus delta sediments and ODP 1148, China South Sea show strong monsoon over the 16 to 10 Ma interval, followed by a gradual weakening between 10 to 3 Ma (Clift et al., 2008).

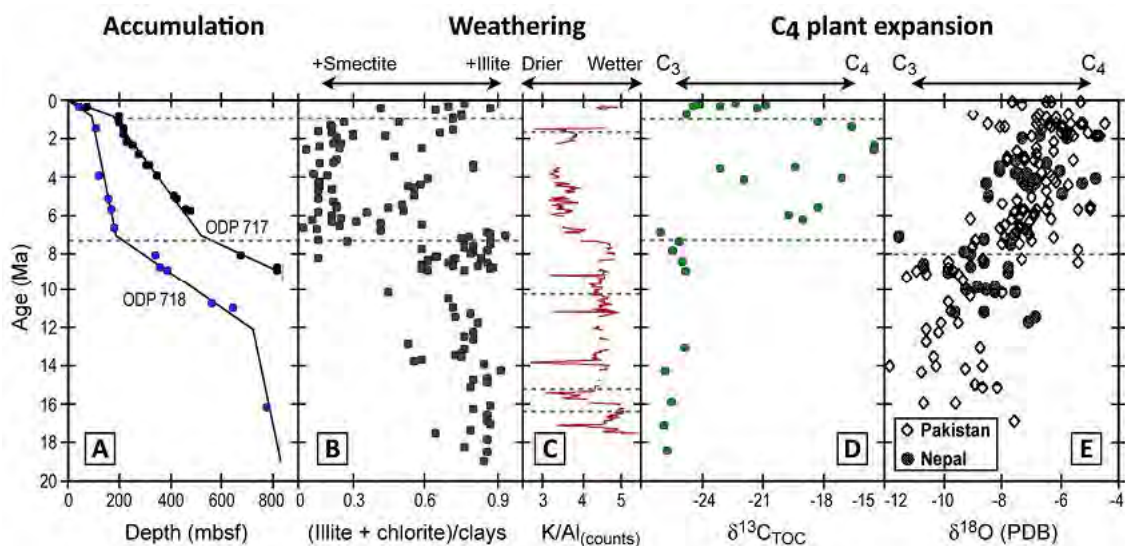


Fig. 9.5 Correlation of climatic indices in the Bengal Fan sediments and the Siwalik Group sediments. A) Accumulation rate, ODP 717 and 718, Bengal Fan (Gartner, 1990). B) Clay mineralogy, ODP 717 and 718, Bengal Fan (Bouquillon et al., 1990). C) Chemical weathering (K/Al), ODP 718, Bengal Fan (Clift et al., 2008). D) TOC isotopic study, ODP 717 and 718, Bengal Fan (France-Lanord and Derry, 1994). E) Oxygen isotopic study of soil carbonate from Pakistan and Nepal by Quade et al. (1989, 1995).

Several researches showed difference in timing of climate change and exhumation of the Himalaya, however, the time of fluvial facies changes around 13.5 Ma in the Khutia Khola and Karnali River section, far western Nepal Himalaya is comparable with the study in western China. Liu et al. (2009) showed the expansion of drier areas in western China and restriction of humid areas to the Southern China around the late middle Miocene (13.5 Ma) which may reflect the early uplift of the western Himalaya (Fig. 9.6). The wind streams originating from Indian Ocean to the Tibetan Plateau was blocked due to uplift of western Himalaya and created a rain shadow zone (drier area) in western China, simultaneously wet and humid climate in the frontal part of the Himalaya which is associated with intensification of Summer Monsoon earlier in the Western Himalaya (Sigdel and Sakai, 2016).

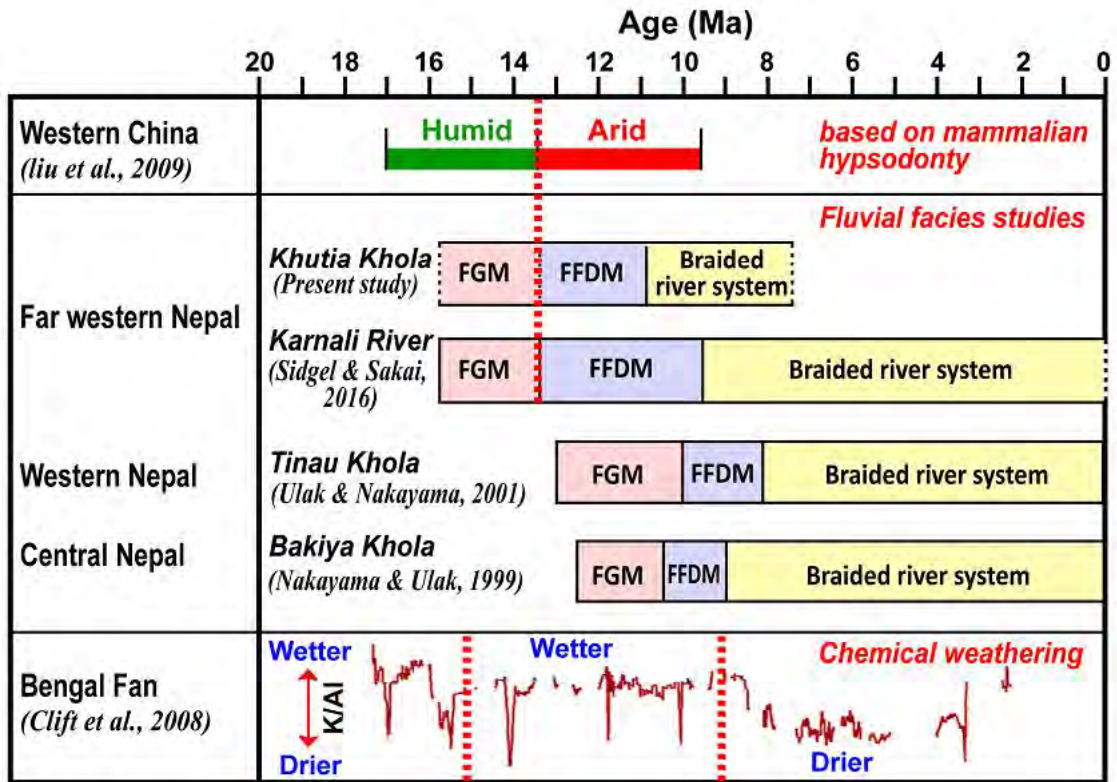


Fig. 9.6 Correlation of the fluvial facies studies with other climatic indices.

CHAPTER TEN

CONCLUSIONS

1. The newly established lithostratigraphy is subdivided into the Jagati Formation (2110 m, equivalent to the Lower Siwalik) and the Kala Formation (2050 m, equivalent to the Middle Siwalik) in ascending order. The Upper Siwalik is not exposed in the area. Each formation is further divided into three members; the lower, middle and upper, based on the ratio of mudstone vs. sandstone beds as well as color and grain size of sandstone.
2. The Jagati Formation is characterized by reddish-brown mudstones interbedded with very fine- to coarse-grained sandstones. Palcosols characterized with burrows, rhizoliths, desiccation cracks, concretions and nodules are present in higher proportion than thinly laminated or massive mudstone beds.
3. The Kala Formation comprises thin- to thick-bedded, very fine- to very coarse-grained sandstones and pebbly sandstones interbedded with reddish-brown, greenish-grey to dark-grey mudstones. Sandstone beds exhibit "salt and pepper" appearance. In the lower part of the upper member sub-rounded to rounded pebbles are scattered along with trough and planar cross-laminations in sandstone

beds, whereas the gravel size tends to be larger and few cobble size gravels also appear in the upper part. Thinly laminated or massive mudstones are common and paleosols are less frequent.

4. The age of the boundary between the Jagati and Kala Formations (Lower-Middle Siwaliks) is around 11.0 Ma. The boundaries age between the middle and upper members of the Jagati Formation is around 12.7 Ma and between the lower and middle members of the Kala Formation is around 9.0 Ma.
5. The dominance of the finer sediments and thinner sandstone units than in the neighboring Siwalik successions indicate that the Khutia Khola section was deposited by small river system and located at the western margin of the palco-Karnali River system or may represent the interfluvic setting of major river systems.
6. Eleven lithofacies, of which three mudstone facies (Fl, Fm and P), six sandstone facies (Sp, St, Sr, Sh, Sc and Sm), and two gravel facies (Gh and Gt) were recognized. Similarly, seven architectural elements (CII, LA, DA, SB, CS, FF and SL) and four facies associations, namely; fine-grained meandering river system (FA1), flood-flow dominated meandering river system (FA2), deep (FA3) and

shallow (FA4) sandy braided river systems, from the oldest to youngest were identified from the Jagati and Kala Formations. FA1-2 corresponds to the Jagati Formation (Lower Siwalik), and FA3-4 to the Kala Formation (Middle Siwalik).

7. Depositional facies description from the Khutia Khola section show same sequences of facies associations that are recognized in other Siwalik sections in Nepal Himalaya. The timing of the appearance of FA2 is crucial for determining the timing of increase in precipitation due to monsoon intensification and sediment supply increment associated with tectonic uplift. FA2 appears at around 13.5 Ma in the Khutia Khola section which corresponds with the adjacent Karnali River section but around 2~3 Ma earlier than in Western and Central Nepal Himalaya. This implies increased discharge and enhanced erosion from the frontal part of the Himalaya at around 13.5 Ma in the Far-western Nepal Himalaya which is earlier than the central and eastern Nepal Himalaya. Similarly, there is no significant variation on the record of monsoon intensification between small river system and the large river system in the Siwalik Group.
8. Whole-rock geochemical analyses of the sandstones and mudstones from the Khutia Khola section show significant compositional changes due to the influence of the provenance, diagenesis, weathering and the river system. Element-Al₂O₃

variation diagrams show considerable scatter due to substantial diagenetic additions of CaO and MgO. The carbonate effects are more intense in sandstones than in mudstones. Na₂O contents are very low, suggesting significant loss of albite during weathering. Elements Fe₂O₃, K₂O, Ba, Cr, Ni, V, Rb, and Ga show regular trends and suggest the control of compositions by separation of quartz, feldspar and lithic fragments from clays. Some elements (CaO, MgO, Sr, and probably MnO, P₂O₅ and Pb) are strongly or moderately influenced by carbonate diagenesis. The elements TiO₂, Nb, Ce and Y show trends that cut the y-axis, consistent with heavy mineral concentration in the meandering river systems of the Jagati Formation (FA1-2). The heavy mineral effect is less marked in the braided river systems of the Kala Formation (FA3-4). Similarly, Zr and Th also show heavy mineral effects.

9. Geochemically the Khutia Khola sandstones and mudstones are classed as sublitharenite, litharenite (LA), wacke (WK) and shale fields. Average UCC_N normalization patterns in all facies associations are remarkably similar, and no provenance change can be detected by using this method. Possibly, diagenetic carbonate has strongly affected these averages, and thus weakened any signals of source change based on them.

10. The oxide/ Al_2O_3 ratio provenance discriminant plot suggests that the provenances of the Khutia Khola sediments and the Karnali River sediments are similar, but are a little different from those in the Bakiya Khola section. With this comparison, it shows that some differences in source composition, weathering intensity, or sedimentary processes related to fluvial system may therefore exist between the Siwalik sections.
11. The stratigraphic variation ratio plots show more intense weathering and uniform source in the meandering river systems in the Jagati Formation (FA1-2). Systematic changes in elemental ratios ($\text{Na}_2\text{O}/\text{Al}_2\text{O}_3$, $\text{K}_2\text{O}/\text{Al}_2\text{O}_3$ and Ga/Rb) suggest change in fluvial style. Comparative studies among the Siwalik sections of the Khutia Khola, Karnali River and Bakiya Khola show that the sandstones and mudstones are distinct in all sections. The similar trend between three different Siwalik sections reflects that the geochemical variations are controlled by fluvial systems.
12. The average modal compositions of the Jagati and Kala Formations are $\text{Q}_{70}\text{F}_7\text{L}_{23}$ and $\text{Q}_{68}\text{F}_{10}\text{L}_{22}$, respectively, and overall average composition is $\text{Q}_{70}\text{F}_8\text{L}_{22}$. Petrographically, these sandstones are lithic arenites (30%) to sub-litharenites (70%) and show that the compositions are similar with other Siwalik sandstones

in the Nepal Himalaya.

13. Provenance analysis indicates that sediments were mainly derived from recycled orogen and fall in transitional recycled block in Qm-F-Lt diagram. The Qp-Lv-Ls diagram suggests that the samples are from collision suture and fold-thrust belt source. The overall stratigraphic trend of the lithic components shows that metamorphic lithic grains are increasing and sedimentary lithic grains are decreasing in upsection, and the Lesser and Higher Himalayas are the mixed sources of these Siwalik sandstones.
14. A bivariate plot of $Q_p/(F+R)$ against $Q_t/(F+R)$ suggests semi-humid to humid climate during sedimentation of the Khutia Khola sandstones and these sandstones are mineralogically immature as well as diminishing compositional maturity towards upsection. Ternary Q-F-R diagram also suggests the deposition under humid climatic condition and metamorphic rock as source. Similarly, bivariate log/log plot of (Q/F) and (Q/R) supports sub-humid climate during deposition and these sediments were mainly derived from high mountains (Higher Himalaya) and moderate hills (Lesser Himalaya).
15. Grain size analyses of the turbidite beds from the Middle Bengal Fan, IODP EXP

354 show that inversely graded beds are dominant in hole U1450 and thicker massive beds are dominant in hole U1451. The ternary plot of sand-silt-clay show that sediments are mostly sandy silt, silty sand and clayey silt, and few are silt and sand. Vertical variation in mean grain size diagram shows tiny coarsening upward and this may be associated with shifting of levees. In the instance, the variation in the grain size in the Middle Bengal Fan turbidites cannot be correlated with lithological changes in the Khutia Khola section of the Siwalik Group, probably because the change around 13.5 Ma was not strong enough to cause the sediment characteristics from the far western Himalaya to be transmitted to the Ganges River mouth.

ACKNOWLEDGEMENTS

I am grateful to the Japanese Ministry of Education, Culture, Sport, Science and Technology (MEXT) for awarding me a scholarship and financing during this research.

I would like to extend my sincere gratitude and appreciation to my academic supervisor Prof. Tetsuya Sakai, Department of Geoscience, Shimane University for his supervision and thoughtful discussion throughout my study. Dr. Sakai's generosity, endless support and encouragement were integral to shape my work as a commendable one. I am always obliged for his moral and physical support in adjusting daily life in Japan.

My deep gratitude goes to Dr. Barry P. Roser for his valuable guidance during geochemical analysis and encouragement throughout the study.

I am equally indebted to Dr. Prakash Das Ulak, Dr. Ananta. Prasad Gajurel and Dr. Danda Pani Adhikari, Tri-Chandra College, Tribhuvan Univeristy, Kathmandu, Nepal for their indispensable support and inspiration regarding the study.

I offer special thanks to Dr. Ashok Sigdel and Dr. Sudarshan Bhandari for their valuable advice in my study and emotional support regarding early life in Japan, and Mr. Sudarshan Prasad Adhikari for his logistic as well as moral support during field visits. Similarly, I am thankful to Mr. Ram Dutta Joshi and Mr. Lokendra Pandey for helping me during several field visits. Mr. Karna Bahadur Saud, Mr. Khem Saud and the village

people of Hatkholi are also sincerely thanked for their continuous aid during my field visits.

I wish to pay my sincere thanks to the Department of Mines and Geology, Government of Nepal for giving me permission to export samples from Nepal to Japan.

I would like to express my thanks to all the staff of the Department of Geoscience, Shimane University for their assistance and support in numerous ways. I also thank all of my Japanese as well as international colleagues in Shimane University for their help in various ways.

My earnest gratitude goes to my mother Mrs. Kamala Adhikari, my siblings Subhashree and Suvakiran, my lovely niece Subhapriya, in-laws Mr. Tulsi Prasad and Mrs. Sumitra Bhandari, Mr. Shyam Prasad and Mrs. Narayani Bhandari, Mr. Pawan Pokharel, Binita Bhandari, Satyawati Bhandari, Rameshwor Bhandari, Ashis Sigdel, Aparna Acharya, Anil Sigdel and Archana Acharya, my co-brothers Kalyan Kishor Ghimire and Sanjaya Chalise, my ever motivating elder brother Madhusudhan Poudyal and entire family for their inspiration to uplift my study. My beloved wife, Mahalaxmi and my sons, Satyam and Shubham are constant motivation in my life.

Swostik Kumar Adhikari
Matsue-Shi, Shimane, Japan
July 2017

REFERENCES

- Adhikar, S. K. and Sakai, T., 2015. Lithostratigraphy of the Siwalik Group, Khutia Khola section, Far Western Nepal Himalaya. *Jour. Nepal Geo. Soc.* **49**, 29-39.
- Aitchison, J., 1986. The statistical analysis of compositional data. Monographs on statistics and applied Probability: Chapman & Hall, London, 416p.
- Allen, J. R. L., 1964. Studies in fluvial sedimentation: six cyclothems from the Lower Old Red Sandstone, Anglo-Welsh Basin. *Sedimentology* **3**, 163-198.
- Allen, J. R. L., 1983. Studies in fluvial sedimentation: bars, bar complexes and sandstone sheets (low-sinuosity braided streams) in the Brownstones (L. Devonian), Welsh Borders. *Sediment. Geol.* **33**, 237-293.
- Amano, K. and Taira, A., 1992. Two-phase uplift of Higher Himalayas since 17 Ma. *Geology*. **20**, 391-394.
- Appel, E., Rosler, W. and Corvinus, G., 1991. Magnetostratigraphy of the Miocene-Pleistocene Surai Khola, Siwaliks in West Nepal. *J. Geophys. Int.* **105**, 191-198.

- Appel, E. and Rosler, W., 1994. Magnetic polarity stratigraphy of the Neogene Surai Khola section (Siwalik, SW Nepal). *Himalayan Geol.* **15**, 63-68.
- Auden, J. B., 1935. Traverses in the Himalaya. *Records of the Geological Survey of India.* **69**, 123-167.
- Basu, A., 1976. Petrology of Holocene fluvial sand derived from plutonic source rocks, implication to plaeoclimatic interpretations. *Jour. Sedi. Petro.* **46**, 694-709.
- Basu, A., Young, S. W., Suttner, L. J., James, W. C. and Mack., G. H., 1975. Re-evaluation of the use of undulatory extinction and polycrystalline in the detrital quartz for provenance interpretation. *Jour. Sedi. Petro.* **45**, 873-882.
- Bernet, M., Van der Beek, P., Pik, R., Huyghe, P., Mugnier, J. L., Labrin, E., and Szulc, A. G., 2006. Miocene to recent exhumation of central Himalaya determined from combined detrital zircon fission-track and U/Pb analysis of Siwalik sediments, western Nepal. *Basin Res.* **18**, 393-412.
- Bhatia, M. R. and Crook, K. A. W., 1986. Trace Elements Characteristics of Greywackes and Tectonic Setting Discrimination of Sedimentary Basins. *Contrib. Mineral. Petrol.* **92**, 181-193.

- Blatt, H., Middleton, G. V. and Murray, R. C., 1980. Origin of sedimentary rocks. Prentice Hall Inc., 87p.
- Bordet, P., Colchen, M. and Le Fort, P., 1972. Some features of the geology of the Annapurna range Nepal Himalaya. *Himalayan Geol.* **2**, 537-563.
- Bouquillon, A., France-Lanord, C., Michard, A., and Tiercelin, J.-J., 1990. Sedimentology and isotopic chemistry of the Bengal Fan sediments: the denudation of the Himalaya. In Cochran, J. R., Stow, D. A. V., et al., *Proceeding of the Ocean Drilling Program, Scientific Results.* **116**, 43-48.
- Bridge, J. S., 2006. Fluvial facies models: recent developments. In: Posamentier, H., Walker, R.G. (Eds.), *Facies Models Revisited: Soc. Eco. Pal. Min. Spec. Pub.* **84**, 85-170.
- Burbank, D. W., Beck, R. A. and Mulder, T., 1996. The Himalayan Foreland: Asian Tectonics. Cambridge Univ. Press, 149-188.
- Burchfiel, B. C., Chen, Z., Hodges, K. V., Liu, Y., Royden, L. H., Deng, C. and Xu, J., 1992. The South Tibetan Detachment System, Himalayan Orogen: Extension contemporaneous with and parallel to shortening in a collisional mountain belt.

Geol. Soc. Am., Sp. Pap., 269p.

Cande, S. C. and Kent, D. V., 1995. Revised calibration of the geomagnetic polarity timescale for the Late Cretaceous and Cenozoic. *J. Geophys. Res.* **100**, 6093-6095.

Capuzzo, N. and Wetzel, A., 2004. Facies and basin architectural of the Late Carboniferous Salvan-Dorenaz continental basin (Western Alps, Switzerland/France). *Sedimentology*, **51**, 675-697.

Chirouze, F., Bernet, M., Huyghe, P., Erens V., Dupont-Nivet, G. and Senebier, F., 2012. Detrital thermochronology and sediment petrology of the middle Siwaliks along the Muksar Khola section in eastern Nepal. *Jour. Asian Earth Sci.* **44**, 94-106.

Cochran, J. R., 1990. Himalayan uplift, sea level, and the record of Bengal Fan sedimentation at the ODP LEG 116 sites. *Proc. Ocean Dril. Prog, Sci. Res.* **116**, 397-414.

- Colchen, M., Le Fort, P. and Pecher, A., 1986. Rescherches reologiques dans l'Himalaya du Nepal, Annapurna-Manaslu-Ganesh Himal: Paris, Editios du Centre National de la Recherche Scientifique, Paris. 136p.
- Collinson, J. D., 1996. Alluvial Sediments, In: Reading, H.G. (Ed.), Sedimentary Environments and Facies, 3rd ed. Blackwell Publishing, Oxford. 37-82.
- Condie, K. C., 1993. Chemical composition and evolution of the upper continental crust: Contrasting results from surface samples and shales. Chem. Geol. **104**, 1-37.
- Corvinus, G. and Nanda, A. C., 1994. Stratigraphy and palcontology of the Siwalik group of Surai khola and Rato khola in Nepal. N. Jb. Geol. Palaont. Abh. **191**, 25-68.
- Critelli, S. and Ingersoll, R. V., 1994. Sandstone petrography and provenance of the Siwalik Group (northwestern Pakistan and western-southeastern Nepal). Jour. Sedi. Res. **A64 (4)**, 815-823.
- Crook, K. A. W., 1974. Lithogenesis and geotectonics, the significance of compositional variations in flysch arenites (graywackes). In: Dott, R. II. and Saver, R. II. (Eds.),

- Modern and Ancient Geosynclinal Sedimentation. Soc. Econ. Paleont. Mineral. Spec. Pub. **91**, 304-310.
- Curry, J. R. and Moore, D. G., 1971. Growth of the Bengal deep-sea fan and denudation of the Himalayas. Geol. Soc. Am. Bull. **82**, 563-572.
- DeCelles, P. G., Gehrels, G. E., Quade, J., Ojha, T. P., Kapp, P. A. and Upreti, B. N., 1998. Neogene foreland basin deposits, erosional unroofing, and the kinematic history of the Himalayan fold-thrust belt, western Nepal. Geol. Soc. Am. Bull. **110**, 2-21.
- DeCelles, P. G., Robinson, D. M., Quade, J., Ojha, T. P., Garzione, C. N., Copeland, P. and Upreti, B. N., 2001. Stratigraphy, structure, and tectonic evolution of the Himalaya fold-thrust belt in western Nepal. Tectonics. **20**, 487-509.
- DeMets, C., Gordon, R. G., Argus, D. F. and Stein, S., 1990. Current plate motions. Geophys. Jour. Int. **101**, 425-478.
- Department of Mines and Geology (DMG/IIMGN), 1987. Geological Map of Far Western Nepal, 1:250,000.

- Department of Mines and Geology (DMG/HMGN), 1994-2007. Geological map of petroleum exploration, Block 1-10, Nepal, 1:250,000.
- Dettman, D. L., Kohn, M. J., Quade, J., Ryerson, F. J., Ojha, T. P. and Hamidullah, S. 2001. Seasonal stable isotope evidence for a strong Asian monsoon throughout the past 10.7 m.y. *Geology*. **29**, 31–34.
- Dhital, M. R., Gajurel, A. P., Pathak, D., Paudel, L. P. and Kizaki, K., 1995. Geology and structure of the Siwaliks and Lesser Himalaya in the Surai khola-Bardanda area, Mid Western Nepal. *Bull. Depart. Geol. Tribhuvan Univ.* **4**, 1-70.
- Dickinson, W. R., 1970. Interpreting detrital modes of greywacke and arkosc. *Jour. Sedi. Petrol.* **40**, 695-707.
- Dickinson, W. R., 1985. Interpreting provenance relations from detrital modes of sandstones. In: Zuffa, G. G. (Ed.), *Provenance of Arenites: North Atlantic Treaty Organization. Advanced Study Institute Series 148*, Reidel Publishing Company, 333-361.
- Dickinson, W. R. and Suczek, C. A., 1979. Plate tectonics and sandstone compositions. *Am Assoc. Petro. Geol. Bull.* **63**, 2164-2182.

- Dickinson, W. R., Beard, L. S., Brakenridge, G. R., Erjavec, J. L., Ferguson, R. C., Inman, K. F., Knepp, R. A., Lindberg, F. A. and Ryberg, P. T., 1983. Provenance of North American Phanerozoic sandstone in relation to tectonic setting. *Geol. Soc. Am. Bull.* **94**, 222–235.
- Dinelli E., Cortecchi G., Lucchini F., Fabbri M. and D’Orazio M., 1999. REE mobility associated to acid mine drainage: investigations in the Libiola area (northern Italy). In: Ármannsson H. (ed.), *Geochemistry of the Earth Surface (GES-5, Reykiavik, 16-20 August 1999)*. Balkema, Rotterdam, 173-176
- Einselc, G., 1992. *Sedimentary Basins: Evolution, Facies, and Sediment Budget*. Springer, Berlin. 628p.
- Emmel, F. J. and Curray, J. R., 1981. Dynamic events near the upper and mid-fan boundary of the Bengal fan. *Geo-Mar. Lett.* **1**, 201-205.
- Folk, R. L., 1980. *Petrology of Sedimentary Rocks*. Austin, Texas, Hemphill. 182p.
- Folk, R. L. and Ward, W. C., 1957. Brazos River Bar, a study in the significance of grain-size parameters. *Jour. Sedi. Petrol.* **27**, 3-27.
- France-Lanord, C., and Derry, L. A., 1994. $\delta^{13}\text{C}$ of organic carbon in the Bengal Fan:

source evolution and transport of C3 and C4 plant carbon to marine sediments.

Geochimica et Cosmochimica Acta. **58(21)**: 4809–4814.

France-Lanord, C., Spiess, V., Klaus, A., Schwenk, T., Adhikari, R.R., Adhikari, S.K., Bahk, J.-J., Baxter, A.T., Cruz, J.W., Das, S.K., Dekens, P., Duleba, W., Fox, L.R., Galy, A., Galy, V., Ge, J., Gleason, J.D., Gyawali, B.R., Huyghe, P., Jia, G., Lantzsch, H., Manoj, M.C., Martos Martin, Y., Meynadier, L., Najman, Y.M.R., Nakajima, A., Ponton, C., Reilly, B.T., Rogers, K.G., Savian, J.F., Selkin, P.A., Weber, M.E., Williams, T., and Yoshida, K., 2016. Expedition 354 summary. In France-Lanord, C., Spiess, V., Klaus, A., Schwenk, T., and the Expedition 354 Scientists, Bengal Fan. Proceedings of the International Ocean Discovery Program, 354: College Station, TX (International Ocean Discovery Program) <http://dx.doi.org/10.14379/iodp.proc.354.101.2016>.

Gansser, A., 1964. *Geology of the Himalayas*. Interscience, London. 289p.

Gartner, S., 1990. Neogene calcareous nannofossil biostratigraphy, Leg 116 (central Indian Ocean). In Cochran, J.R., Stow, D.A.V., et al., *Proc. ODP, Sci. Results.* **116**, 165–187.

- Garzanti, E., Vezzoli, G., Ando, S., Lave, J., Attal, M., France-Lanord, C. and DeCelles, P., 2007. Quantifying sand provenance and erosion (Marsyandi River, Nepal Himalaya). *Earth Planet. Sci. Lett.* **258**, 500-515.
- Gautam, P. and Appel, E., 1994. Magnetic polarity stratigraphy of the Siwalik Group sediments of Tinau Khola section in West Central Nepal. revised. *Geophys. J. Int.* **117**, 223-234.
- Gautam, P. and Fujiwara, Y., 2000. Magnetic polarity stratigraphy of Siwalik Group sediments of the Karnali River section in western Nepal. *Geophys. J. Intern.* **142**, 812-824.
- Gahzi, S. and Mountney, N. P., 2009. Facies and architectural element analysis of a meandering fluvial succession: the Permian Warchha Sandstone, Salt Range, Pakistan. *Sedi. Geol.* **221**, 99-126.
- Glennie, K. W. and Ziegler, M. A. 1964. The Siwalik formations of Nepal. *Internat. Geol. Congr.*, 22, Sess. Rep. Pt. **25**, 82-95.
- Guilbaud, R., Bernet, M., Huyghe, P., Erens, V., Chirouze, F. and Dupont-Nivet, G., 2012. On the influence of diagenesis on the original petrographic composition of

- Miocene-Pliocene fluvial sandstone in the Himalayan foreland basin of western-central Nepal. *Jour. Asian Earth Sci.* **44**, 107-116.
- Hagen, T., 1969. Report on the Geological Survey of Nepal, vol. 1. Preliminary Reconnaissance, Druk von Art. Institut. orell Füssli Agi Zürich, Kommissionverlag von Gerbüder Fretzag , Zürich .
- Harrison, T. M., Copeland, P., Hall, S. A., Quade, J., Burner, S., Ojha, T. P. and Kidd, W. S. F., 1993. Isotopic preservation of Himalaya/Tibetan uplift, denudation and climate histories in two molasses deposits. *J. Geol.* **101**, 157-175.
- Harrison, T. M., Grove, M., Lovera, O. M. and Catlos, E. J., 1998. A model for the origin of Himalayan anatexis and inverted meta-morphism. *J. Geophys. Res.* **103**, 27,017-27,032.
- Heim, A. and Gansser, A. 1939. Central Himalaya: Geological observations of the Swiss expedition 1936. *Mem. Soc. Helv. Sci. Nat.* **73 (1)**, 1-245.
- Herron M., 1988. Geochemical classification of terrigenous sands and shales from core data. *Jour. Sed. Petrol.* **58**, 820-829.
- Hisatomi, K., 1990. The sandstone petrology and the provenance of the Churia Group

- in the Arung Khola – Binai Khola area, west central Nepal. *Bulletin Fac. Edu. Wakayama Univ. Nat. Sci.* **39**, 5-29.
- Hisatomi, K. and Tanaka, S. 1994. Climatic and environmental changes at 9.0 and 7.5 Ma in the Churia (Siwalik) Group, West Central Nepal. *Himalayan Geol.* **15**, 161–180.
- Hjellbakk, A., 1997. Facies and fluvial architecture of a high-energy braided river: the Upper Proterozoic Segloddan Member, Varanger Peninsula, northern Norway. *Sediment. Geol.* **114**, 131-161.
- Hossain, H. M. Z., Ulak, P. D. and Roser, B., 2008. Geochemical analyses of sandstones and mudstones from the Siwalik succession, Surai Khola, Western Nepal. *Geosci. Rept. Shimane Univ.* **27**, 53-60.
- Huyghe, P., Galy, A., Mugnier, J. L. and France-Lanord, C., 2001. Propagation of the thrust system and erosion in the Lesser Himalaya: Geochemical and sedimentological evidence. *Geology.* **29**, 1007-1010.
- Huyghe, P., Mugnier, J. L., Gajurel, A. P, and Decaillau, B., 2005. Tectonic and climatic control of the changes in the sedimentary record of the Karnali river

- section (Siwaliks of western Nepal). *The Island Arc*. **14**, 311-327.
- Ingersoll, R. V. and Suczek, C. A., 1979. Petrology and Provenance Neogene sand from Nicobar and Bengal fans. DSDP site 211 and 218. *Jour. of Sedi. Petrol.* **49**, 1217-1228.
- Ingersoll, R. V., Bullard, T. F., Ford, R. L., Grimm, J. P., Pickle, J. D. and Sares, S. W., 1984. The effect of grain size on detrital modes: A test of the Gazzi-Dickinson pointcounting method. *Jour. Sedi. Petrol.* **54**, 103-116.
- Jackson, M. and Bilham, R., 1994. Constraints on Himalayan deformation inferred from vertical velocity fields in Nepal and Tibet. *J. Geophys. Res.* 99 (B7). **13**, 897-13, 912.
- Johnsson, M. J., 1993. The system controlling the composition of clastic sediments. *Geol. Soc. Am. Spec. Pap.*, **284**, 1-19.
- Johnson, M. R. W., Oliver, G. J. G., Parrish, R. K. and Johnson, S. P., 2001. Synthrusting metamorphism, cooling and erosion of the Himalaya, Kathmandu Complex, Nepal. *Tecto.* **20**, 394-415.
- Khan, I. A., Bridge, J. S., Kappelman, J. and Wilson, R., 1997. Evolution of Miocene

- fluvial environments, eastern Potwar Plateau, northern Pakistan. *Sedimentology*, **44**, 221–251.
- Kimura, J. I. and Yamada, Y., 1996. Evaluation of major and trace element XRF analyses using a flux to sample ratio of two to one glass beads. *J. Min. Petr. Econ. Geol.* **91**, 62-72.
- Kroonenberg, S. B., 1994. Effect of provenance, sorting and weathering on the geochemistry of fluvial sands from different tectonic and climatic environments. *Proceedings of the 29th International Geological Congress, Part A*, pp. 69–81, VSP BV, Utrecht, The Netherlands.
- Kumar, R., Ghosh, S. K., and Sangode, S. J., 2003. Mio–Pliocene sedimentation history in the northwestern part of the Himalayan foreland basin, India. *Current Science*, **84**, 1006–1013.
- Kumar, R. and Nanda, A. C., 1989. Sedimentology of the Middle Siwalik Subgroup of Mohand area, Dehara Dun valley, India. *Geol. Soc. India.* **34**, 597–616.
- Kundu, A., Matin, A. and Mukul, M., 2012. Depositional environment and provenance of Middle Siwalik sediments in Tista Valley, Darjiling District, Eastern Himalaya,

- India. *Jour. Earth System Sci.* **121(1)**, 73-89.
- Le Fort, P. 1975. Himalayas: The collided range, Present Knowledge of the continental arc. *Am. J. Sci.* **275-A**, 1-44.
- Le Fort, P., 1996. The Himalayan evolution. In: Yin, A., Harrison, T.M. (Eds.), *The tectonics of Asia*. Cambridge University Press, New York. 95-109 p.
- Le Maitre, R.W., 1976. The chemical variability of some common igneous rocks. *Jour. Petrol.* **17**, 589-637.
- McLennan, S. M., 1993. Weathering and global denudation. *Jour. Geol.* **101**, 295-303.
- McLennan, S. M., Hemming, S., McDaniel, D. K., Hanson and G. N., 1993. Geochemical approaches to sedimentation, provenance, and tectonics. *Spec. Pap. Geol. Soc. Am.* **284**, 21-40.
- Medlicott, H. B., 1875. Note on the geology of Nepal. *Rec. Geol. Surv. India.* **8**, 93-101.
- Miall, A. D., 1985. Architectural-element analysis: a new method of facies analysis applied to fluvial deposits. *Earth Sci., Rev.* **22**, 261-308.
- Miall, A. D., 1996. *The Geology of Fluvial Deposits: Sedimentary Facies, Basin*

Analysis and Petroleum Geology. Springer-Verlag, New York. 528p.

Mugnier, J. L., Delcaillau, B., Huyghe, P. and Leturmy, P., 1998. The break-back thrust splay of the Main Dun Thrust (Himalayas of western Nepal): evidence of an intermediate displacement scale between earthquake slip and finite geometry of thrust systems. *J. Struct. Geol.* **20**, 857-864.

Munsell Color., 2000, *Munsell Soil Color Charts*. Gretag Macbeth, New Windsor.

Nadon, G .C., and Middleton, G. V., 1985. The stratigraphy and sedimentology of the Fundy Group (Triassic) of the St. Martins area, New Brunswick. *Canadian Jour. Earth Sci.* **22**, 1183-1203.

Nakayama, K. and Ulak, P. D., 1999. Evolution of fluvial style in the Siwalik Group in the foothills of the Nepal Himalaya. *Sediment. Geol.* **125**, 205-224.

Nesbitt, H. W. and Young, G. M., 1982. Early Proterozoic climates and plate motions inferred from major element chemistry of lutites. *Nature.* **299**, 715-715.

Nesbitt, H. W. and Young, G. M., 1984. Prediction of some weathering trends of plutonic and volcanic rocks based on thermodynamic and kinetic considerations. *Geochim. Cosmochim. Acta.* **48**, 1523–1534.

- Nesbitt, H.W. and Young, G.M., 1989. Formation and diagenesis of weathering profiles. *Jour. Geol.* **97**, 129–147.
- Ohta, T. and Arai, H. (2007). Statistical empirical index of chemical weathering in igneous rocks: A new tool for evaluating the degree of weathering. *Chem. Geol.* **240**, 280-297.
- Ojha, T. P., Butler R. F., Quade, J., DeCelles, P. G., Richards, D. and Upreti, B. N., 2000. Magnetic polarity stratigraphy of the Neogene Siwalik Group at Khutia Kholā, far western Nepal. *Geol. Soc. Am. Bull.* **112**, 424-434.
- Olsen, H., 1988. The architecture of a sandy braided-meandering river system: an example from the Lower Triassic Solling Formation (M. Buntsandstein) in W-Germany. *Geol. Rundschau.* **77**, 797-814.
- Pandey, M. R., Tandukar, R. P., Avouac, J. P., Lavce, J. and Massot, J. P., 1995. Interscismic strain accumulation on the Himalayan crustal ramp (Nepal). *Geophys. Res. Lett.* **22**, 751-754.
- Paredes, J. M., Foix, N., Pinol, F. C., Nillni, A., Allard, J. and Marquillas, R. A., 2007. Volcanic and climatic controls on fluvial style in a high-energy system: the Lower

- Cretaceous Matasiete Formation, Golfo San Jorge basin, Argentina. *Sediment. Geol.* **202**, 96-123.
- Patriat, P. and Acheche, J., 1984. India-Eurasia collision chronology has implications for crustal shortening and driving mechanism of plates. *Nature.* **311**, 615-621.
- Pettijohn, F. J., 1975. *Sedimentary Rocks*. 3rd ed. Harper & Row, New York. 628p.
- Pettijohn, F. J., Potter, P. E. and Siever, R., 1987. *Sand and sandstone*. 2nd ed. Springer-Verlag. 533p.
- Pilgram, G. E., 1913. The correlation of the Siwaliks with mammal horizons of Europe. *Rec. Geol. Sur. In.* **43 (4)**, 264-326.
- Powers, P. M., Lillie, R. J. and Yeats, R. S., 1998. Structure and shortening of the Kangra and Dehra Dun re-entrants, sub-Himalaya, India. *Geol. Soc. Am. Bull.* **110**, 1010-1027.
- Prakash, B., Sharma, R. P. and Roy, A. K., 1980. The Siwalik Group (molasses) – sediments shed by collision of continental plates. *Sediment. Geol.* **25**, 127-159.
- Prell W. L. & Kutzbach, J. E., 1992. Sensitivity of the Indian monsoon to forcing parameters and implications for its evolution. *Nature.* **360**, 647-652.

- Quade J., Cater, J. M. L, Ojha, T. P., Adam J. and Harrison, T. M. 1995. Late Miocene environmental change in Nepal and the northern Indian subcontinent: Stable isotope evidence from paleosols. *Geol. Soc. Am. Bull.* **107**, 1381-1297.
- Quade, J., Cerling, T. E., and Bowman, J. R., 1989. Development of the Asian monsoon revealed by marked ecologic shift in the latest Miocene of northern Pakistan: *Nature*. **342**, 117–119.
- Raymo, M. E. & Ruddiman, W. F., 1992. Tectonic forcing of Late Cenozoic climate. *Nature*. **359**, 117-122.
- Reading, H. G., ed., 2004. *Sedimentary environments: processes, facies and stratigraphy*. Blackwell Science, Oxford. 3rd ed. 688p.
- Reed, W. E., 1991. Genesis of calcrete in the Devonian Wood Bay Group, Dicksonland, Spitsbergen. *Sediment. Geol.* **75**, 149-161.
- Robinson, D. M., DeCelles, P. G. and Copeland, P. 2006. Tectonic evolution of the Himalaya thrust belt in western Nepal: Implication for channel flow models. *Geol. Soc. Am. Bull.* **118**, 868-885.
- Roser, B. P., 2000. Whole-rock geochemical studies of clastic sedimentary suites. *Mém.*

Geol. Soc. Japan. **57**, 73-89.

Roser, B. P. and Korsch, R. J., 1986. Determination of tectonic setting of sandstone-mudstone suites using SiO₂ content and K₂O/Na₂O ratio. *J. Geol.* **94**, 635-650.

Roser, B. P. and Korsch, R. J., 1988. Provenance signatures of sandstone-mudstone suites determined using discriminant function analysis of major-element data. *Chem. Geol.* **67**, 119-139.

Roser, B. P., Sawada, Y. and Kabeto, K., 1998. Crushing performance and contamination trails of a tungsten carbide ring mill compared to agate grinding. *Geoscience Reports of Shimane University.* **17**, 1-11.

Roser, B. P., Ulak, P. D., Nakayama, K., Kimura J. I. and Mori, H., 2002. Major element geochemistry of the Upper Cenozoic Siwalik Group along the Bakiya Khola Section, Central Nepal. In: Charu C. Pant and Arun K. Sharma (eds). *Aspects of Geology and Environment of the Himalaya*. Nainital, Gyanodaya Prakashan. 41-62p.

- Rosler, W., Metzler, W. and Appel, E., 1997. Neogene magnetic polarity stratigraphy of some fluvial Siwalik sections, Nepal. *Geophysics Journal of International*. **130**, 89-111.
- Rowley, D. B., 1996. Age of initiation of collision between India and Asia: A review of stratigraphic data. *Earth Planet. Sci. Lett.* **145**, 1-13.
- Roy, D. K. and Roser, B. P., 2013. Climatic control on the composition of the Carboniferous-Permian Gondwana sediments, Khalaspir basin, Bangladesh. *Gondwana Res.* **23**, 1163-1171.
- Ruddiman, W. F. & Kutzbach, J. E., 1989. Forcing of the late Cenozoic Northern Hemisphere climate by plateau uplift in southeast Asia and the American southwest. *J. Geoph. Res.* **94**, 8409-18427.
- Rudnick, R. L. and Gao, S., 2005. Composition of the Continental Crust. In: Rudnick, R.L., Holland, H.D., Turckian, K.K. (Eds.), *The Crust*. Vol. 3. *Treatise on Geochemistry*. Elsevier-Pergamon, Oxford. 1-64p.
- Sah, R. B., Ulak, P. D., Gajurel, A. P. and Rimal, L. N., 1994. Lithostratigraphy of the Siwalik sediments of the Amlekhganj-Iktauda area, sub-Himalaya of Nepal. *Him.*

Geol. **15**, 37-48.

Sakai, T., Saneyoshi, M., Tanaka, S., Sawada, Y., Nakatsukasa, M., Mbua, E., and Ishida, H., 2010. Climate shift recorded at around 10 Ma in Miocene succession of Samburu Hills, northern Kenya Rift, and its significance. From: Clift, P. D., Tada, R. and Zheng, H. (eds) Monsoon Evolution and Tectonics-Climate Linkage in Asia. Geol. Soc. Lon, Sp. Pub. **34**, 109-127.

Schelling, D., 1992. The tectonostratigraphy and structure of the eastern Nepal Himalaya. Tecto. **11**, 925-943.

Schwenk, T., and Spieß, V., 2009. Architecture and stratigraphy of the Bengal Fan as response to tectonic and climate revealed from high-resolution seismic data. In Kneller, B.C., Martinsen, O.J., and McCaffrey, B. (Eds.), External Controls on Deep-Water Depositional Systems. Sp. Pub., Soc. Sedi. Geol. **92**, 107-131.

Seeber, L. and Armbruster, J. G., 1981. Great detachment earthquakes along the Himalayan arc and long-term faulting. Earthquake prediction. An International review Maurice Ewing Series 4. Am. Geol. Union. 259-277.

Sengupta, S. M., 1994. Introduction to Sedimentology. A. A. Balkema/ Rotterdam/

Brookfield.

Sharma, C. K., 1973. Geology of Nepal. Education Enterprises, Kathmandu. 164p.

Sharma, S. R., Subedi, D. N., KC, S. B., Khanal, R. P. and Tripathi, G. N., 2007.

Geological Map of Petroleum Exploration Block-1, Dhangadi, Far Western Nepal

(Scale: 1:250,000). Petroleum Exploration Promotion Project, Depart. Mines and

Geol., Kathmandu, Nepal.

Shimizu, 2013. Geochemistry of Siwalik sedimentary rocks in the Karnali River section,

Nepal. Unpublished Undergraduate Thesis, Shimane University, Matsue, Shimane,

Japan. 90p.

Sigdel, A. and Sakai, T., 2013. Petrography of Miocene Siwalik Group sandstones,

Karnali River section, Nepal Himalaya: Implications for source lithology and

tectonic setting. Jour. Nepal Geol. Soc. **46**, 95-110.

Sigdel, A. and Sakai, T., 2016, Sedimentary facies analysis of the fluvial systems in the

Siwalik Group, Karnali River section, Nepal Himalaya, and their significance for

understanding the paleoclimate and Himalayan tectonics. Jour. Nepal Geol. Soc.

51, 11-26.

- Sigdel, A., Sakai, T., Ulak, P. D., Gajurel, A. P. and Upreti, B. N., 2011. Lithostratigraphy of the Siwalik Group, Karnali River section, far-west Nepal Himalaya. *Jour. Nepal Geol. Soc.* **43**, 83–101.
- Suttner, L. J. and Dutta, P. K., 1986. Alluvial sandstone composition and paleoclimate. 1. Framework mineralogy. *Jour. Sedi. Petrol.* **56**, 329-345.
- Suttner, L. J., Basu, A. and Mack, G. H., 1981. Climate and the origin of quartz arenite. *Jour. Sedi. Petrol.* **51**, 1235-1244.
- Szule, A. G., Najman, Y., Sinclair, H., Pringle, M., Bickle, M., Chapman, H., Garzanti, E., Ando, S., Huyghe, P., Mugnier, J. L., Ojha, T. P. and DeCelles, P. G. 2006. Tectonic evolution of the Himalaya constrained by detrital ^{40}Ar - ^{39}Ar , Sm-Nd and petrographic data from the Siwalik foreland basin succession, SW Nepal. *Basin Res.* **18**, 375-391.
- Tamrakar, N. K., Yokota, S. and Shrestha, S. D., 2003. Petrography of the Siwalik sandstones, Amlekhganj-Suparitar area, central Nepal Himalaya. *Jour. Nepal Geol. Soc.* **28**, 41-56.

- Tamrakar, N. K. and Syangbo, D. K., 2014. Petrography and provenance of the Siwalik Group sandstones from the Main Boundary Thrust region, Samari River area, Central Nepal, Sub-himalaya. *Boletin de Geologia* 36 (2).
- Tanaka, S. 1997. Uplift of the Himalaya and climate changes at 10.0 Ma evidence from records of the carbon stable isotopes and fluvial sediments in the Churia Group Nepal. *J. Geol. Soc. Japan.* **103 (3)**, 253–264.
- Taylor, S. R. and McLenan, S. M., 1985. The continental crust: its composition and evolution. Blackwell Scientific, Oxford. 312p.
- Thomas, J. V., Parkash, B. and Mohindra, R., 2002. Lithofacies and palacosol analysis of the Middle and Upper Siwalik Group (Plio-Pleistocene), Haripur-Kolar section, Himachal Pradesh, India. *Sediment. Geol.* **150**, 343-366.
- Tokuoka, T. and Yoshida, M., 1984. Some characteristics of Siwalik (Churia) Group in Chitwan Dun, Central Nepal. *Jour. Nepal Geol. Soc.* **4**, Special Issuc, 26-55.
- Tokuoka, T., Takayasu, K., Yoshida, M. and Hisatomi, K., 1986. The Churia (Siwalik) Group of the Arung Kholā area, west-central Nepal. *Mem. Fac. Sci. Shimane Univ.* **20**, 135-210.

- Tokuoka, T., Takeda, S., Yoshida, M. and Upreti, B. N., 1988. The Churia (Siwalik) Group in the Western Part of the Arung Khola area, west central Nepal. Mem. Fac. Sci. Shimane Univ. **22**, 131-140.
- Tokuoka, T., Takayasu, K., Hisatomi, K., Yamasaki, H., Tanaka S., Konomatu M., Sah R. B. and Roy S. M., 1990. The Churia (Siwalik) Group of Tinau Khola-Binai Khola area, West Central Nepal. Mem. Fac. Sci. Shimane Univ. **24**, 71-88.
- Tokuoka, T., Takayasu, K., Hisatomi, K., Tanaka, S., Yamasaki, H., and Konomatsu, M., 1994. The Churia Siwalik Group in West Central Nepal. Himalayan Geol. **15**, 23–35.
- Tucker, M. E., 1982. Sedimentary Rocks in the Field. Third ed. John Wiley & Sons, New York. 234p.
- Turner, P., 1980. Continental Red Beds. Developments in Sedimentology. **29**. Elsevier, Amsterdam. 562p.
- Ulak, P. D., 2004. Evolution of fluvial system in Siwalik Group of Chatara-Barahakshetra area, east Nepal Himalaya. Jour. Nepal Geol. Soc. **30**,

67–74.

Ulak, P. D., 2009. Lithostratigraphy and late Cenozoic fluvial styles of Siwalik Group along Kankai River section, East Nepal Himalaya. *Bull. Dep. Geol., Tribhuvan University*, **12**, 63–74.

Ulak, P. D. and Nakayama, K., 1998. Lithostratigraphy and evolution of the fluvial style in the Siwalik Group in the Hetauda-Bakiya Khola area, Central Nepal. *Bull. Dep. Geol., Tribhuvan University*, **6**, 1–14.

Ulak, P. D. and Nakayama, K., 2001. Neogene fluvial systems in the Siwalik Group along Tinau Khola section, west central Nepal Himalaya. *Jour. Nepal Geol. Soc.* **25**, 111–122.

Ullah, K., Arif, M. and Shah, T. M., 2006. Petrography of sandstones from the Kamliak and Chinji Formations, southwestern Kohat Plateau, NW Pakistan: Implications for source lithology and palaeoclimate. *Jour. Himalayan Earth Sci.* **39**, 1–13.

Upreti, B. N. 1999. An overview of the stratigraphy and tectonics of the Nepal Himalaya. *J. Asian Earth Sci.* **17**, 577–606.

Upreti, B. N. and Le Fort, P. 1999. Lesser Himalayan crystalline nappes of Nepal:

problem of their origin. In: Macfarlane, A., Quade, J., and Sorkhabi, R. (des.), Himalaya and Tibet: Mountain root to tops. Geol. Soc. Am., Special Paper. **328**, 225-238.

Valdiya, K. S., 1998. In: Dynamic Himalaya. Universities Press (India) Ltd, Hyderabad. 178p.

Wadia, D. N., 1975. Geology of India. Tata McGraw Hill Publ. Corp., New Delhi, India. 508p.

Weltje, G. J., 1994. Provenance and dispersal of sand-sized sediments: reconstruction of dispersal patterns and sources of sand-size sediments by means of inverse modeling techniques. PhD thesis, Geologicaa Ultraicctina.

Weltje, G. J., 2002. Quantitative analysis of detrital modes: statistically rigorous confidence region in ternary diagrams and their use in sedimentary petrology. Earth Sci. Rev. **57**, 211–253.

Weltje, G. J., Meijer, X. D. and De Boer, P. L., 1998. Stratigraphic inversion of siliciclastic basin fills: a note on the distinction between supply signals resulting

- from tectonic and climatic forcing. In: Hovius, N., Leeder, M. (Eds.), Thematic Set on Sediment Supply to Basins. *Basin Research*. **10**, 129-153.
- West R. M., Munthe, J., Lakacks, J. R. and Shrestha, T. B., 1975. Fossils mollusca from the Siwalik of eastern Nepal. *Cur. Sci.* **44 (14)**, 497-498.
- West, R. M., Hitchinson, J. H. and Munthe, J., 1991. Miocene vertebrates from the Siwalik Group, Western Nepal. *Jour. Vertb. Paleontol.* **11 (1)**, 108-129.
- Willis, B. J., 1993a. Ancient river systems in the Himalayan foredeep, Chinji village area, northern Pakistan. *Sediment. Geol.* **88**, 1-76.
- Willis, B. J., 1993b. Evolution of Miocene fluvial systems in the Himalayan foredeep through a two kilometer-thick succession in northern Pakistan. *Sediment. Geol.* **88**, 77-121.
- Willis, B. J., and Behrensmeyer, A. K. 1994. Architecture of Miocene overbank deposits in northern Pakistan. *Jour. Sedi. Res.* **B64 (1)**, 60-67.
- Ycats, R. S., Nakata, T., Farah, A., Fort, M., Mirza, M. A., Pandey, M. R. and Stein, R. S., 1992. The Himalayan Frontal Fault System. *Annales Tectonicae.* **6**, (Suppl.), 85-98.

- Yoshida, M. and Arita, K., 1982. On the Siwaliks observed along some routes in Central
Jour. Nepal Geol. Soc. **2**, Spec. Issue, 51-58.
- Young, S. W., 1976. Petrographic textures of detrital polycrystalline quartz as an aid to
interpreting crystalline source rocks. Jour. Sedi. Petro. **46**, 595-603.
- Zaleha, M. J., 1997. Intra-and extrabasinal controls on fluvial deposition in the Miocene
Indo Gangatic foreland basin, northern Pakistan. Sedimentology. **44**, 369-390.